The Use of Temperature and Environmental Isotopes as Tools to Characterize Groundwater Discharge to the Grand River, Ontario, Canada

by

Robert Westberg

A thesis
presented to the University of Waterloo
in fulfillment of the
thesis requirement for the degree of
Master of Science
in
Earth Sciences

Waterloo, Ontario, Canada, 2012

AUTHOR'S DECLARATION

I hereby declare that I am the sole author of this thesis. This is a true copy of the thesis, including any required final revisions, as accepted by my examiners.

I understand that my thesis may be made electronically available to the public.

Abstract

The Grand River Watershed, in southern Ontario, is home to approximately 900,000 people and one of the fastest growing regions in Canada; specifically, in the urban areas of Guelph, Cambridge, Kitchener, and Waterloo. This growth strains the watershed's capacity to supply adequate water resources to these municipalities, as well as manage the waste-water treatment effluent discharged from them. Nowhere in the watershed is this juxtaposition in water resource function more apparent than at the city of Brantford, with a population of approximately 100,000 people. Located forty-two kilometers downstream from the major urban areas, Brantford is unique in the watershed in that it obtains its entire municipal water supply directly from the Grand River, into which the upstream municipalities discharge 77% of the total waste-water treatment plant effluent emitted to the watershed. One contaminant of concern is nitrate, which, for decades, has been linked to numerous human and aquatic health complications. The input of nitrate from these upstream WWTP's is considerable; the WWTP's have a combined flow rate of 2.3 m^3s^{-1}, and a mean nitrate concentration of 10.4 mg $N \cdot L^{-1}$ (data from Anderson, 2012). As a comparison, the Nith River, the largest tributary to the Grand River between Cambridge and Brantford, has a summer baseflow of 2.9 m^3s^{-1} and, from 2000 to 2004, had a mean nitrate concentration of 4.4 mg $N \cdot L^{-1}$ (Cooke, 2006).

Brantford, in addition to treating their water supply, relies on the dilution of in-stream nitrate from groundwater that is thought to discharge along the Grand between Cambridge and the Brantford municipal water intake. This 40-km reach of the Grand River is colloquially referred to as either the discharge reach or the recovery reach. Recent data from various authors indicate that groundwater may not always act to dilute in-stream nitrate from upstream WWTPs (Encalata, 2008; Pastora, 2009; Rosamond 2009).

The main objective of the research completed in this thesis was to refine the conceptual model of groundwater/surface water interaction along the Grand River between Cambridge and Brantford. Refinement of this conceptual model was accomplished in two parts. First, groundwater discharge, from bank seepage and direct discharge through the riverbed, was located using a variety of methods; a simple reconnaissance survey by canoe, a FLIR thermography survey, drag probe surveys, and a temperature profiling method. Then domestic wells, seeps, tributaries, riverbed discharge, and WWTP effluent were sampled to geochemically characterize inputs to the Grand River. Sulfate concentrations and $^{34}S/^{32}S$ and $^{18}O/^{16}O$ isotopic ratios of sulfate were used to classify discharge as

originating from shallow vs. deep flow systems. Nitrate concentrations in all inputs were surveyed, and $^{15}N/^{14}N$ and $^{18}O/^{16}O$ ratios of nitrate were used to identify possible nitrate sources and cycling processes. To explore how these inputs affect the Grand River, two geochemical surveys - the first in June, at flow 70% greater than baseflow, and the second in early September, under baseflow conditions - were conducted to compare river chemistry at various flow rates.

Combined, the temperature methods were successful in locating both seep and riverbed discharge. The utility of the FLIR thermography survey was highlighted along several reaches, where considerable bank seepage was found that had been missed by previously conducted reconnaissance surveys. The drag probe surveys indicated an appreciable groundwater input along one six to ten km stretch of the discharge reach where downstream river temperatures decreased while temperatures recorded by stationary dataloggers continually increased. Riverbed temperatures along this reach, and other, less promising ones, were explored by temperature profiling. Using a method similar to that of Conant (2004) and an analytical solution to the one dimensional steady state heat advection-diffusion equation developed by Schmidt et al. (2007), a wide range of vertical groundwater discharge flux rates were estimated, from non-detectable discharge to a maximum value of 122.32 $cm \cdot d^{-1}$. Various locations, selected to capture a range of groundwater discharge rates, were chosen for sampling, to compare the geochemistry in the riverbed to a variety of riverbed environments indicated by the flux estimates.

$\delta^{34}S$ and $\delta^{18}O$ values of sulfate showed a clear distinction between sulfate from the dissolution of marine evaporites, found within one of the two predominant bedrock formations in the region, and sulfate from the oxidation of sulfides and organic materials, ubiquitous throughout the overburden. This, along with agreement in sample location, chloride concentrations, vertical flux calculations, and general redox conditions within the subsurface allowed for the distinction between groundwater discharging from shallow and deeper, more regional flow-systems.

This distinction, combined with downstream geochemical trends and seasonal differences in river chemistry, was used to refine the conceptual model of how discharge affects the recovery reach. Discharge from each flow-system has different effects on in-stream nitrate from upstream WWTPs. Discharge from the deeper system tends to be anoxic and contains lower nitrate due, at least in part, to denitrification reactions. Considered individually, this groundwater input dilutes in-stream nitrate concentrations, likely consistently throughout the year. The shallow flow-system is characterized by more oxic conditions and variable nitrate concentrations, and does not always dilute in-stream nitrate

concentrations. As the discharge from the deeper system is relatively consistent over annual timescales (driven by relatively consistent regional hydraulic gradients), it is suggested that any variation in the effect of groundwater on in-stream nitrate comes from fluctuations in the shallow system discharge and nitrate concentrations. However, both a stream-flow mass balance and downstream geochemical trends suggested that discharge to the Grand River during the summer of 2011 was considerably lower than pervious estimates. With other inputs removed, only 6.4% of riverflow at Brantford during September lowflow conditions was available to have come from groundwater discharge. Previous estimates, in contrast, have the discharge component at Brantford as high as 25% of riverflow. Thus, groundwater many not play as large a role in the recovery of this reach as the present conceptual model of groundwater discharge suggests, and the importance of in-stream nitrate cycling processes may be relatively greater.

Acknowledgements

I would like to thank Dr. Ramon Aravena for his guidance and support during the entirety of this research. Further thanks go to Dr. John Spoelstra, Dr. Sherry Schiff , and Dr. Will Robertson for their participation as my committee members, as well as providing support and wisdom throughout my degree. A sincere thank-you goes to Richard Elgood, the coordinator of our lab group at the University of Waterloo, who provided invaluable logistical help as well as insight on, well, pretty much everything. Others in the lab group helped with fieldwork, taught me laboratory procedures, or gave me suggestions on various presentations, so thank you to Maddy Rosamond, Natalie Senger, Jason Venkiteswaran, Janessa Zheng, Justin Harbin, Eduardo Cejudo, Rodrigo Herrera, Gonzalo Huerta, Nicholas Flinn, Pieter Aukes, Xu Zang, Bonnie Debaets, and Fraiser Cummings.

Funding for this research was provided by Waterline Resources, Inc., NSERC (Natural Sciences and Engineering Research Council of Canada), OGS (Ontario Graduate Scholarships), and the University of Waterloo.

Table of Contents

List of Figures

List of Tables

Chapter 1 – Introduction

1.1 Groundwater and the Grand River Discharge Reach

The Grand River Watershed, in southern Ontario, Canada, is home to approximately 900,000 people and one of the most rapidly increasing populations in Canada, with most of this growth occurring in the municipalities of Waterloo, Kitchener, Cambridge, and Guelph (Figure 1.1). This growth increasingly strains the watershed in terms of supplying adequate water resources to these municipalities, as well as managing wastewater treatment effluent from them. Although a large proportion of the watershed relies on groundwater for municipal water supplies, approximately 200,000 people rely on the Grand River for some fraction of their water source (Bellamy and Boyd, 2005). Brantford, a community in the southern portion of the watershed, relies exclusively on the Grand River for its water supply but, because of its location, is downstream of 77% of all the wastewater effluent discharged in the watershed (Figure 1.2, modified from Anderson, 2012). In addition to treating their water source, the municipality of Brantford also relies on the natural attenuation capacity of groundwater discharging upstream. The Grand River between Cambridge and Brantford is colloquially known as the discharge reach, and numerous researchers have documented a considerable flux of groundwater entering the river along this 40-km reach (Holysh et. al., 2001; Singer et. al., 2003; Scott and Imhof, 2005; LESPRTT, 2008; AquaResource Inc. 2009).

The current conceptual model of the interaction between groundwater discharge and the Grand River is that the discharge acts to dilute and otherwise attenuate in-stream contaminants from upstream WWTPs (LSPRTT, 2008; Scott and Imhof, 2005). Accordingly, this groundwater discharge is incorporated into the conceptual framework for how wastewater effluent in the Grand River, and in the watershed as a whole, is managed. Of the thirty wastewater treatment plants (WWTPs) located throughout the watershed, eight release effluent downstream of the discharge reach (Figure 1.2). Of these eight, the only WWTP of significant size is from Brantford itself, with a current discharge of 36,957 m^3d^{-1}; the other seven WWTPs combined have current flows of less than 15,000 m^3d^{-1}. In contrast, the volume of WWTP discharge from the upstream urban area of Kitchener, Waterloo, Cambridge, and Guelph totals 192,172 m^3d^{-1} (Anderson, 2012).

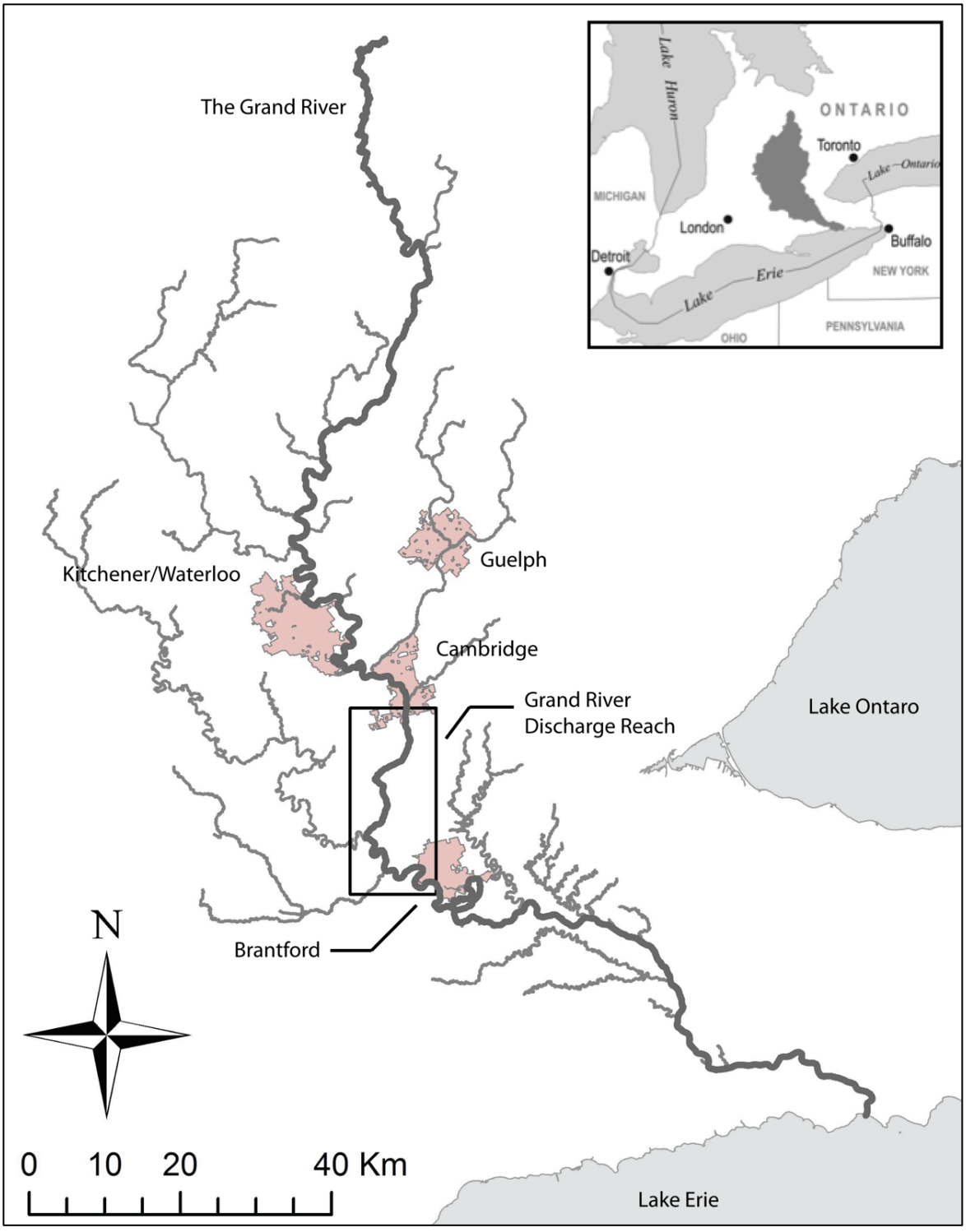

Figure 1.1 The Grand River discharge reach.

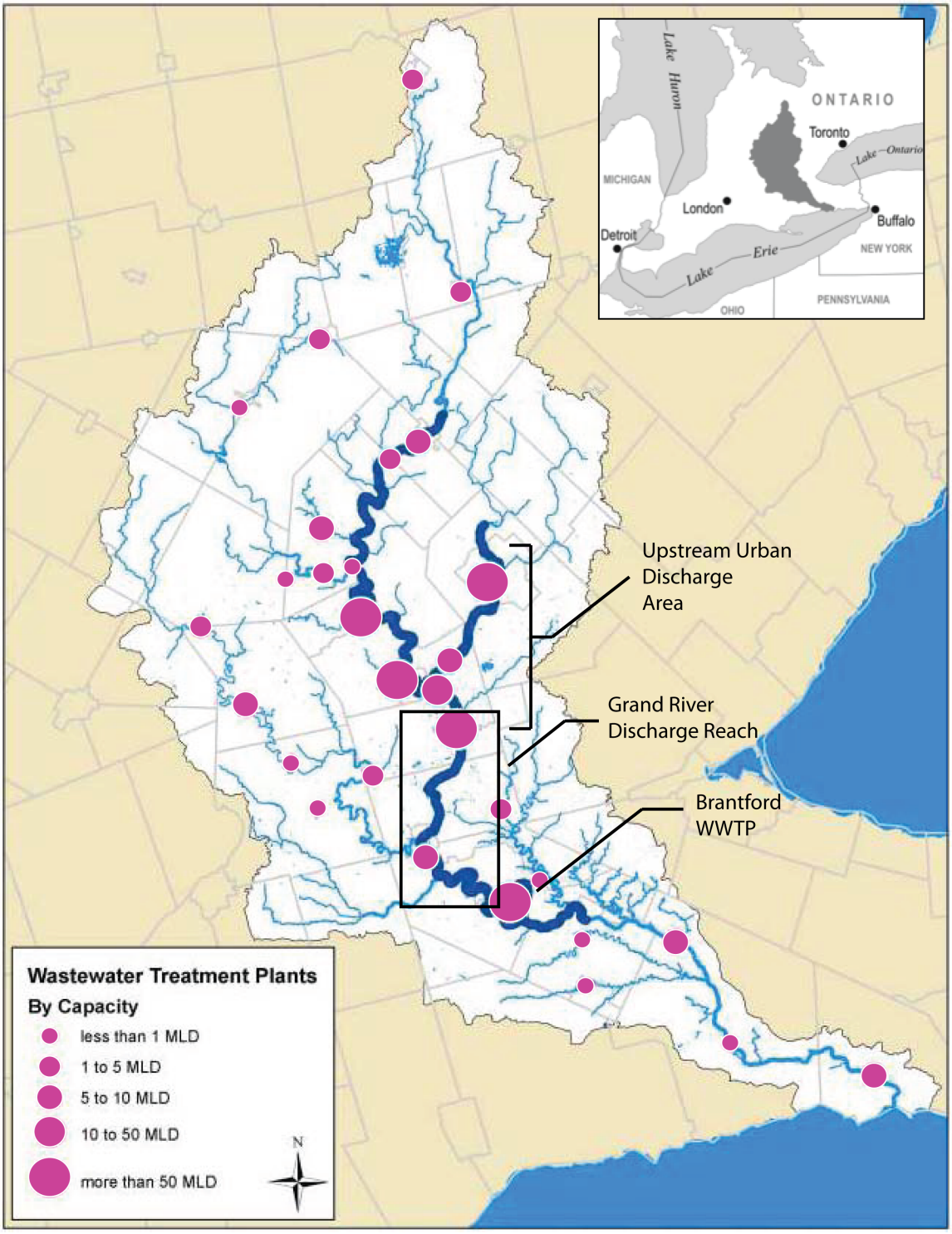

Figure 1.2 The distribution of WWTPs (Waste Water Treatment Plants) and current capacities in the Grand River watershed, in millions of liters per day (MLD). Modified from Anderson, 2012.

One in-stream contaminant of considerable interest is nitrate. Above 10 mg $N \cdot L^{-1}$, nitrate can interfere with the oxygen carrying capacity of haemoglobin in the bloodstream of infants, a condition known as "blue baby syndrome" (Clark and Fritz, 1997). Nitrogen has also been linked to eutrophication in surface waters (Burjin and Hamilton, 2007), and is toxic to aquatic life at concentrations over 2 mg $N \cdot L^{-1}$(Carmago et al., 2005). The current conceptual model that discharging groundwater dilutes nitrate in the Grand River from upstream WWTPs may be contradicted by numerous studies that document high concentrations of nitrate in shallow aquifers throughout the watershed and southern Ontario, due to agricultural activities and septic system effluent (Starr et. al., 1987; Aravena and Robertson, 1998; Vidon and Hill, 2004; Shabaga and Hill, 2010; Senger, 2012). While many groundwater systems have strong, natural denitrification capacities, especially in near-stream environments, it is not clear to what extent nitrate concentrations are, or remain, elevated in groundwater entering the Grand River. Previous studies exploring nitrate concentrations and cycling in riparian zones and riverbed sediments along the Grand produced mixed conclusions (Loreto, 2008; Pastora, 2009). Although low nitrate concentrations were found throughout riparian zones, higher concentrations were observed in riverbed sediments, above 13.0 mg $N \cdot L^{-1}$ and 7.8 mg $N \cdot L^{-1}$, from Loreto (2008) and Pastora (2009), respectively (Figures 1.3 and 1.4). It was not clear whether riparian zones were actively removing nitrate, or if, at these specific sites, nitrate in groundwater from adjacent uplands was simply low to begin with (Figure 1.4). Other studies conducted in the region have shown the capacity of riparian zones to lower nitrate concentrations through denitrification and assimilation, under favourable flow conditions (Devito et. al., 2000; Vidon and Hill, 2004; Shabaga and Hill, 2010).

In another study, Rosamond (2009) conducted a geochemical survey along the entire 300 km length of the Grand River (Figure 1.5). Samples were collected from twenty-three sites down the river at three different times, chosen to characterize the geochemistry of the river during spring, early summer, and later summer flow conditions. During all three surveys, river continuum plots show nitrate concentrations rising sharply through the urban area of Kitchener/Cambridge/Waterloo. Along the discharge reach downstream of the urban area, nitrate concentrations vary considerably during different times of the year. In early summer 2007, nitrate decreases through the discharge reach, in good agreement with the general dilution/assimilation model of groundwater discharge. In late summer 2007, nitrate shows an initial decrease in concentration followed by a slight increase beginning approximately halfway down the discharge reach. Nitrate concentrations, in the spring of 2009 initially decrease, but a subsequent increase through the latter half of the discharge reach brings

concentrations almost back up to those found in the urban area. Amongst other complexities, there appears to be a temporal element to how inputs and processes along the discharge reach, including groundwater discharge, affects in-stream nitrate not addressed by the current conceptual model.

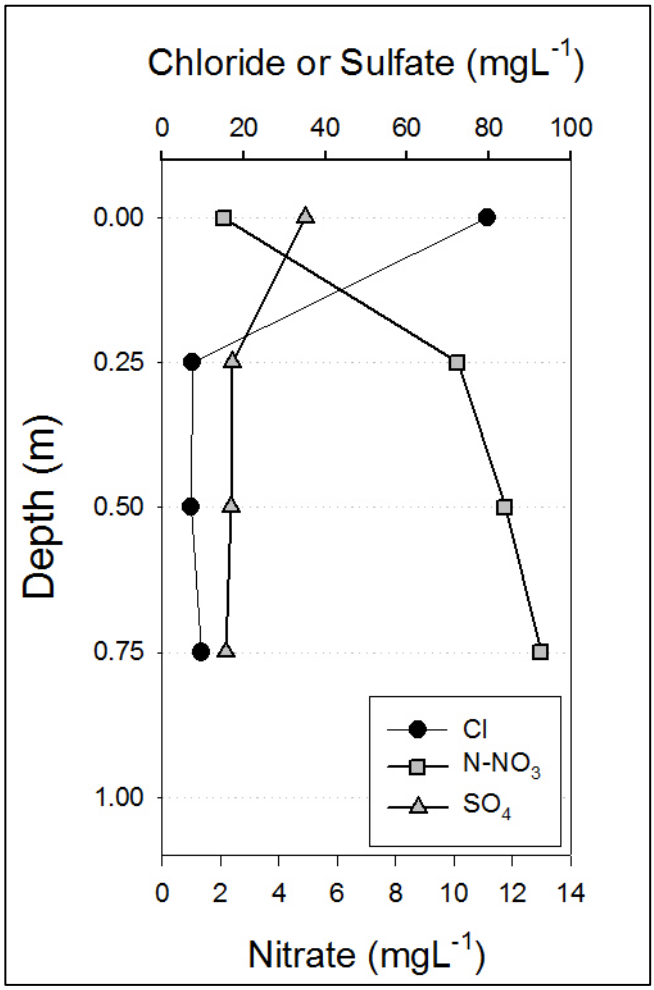

Figure 1.3 A vertical profile into the Grand River streambed at a study site in the discharge reach. Groundwater is distinguished from the overlying river based on a considerable change in chloride concentrations at the stream/streambed interface. The high degree of consistency of chloride concentrations in the riverbed may suggest a moderate to strong vertical groundwater flux. Riverbed samples have higher nitrate concentrations than the river, suggesting nitrate from a source other than the upstream WWTPs is in present in the riverbed, further indicating the presence of groundwater. Data from Encalada, 2008.

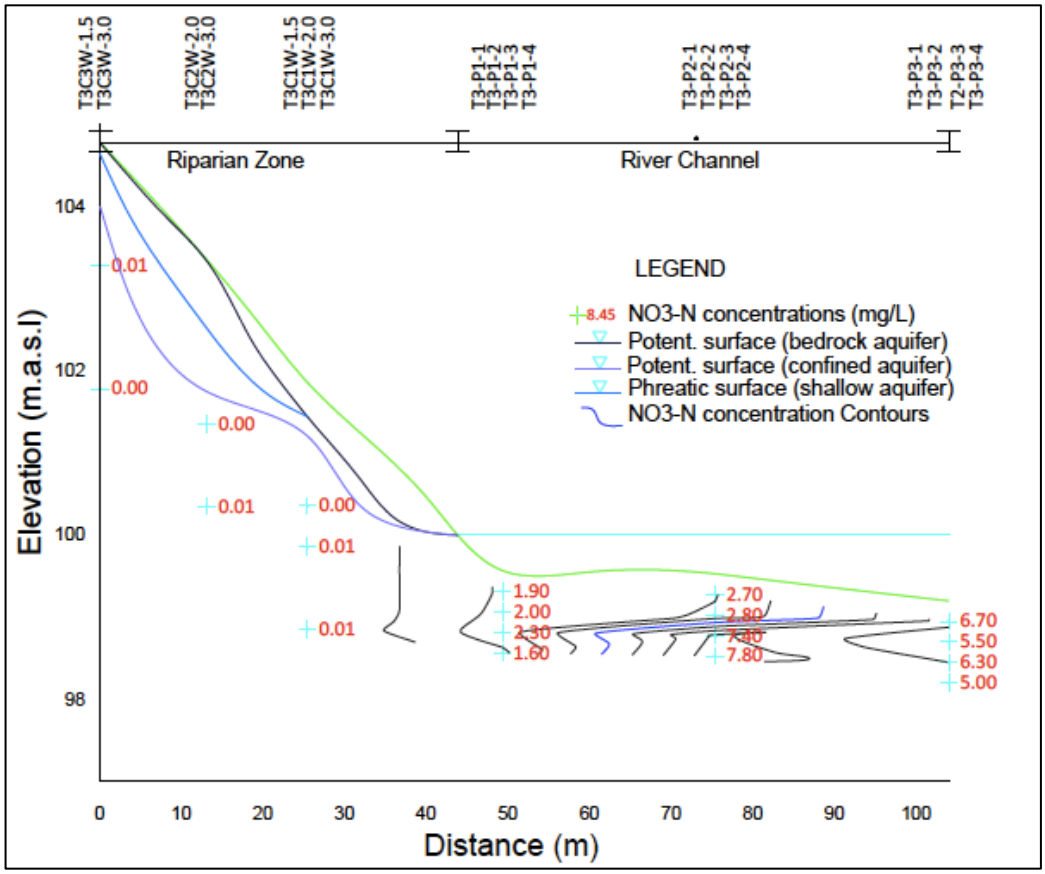

Figure 1.4 Riparian zone and riverbed nitrate concentrations at a second study site in the Grand River discharge reach. In some sampling locations, nitrate is higher in the riverbed than the river (river nitrate averaged 2.8 mg $N \cdot L^{-1}$ during this study). The riparian zone shows no spatial patterns of nitrate concentrations, so it is unclear whether the riparian zone is removing nitrate or if the groundwater from adjacent uplands is simply low in nitrate at the time it was sampled. From Pastora, 2008.

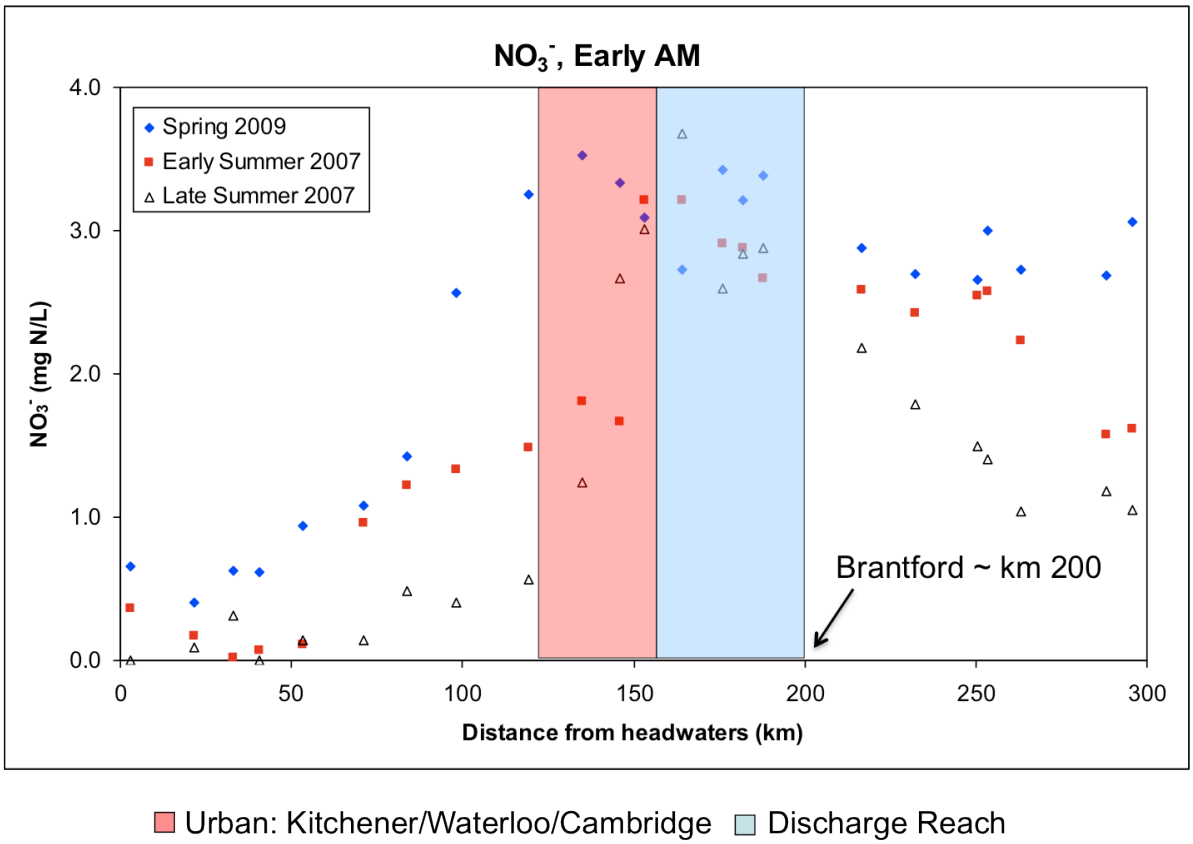

Figure 1.5 Nitrate continuum surveys along the entire length of the Grand River. During all surveys nitrate increases though the urban portion of the watershed, but there is a temporal element to how nitrate behaves through the discharge reach immediately downstream. In early summer 2007, concentrations decrease. In late summer 2007, concentrations initially decrease but show a small increase soon afterwards. In spring 2009, initial nitrate concentrations decrease into the discharge reach, but subsequently rebound to concentrations similar to what is found in the urban area. Therefore, flow additions from groundwater and other inputs do not necessarily dilute in-stream nitrate concentrations. Modified from Rosamond (2009).

The overall goal of the research presented in this thesis was to refine the conceptual model of how groundwater discharge occurs along the Grand River, between Cambridge and Brantford, towards accounting for the temporal and spatial characteristics of the in-stream nitrate concentrations described above. To do this, three main objectives were identified:

1. Map out major areas of groundwater discharge between Cambridge and Brantford, both from seeps along the riverbanks and directly from the riverbed. Although previous work has been done to constrain the overall flux of groundwater entering the river along this stretch, more needs to be done in terms of monitoring its quality. To do this, discharge needs to be located on a scale specific enough that allows for geochemical sampling. This is more easily accomplished for seep discharge than it is for riverbed discharge. Sampling groundwater discharging directly from the streambed along a 40-km river as wide as the Grand presents considerable methodological and logistical problems.

2. Differentiate between groundwater discharge from shallow and deeper flow-systems. The underlying assumption is that the regional flow-systems are deeper, older, and more geochemically evolved than the younger, shallower, and more local flow-systems. As a result, discharge from regional flow systems may be less impacted from anthropogenic activities and may conform better to the dilution conceptual model than local flow-systems.

3. From the discharge locations identified in objective one, find examples of these different groundwater types discharging to the Grand River. Summarize the geochemistry of each flow-system, and evaluate how each affects in-stream nitrate concentrations from upstream urban wastewater treatment plants.

1.2 Thesis Organization

The research conducted to address these objectives made use of two distinct but complimentary methodologies: a) using temperature and heat as a tracer for groundwater to map discharge locations along the reach, and b) a subsequent sampling campaign to geochemically characterize the mapped discharge. This thesis is organized to reflect the order in which these methodologies were utilized. Chapter one has introduced the overall objectives that served as the framework for this research. Chapter two introduces the study area, the Grand River discharge reach, and reviews the local

hydrogeologic characteristics that affect groundwater discharge in the region. Chapter three provides background information on the temperature method and the use of environmental isotopes as groundwater tracers, providing justification as to why these techniques were appropriate to accomplish the research objectives of this study. Chapter four focuses on the first phase of the temperature method: a FLIR camera survey using infrared video and photographs to locate groundwater seeps along the banks of the Grand River between. Chapter five focuses on the second phase of the temperature method: drag probe surveys and streambed temperature profiling utilized to investigate groundwater discharge directly through the riverbed. Chapter six is written along the lines of a stand-alone paper on using $^{34}S/^{32}S$ and $^{18}O/^{16}O$ isotopic ratios of sulfate to identify groundwater discharge from deeper, regional groundwater flow-systems. Based on the geochemical data presented in this chapter, a refined conceptual model of groundwater discharge between Cambridge and Brantford is suggested. Chapter seven, written in a manner similar to chapter six, surveys nitrate concentrations in the study area as well as possible sources and cycling processes, and discusses the implications of the conceptual model, introduced in chapter six, on in-stream nitrate. Finally, chapter eight briefly summarizes the individual conclusions from chapters four through seven, presents the complete refined conceptual model of how groundwater discharge behaviour between Cambridge and Brantford affects in-stream nitrate, and proposes recommendations for further research directions. References are given at the end of the thesis.

Appendix A presents all of the vertical groundwater flux estimates calculated along the discharge reach. Appendix B gives the geochemical data for the domestic well samples, Appendix C the geochemical data for the seep samples, and Appendix D the geochemical data for the riverbed samples. Appendix E shows, and discusses, the vertical profiles of samples from riverbed locations that were not analyzed for sulfate isotopes, and therefore not included in chapter six. Finally, Appendix F presents the geochemical data for the two Grand River surveys.

Chapter 2 – Study Area Characterization: The Grand River Discharge Reach

2.1 Introduction

The Grand River Watershed, located in southern Ontario, drains an area of approximately 6,800 km^2 (AquaResource Inc. 2009). The term *discharge reach* applies to a 40-km stretch of the Grand River, from Cambridge to Brantford, where large volumes of groundwater are thought to enter the river (Figure 2.1). The magnitude of this discharge is moderately well constrained, and various flux estimates during low-flow conditions range from 1.6 m^3s^{-1} to 4.0 m^3s^{-1}, or approximately 8% to 18% of the river flow at Brantford (Scott and Imhof, 2005; Lake Erie Source Protection Region Technical Team 2008; AquaResource Inc. 2009). The source of this groundwater is contested; authors alternatively suggest the discharge originates predominately from either deep, bedrock aquifers underlying the region (AquaResource Inc. 2009), or from shallow, overburden aquifers to the east and west of the river channel (Cooke, 2006; LESPRTT, 2008).

The size of the study area for this research is approximately 400 km^2. North to south, it extends from the lower suburbs of Cambridge to just downstream of the municipal water intake in Brantford. East to west, it spans a distance of approximately ten kilometers, covering the sub-watersheds through which the Grand flows (Figure 2.1). A detailed characterization of this study area is provided to put the methodologies and the results of this research into context. This characterization focuses on the aspects of the region that affect both groundwater geochemical characteristics and groundwater discharge patterns: climate, quaternary geology, bedrock geology, Grand River hydrology and geomorphology, the general flow characteristics of shallow and deep groundwater systems in the area, and the geochemistry of effluent from upstream waste-water treatment plants. Although the latter has no influence on groundwater chemistry or discharge patterns, it is needed to put the geochemistry of the groundwater discharge into context.

2.2 Climate

The climate in the study area is moderately temperate (LSPRTT, 2008). Winters are mild. Summers are humid and hot. Precipitation follows no discernable seasonal tendency, and varies considerably from month to month. During 2011, mean monthly temperatures fell to -12°C in January, and peaked at 29°C in July. Minimum and maximum temperatures ranged from below -20°C to 35°C degrees,

respectively, in January and July (National Climate Archives: http://climate.weatheroffice.gc.ca-/climateData/canada_e.html). Precipitation was fairly consistent over the year, with the exception of a long, dry spell in July (Figure 2.2).

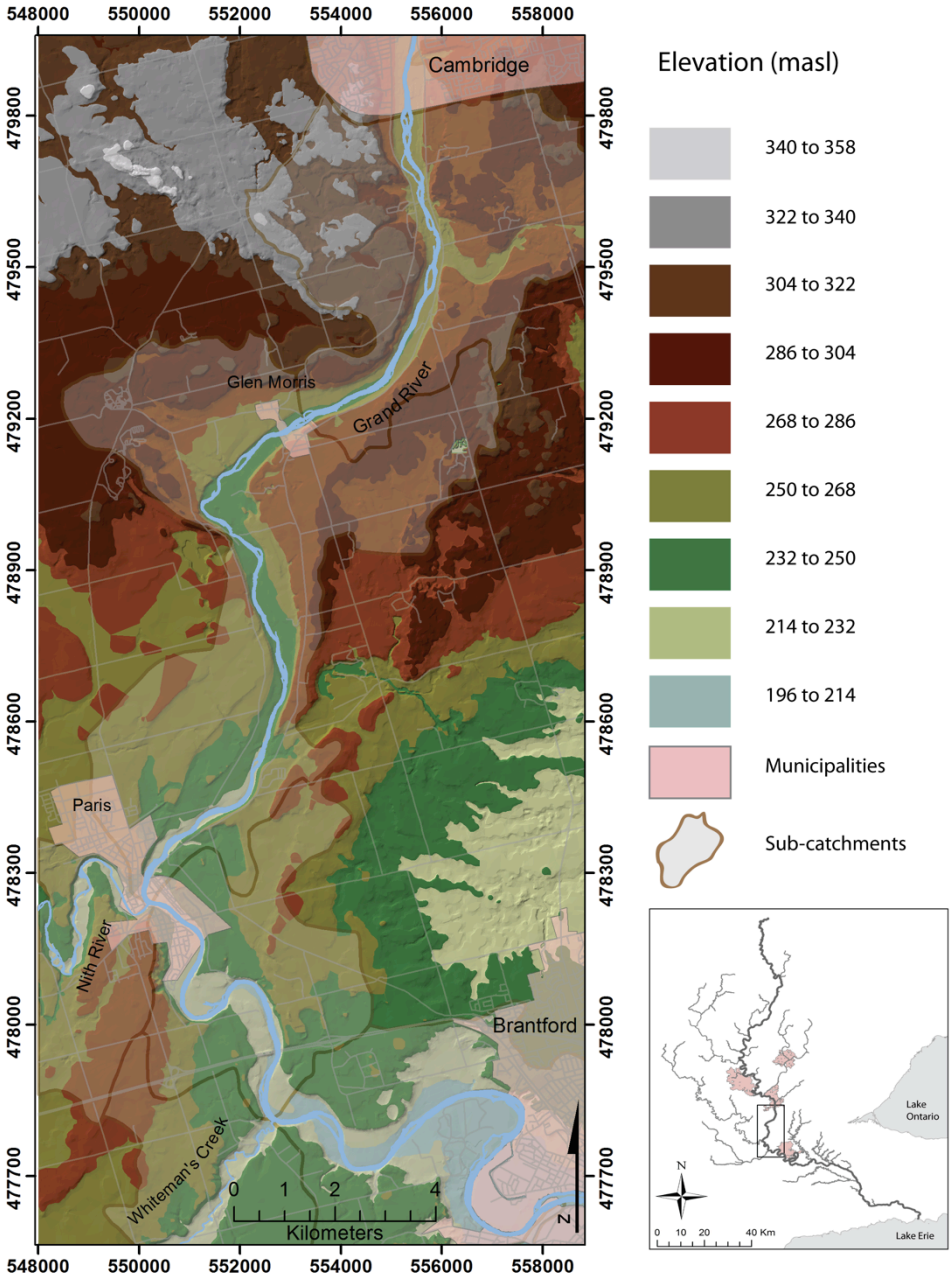

Figure 2.1 The study area: the Grand River discharge reach. Light purple polygons indicate sub-catchments through which the Grand River flows in this portion of the watershed.

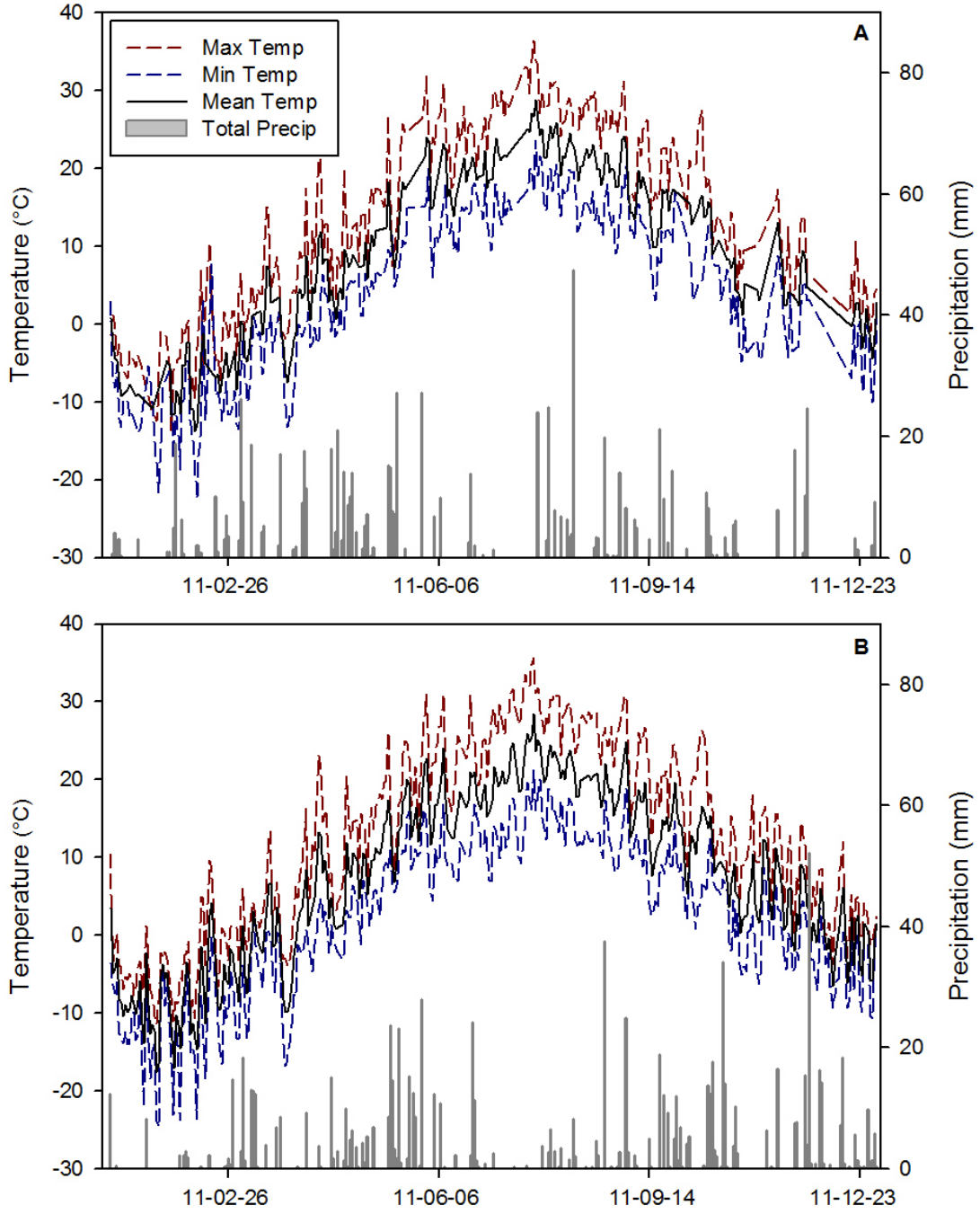

Figure 2.2 Mean, minimum, and maximum temperatures, as well as month precipitation, at A) the Brantford weather station and B) the Kitchener/Waterloo weather station for the year 2011. Data from the NCA: http//:climate.weatheroffice.gc.ca/climateData.canada_e.html.

http://climate.weatheroffice.gc.ca/climateData/canada_e.html). Precipitation was fairly consistent over the year, with the exception of a long, dry spell in July (Figure 2.2).

2.3 Quaternary Geology

The quaternary geology within the study area is depositionally and stratigraphically complex. The main physiological features are recessional and kame moraines, and deposits of outwash sands and gravels associated with the latter. Of these features, the Paris and Galt recessional moraines generally lie to the east of the river channel, while outwash sands and gravels related to the Waterloo Kame moraine complex lie to the west (Figure 2.3).

The Paris moraine is the result of the advance, stagnation, and eventual retreat of the Ontario ice lobe 12,000 to 13,000 years ago (Blackport Hydrogeology Inc., 2009). The Galt moraine formed from a subsequent glacial retreat, re-advance, and stagnation episode, although the dates of these events are not well constrained. Both moraines are oriented northeast to southwest across the study area. Near Cambridge, the moraines are adjacent to one another with the Paris moraine just north of the Galt moraine. Topographic relief is on the order of 20 to 30 meters. To the southwest, the Paris moraine disappears in the Glen Morris region, while the Galt moraine forms the southern bank of the Grand River (LESPRTT, 2008). Downstream of Paris, the Grand River cuts through both moraines as it heads southeast to Brantford while the moraines continue to the southwest. Here, relief from the moraines is more subdued; more on the order of 10 to 20 meters. The presence of these moraines throughout the study area results in a widespread hummocky topography, and numerous kettle lakes dot the landscape. This topography plays an important hydrogeological role in this area of the watershed; it reduces local surface water runoff and increases groundwater recharge rates (Blackport Hydrogeology Inc., 2009).

The main geologic unit of both the Paris and Galt moraines is the Wentworth till, a brown to reddish brown silty sand or sandy silt till (Figure 2.3). It tends to be coarse-grained north of Guelph and Cambridge, but fines downwards throughout the study area, towards the south, as sediments from glaciolacustrine clays are increasingly incorporated into its matrix. In both moraines, the till has a complex internal structure, with numerous sandy silt lenses and sandy gravel units commonly documented in well logs (Blackport Hydrogeology Inc., 2009). Some hydrogeologic data on the Wentworth till is available. Singer et al. (2003) summarized the specific capacity of 662 wells

screened in the Wentworth till throughout southern Ontario. The specific capacity of a well is the pumping rate divided by the height of the drawdown curve and, although generally used to evaluate the quality of the well construction and efficiency of the well, can also be used to infer the transmissivity of an aquifer. The greater an aquifer's transmissivity, the smaller the drawdown cone caused by pumping, so in general, higher specific capacities are indicative of high transmissivities (Singer et al., 2003). Minimum and maximum specific capacities in the Wentworth till were 0.2 $L \cdot min^{-1}m^{-1}$ and 298 $L \cdot min^{-1}m^{-1}$, respectively. 10^{th} and 90^{th} percentiles were 2.8 $L \cdot min^{-1}m^{-1}$ and 74.6 $L \cdot min^{-1}m^{-1}$, and the geometric mean specific capacity was 6.6 $L \cdot min^{-1}m^{-1}$.

The Port Stanley till, one of the first deposited in the region and a unit with a significant proportion of silts and clays, may be present between the bedrock units and overlying moraine features. This till, which outcrops throughout the entire Grand River Watershed, may act as a confining layer between the bedrock and the overburden, depending on its local thickness and continuity. The extent of this till in the study area is not well known, although its presence has been noted in drill logs in the Cambridge area (Blackport Hydrology Inc., 2009).

The kame moraines (ice-contact deposits) in the study area formed as till units were deposited by advancing glaciers and subsequently covered by sand and gravels from stagnant and retreating glacial events during the late Wisconsinan (Blackport Hydrogeology Inc., 2009)). The result is a heterogeneous sediment that can be quite permeable and often has considerable potential as an aquifer. Singer et al. (2003) summarized the aquifer potential of kame moraines throughout Southern Ontario from 5628 wells screened in ice contact deposits. Minimum and maximum specific capacities were 0.1 $L \cdot min^{-1}m^{-1}$ and 5384 $L \cdot min^{-1}m^{-1}$, respectively. 10^{th} and 90^{th} percentiles were 1.3 $L \cdot min^{-1}m^{-1}$ and 37.3 $L \cdot min^{-1}m^{-1}$, and the geometric mean specific capacity was 6.0 $L \cdot min^{-1}m^{-1}$. Kame moraines are generally sub-divided into ice-contact gravels and ice-contact sands, and both are present north of the Grand River between Cambridge and Paris (Karrow, 1987).

As the glaciers retreated, sediment became entrained by melt-water and deposited various distances from the glacier margin, depending on the size and density of the sediment, and the energy in the melt-water channel. Generally, gravels were deposited closest to the glacier margins, sands were carried farther, and silts and clays carried still further (Blackport Hydrogeology Inc., 2009). Outwash sand and gravel deposits are significant features within the study area. Numerous occurrences of both are found amongst the kame moraines northwest of the Grand River channel (Figure 2.3). Singer et al. (2003) summarized the specific capacity of these deposits throughout

Southern Ontario from 3341 wells screened in sand and gravel outwash deposits. Minimum and maximum specific capacities were 0.1 $L \cdot min^{-1}m^{-1}$ and 4823 $L \cdot min^{-1}m^{-1}$, respectively. 10^{th} and 90^{th} percentiles were 1.9 $L \cdot min^{-1}m^{-1}$ and 74.6 $L \cdot min^{-1}m^{-1}$, and the geometric mean specific capacity was 10.6 $L \cdot min^{-1}m^{-1}$. Table 2.1 summarizes the specific capacity data from the Wentworth till, kame moraines, and outwash deposits present in the study area.

2.4 Bedrock Geology

There are two main bedrock formations present in the study area; the Guelph formation, composed of dolostone and limestone in the north, and the Salina formation, composed of interbedded evaporites, dolostone, and shales, in the south (Figure 2.4). In the study area, the inferred contact between these two bedrock units runs approximately southeast to northwest. Upstream of the study area, it turns northward and for the majority of the Grand River Watershed the contact runs closer to the north-south strike of the units. Throughout the watershed, these bedrock units have a shallow dip of approximately 2 degrees to the west (Holysh et al., 2001).

2.4.1 Guelph Formation

Formed during the middle Silurian period (~443 to 418 Ma), the Guelph formation is mostly brown to tan fine- to medium- crystalline dolostone ranging in thickness from 4m to 100m (Thurston et al., 1992). It is extensively fractured and represents an important water resource to the region of Waterloo and the city of Guelph, with both municipalities using water extracted from this formation as part of their water supply. Singer et al. (2003) summarized the Guelph formation's hydrogeologic characteristics using data from an MOE (Ministry Of Environment) database of 6072 wells screened in the formation throughout Southern Ontario. Minimum and maximum specific capacities ranged from 0.1 to 2076 $L \cdot min^{-1}m^{-1}$. The 10^{th} and 90^{th} percentile values were 0.8 and 49.7 $L \cdot min^{-1}m^{-1}$, respectively, with a geometric mean specific capacity of 6.2 $L \cdot min^{-1}m^{-1}$. Transmissivity values, calculated from these specific capacities, ranged from 0.1 and 5719.0 m^2day^{-1}. The 10^{th} and 90^{th} percentiles were 1.4 and 104.9 m^2day^{-1}, respectively, and the geometric mean was 12.1 m^2day^{-1}. Guelph formation flow data is summarized in table 2.2.

Similarly, Singer et al. (2003) also summarized the known water quality data of the formation from 48 wells from the MOE well database. The geochemistry of the Guelph formation is summarized, and compared to that of the Salina formation and overburden sediments, in figure 2.5.

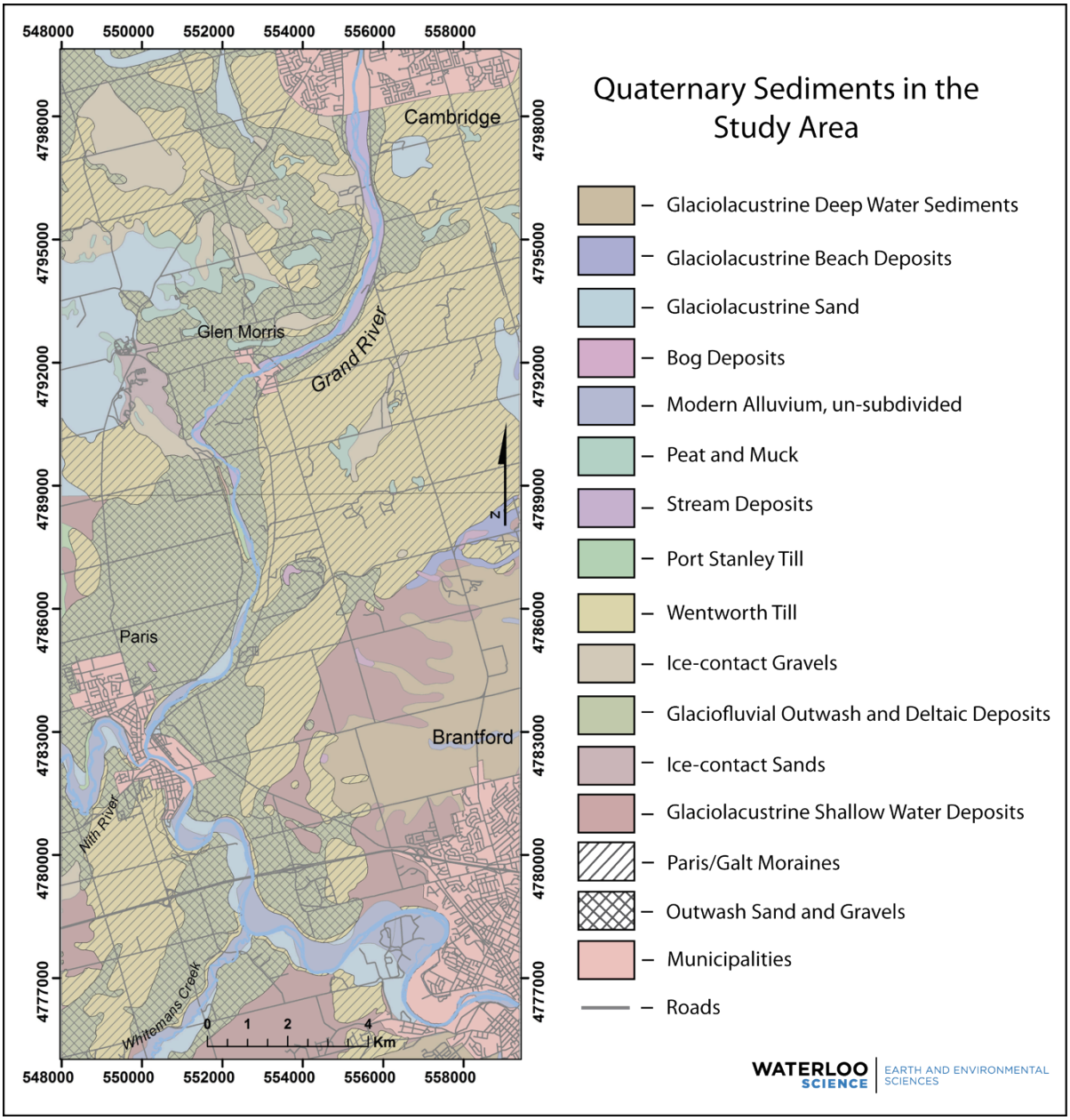

Figure 2.3 Quaternary geology and associated physiological features in the study area. The main features with considerable aquifer potential are the Paris and Galt moraines (Wentworth till), the Waterloo kame moraine complex (ice-contact sands and gravels) and deposits of glacio-fluvial outwash sands and gravels associated with the kame moraines.

2.4.2 Salina Formation

In the southern half of the study area the Salina formation, formed during the upper Silurian (422 to 416 Ma) overlies the Guelph formation. The type of contact between the two is the subject of some controversy, partly because it doesn't outcrop within southern Ontario (Thurston et al., 1992). The Salina formation consists of eight units, four of which outcrop in the Grand River watershed but only two of which outcrop in the study area. The lowermost unit, in contact (conformable or not) with the Guelph formation is primarily composed of dolostones and interbedded mudstones. The upper unit consists of grey to olive green shales containing anhydrite and gypsum lenses (LESPRTT, 2008). Together, the two units in the study area have a combined thickness ranging between 45m and 120m (Thurston et al., 1992).

Singer et al. (2003) summarized the hydrogeologic characteristics of the Salina formation using 2994 wells screened in the formation throughout southern Ontario. Minimum and maximum specific capacities ranged from 0.1 and 3729.0 $L \cdot min^{-1}m^{-1}$. The 10^{th} and 90^{th} percentiles were 1.7 and 82.9 $L \cdot min^{-1}m^{-1}$, respectively, with a geometric mean specific capacity of 13.2 $L \cdot min^{-1}m^{-1}$. Transmissivity values, calculated from these specific capacities, ranged from 0.1 and 10,197 m^2day^{-1}. The 10^{th} and 90^{th} percentiles were 3.2 and 189 m^2day^{-1}, respectively, and the geometric mean was 28.2 m^2day^{-1}. Salina flow formation is summarized in table 2.2.

Singer et al. (2003) also summarized the known water quality data from 63 wells from the MOE well database. The geochemistry of the Salina formation is summarized, and compared to that of the Guelph formation and overburden sediments, in figure 2.5.

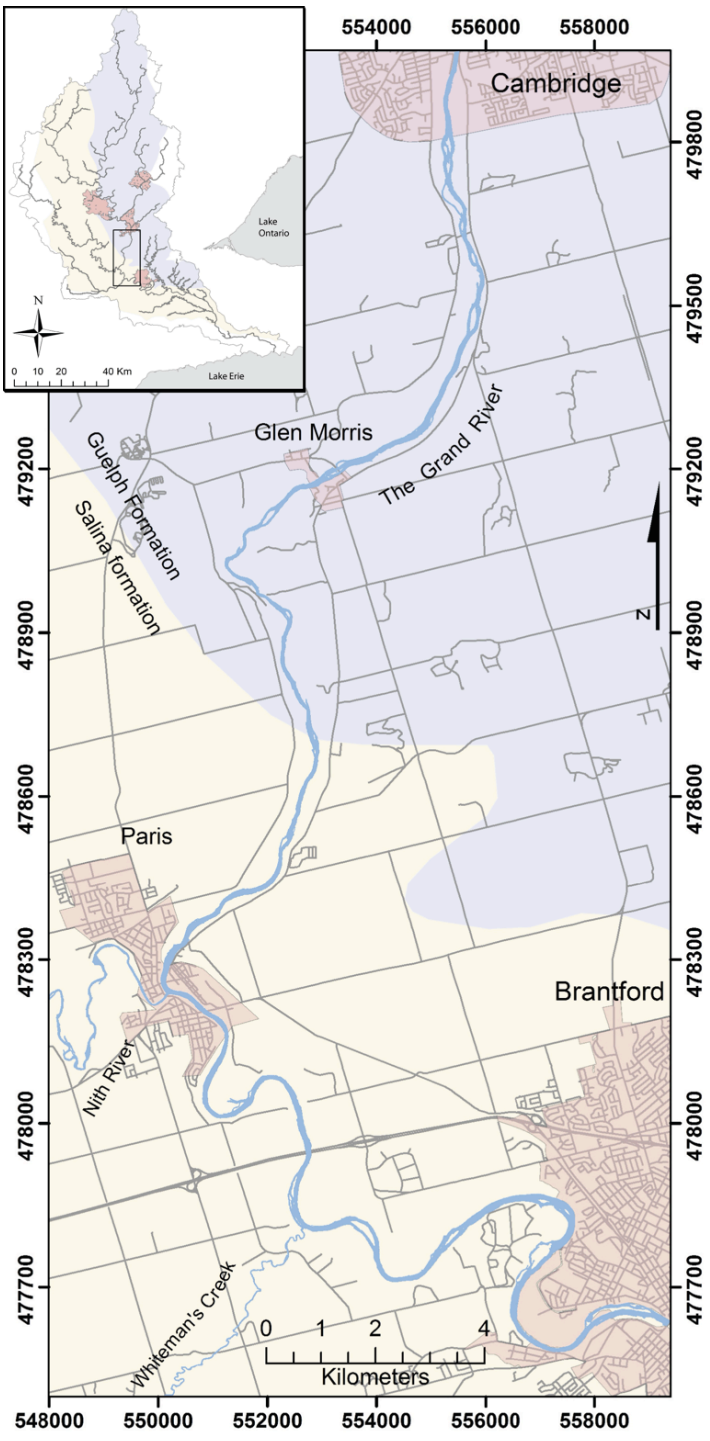

Figure 2.4 Bedrock geology in the study area. The contact between the Salina and Guelph formations does not outcrop in the region, and is therefore only inferred. The southeast to northwest trending contact is actually orientated more closely to north-south in much of the northern portion of the Grand River Watershed (See inset map).

2.5 Comparisons Between the Guelph, Salina, and Overburden Formations

Table 2.1 indicates that outwash deposits have a slightly greater geometric mean specific capacity than either the Wentworth tills (Paris and Galt moraines) or the kame moraines. The kame moraines have a similar specific capacity to that of the Wentworth till, but a 90th percentile value of only about half. The Guelph formation has a geometric mean similar to the Wentworth till and kame moraines, and a 90^{th} percentile value similar to the kame moraines as well. In contrast, both the geometric mean and 90^{th} percentile specific capacities of the Salina formation are about twice the values of the Guelph formation. This may indicate that the Salina formation is a more transmissive aquifer body than either the overburden or the Guelph formation. Because of the large number of wells compared, it is assumed that differences in specific capacities are due to aquifer properties, not a systematic difference in the quality of the construction of wells screened in each sediment type.

Geochemically, the Guelph formation and overburden are fairly similar. The Salina formation can be distinguished from the other two formations by higher calcium and sulfate concentrations, and to a lesser extent potassium, sodium, and magnesium (Figure 2.5). Chloride and bicarbonate concentrations are similar in all three aquifer types. Nitrate concentrations are low in all three units, with the overburden having a slightly higher median value than the bedrock formations. The Salina formation appears to have more consistently low nitrate concentrations than either the Guelph formation or the overburden. All three aquifer types have samples with high nitrate concentrations.

Table 2.1 Specific capacities of the Paris and Galt moraines (Wentworth till), kame moraines (ice-contact deposits), outwash deposits (outwash sands and gravels), and the Guelph and Salina bedrock formations

	*Specific Capacity ($L \cdot min^{-1} m^{-1}$)				
	Wentworth Till	Ice Contact Deposits	Outwash Deposits	Guelph	Salina
Min	0.2	0.1	0.1	0.1	0.1
10th Percentile	2.8	1.3	1.9	0.8	1.7
Geometric Mean	6.6	6	10.6	6.2	13.2
90th Percentile	74.6	37.3	74.6	49.7	82.9
Max	298	5384	4823	2076	3729
Number of Wells	662	5628	3341	6072	2994

*Data from Singer et al. (2003).

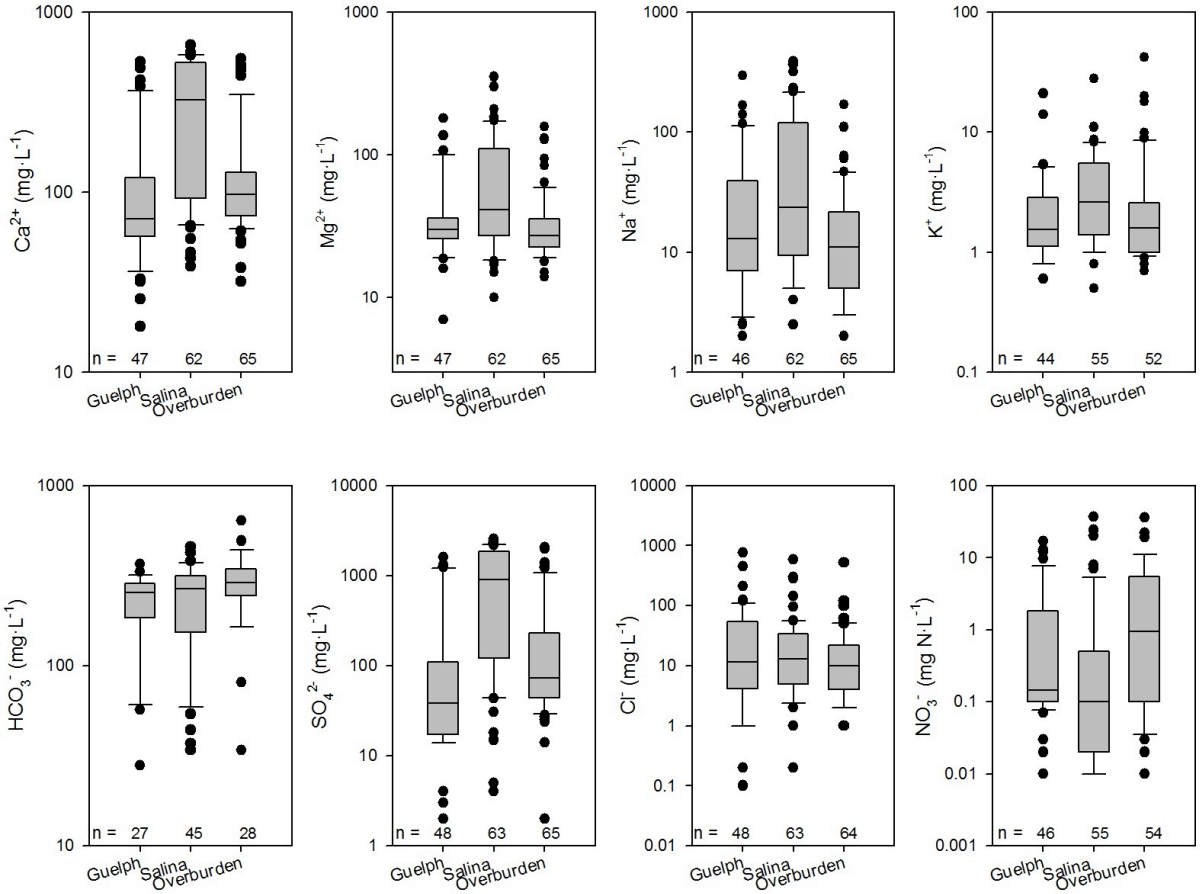

Figure 2.5 A geochemical comparison between the Guelph bedrock formation, the Salina bedrock formation, and the overburden sediments. Data from Singer et al. (2003). Overburden data has been compiled from various sediment types that are all present in the study area: Wentworth till, Port Stanley till, ice-contact sands and gravels, and glacio-fluvial sands and gravels.

2.6 Grand River Geomorphology

The geomorphology of the Grand River channel changes considerably between Cambridge and Brantford. From Cambridge to Paris, it has relatively straight banks and a steep gradient, losing approximately 40m of elevation between Cambridge and Paris (from GIS data accessed from www.grandriver.ca). Between Paris and Brantford it has a shallower gradient, losing 18m of elevation, and a greater meander (Figure 2.1). Along the whole discharge reach there are sections where the river flows directly on bedrock. A significant stretch occurs immediately below Cambridge, and another extends from just below Shep's footbridge into Glen Morris. Along both of these reaches, the Grand River flows directly over the Guelph formation. Farther south, a third stretch occurs just

north of the 403 bridge; here, the river flows over the Salina formation. In terms of groundwater flow-paths, the effects of this incision are unclear but potentially important, depending on other characteristics of the groundwater environment. Groundwater flow within the overburden on the east and west sides of the Grand River may operate under separate gradients. Hydraulic pressure on the riverbanks may be increased in areas lacking considerable fracture networks. This may induce groundwater recharge, or at least retard discharge and increase bank erosion (Scott and Imhof, 2005). Depending on the nature of the fractures in the bedrock formations, discharge could result from several *hotspot* locations, rather than a more diffuse discharge pattern generally conceptualized from more uniform overburden aquifers.

2.7 Study Area Hydrology

Two major tributaries converge with the Grand River in the study area; the Nith River, which joins at Paris, and Whiteman's Creek, which joins several kilometers to the south (Figure 2.1). Several small creeks – for example, Horner's creek in Brantford, and Mill Creek in Cambridge –also converge with the Grand, although these additions are relatively insignificant in terms of the cumulative flow of the Grand River at Brantford. Other smaller tributaries drain local bodies of water fed by groundwater discharge such as wetlands or kettle lakes, or are fed by the confluence of seep discharge higher up the flanks of the moraines. Based on flow gauges operated by the GRCA, baseflow during summer 2011 was approximately 17 m^3s^{-1} in Cambridge and 22 m^3s^{-1} in Brantford; slightly greater than the baseflow values of 15.1 m^3s^{-1} and 20.7 m^3s^{-1} for Cambridge and Brantford, respectively, derived by the GRCA from longer term trends (Figure 2.6).

2.7.1 The Nith River

The Nith is the largest tributary to the Grand River in the study area, and the largest unregulated tributary in the watershed (Cooke, 2006). During baseflow conditions in 2011, flow at the mouth was 2.9 m^3s^{-1}, or 13% of the flow at Brantford. The upper portion of the Nith River catchment drains a portion of the silty till plains that cover large areas of the northern Grand River watershed. Downstream towards the Grand River, the Nith flows through the Paris and Galt moraine complex (Holysh et al., 2001). In terms of bedrock, the Salina formation underlies most of the flow-path of the Nith, and in some areas, like the Grand, the river has incised completely through the overburden and flows directly on top of bedrock.

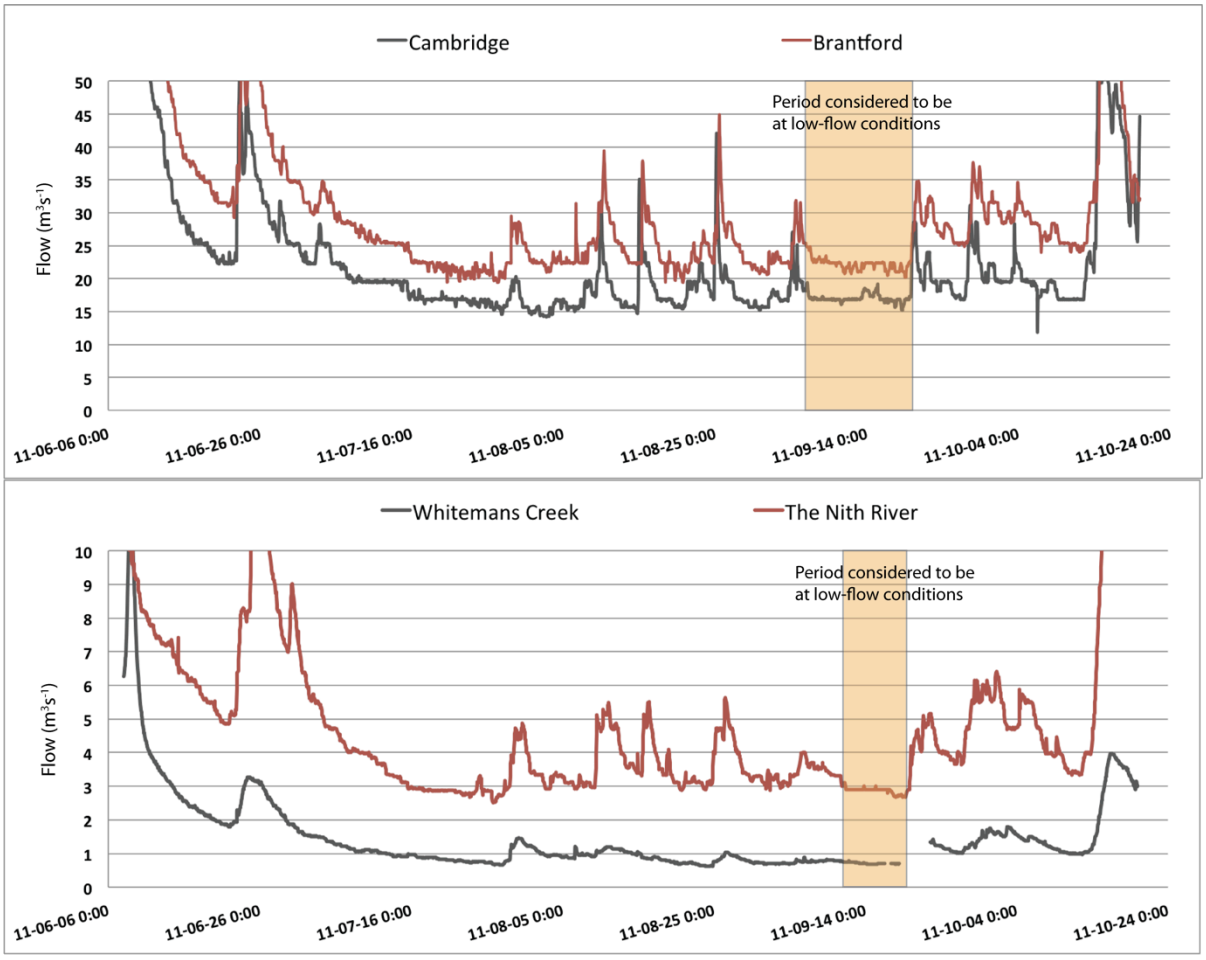

Figure 2.6 Flow (m^3s^{-1}) along the Grand River at Cambridge and Brantford, as well as in Whiteman's Creek at Mt. Vernon and the Nith River at Canning, from the beginning of June until the end of October, 2011. Summer baseflow values were 17 m^3s^{-1} at Cambridge, 22 m^3s^{-1} at Brantford, 2.9 m^3s^{-1} for the Nith River, and 0.69 m^3s^{-1} for Whiteman's Creek. Baseflow occurred near the middle to end of August. The level recorded by Whiteman's Creek datalogger may not be accurate, due to continual problems with debris catching on the datalogger (Schifflet, personal communication). Data from GRCA leveloggers (Available on request from the GRCA).

Water quality in the Nith tends to improve downstream from the silty till plane headwater region towards the Paris/Galt moraine complex. The improvement in water quality has been attributed to contributions from shallow groundwater discharge as the Nith flows through the moraines (Cooke, 2006). Even with improved water quality, however, the Nith tends to add nutrients to the Grand; nitrate concentrations in the Nith are both generally higher and exhibit a greater interquartile range than nitrate in the Grand River (Figure 2.7). As a result of the northern till plains, the Nith has a

considerably greater TSS (Total Suspended Solids) than the Grand, a characteristic that is quite apparent when the rivers meet. The Nith may also add considerable concentrations of phosphorus to the Grand (Cooke, 2006).

2.7.2 Whiteman's Creek

Whiteman's Creek is the second largest tributary in the study area and also enters the Grand River from the west. During summer baseflow conditions in 2011, the flow rate of Whiteman's Creek was 0.69 m^3s^{-1}, or 3% of the Grand River flow at Brantford. Only a small portion of its headwaters drain the till plains that contribute so much sediment to the Nith, and, as a result, Whiteman's Creek is much lower in TSS (Cooke, 2006). Like the Nith, it tends to have higher nitrate concentrations than the Grand River, but, unlike the Nith, generally has considerably lower concentrations of phosphorus. Nitrate concentrations are higher in the winter than the summer, and show a clear annual variation (Figure 2.7).

The origin of the nitrate in Whiteman's Creek is a subject of current research (not by this author). The lower portion of the creek flows over an unconfined, sandy aquifer in a heavily agricultural portion of the watershed (Holysh et al., 2001). Numerous researchers have suggested a large portion of the creek's flow is derived from groundwater discharge, as, during the summer, it has a considerably lower temperature than the Grand - low enough to support brown and rainbow trout populations (www.grandriver.ca). Therefore, from the implied hydraulic connection between the unconfined aquifer and the overlying river, the nitrate may be agricultural in origin.

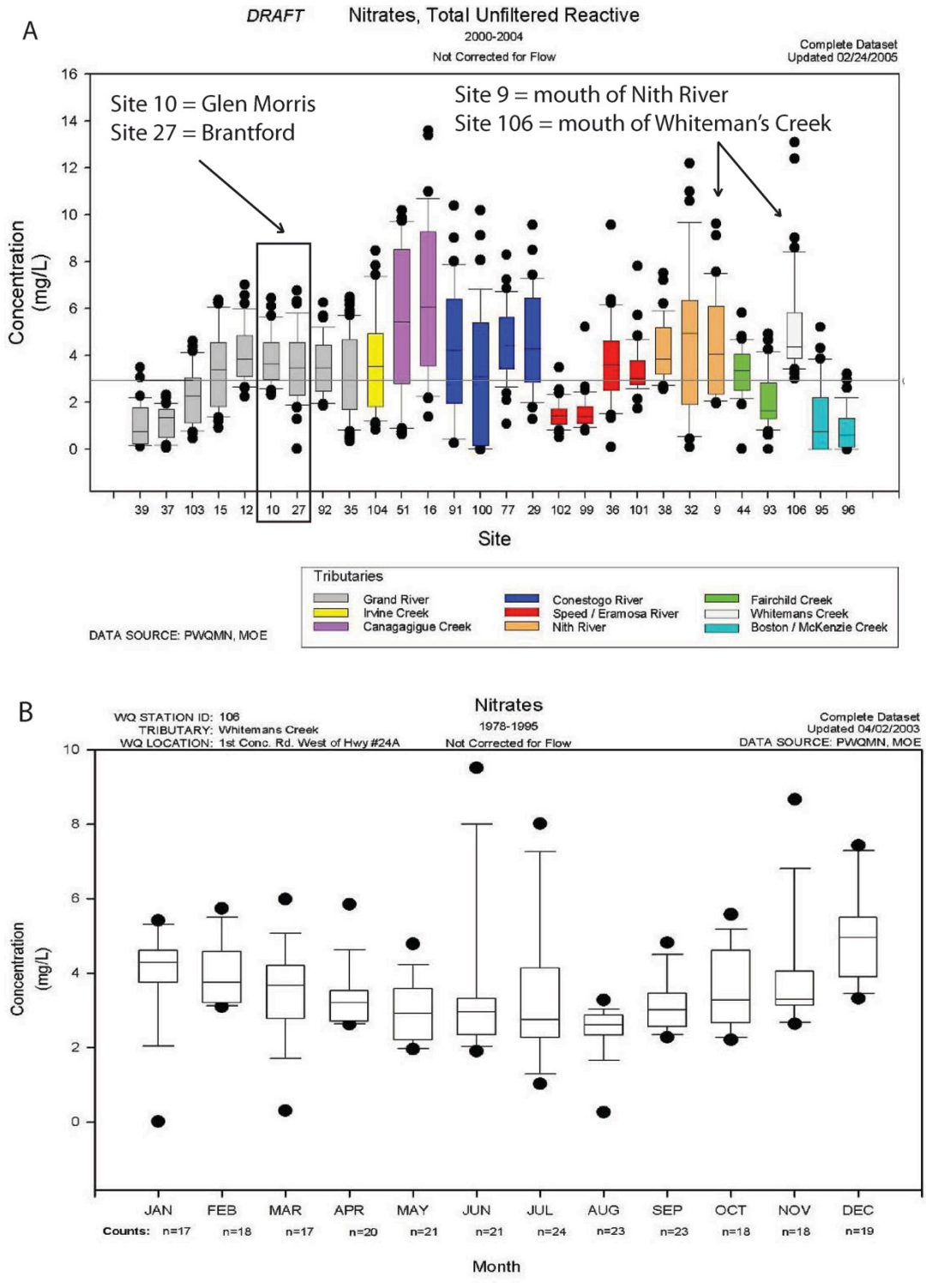

Figure 2.7 A) Boxplots of nitrate concentrations for various rivers in the Grand River watershed. B) Seasonal trends of nitrate concentrations (axis is labeled as mg·L^{-1}, but likely intended to be in mg N·L^{-1}) in Whiteman's Creek. Modified from Cooke (2006).

2.7.3 Other Surface Water Features

The other major surface-water features in the study area reflect weathering patterns and hydrogeologic characteristics of the underlying geology. There are five separate sub-catchments through which the Grand River flows along the discharge reach (Figure 2.1). In part, this is due to the hummocky nature of the moraines in the region; only a short distance away from the river channel surface-water divides are present, and tributaries flow down the distal flanks of these features into other drainage basins such as the Nith River and Fairchild Creek sub-watersheds. Both rivers eventually converge with the Grand, although Fairchild Creek doesn't until downstream of Brantford; i.e., downstream of the discharge reach.

The hummocky nature of the moraines also results in numerous kettle lakes and wetlands in the local sub-watersheds (Karrow, 1987). This reduces the number of local, surface-water tributaries that feed the Grand. Instead, runoff collects in surface depressions, percolates downwards, and recharges local aquifers. Because this groundwater may eventually end up in the Grand River anyways, the hummocky topography acts as a natural flow-control feature, and results in a temporally more consistent flow input to the Grand than the highly variable flow-rates of surface-water tributaries fed by storm events. Thus, the interaction between kettle lakes, wetlands, and groundwater discharge to the Grand could be critical in maintaining healthy flow levels during periods of sustained drought (AquaResource Inc., 2009).

Several dams along the Grand River upstream of the discharge reach act as man-made flow augmentation. During periods of sustained low flow conditions, a considerable portion of the Grand River is attributable to water released from dams upstream (www.grandriver.ca). Other than low flow augmentation, the main purpose of these dams is flood control, and they could also important for the assimilation of wastewater treatment plant effluent (AquaResource Inc., 2009), although that topic is outside the scope of this research.

2.8 Local and Regional Groundwater Flow

To provide a characterization of groundwater flow within the study area, well records from the Ontario MOE (Ministry Of Environment) were used to produce two hydraulic potential maps; a potentiometric surface map from wells screened within the bedrock, and a watertable surface map from wells screened in overburden material (Figure 2.8). Defining all groundwater in the overburden as a single, connected aquifer is a significant over-simplification of the complexity of these highly

heterogeneous aquifer complexes. Other authors have noted that bedrock and overburden wells in the Grand River Watershed do not always conform to the assumption that the bedrock wells are screened in deeper, confined aquifers, while wells screened in the overburden draw from overlying, unconfined systems. Numerous overburden wells are drilled deep into moraine complexes, likely drawing from confined aquifers, and in other areas bedrock is only meters from the surface. Bedrock wells at these locations probably more accurately define the water table (Holysh et al., 2001). In the study area, however, overburden sediments tend to be fairly thick, with the exception of a small portion of the map-sheet directly east of Cambridge. Bedrock wells are generally screened at greater depths than the overburden. Thus, the assumption that bedrock wells define the potentiometric surface and overburden wells define the water table - as much as any set of wells drilled in heterogeneous sediments can be said to define a water table - may be appropriate in this part of the Grand River watershed.

The depth to water-level values used to calculate these hydraulic surfaces is from an MOE database of all the wells drilled in the study area over the last 50 years. These surfaces, then, do not provide an accurate depiction of flow in 2011. Instead, they provide a general, conceptual interpretation of groundwater flow direction in the overburden and underlying bedrock in the study area. Both surfaces have been drawn so that they interact with river stage. Although this is a generally accepted practice for unconfined aquifers and water table surfaces, the underlying confined aquifers may or may not be hydraulically connected to the river channel.

Both surfaces show the same general features, with greatest hydraulic potential northwest of the Grand River and the lowest potential to the southeast, near Brantford. Along the western bank of the Grand, the contours of hydraulic potential on both maps more or less parallel the river channel, suggesting groundwater flow to, and eventual discharge at, the river. These contours do not follow the surface-water divides indicated by the overlying sub-catchment outlines. Therefore, even while surface-water catchments quite close to the Grand drain away from the river, the dominant direction of underlying groundwater flow is still towards the river. West of the Grand River, the overburden wells show a greater topographic influence then the bedrock wells, in good agreement with most conceptualized models of the effects of topography on hierarchical groundwater flow-systems (Freeze and Witherspoon, 1967).

Along the eastern bank of the Grand, the maps suggest that the flow behaviour of the overburden and bedrock aquifers diverge. On the watertable map, the topographic influence of the Paris/Galt

moraine complex is clear; flow lines near the Grand River channel are to the south and west, while further east, flow lines are to the south and east - clearly following the overlying topography of the moraines. Directly adjacent to the Grand River, the overburden aquifer system flows towards the river channel, while a short distance farther east, groundwater appears to predominately flow south and southeast. South of Glen Morris, hydraulic potential declines as moraine topography becomes more subdued. The potentiometric map shows less topographic influence, and suggests that the deeper flow-system mainly moves south and east, with a minimal component west towards the river. Although both maps show that groundwater flow does not necessarily follow surface-water divides, there is better agreement with overlying drainage patterns here than in the western portion of the study area. The most obvious contradiction of this is illustrated on the watertable map just southeast of Glen Morris. Flow-lines here cross the surface-water divide to converge with the Grand River.

Figure 2.9 shows the results of a particle-tracking model developed by the GRCA that illustrates to which sub-watershed areas of groundwater recharge end up discharging at. Based on the results, there are several areas in the Lower Nith and Fairchild creek watersheds that cross surface water boundaries and discharge directly into the Grand River. Generally, the particle tracking model agrees with the maps discussed above; groundwater discharges from the west bank (below the Nith sub-watershed) to the Grand, while groundwater along the east bank mimics surface water divides and flows into the Fairchild creek watershed. The cross section *A to A'*, shown in figure 2.9, suggests that even local recharge areas may follow flow paths deep into bedrock aquifers before discharging to the Grand River; this is contrary to the conclusions of other authors, who summarize that the Paris and Galt moraines supply the majority of the groundwater to the river systems in the area (Cooke, 2006; Scott and Imhof, 2005).

The total amount of groundwater that discharges to the Grand River flow is also the subject of some debate. Previous researchers, based on sequential stream-gauge mass balances or modeling techniques, suggest that up to 25% of the streamflow at Brantford may be from groundwater (Scott and Imhof, 2005). A quick calculation from the streamflow gauges in 2011 shows that, at Brantford, 22 m^3s^{-1} is a reasonable baseflow rate (Figure 2.6). Of this baseflow, 2.9 m^3s^{-1} comes from the Nith and 0.69 m^3s^{-1} comes from Whiteman's Creek. As the flow at Cambridge is 17 m^3s^{-1}, only 1.41 m^3s^{-1}, or 6.4% of flow at Brantford, remains as possible contributions from all other sources between Cambridge and Brantford. This does not account for river flow lost to adjacent aquifers a recharge, although both maps in figure 2.8 suggest this component would be minimal.

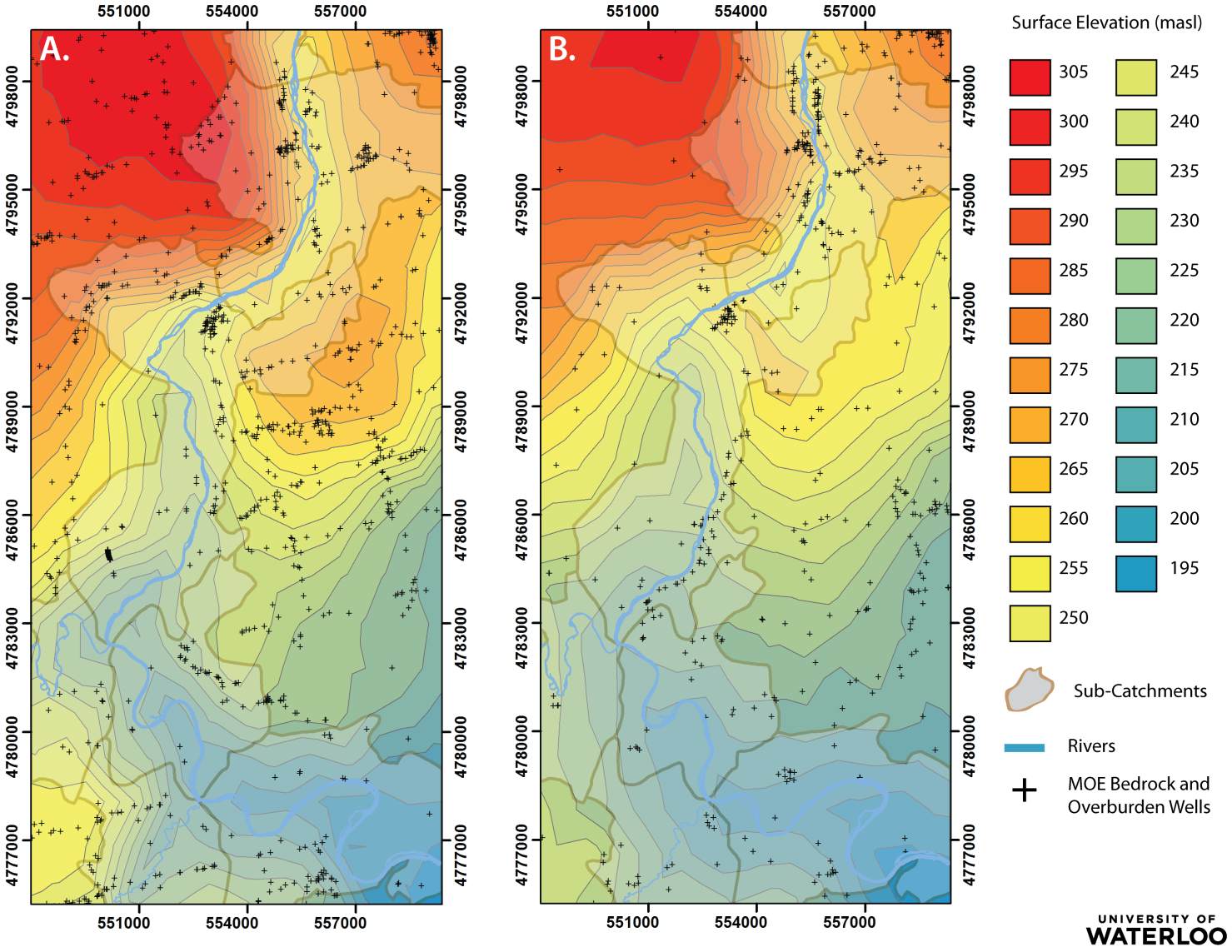

Figure 2.8 Maps of potentiometric surfaces from wells screened in the overburden sediments (A) and bedrock formations (B).

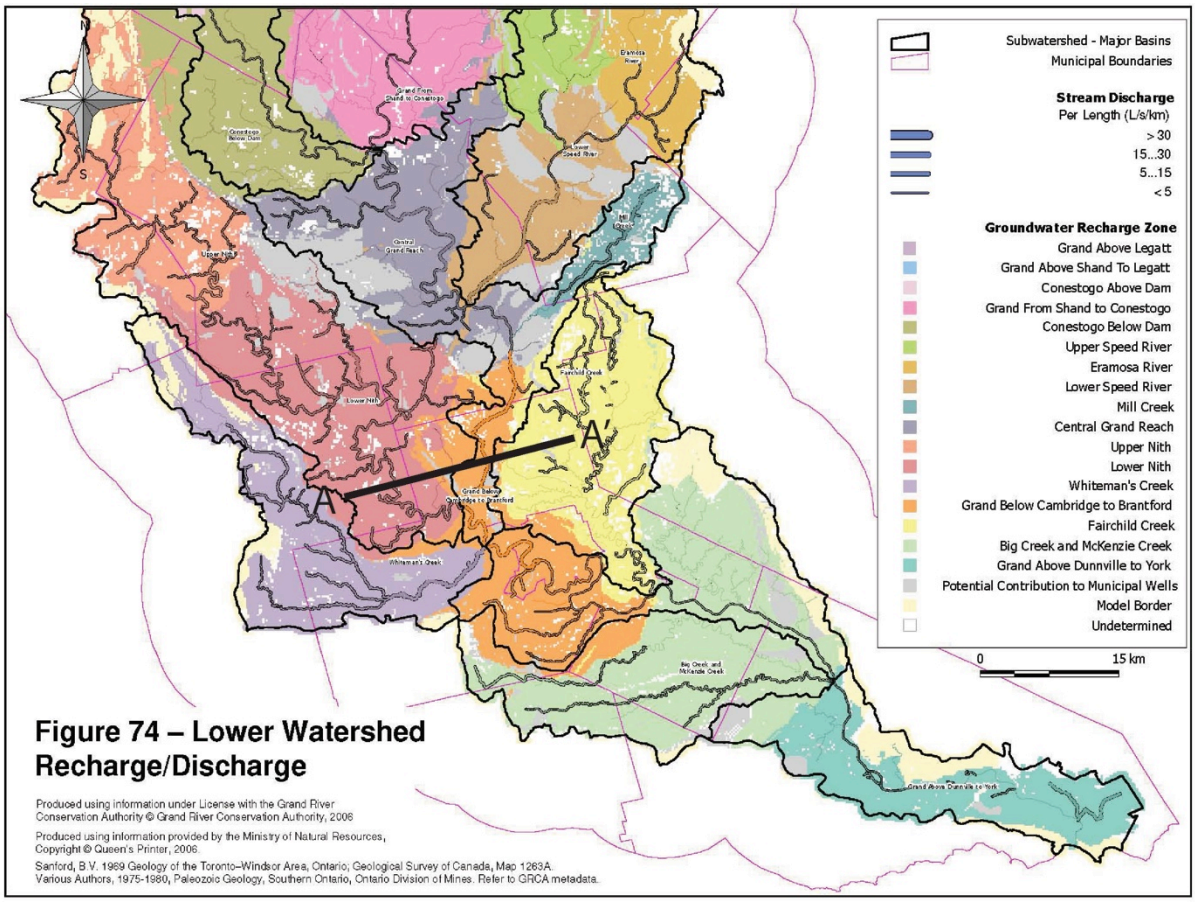

Figure 2.9 Groundwater recharge and discharge areas in the lower half of the Grand River watershed from a particle tracking model. In the study area, precipitation that falls on the lower reaches of the Nith Sub-watershed can recharge groundwater pathways that flow directly to the Grand River rather than the Nith (observe area directly above the A – A' cross-section). This is in good agreement with the surface maps produced in figure 2.8. The same occurs in the lower areas of Whiteman's Creek sub-watershed, and in small portions of the Fairchild Creek sub-watershed just north of Brantford. From AquaResource Inc. (2009).

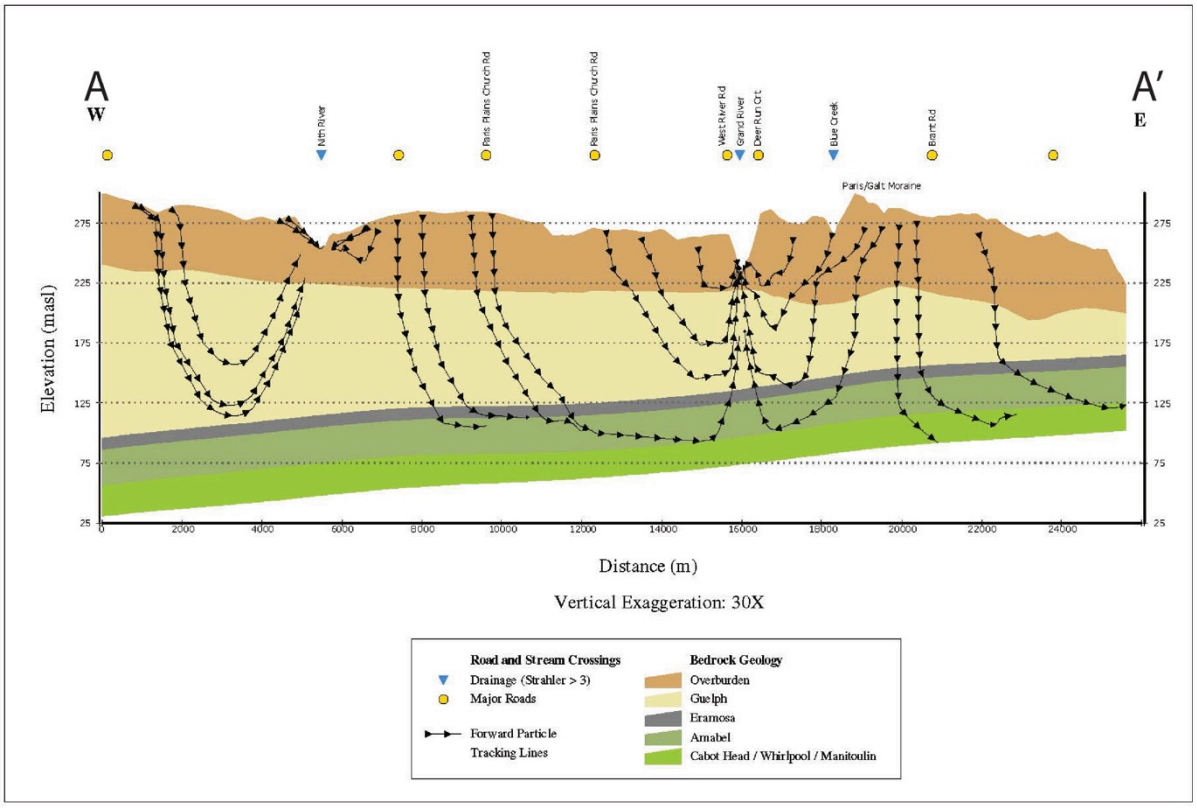

Figure 2.10 Cross-section A to A' on figure 2.9. The particle tracking model suggests that discharge to the riverbed comes predominately from flow-paths that have moved deep into the bedrock, whereas riverbank discharge is predominately from relatively short, local flow-paths. From AquaResource Inc. (2009).

2.9 Waste Water Treatment Plant Effluent in the Grand

There are 30 WWTPs along the Grand River and its tributaries (Table 2.2, adapted from Anderson 2012). The highest capacity plants treat waste from Waterloo, Kitchener, Cambridge, Guelph, and Brantford. Of these five treatment plants, only effluent from Brantford discharges to the Grand downstream of the Brantford municipal water intake. The input of nitrate from these upstream WWTP's is considerable, with a combined flow rate of 2.26 m^3s^{-1}, comparable to that of the Nith River, and a mean nitrate concentration of 10.4 mg $N \cdot L^{-1}$. Several WWTPs, the Kitchener plant specifically, discharge nitrogen as ammonia rather than nitrate. Upon entering the Grand this ammonia is either volatilized to ammonia gas and lost to the atmosphere, or oxidized to nitrate, further increasing concentrations from upstream of the discharge reach.

Table 2.2 Current* flow and geochemistry of select WWTP's in the Grand River Watershed

WWTP	Flow (m^3d^{-1})	cBOD ($mg \cdot L^{-1}$)			TP ($mg \cdot L^{-1}$)			NH_3 ($mg\ N \cdot L^{-1}$)			NO_3 ($mg\ N \cdot L^{-1}$)		
		Min	Med	Max	Min	Med	Max	Min	Med	Max	Min	Med	Max
Brantford	36,957	2.0	7.5	31.0	0.26	0.43	0.72	0.1	2.57	11.68	0.1	4.2	13.2
Galt	35,635	1.0	2.0	9.8	0.17	0.31	0.93	0.1	0.21	18.9	0.5	18.0	24.6
Guelph	46,214	2.0	2.0	4.0	0.04	0.16	0.63	0.01	0.2	4.8	14.4	20.6	31.1
Kitchener	64,329	2.0	6.0	20.0	0.23	0.55	1.68	12.8	21.7	38.7	0.1	1.2	2.4
Paris	3,310	1.0	3.0	27.0	0.30	0.60	0.94	0.1	0.25	13.3	0.1	6.5	19.1
Waterloo	45,994	2.0	4.5	32.8	0.17	0.44	2.06	0.23	7.83	29.3	0.1	7.5	23.5

*Data from Anderson (2012).

Chapter 3 – Background Theory on Methods

3.1 Groundwater Surface-Water Interactions Along the Grand River

Historically, research on groundwater and surface-water systems has treated each as a separate, isolated entity (Brunke and Gonser, 1997; Boulton, 1998; Sophocleous, 2002; Stonestrom and Constantz, 2003). More recently, their hydraulic connection has become widely acknowledged, and the general conceptual model has been modified to view each as part of a whole, integrated system. This initially led to the definitions of gaining and loosing streams, but there is widespread agreement that this too is an oversimplification, and other types of interactions are increasingly conceptualized; flow-through reaches and underflow conditions are two such examples (Larkin and sharp, 1992; Woessner, 2000).

The concept of a hyporheic zone has similarly evolved from its biological roots (White, 1993; Brunke and Gonser, 1997). Today, it is loosely defined as a chemically and biologically distinct, transitory ecotone that exists within a streambed where the characteristics of a surface water environment transition towards those of a groundwater system (Bencala, 2000; Sophocleous, 2002). The actual physical boundaries of the hyporheic zone are difficult to delineate, as these characteristics tend to be both spatially and temporally variable (Boulton et al., 1998).

There are at least two differing, more specific definitions of the hyporheic zone. Hydrogeologists tend to define the hyporheic zone as a mixing zone defined by the spatial boundaries between upwelling groundwater and downwelling surface water (Sophocleous, 2002). A second definition, perhaps more familiar to hydrologists and limnologists is (from Harvey and Bencala, 1993):

"A subsurface flow-path along which water 'recently' from the stream will mix with subsurface water to 'soon' return to the stream".

In this interpretation, surface water is not downwelling in the sense that it is providing recharge to aquifers adjacent to the river channel, but taking the most energy efficient route downstream. This is derived from extensive literature documenting how riverbed topography – specifically riffle and pool sequences – cause stream-water to take alternate flow-paths downstream (Harvey and Wagner, 2000; Storey et al., 2003). It is not groundwater in the sense that it did not come from beneath the water table, and has been heavily influenced by in-stream processes (White, 1993). This is the conceptual definition of a hyporheic zone used in this study. Because this research is focused on the geochemical implications of groundwater discharge in the Grand River, it is necessary to be able to clearly

distinguish groundwater discharge through the riverbed from surface water flowing through the streambed.

The larger conceptual model of groundwater/surface-water interactions under which this research was conducted can be described as follows: groundwater flow systems form a hierarchical 'nest' of spatial scales, from local, to intermediate, to regional flow systems (Freeze and Witherspoon, 1967). Groundwater flowing under all three spatial scales can interact with the Grand River. Interactions include gaining reaches, whereby groundwater hydraulic gradients are parallel to the river and groundwater flowlines enter the river when the hydraulic head is greater in the aquifer than it is in the river (Sophocleous, 2002). Losing reaches occur when hydraulic gradients are parallel to the river channel, but hydraulic head in the aquifer is lower than that of the river stage (Sophocleous, 2002). Flow-through reaches occur when hydraulic gradients are parallel to the river, and the hydraulic head is greater than the river stage on one side, but lower than the river stage on the other. Thus the river gains groundwater along one vector of the flow system while losing stream-flow along another (Woessner, 2000). 'Underflow' or 'parallel-flow' occurs when hydraulic gradients are perpendicular to the river channel and groundwater flow is therefore parallel, but below, the streambed (Larkin and Sharp, 1992; Woessner, 2000). Although following a flow-line similar to hyporheic zone stream-water, this groundwater will be chemically distinct from river water.

These flow types are essentially end-members on a multi-dimensional spectrum that are easily combined. As an example, flow in one reach could have a considerable parallel flow component while under a hydraulic gradient higher than the river stage – i.e., also discharging to the river. As another, hydraulic head along a flow-through reach may not be perfectly parallel to the river. Hydraulic head may be orientated such that there is a component of parallel flow to the groundwater as well.

There are several ways in which this conceptual flow model is specifically applied to the Grand River. First, overburden sediments tend to be thick in the area due to the presence of the Paris, Galt, and Kame moraines, and topography tends to be hummocky throughout the region (Holysh et al., 2001; AquaResource Inc., 2009). Thus, it is assumed that local flow systems are completely contained within the overburden with relatively short flow-paths (less than one km). Intermediate flow systems may or may not enter the underlying bedrock; this depends on the hydraulic connectivity between the bedrock and the overburden, which may in turn depend on the extent and thickness of the Port Stanley till in the region (Blackport Hydrogeologic Inc., 2009). Regional flow

systems are older and deeper flow-paths from recharge areas up to tens of kilometers way, which have been constrained almost entirely to the underlying bedrock aquifers for a considerable time period.

Second, as previously discussed in Chapter two, in many areas of the discharge reach the Grand has incised completely through the overburden sediments (Figure 3.1). This separates local - and possibly intermediate - scale flow systems on one side of the river from those on the other, and it is assumed that, in these areas, local and intermediate flow systems discharge along the banks of the Grand whereas only intermediate and regional flow systems discharge beneath the river. In other locations, overburden material still exists below the river channel (Figure 3.1). The study areas of Herrera (2012) are two examples. Monitoring wells were drilled, one on either side of the river, in uplands quite close to the riparian zone, in an effort to sample nitrate concentrations from adjacent crop fields (Figure 3.2). The well on the east side of the river was drilled approximately 10m deeper than the riverbed without encountering bedrock (Figure 3.3). In areas such as these, there may still be considerable overburden discharge directly to the riverbed.

Third, there is a clear change in river morphology between the reach from Cambridge to Paris and the reach from Paris down to Brantford (see section 2.6 for details). Due to these differences, it is assumed that parallel or under-flow, if occurring, would be a greater component of groundwater flow between Cambridge and Paris than between Paris and Brantford. Conversely, one expects flow-through reaches to be more common between Paris and Brantford than upriver.

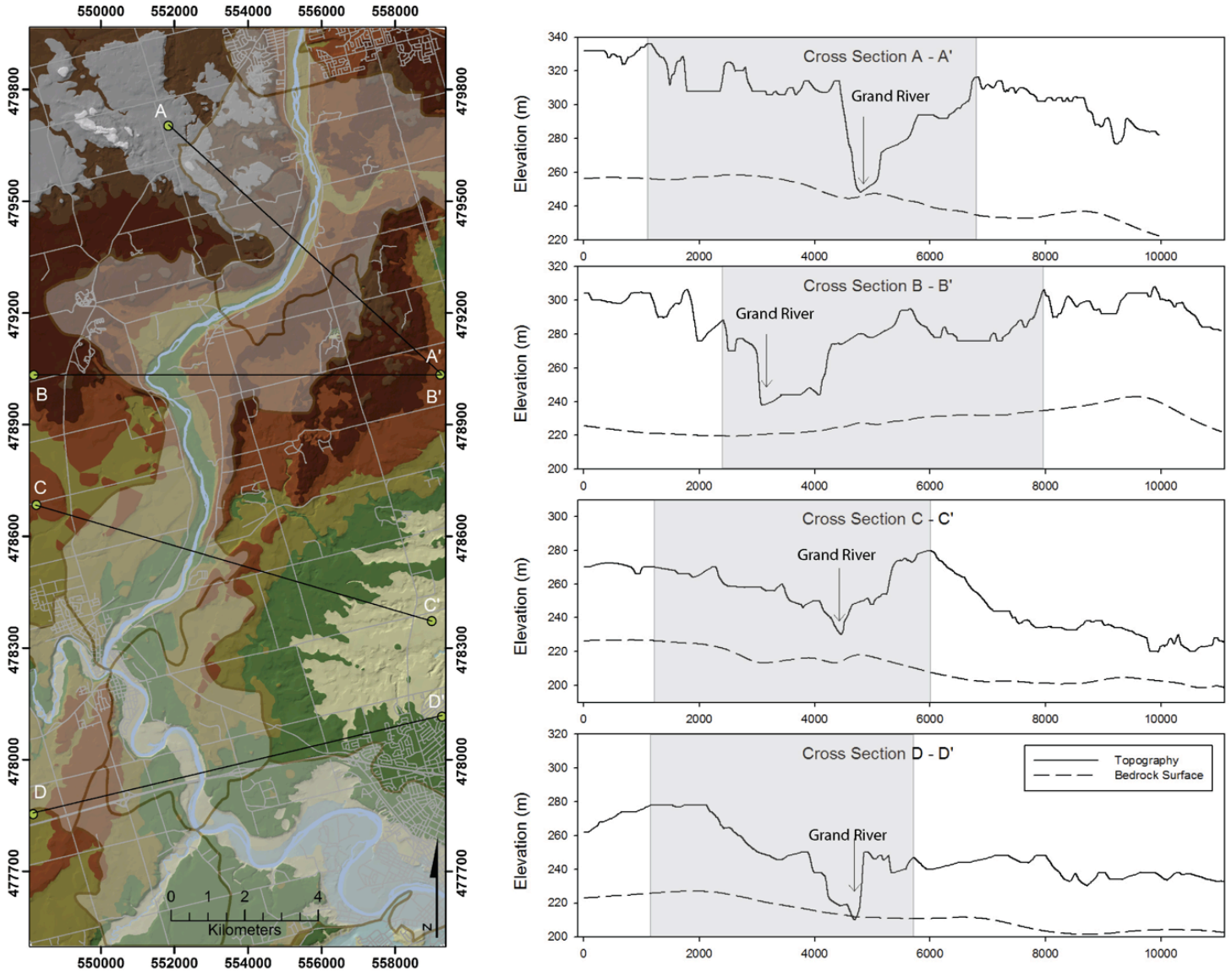

Figure 3.1 Elevation plan map and topographic and bedrock surface cross-sections through the discharge reach. The grey shaded areas on the cross-sections illustrate where the surface water divides are present on the plan map.

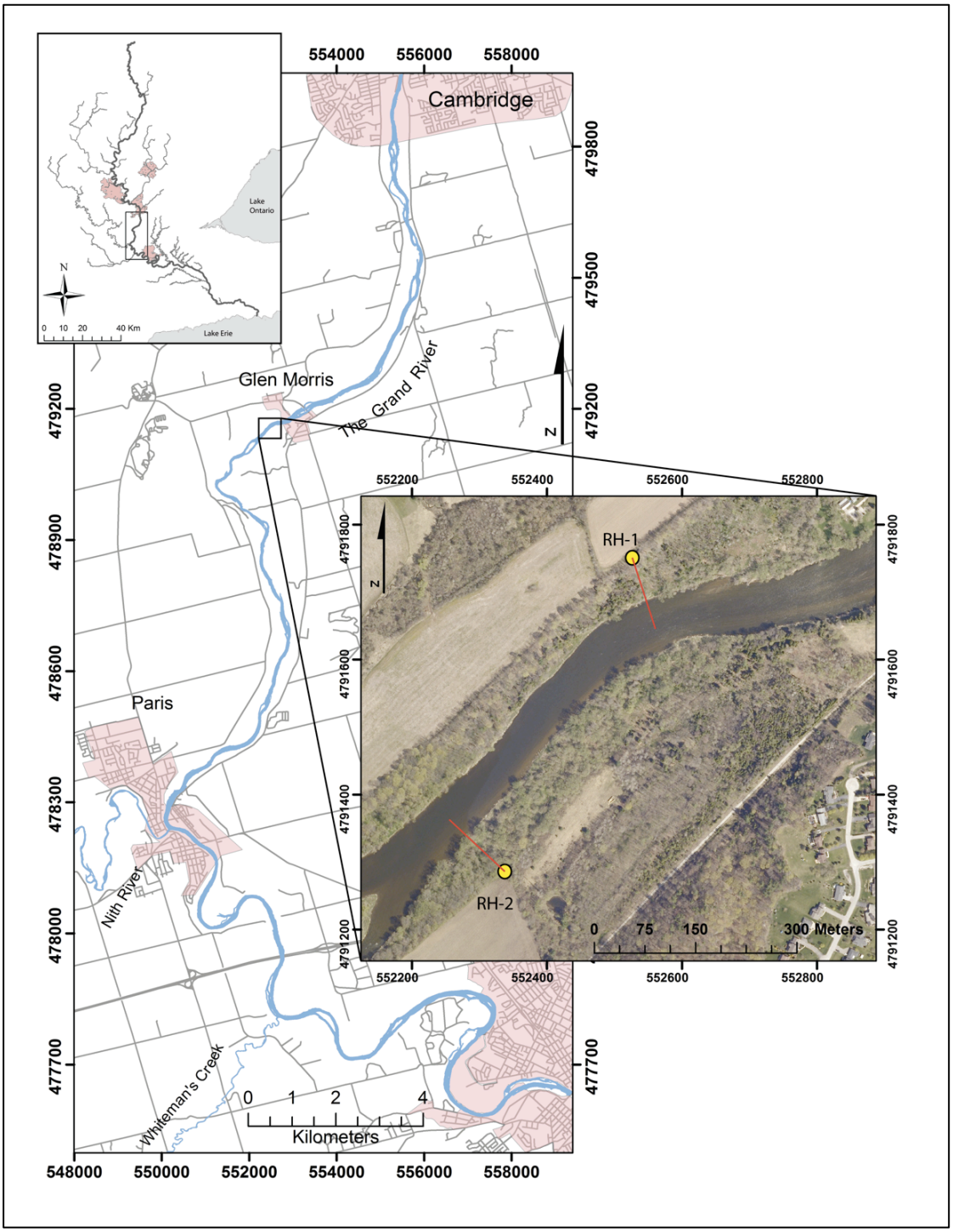

Figure 3.2 Study site of Herrera (2012) where two monitoring wells, RH-1 and RH-2, were drilled adjacent to riparian zones along the Grand River. The red lines from boreholes represent the cross-sections in figures 3.2 and 3.3.

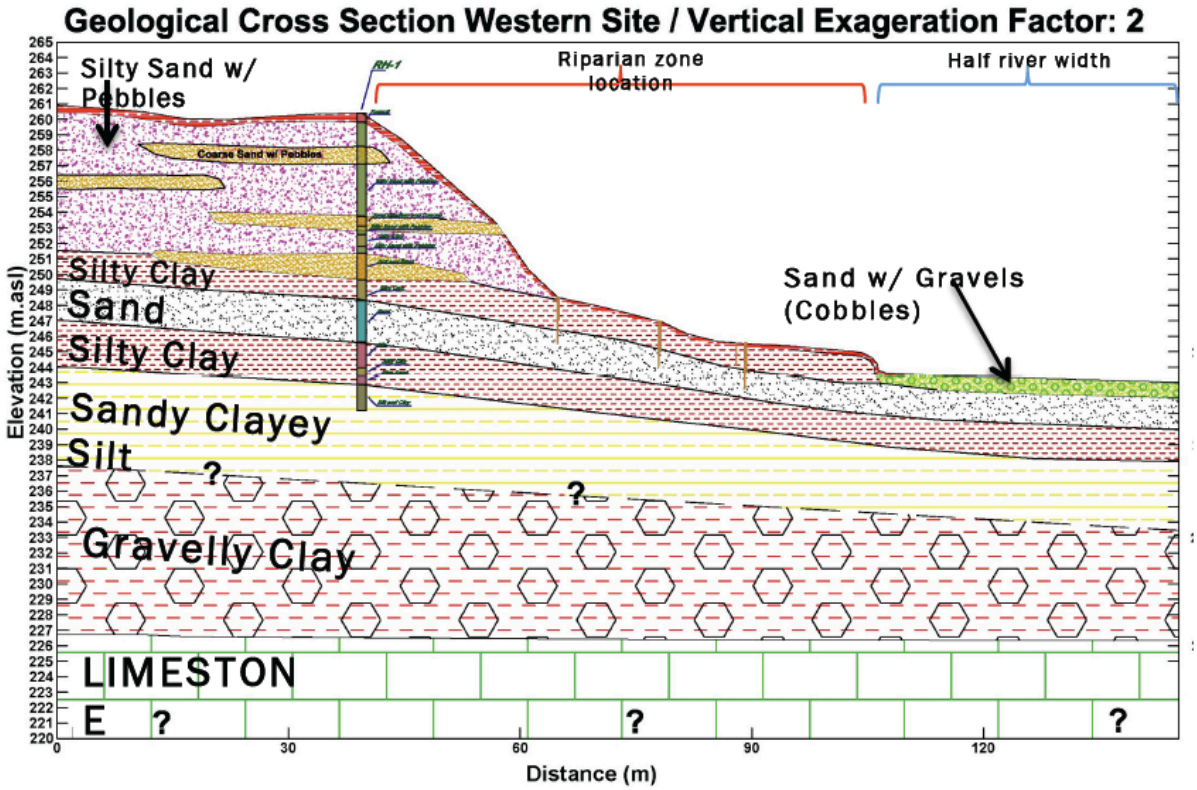

Figure 3.3 Geological cross-section of RH-1. As the well was only drilled a meter or two below the riverbed, further extrapolation is uncertain. Depth to the bedrock unit is based on modeled overburden thicknesses from Holysh et al. (2001), completed at a watershed scale. From Herrera (2012).

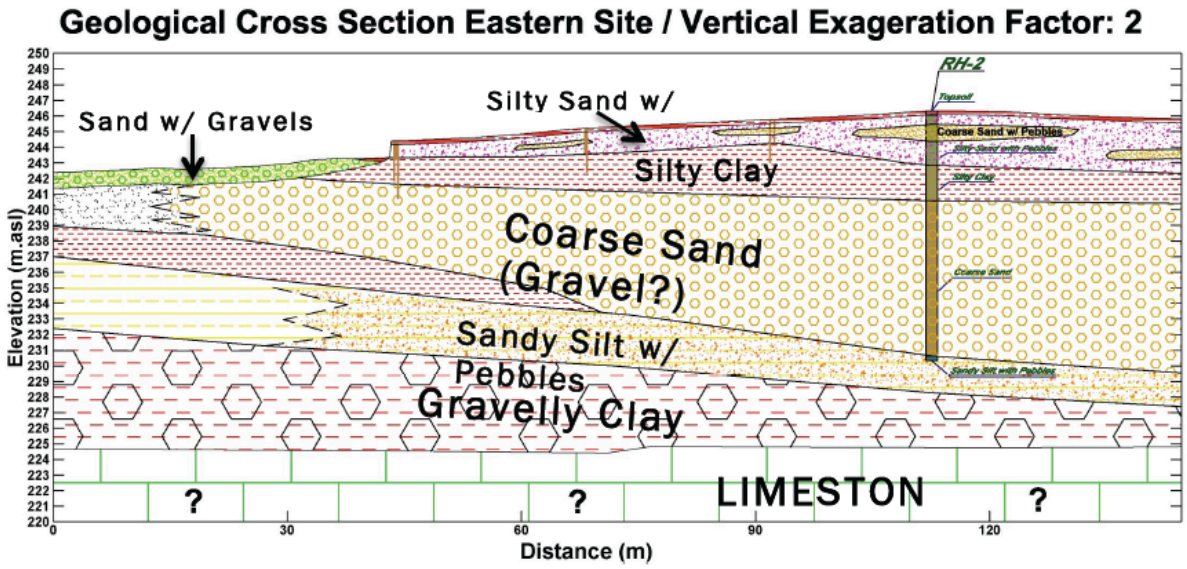

Figure 3.4 Geological cross-section of RH-2. As the well was drilled well below the riverbed and supports the assumation that at least 10m of overburden material is present below the Grand River, discharge from overburden aquifers may be occurring directly to the riverbed. From Herrera (2012).

3.2 Introduction to the Temperature Method

The fundamental utility of using temperature and heat flow as a tracer for groundwater surface-water interactions is that the temperature of groundwater is relatively constant, whereas the temperature of surface-water bodies fluctuate on diurnal and annual timescales (Conant, 2004). During optimal conditions, this results in clear temperature contrasts between the two. The temporal and spatial patterns of simultaneous heat transfers from the groundwater to surface water and vice versa allows researchers to distinguish one from the other (Stonestrom and Constantz, 2003). The climate in southern Ontario allows for two fairly long field seasons in which groundwater discharge has a distinct temperature relative to surface water: during winter, it is significantly warmer, and during summer, significantly cooler. One advantage of this research locating groundwater discharge compared to other studies was that it was already known - through previous incremental stream-flow, mass balance approaches, and particle tracking studies – that groundwater discharges along the Grand from Cambridge down to Brantford (Holysh et al., 2001; LESPRTT, 2008; AquaResource Inc., 2009; Colautti, 2010; Herrera, 2012). Equipped with this knowledge, the first objective of this research, then, was to specify *where* the groundwater was discharging, rather than trying to determine if it was discharging in the first place. Thus, the employed reconnaissance method needed to resolve a fundamental issue of groundwater discharge and scale; how does one locate specific points of discharge, to allow for geochemical sampling, along a 40-kilometer, 50-80 meter wide river? Of the numerous methods to locate groundwater discharge reviewed in the literature, using temperature and heat-flow as a tracer seemed the most appropriate choice for tackling this issue of scale.

The Grand River presents several complications other than the scale issue that also factored into the decision to use temperature and heat flow. One is that the riverbed alternates between bedrock and cobble alluvium. Complicated instrumentation of such a riverbed is not practical; it is very difficult, and requires considerable effort, to insert anything into the riverbed. The Grand River discharge reach is also one of the most frequently used areas for public recreation in southern Ontario (Scott and Imhof, 2005). Instrumentation cannot be left in the riverbed, as it poses a hazard to recreational users and presents a liability to the research project, in terms of cost, if anything is stolen. Not being able to leave permanent instrumentation in the river severely restricts the research methods available, and temperature and heat was left as an obvious choice. More specifically, three temperature methods were selected: The FLIR survey, drag probe surveys, and temperature profiling. The FLIR survey was

utilized to locate discharge along the banks of the Grand, while the other two methods were utilized to locate discharge directly through the streambed.

3.2.1 Bank Discharge - The FLIR Survey

FLIR (Forward Looking InfraRed) Systems, Inc., is a company that manufactures thermal imaging cameras. These are cameras capable of detecting infrared radiation emitted from the surface objects, and processing that into an image (Figure 3.5). The radiation emitted from objects, and ultimately the resulting image, depends on their thermal properties, which vary considerably from material to material. These contrasts can be used to identify objects that are not visible to the naked eye. For this research, the FLIR camera was used to locate and categorize groundwater discharging from the banks of the Grand River.

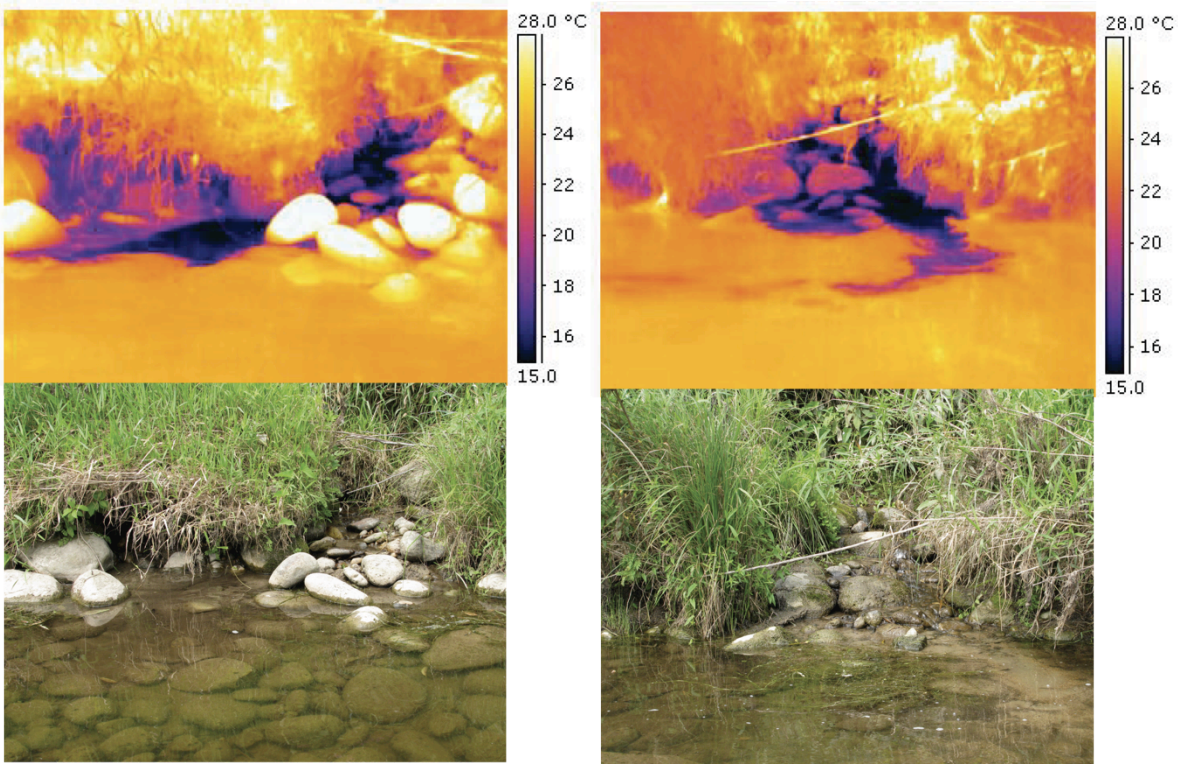

Figure 3.5 Examples of FLIR photos and visual equivalents. These are close-up shots, taken from several meters away where the discharge is also clearly evident in the visual photos. Other discharge types are not easily seen in visual photos.

Groundwater in the study area ranges, on annual timescales, between 8.01°C and 9.33°C (Herrera, 2012). Water also has a high specific heat capacity; 4.18 $J \cdot g^{-1}K^{-1}$ of heat energy is needed to raise the

temperature of one gram of water by one degree Kelvin (or Celsius). In contrast, other bank materials – leaves, rocks, wood, bare earth, and man-made materials – are both exposed to oscillations in ambient temperatures and tend to have lower, more variable heat capacities (Conant, personal communication). Therefore, during hot summer days (or cold winter days) groundwater will have a unique temperature relative to other objects along the banks, and this temperature contrast can be used to identify seeps not visible to the eye. While surface-water bodies will also have high heat capacities, they are not thermally insulated from either ambient temperature conditions or solar radiation by the subsurface environment, and so these features tend to have temperatures similar to other bank materials. In addition to locating seeps, therefore, the FLIR survey can also be used to distinguish between tributaries fed by groundwater or surface water sources.

3.2.2 Temperature and Heat Exchange in the Streambed – Drag Probe Surveys and Temperature Profiling

Temperature and heat flow as a tracer in the subsurface began as a tool to estimate groundwater flow velocity (Suzuki, 1960; Stallman, 1963). More recently, numerous researchers have used heat flow and spatial and temporal temperature variations to examine groundwater/surface-water interactions in streambeds (Stonestrom and Constantz, 2003; Becker et al., 2004; Conant, 2004; Schmidt et al., 2007).

Heat is transferred through streambed sediments by four mechanisms: conduction, advection, convection, and radiation (Stonestrom and Constantz, 2003). Radiative heat transfers occur when solar radiation is adsorbed by the overlying stream and streambed materials. Heat conduction is a diffusive process, transferring thermal energy along temperature gradients. Both convection and advection occur as moving water carries heat energy; the former occurs as stream water flows downstream, and the latter as fluid flows through the streambed sediments (Constantz, 2008). These four processes of heat transfer produce spatially and temporally heterogeneous patterns of temperature within streambed sediments that can be used to qualitatively or quantitatively describe groundwater/surface-water interactions.

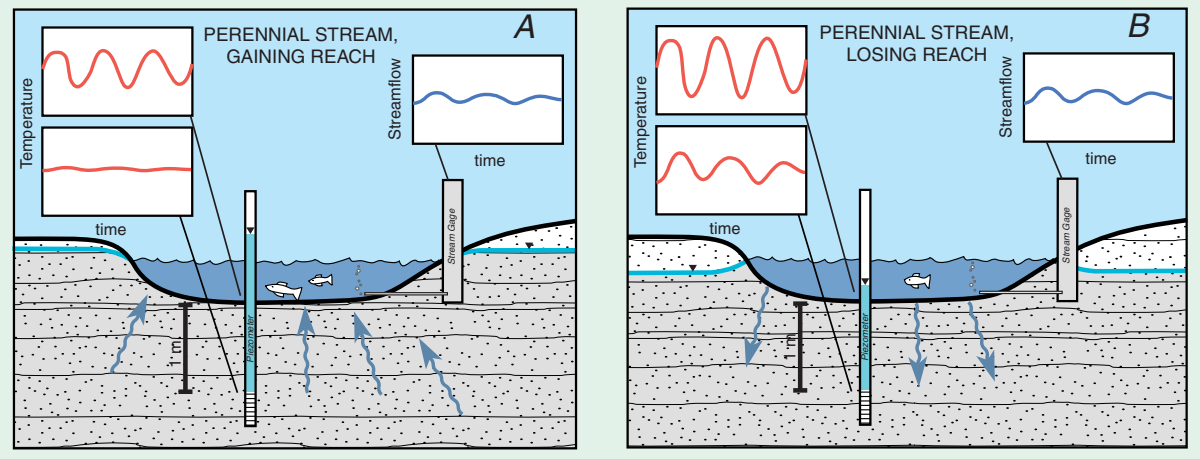

Figure 3.6 Type examples of temperatures in the streambed in a gaining (A) and loosing (B) reach of a perennial stream. In a gaining stream, the vertical groundwater flux dampens downward heat conduction from the overlying stream. In a loosing stream, temperature fluctuations in the streambed are more exaggerated, without the moderating influence of groundwater discharge. From Stonestrom and Constantz (2003).

The value of using temperature and heat as a tracer is that unique, predictable temperature patterns within a streambed are indicative of various types of groundwater/surface-water interactions (Constantz, 2008). Stonestrom and Constantz (2003), give two type examples of these interactions and describe what the temperature signal measured in the subsurface looks like for each (Figure 3.3). Due to the objectives of this research, this study is mainly concerned with type example A; in a gaining stream, temperature within the streambed is a function of downward heat conduction from the overlying stream and upward heat advection from the underlying aquifer. Conduction from the streambed will exhibit a diurnal variation due to daily streambed temperature fluctuations. Upward advection will be constant, given a consistent vertical groundwater flux, as the temperature of groundwater exhibits minimal variation on daily timescales (Schmidt et al., 2007). Thus, the temperature of groundwater moving up through the streambed acts to dampen temperature fluctuations caused by heat conducting down from the overlying stream. The magnitude of the dampening is a function of how deep in the subsurface the parameter is measured and the vertical flux rate of the groundwater discharge (Blasch, USGS paper 1703). The actual temperature measured will be a function, then, of the rate at which groundwater is discharging to the river – itself a function of vertical gradients and permeability of the streambed sediments. Conant (2004), expanded upon this idea by mapping the temperature at 20 cm depth in the streambed, on a 1x2m grid scale, along a 60m long stretch of the Pine River, Ontario, Canada. It was shown that the spatial variability in streambed

temperatures, across the 60m reach, could be used to infer rates of groundwater flux to the river through an empirical equation relating temperature measurements to actual groundwater fluxes, measured through slug tests and head height measurements of 34 mini-piezometers installed throughout the reach.

Schmidt et al. (2007), in a continuation of the methodology of Conant (2004), produced an equation that directly relates temperature in the riverbed to a vertical groundwater flux. Equation 3.1 from Schmidt et al. (2007), is the Turcotte and Schubert (1982) analytical solution to the one-dimensional steady-state heat-diffusion-advection equation:

$$q_z = -\frac{K_{fs}}{\rho_f C_f Z} \ln \frac{T_{(z)} - T_L}{T_O - T_L} \quad (3.1)$$

Where:

q_z = Specific Darcy flux ($m \cdot s^{-1}$)

K_{fs} = Geometric mean of the thermal conductivity of the solid-fluid system ($J \cdot s^{-1} m^{-1} K^{-1}$)

ρ_f = Density of the fluid ($kg \cdot m^{-3}$)

C_f = Heat capacity of the fluid ($J \cdot kg^{-1} K^{-1}$)

z = Depth into the riverbed the probe is driven (m)

$T_{(z)}$ = Temperature at depth (z) (°C)

T_L = Temperature at the aquifer bottom (°C)

T_O = Temperature at the riverbed/river interface (°C)

$$K_{fs} = K_s^{(1-n)} + K_f^n \quad (3.2)$$

Where:

$K_s^{(1-n)}$ = Thermal conductivity of solids ($J \cdot s^{-1} m^{-1} K^{-1}$)

K_f^n = Thermal conductivity of the water ($J \cdot s^{-1} m^{-1} K^{-1}$)

n = porosity of the subsurface (-)

Using equation 3.1, it is possible to gain estimates of the vertical groundwater flux through the riverbed using only two temperature measurements, T_Z and T_O. This estimate is based on two

assumptions that may not be valid for all discharge locations; 1) flow at depth is at steady-state, and 2) the groundwater flux is entirely vertical (Schmidt et al., 2007).

Of the two temperature measurements, obtaining an accurate estimate of T_O is more difficult. This is because the profiling takes time; surface water temperatures can oscillate considerably on daily time-scales, so if the survey takes longer than this, T_O must be approximated by averaging the surface-water temperatures during the time the profiling takes place. As long as there are no long-term trends evident in the surface water temperature fluctuations, the average temperature will be a reasonable approximation of T_O (Schmidt et al., 2007).

One of the more innovative qualities of this equation is that in calculating a flux estimate, thermal conductivity is utilized rather than hydraulic conductivity. In any subsurface environment, hydraulic conductivity is strongly dependant on sediment texture, varies by several orders of magnitude, and is rarely more precisely constrained than one order of magnitude. Thermal conductivity, on the other hand, is only slightly dependent on sediment texture and tends to range between 0.8 and 2.5 $J \cdot s^{-1} m^{-1} K^{-1}$ (Figure 3.4, Schmidt et al., 2007). This has the potential to greatly increase the precision of vertical groundwater flux estimates.

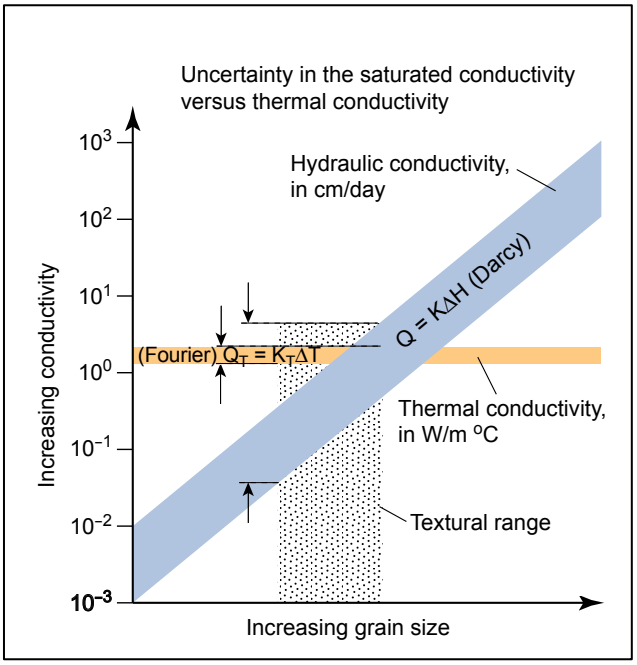

Figure 3.7 The effect of increasing grain size on thermal and hydraulic conductivities. Hydraulic conductivity varies considerably relative to thermal conductivity. From Stonestrom and Constantz (2003).

3.3 Introduction to the Isotopes of Sulfate and Nitrate

Isotopes are atoms, or nuclides, of a given element with the same number of protons but varying numbers of neutrons. Of approximately 2500 known nuclides, 270 are stable; i.e., whose protons or neutrons do not spontaneously undergo radioactive decay to another element (Faure and Mensing, 2005). These stable nuclides, along with several radioactive nuclides with long half-lives, make up the periodic table of elements.

Many elements have more than one naturally occurring isotope. *Environmental isotopes* is a term that refers to the stable and radioactive isotopes of hydrogen, carbon, nitrogen, oxygen, sulfur and phosphorous; the principal elements involved in biogeochemical cycling. These are often used to study the transfer of elements between various reservoirs in these systems (Clark and Fritz, 1997). Part of their usefulness is derived from the fact that, as elements with relatively low mass numbers, the addition of one or more neutrons results in a mass difference large enough to elicit changes in behaviour during physical, chemical, and/or biological reactions.

The whole earth abundance of environmental isotopes are expressed as percentages; e.g., of the four naturally occurring isotopes of sulfur, 95.02% is ^{32}S, 4.212% is ^{34}S, 0.760% is ^{33}S, and a mere 0.0136% is ^{36}S (Canfield, 2001). Specific sulfur compounds will have different abundance ratios of these isotopes, however, due to reactions that continuously occur as sulfur is cycled through the earth system. Due to the difficulty in precisely and accurately determining the absolute abundances of isotopes in any given compound, isotope analyses are routinely expressed as the ratio of the two most abundant isotopes in a sample relative to the ratio of the same two isotopes in a recognized standard (Kendall, 1998). This ratio of ratios, between the sample and the standard, is known as delta notation. Continuing with the example of sulfur above:

$$\delta^{34}S = \left(\frac{\left(\frac{^{34}S}{^{32}S}\right)_{sample}}{\left(\frac{^{34}S}{^{32}S}\right)_{standard}} - 1 \right) x\ 1000 \qquad (3.3)$$

$\delta^{34}S$ is the 'delta value' in per mil, ‰, (per mil = parts per thousand), in terms of the standard used. For example, a delta value from equation 3.2 might be recorded as $\delta^{34}S$ = +20.8‰ VCDT; i.e., plus 20.8 per mil relative to the standard Vienna Cañon Diablo Trolite. The delta value is positive, and therefore the sample is enriched in ^{34}S relative to the standard. If a sample has the exact same ratio of $^{34}S/^{32}S$ as the standard (VCDT), then the delta value is zero, and the sample contains the same amount

of ^{34}S as the standard. If the ratio is smaller then that of the standard, then the delta value is negative, or depleted in ^{34}S; the sample has a lower abundance of ^{34}S than the standard.

Chemical compounds that contain sulfur can be thought of as a series of reservoirs through which sulfur, as various isotopes, cycle. The processes by which sulfur moves from one reservoir to another – for example, sulfate from the oxidation of pyrite in sediments (reservoir 1) is ultimately carried to the ocean (reservoir 2) via drainage systems – may cause changes in the isotopic ratios of sulfur within those reservoirs. These changes are called fractionations, and fundamentally occur because of the mass differences between isotopes of a given element. Heavier isotopes form stronger bonds than lighter isotopes (Krouse and Grinenko, 1991). These bonds require a higher energy investment to break, so lighter isotopes tend to react more rapidly than their heavier counterparts. This causes the relative abundance of each isotope to change, both in the substrate undergoing reaction and the product formed. Numerous types of reactions cause isotope fractionations, such as changes of state or inorganic or biologically mediated chemical reactions (Clark and Fritz, 1997). The fractionation of isotopes between a substrate compound and resulting product can be written either as exactly:

$$\varepsilon_{(A-B)} = 1000\, x\, (\alpha_{(A-B)} - 1) \tag{3.4}$$

Where alpha is defined as:

$$\alpha_{(A-B)} = \left({}^{R_A}/_{R_B}\right) \tag{3.5}$$

or as approximately:

$$\Delta_{A-B} = \delta^{34}S_A - \delta^{34}S_B \cong \varepsilon_{A-B} \tag{3.4}$$

Equation 3.4 is referred to as the fractionation factor, and expresses the ratio of heavy to light isotopes in the reactant, (R_A), to the product, (R_B), that result from a fractionation reaction.

Fractionations can be either equilibrium or kinetic (Kendall and MacDonnell, 1998). The former implies isotopic equilibrium between the substrate and the products, which necessarily implies chemical equilibrium as well; i.e., the forward and backward reaction rates are equal. In equilibrium fractionations, the heaver isotope tends to be enriched in the species or compound with the higher oxidation state (Kendall and MacDonnell, 1998). Kinetic fractionations are uni-directional, irreversible reactions. Forward and back reaction rates are not equal, and because bonds are more easily broken between lighter isotope species, these react faster and are concentrated (enriched) in the products. Therefore, the heaver isotopes become enriched in the substrate (depleted in the product).

For a given temperature, kinetic fractionations generally result in considerably greater isotope fractionations than equilibrium fractionations (Clark and Fritz, 1997).

Mixing relationships can also alter isotopic ratios. If sulfate, formed from the oxidation of pyrite, mixes with sulfate from the dissolution of gypsum – the latter being considerably enriched in ^{34}S relative to the former – the resulting pool of sulfate will be chemically identical to the initial groups, but will have a $^{34}S/^{32}S$ isotope ratio intermediate between the two. What the actual ratio will be depends on the mixing fractions involved.

3.3.1 Sulfate in the Grand River Discharge Reach

Sulfur exists in a wide range of compounds and oxidation states throughout the natural environment, from (-2) in iron sulfides to (+6) in sulfate (Krouse and Grinenko, 1991). In stream environments, sulfur is usually found as dissolved sulfate or in suspended plant or mineral materials. Conceptually, the Grand River discharge reach can be thought of as a through-flow reservoir receiving sulfate from, and loosing sulfate to, other reservoirs. The major inputs of sulfur to the Grand River are expected to be sulfate dissolved in groundwater discharge, surface water run-off, direct precipitation, and WWTP effluent. The sulfate itself may come from a variety of sources: geological units, the oxidation of organic materials, ammonium fertilizers, or wet and dry atmospheric fallout.

In the discharge area, geologic sources of sulfate are likely either from minerals in the evaporite units of the Salina formation, or sulfate produced from the oxidation of sulfides and organic matter, found throughout the overburden sediments. The evaporite minerals of the Salina formation, mostly anhydrite with minor gypsum, retain the $^{34}S/^{32}S$ ratios of the Permian ocean basin in which they precipitated, with delta values ranging from 27.3‰ to 29.6‰. Maximum $\delta^{34}S$ values found were just above 30‰ (Fritz et al., 1989). Only a minor isotopic fractionation is associated with the precipitation of sulfate minerals, on the order of +1.7‰, and a similar fractionation associated with their subsequent dissolution in groundwater environments. $^{18}O/^{16}O$ isotopic ratios show a greater fractionation, on the order of +3.5‰, during the formation of evaporite minerals (Faure and Mensing, 2005).

Sulfides, mostly pyrite, are found ubiquitously throughout the overburden material in the Grand River Watershed at weight percentages of 0.01% to 0.1% (Robertson et al., 1996). While no Grand River specific data was available on $^{34}S/^{32}S$ or $^{18}O/^{16}O$ values of sulfate derived from the oxidation of sulfide minerals, compilations by Krouse and Grinenko (1991), show worldwide average isotopic

composition of $\delta^{34}S$ in pyrites (Figure 3.5) and sulfide mineral deposits (Figure 3.6) to be about 3.4‰. A compilation by Brabec et al. (2012), shows $\varepsilon^{34}S_{(SO4-FeS2)}$ values are generally slightly negative, but can range from -13.2‰ up to 5‰, in rarer cases. Even at the margins of this range, however, the $\delta^{34}S$ values of sulfate derived from sulfides is clearly distinct from sulfate derived from the Salina bedrock formation.

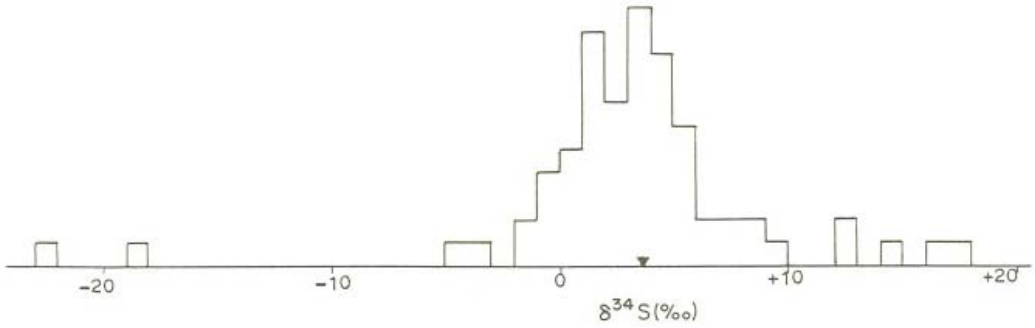

Figure 3.8 Worldwide $\delta^{34}S$ values (‰, CDT) from pyrite samples (n = 70). Samples are from the Soviet Union, Japan, Canada, Australia, Africa, and Central Europe. From Krouse and Grinenko (1991).

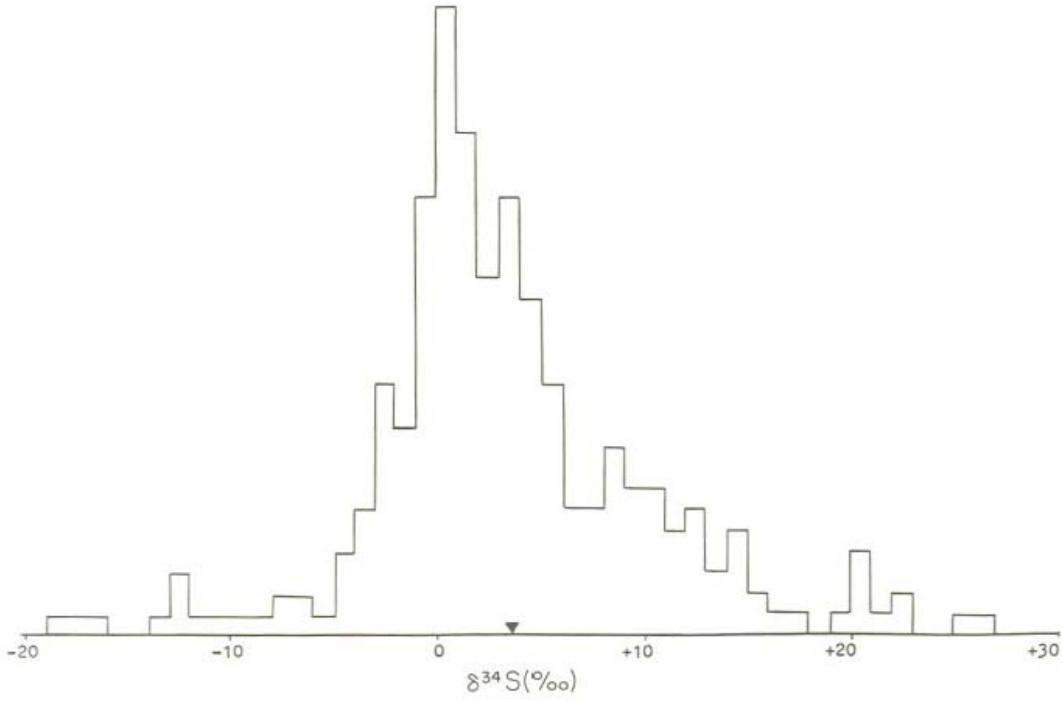

Figure 3.9 Worldwide distribution of $\delta^{34}S$ values (‰ CDT) from sulfide deposits (sample size is unclear, but greater than 120). From Krouse and Grinenko (1991).

Oxygen in sulfate derived from the oxidation of sulphides is generally conceptualized as coming from both liquid water and molecular oxygen via several reactions, and the $\delta^{18}O$ values of such sulfate will reflect, in part, the stoichiometry of this mixture (Taylor et al., 1984; Lloyd, 1967: in Krouse and Grinenko, 1991). Other researchers have reported $\delta^{18}O$ and $\delta^{2}H$ values of groundwater in the Grand River Watershed, documenting $\delta^{18}O$ values close to -10‰ (Encalada, 2008; Pastora 2009; Stotler et al., 2011). Thus, depending on what fraction of ^{18}O comes from which reaction (Van Everdingen and Krouse, 1985), $\delta^{18}O$ values of sulfate derived from sulfide oxidation should range between -12‰ and +8‰, in close agreement with the range of -10‰ to 5‰ used, from Krouse and Grinenko (1991), to characterize terrestrial sulfates (Figure 3.10).

The range of $\delta^{34}S$ values found in organic material tends to reflect the original source the sulfur came from. In many terrestrial environments, plants absorb inorganic SO_4^{2-} from the soil pool, which in turn has come from fertilizers, geologic sources (in this case, likely sulfides), or atmospheric deposition (Kendall, 1998). In many cases, previous researchers have reported similar isotopic ratios in organic matter and from the soil sulfate pool (Krouse and Grinenko, 1991). In the absence of fertilizer or atmospheric inputs, the isotopic ratios of sulfate from the oxidation of sulfides, organic matter, and the soil pool should all plot within similar ranges. Here, this is termed 'terrestrial sulfates' (after Krouse and Grinenko, 1991; Figure 3.10).

Another possible sulfur input to the discharge reach is from aerosols and atmospheric sulfate dissolved in rain droplets. Good $\delta^{34}S$ data is available from Nriagu and Croker, 1978, which gives a range of $\delta^{34}S$ values, from Dec 1973 to June 1975, of +3‰ to +7‰, for a selection of locations across southern Ontario. A large part of this range is seasonal variation; samples taken during the winter average 4‰ heavier than those taken during the summer. Other researchers have documented similar values (Nowicki, 1976). Most of the atmospheric sulfate in Ontario is attributed to anthropogenic and bacteriogenic sources; sea salt spray accounts less than 10% of the total sulfate (Nriagu et al., 1975). Aerosols in southern Ontario are strongly influenced by industrial emissions. Typical $\delta^{18}O$ values of aerosol sulfate range between 7‰ and 15‰ (Krouse and Grinenko, 1991).

Anthropogenic sulfur must also be considered in agricultural watersheds such as the Grand. Ammonium sulfate fertilizers have a significant sulfate component, which, after application, can dissolve into runoff or leach into groundwater and ultimately may end up in the Grand River. Although no Grand River specific data was found, literature compilations of isotope values of sulfate in ammonium sulfate fertilizers used in Italy show a range between -8‰ and +13‰ for $\delta^{34}S$, with

outliers up to +22‰, and a range of +7‰ to +15‰ for $\delta^{18}O$ values (Vitoria et al., 2004). These values may not accurately represent sulfate fertilizers applied in the Grand River Watershed, as the isotopic composition of the sulfate will surely depend on the source of sulfate used to produce the fertilizer. These sources are probably not the same in Italy and central Canada.

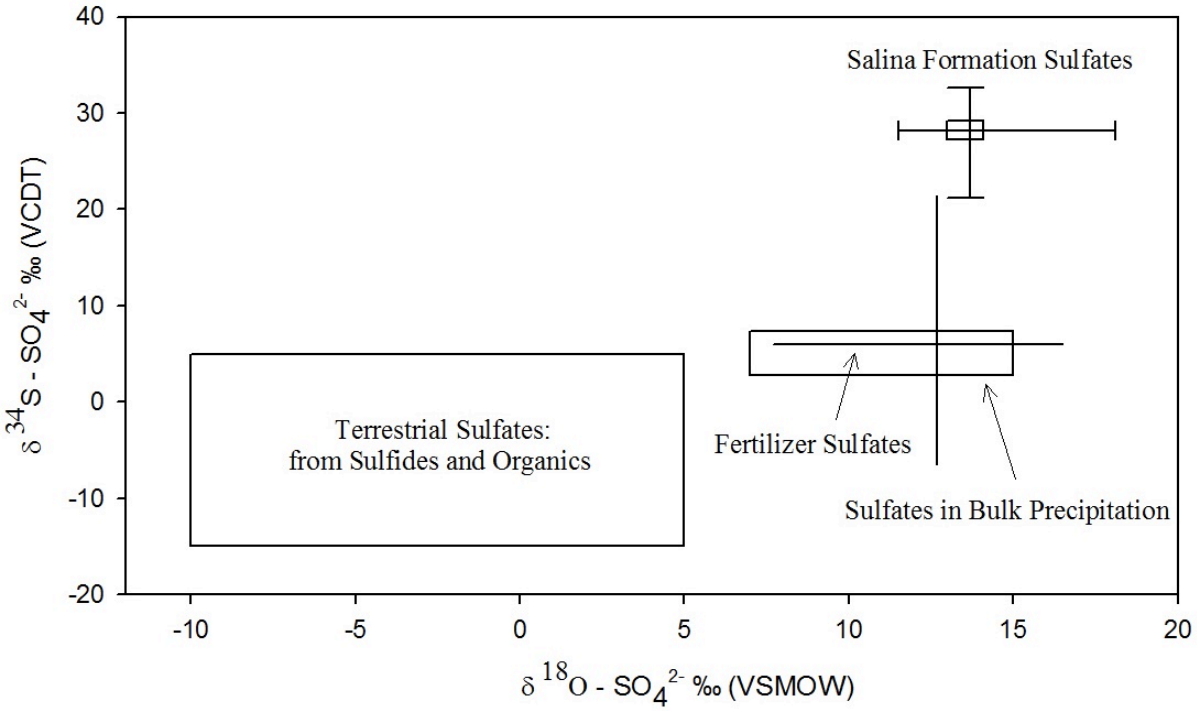

Figure 3.10 Literature isotopic end-member ranges of possible sulfate sources to the Grand River. Overburden terrestrial sulfates from Kendall and MacDonnell (1998). Fertilizer sulfates from Vitoria et al. (2004). Bulk precipitation sulfate from Nriagu and Coker (1978), *in* Krouse and Grinenko (1991). Salina formation sulfates from Fritz et al. (1989).

All of these sources of sulfate to the Grand River are subject to fractionations that occur during sulfate reduction. This occurs as either assimilatory or dissimilatory reduction of sulfate. During the former, sulfate is actively taken in by cells and reduced to sulfide, eventually to be incorporated into sulfur compounds within cells; during the later, facultative bacteria in anoxic environments use sulfate as an electron acceptor for the oxidation of carbon, through which they gain energy for metabolic functions (Canfield, 2001). Assimilatory sulfate fractionation seems to result in only minimal $^{34}S/^{32}S$ fractionations, with average epsilon values of 1.5‰ within a range of 4‰ or 5‰ (Trust and Fry, 1992). Dissimilatory sulfate reduction, on the other hand, can produce very large

fractionations, up to 46‰, given several conditions that seem ubiquitous throughout environments where sulfate is reduced (Canfield, 2001):

1) The extent of isotope fractionations tends to be inversely proportional to the rate of the reaction. The quicker reaction rates, the smaller the ^{34}S fractionation. It is thought that slower reaction times allow the prokaryote to be more selective in which sulfate ions are used.

2) Reactions in which organisms utilize organic compounds as electron donors tend to result in greater fractionations than those in which H_2 is used.

3) Fractionations are minimal if sulfate concentrations are below 1mM

4) Fractionations can range widely when sulfate concentrations are above 1mM

Even given conditions in which there are large amounts of sulfate, and DOC is utilized as an electron donor, fractionations show considerable variation (Kendall and MacDonnell, 1998). Furthermore, if substrate sulfate concentrations are high enough, fractionation during reduction will be obscured, as the fraction of substrate affected by the enrichment in ^{34}S will be negligible compared the unaffected sulfate that remains in the system (Kendall and MacDonnell, 1998). Salina formation groundwater is a candidate environment where this could occur. The generally accepted geochemical progression of groundwater (Freeze and Cherry, 1979) suggests that conditions within deep, old Salina formation groundwater may be sufficiently reduced to favour sulfate reduction. There are also large volumes of anhydrite and gypsum precipitates available to dissolve (see Chapter 2.4.2). Therefore, in Salina groundwater where sulfate concentrations are low, fractionations should be evident. In Salina groundwater where sulfate concentrations are high, fractionations may be obscured.

Sulfate reduction occurring in other environments with sufficient electron donors and bacteria such as wetlands, shallow groundwater, or the hyporheic zone, may show significant fractionations, as sulfate concentrations are unlikely to be high enough to obscure fractionations. In all environments, redox conditions will help confirm if sulfate reduction has or has not occurred.

3.3.2 Nitrate in the Grand River Discharge Reach

Like sulfur, nitrogen exists in a wide range of oxidations states in the natural environment, from (-3) in ammonium to (+5) in nitrate. Nitrogen is essential for biological activity and a critical element for all forms of life (White, 2005). It must also be considered when the quality of surface or groundwater is of concern. Above 10 mg $N \cdot L^{-1}$, nitrate can interfere with the oxygen carrying capacity of

haemoglobin in the bloodstream of infants, a condition known as “blue baby syndrome” (Clark and Fritz, 1997). Nitrogen has also been linked to eutrophication in surface waters (Burjin and Hamilton, 2007), and nitrate is toxic to aquatic life at concentrations over 2 mg $N \cdot L^{-1}$. Thus, there are numerous reasons related to water quality why nitrogen cycling in the Grand River is of considerable interest.

Nitrogen cycling in the Grand River discharge reach can be conceptualized as a flowing reservoir with inputs and sinks of nitrogen occurring at various locations down-reach, with additional, internal cycling processes occurring within the reservoir as it flows downstream. Major inputs of nitrogen to the Grand River include groundwater discharge, surface water tributaries, and upstream WWTPs. Each of these inputs carries with it nitrogen from various sources; nitrate, for example, from the oxidation of plant compounds, ammonium fertilizers, or septic tank urea (Kendall and MacDonnell, 1998). Additionally, numerous cycling processes have already affected nitrogen isotopic ranges of these sources. Nitrogen incorporated into plant compounds and organic material has already been fixed from atmospheric N_2, or ammonium or nitrate sources from atmospheric particles and soil nitrate pools. Upon decay, compounds are mineralized to ammonium and then nitrified to nitrate (Kendall and MacDonnell, 1998), then further recycled or leached into groundwater. Fertilizers are either leached directly to the watertable, in the case of nitrate fertilizers, or undergo nitrification, in the case of ammonium fertilizers, before subsequent leaching. Septic system nitrogen waste is in a reduced form (e.g., organic N, NH_4^+), and upon entering the subsurface, is oxidized, or nitrified, to nitrate by various electron donors depending on prevailing geochemical conditions (Robertson et al., 1991; Aravena et al., 1993).

In terms of non-point source nitrate contamination of rivers, some researchers have stressed the importance of considering the flow-path groundwater takes on route to the discharge point (Maitre et al., 2002; Vidon and Hill, 2004; Burgin and Hamilton, 2007; Shabaga and Hill, 2010). Nitrate in shallow groundwater, flowing through wide riparian zones with considerable DOC, may be strongly denitrified. Nitrate in groundwater that bypasses riparian zones, flows through them too quickly, or moves through riparian zones lacking either sufficient width and/or DOC content may not be strongly attenuated by denitrification (Hill et al., 2000). An example environment where denitrification may be minimal is along steep cutbanks with little or no riparian buffer; others, however, have shown that, even without a DOC source, nitrate can undergo dentrification via oxidation of other compounds such as sulphides (Aravena and Robertson, 1998). Another groundwater flow-path that bypasses the

riparian zone altogether is discharge from deeper, regional aquifers, which could have redox conditions where nitrate will be strongly denitrified, directly to the streambed.

All of these processes above can impart fractionations to the isotopic ratios of these nitrogen sources. Thus, nitrate carried by inputs to the Grand are not easily characterized in terms of isotopic signatures, and care must be taken to distinguish source signatures from fractionation processes. Due to the water quality concerns posed by nitrate, there are various compilations of the expected range of $\delta^{15}N$ and $\delta^{18}O$ values for various sources (Clark and Fritz, 1997; Kendall and MacDonnell, 1998). Figure 3.8, using literature data summaries from Kendall and MacDonnell (1998), shows areas in $\delta^{18}O\text{-}NO_3^-$ vs. $\delta^{15}N\text{-}NO_3^-$ space where sources of nitrate are expected to plot. Denitrification activity can be identified by comparing relative increases of $\delta^{18}O\text{-}NO_3^-$ and $\delta^{15}N\text{-}NO_3^-$ values or by comparing $\delta^{15}N$ values with nitrate concentrations. Various researchers have noted that samples affected by denitrification, on a $\delta^{18}O\text{-}NO_3^-$ vs. $\delta^{15}N\text{-}NO_3^-$ plot, tend to conform to a linear relationship characterized by a 1.3:1 to a 2.1:1 increase between $\delta^{15}N$ and $\delta^{18}O$ values (Aravena and Robertson, 1998; Mengis et al., 1999; Xue et al., 2009). Thus, samples that plot along an enrichment trend with a slope near these values may have been influenced by denitrification and are worth further inspection. As denitrification is a multi-step, overall uni-directional kinetic fractionation process, $\delta^{15}N$ values of residual nitrate will increase exponentially as nitrate concentrations decrease (Kendall and MacDonnell, 1998). Thus, samples of groundwater in which denitrification has occurred should conform to Rayleigh-type fractionation curves for a given enrichment factor. This can be distinguished from hyperbolic mixing curves between two sources of nitrate by plotting $\delta^{15}N$ values vs. the natural logarithm of nitrate concentrations, which convert exponential fractionation curves into straight lines (Faure and Mensing, 2005).

As with the sulfate reduction processes, redox conditions and major ion chemistry can add evidence for or against the plausibility of denitrification occurring. For facultative bacteria to choose nitrate as an electron acceptor, conditions are must be anoxic with considerable concentrations of DOC or some other electron donor (such as sulfides). For anammox reactions to occur, high concentrations of both ammonium and nitrate should be present (Robertson et al., 2012); a condition not expected to be found in the discharge area.

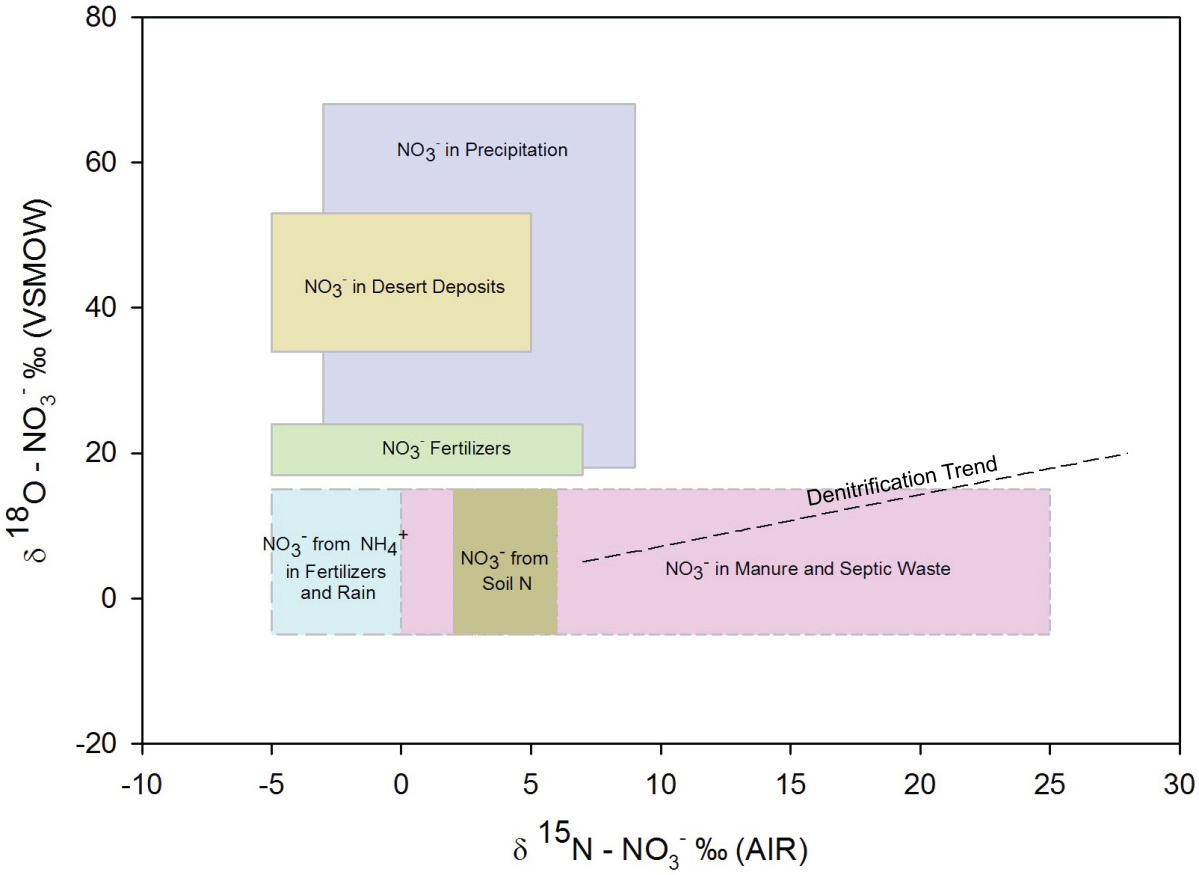

Figure 3.11 Literature summary of where nitrate, from various sources, tends to fall on a $\delta^{18}O$ vs. $\delta^{15}N$ plot. Summary box values are from Kendall and MacDonnell (1998).

Chapter 4 – FLIR Survey

4.1 Introduction

The first objective of this research was to map out the major groundwater discharge locations in the study area. It was already known, through previous work, that a groundwater discharges between Cambridge and Brantford, but to the author's knowledge, no work had yet been done locating specific discharge points. Identifying these locations is important for a number of reasons. It allows researchers to sample seeps, which may result in a more complete understanding of the discharge source. It provides the local conservation authority the option to continually monitor specific discharge areas that may impact the water quality of the Grand River. It allows the discussion of point WWTP contamination vs. non-point agricultural contamination to be refined towards specific locations and plumes of contaminated discharge. It can improve the conceptual model for groundwater/surface-water interactions along the reach: does discharge occur diffusively along the reach, or from localized *hotspots*? Finally, using FLIR thermography to prospect for groundwater discharge is a relatively new research method. Employing it along a reach where groundwater is already known to discharge allows for refinement of the method not possible were it being used without that background context.

4.2 Methods

4.2.1 Survey

The FLIR camera survey methodology was based upon the previous work of Dr. Brewster Conant Jr. and others within the groundwater/surface-water research community (Loheide and Gorelick, 2006; Conant, 2008; Drake, 2009). The idea is to use the FLIR camera's ability to record infrared radiation emitted from objects to locate groundwater seeps and springs discharging along a river's banks. The temperature of groundwater will reflect the average annual temperature of the region, which, if the survey is done at an appropriate time, will differ significantly from the temperature of the surrounding banks. Thus groundwater discharging to the river can be quickly located for further study.

Although it was known that, in southern Ontario, work using temperature as a tracer should done during winter or summer to ensure adequate differences between ambient and groundwater temperatures, it was not immediately apparent what time of day would result in the largest

temperature contrast. Several factors needed to be considered. The temperature of groundwater in the discharge reach ranged between 8.01 °C and 9.33 °C in 2011 (Herrera, 2012). Therefore, the best time to conduct the survey is whenever other objects along the banks – foliage, rocks, exposed ground, deadfall – have temperatures as different from this range as possible. At first guess, this would be just after the maximum peak in the diurnal ambient temperature cycle, i.e., sometime mid to late afternoon. If discharging at a low flow rate, however, the groundwater may absorb enough radiation to increase its temperature to values similar to that of other bank objects. Heat transfers from surrounding objects may also occur, resulting in a homogenized, unhelpful thermal image. Thus, the time when the temperature of objects is maximized may also be the time when heat transfers are maximized, and this may not necessarily be when temperature contrasts *between* groundwater and bank objects are maximized.

To determine the optimal time to conduct the FLIR survey, the camera was field tested just south of Glen Morris Bridge (Figure 4.1). FLIR photographs of several seeps were taken repeatedly from approximately 5:00am until about 3:00pm. Figure 4.2 is an example of typical results: photo A) was taken at 7:30am, before incoming solar radiation begins to increase the temperature of bank objects. In this photo, the seep has a fairly uniform temperature of 16.5°C to 16.6°C. Most of the actual seep is indistinguishable from the rock under which it emerges, and is most clearly defined as it enters the Grand River. Temperatures across the image are fairly homogeneous. Photo B) shows the same seep, photographed at 12:45pm. In this second picture, the temperature of the seep, from the top of the frame to the bottom, ranges from 17.6°C up to 20.6°C. The rock and the seep are clearly distinguished; despite the temperature of the seep having increased, the temperature of the rock has increased considerably more, and the contrast between the two has improved. Even though the seep's temperature is both higher and less uniform in the second frame, mid-afternoon appeared to maximize the capacity of the FLIR camera to detect groundwater seeps.

This may not be true for tributaries draining surface water sources. These tributaries have higher initial temperatures, and lower temperature contrasts, with other bank objects to begin with – and they are all subject to diurnal fluctuations in ambient temperatures. The defining temperature contrasts of these tributaries, therefore, may not increase to the same degree as the groundwater seeps as solar radiation increases throughout the day. No seeps photographed at Glen Morris showed this trend, but none of the seeps were definitively known to be draining surface water sources.

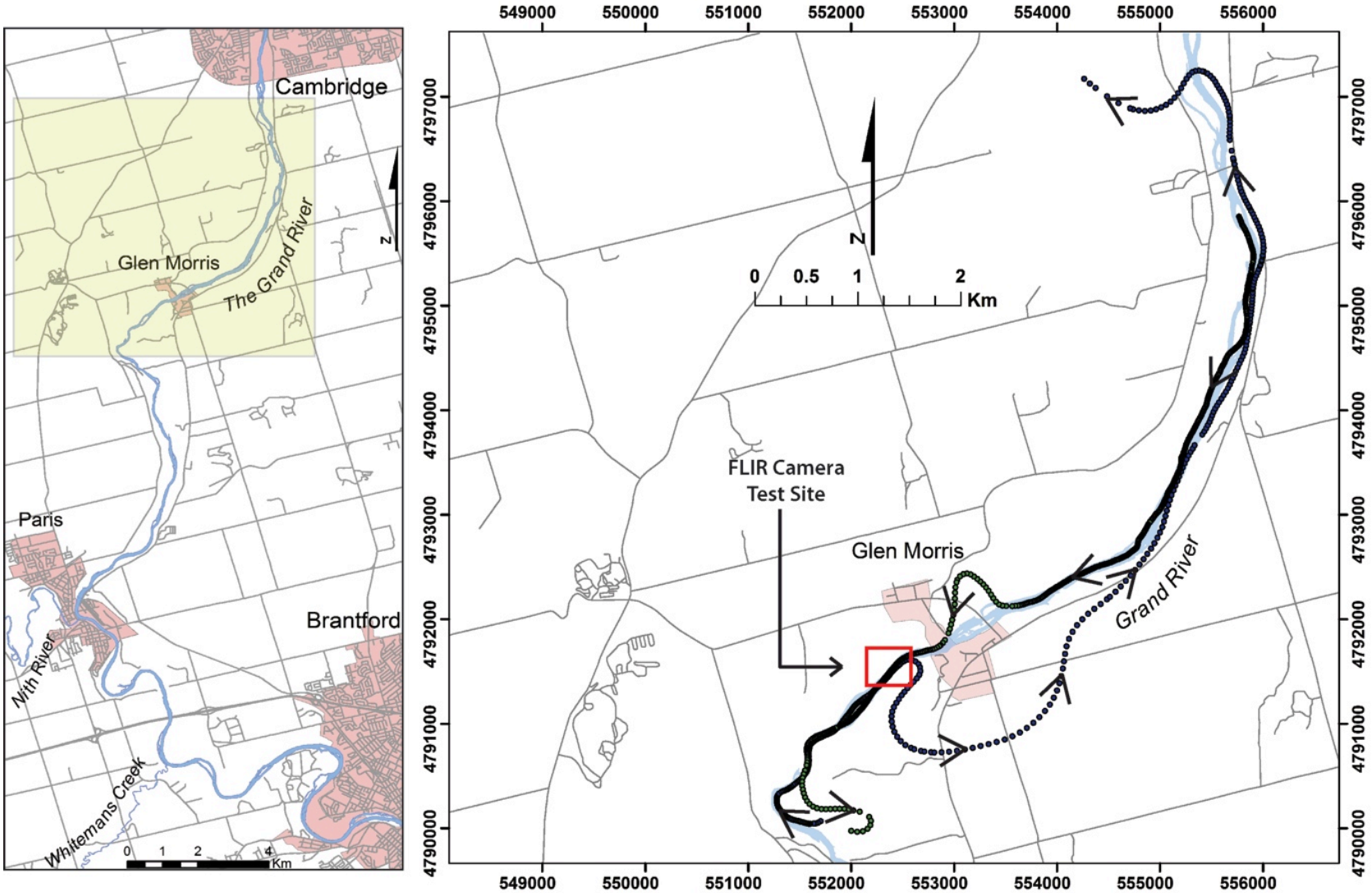

Figure 4.1 Helicopter traces of the southwest and northwest bank FLIR thermography surveys. Arrows indicate the direction of flight. The red square shows the general location where the camera was field tested prior to the actual survey.

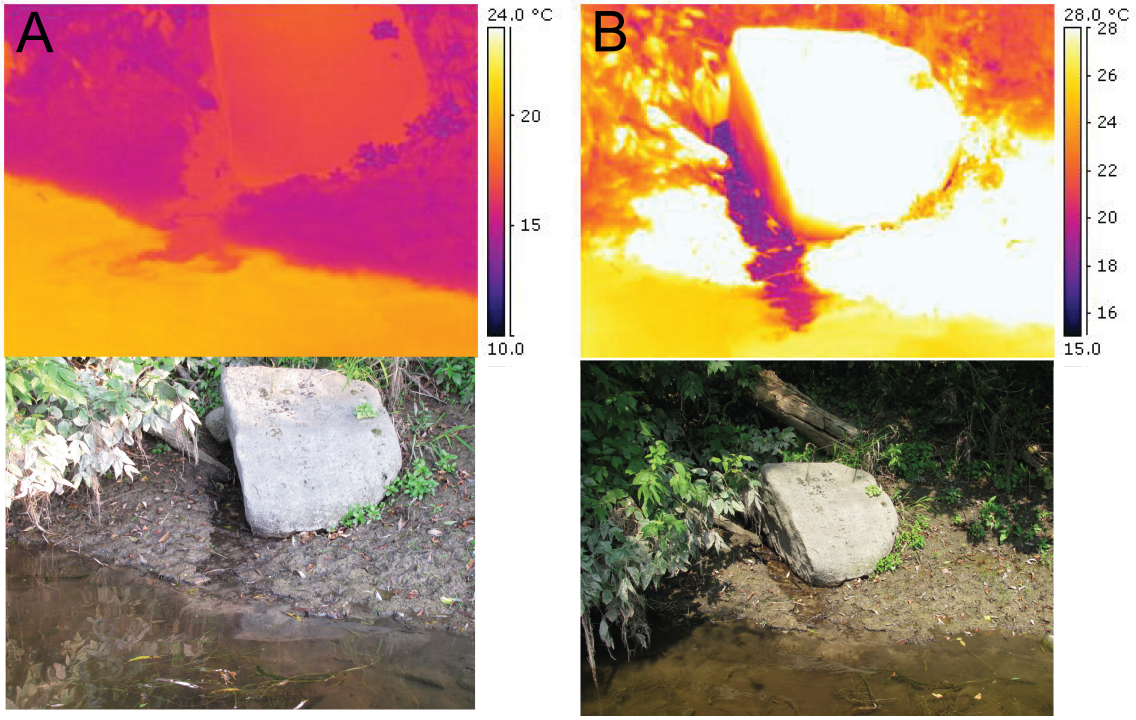

Figure 4.2 Thermal comparisons of the same seep photographed at two different times during the day. Photo (A) was taken at 7:30am on August 21st 2011. Photo (B) was taken at 12:45pm, August 21st 2011. At 7:30am, the seep has been less affected by thermal radiation and ambient temperature increases, but so has the rock, and the two are virtually indistinguishable in the thermal photograph. At 12:45pm, the temperature of the seep has increased, but the temperature of the rock has increased considerably more, and the contrast between the seep and the surrounding bank features has been greatly improved.

To perform the FLIR survey, two cameras were used: one to record thermal images, and a second to record visual images. The IR camera was a FLIR thermaCAM Model P25, with a resolution of 320 x 240 pixels, spectral range of 7.5um to 13um, and error in temperature measurement of +/- 2°C. The video camera was a Panasonic 3CCD handheld camcorder. The visual images are needed in order to identify and locate the features noted using the IR camera, as alone, the IR pictures can be difficult to interpret. In addition to the cameras, a GPS system was used record the helicopter's location every one or two seconds (Figure 4.1). This allowed for concurrent capture of location, thermal image, and visual image data. It is important to note that the helicopter always flew on the opposite bank from the one being filmed. Finally, a wristwatch was used to record the time at which observations during the flight where made. The clocks on all devices used were synched before the survey began.

The FLIR Camera survey was completed on August 31st, 2010, between 1:45pm and 3:00pm. Ambient temperature was 32°C. The survey began under clear skies, with considerable cloud development by 3:00pm. Relative humidity was recorded at 63.6% and the dew point was at 16°C.

The survey began at Footbridge St. Bridge south of Cambridge and finished approximately two kilometers south of Glen Morris (Figure 4.1). This reach was flown twice. During the first pass, the banks were filmed using both cameras. During the second, the IR camera was used to take photographs of the major features noted during the first. The FLIR video data was used to locate temperature anomalies along the banks of the Grand that could potentially be caused by groundwater discharge. These locations were then studied in closer detail in the still photos.

To provide a standard with which to judge the effectiveness of the thermal survey, visual surveys down the discharge reach were also completed. These were relatively simple; two researchers canoed slowly down the reach, first along one bank and then the other, and recorded GPS locations when discharge, either tributary or seep, was noticed. The two surveys were then compared to see which survey had missed what seep/tributary, so that the FLIR survey method could be improved upon for subsequent surveys.

4.2.2 Photo Analysis

To analyze the FLIR data, photos were imported to FLIR Quickreport™, a program that allows rudimentary analysis of photographs taken using a FLIR camera (software available for free download from www.flir.com). The program assigns user chosen color ramps to the temperature range captured in each photograph by the camera. The color ramp used in this research started at black for the coldest temperature recorded in the frame, and moved through dark purple, red, orange, yellow, and finally white for the highest temperatures. The program allows the user to define the temperature range this color ramp covers – essentially, allowing the user to vary color contrasts within the photo to tease out features that may not be obvious at the default scale. The minimum temperature within the frame was usually associated with some sort of bank discharge feature: bank seepage, runoff, or sometimes just a darkly shaded portion of the bank. Each of these *features* was also evaluated according to its spatial characteristics, and placed into one of three categories: seeps or shade, seeps and/or runoff, and runoff. The categories are defined as:

1. **Seeps or Shade:** Patchworks of clear temperature contrasts within the surrounding bank and lack a defined channel structure. They could be caused either by seepage or shading.

2. **Seeps and/or Runoff**: Discrete temperature contrasts that could be the result of either seeps or tributaries whose channels are obscured by thick vegetation and are only seen right at the edge of the Grand River. Some photos contained areas where both seeps and runoff feature types are present. These compound feature types are also included in this category.
3. **Runoff:** Clear, defined channels of temperature anomalies meandering through the riparian zone and ending at the edge of the Grand River.

Implicit in these categories is a relative scale of uncertainty: the weaker the temperature contrast between the feature and the bank, the more uncertainty exists with regards to what the feature is. Thus, *seeps or shade* with a small temperature contrast to the bank could be a low flow seep, but could also just be a patch of shade. On the other hand, a *seeps or shade* feature with a large temperature anomaly is almost certainly a seep. This scale applied to the other two categories as well.

4.3 Results

The photo survey down the northwest bank of the Grand River yielded 132 IR photos, in which features clearly or possibly caused by groundwater or surface-water discharge were found in 42. The photo survey down the southwest bank of the Grand River yielded 181 IR photos, 60 of which contained some sort of discharge feature. These results were compiled into a map, showing the feature distribution, intensity of the temperature anomaly, type of feature, and relative size of the feature noted during the FLIR survey. The map is super-imposed on an elevation profile map of the FLIR survey reach, to compare local elevations with discharge features. The map also shows the locations where discharge was noted during a canoe survey completed several days prior to the FLIR survey (Figure 4.3).

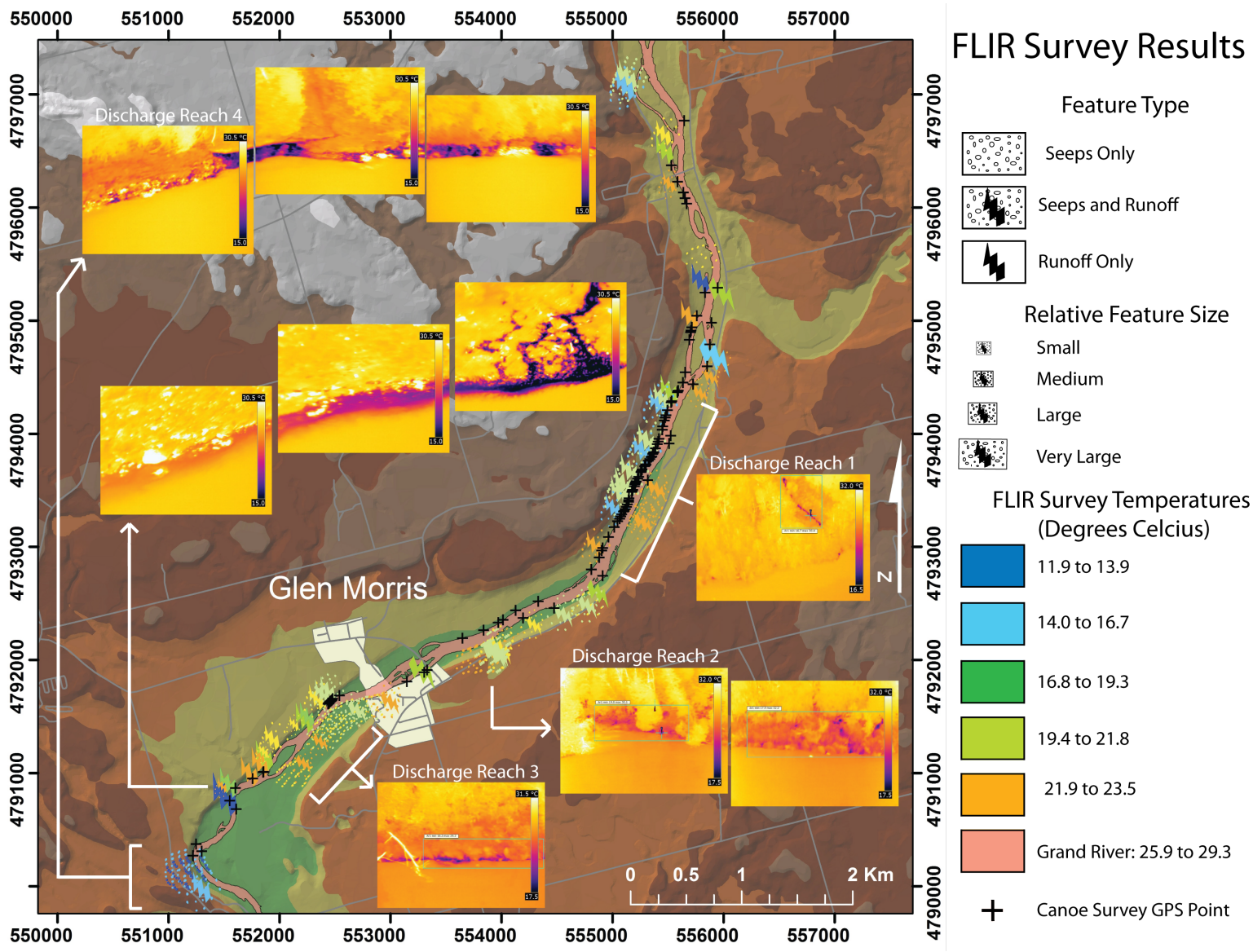

Figure.1 Results of the FLIR photo survey. Four sub-reaches of considerable bank discharge were noted, only one of which (discharge reach one) was obvious from previous visual surveys completed by canoe.

4.4 Discussion

4.4.1 Drawbacks to the FLIR Survey

The FLIR camera does not necessarily provide accurate or precise measurements of a feature's temperature. The angle of the camera relative to the object, the distance from the camera to the feature, where the object sits in the frame, and the influence of reflections and 'shadows' from nearby objects all contribute to its apparent temperature. The feature will appear to have different temperatures as these factors vary. The feature in figure 4.4A is a cold-water tributary entering the Grand from the northwest bank several kilometers upstream of the Glen Morris Bridge. Figure 4.4B, taken seconds after, is of the exact same tributary, but the minimum temperature in this figure is 4.2 °C higher than in the first.

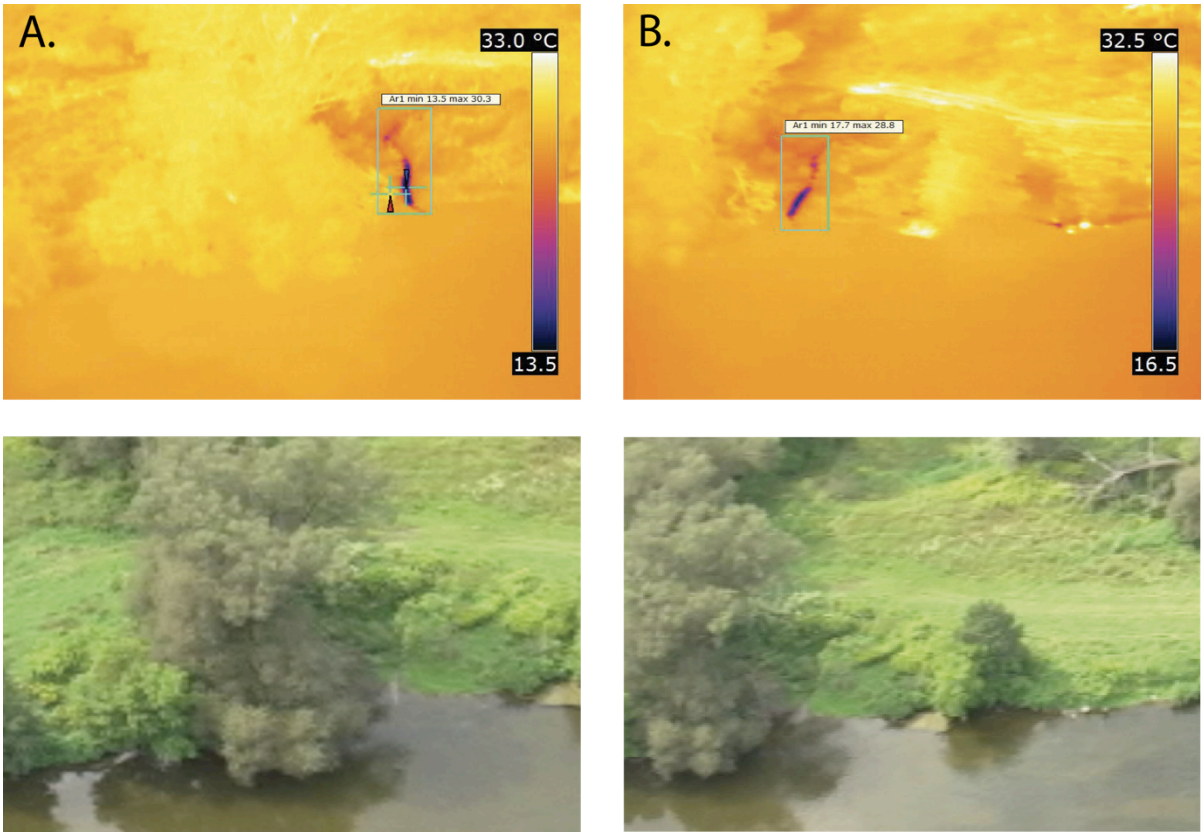

Figure 4.4 Temperature differences from successive photos of the same discharge feature. The feature is 13.5°C in photo (A), but 17.7°C in photo (B).

One of the factors that created the most uncertainty in the FLIR survey results was the variability of the distance the helicopter, and therefore the camera, was situated from the bank as the survey progressed. The pilot was constrained in terms of how close he can fly to each bank through a bylaw which states that he must remain at least 500ft away from any "built up" region – e.g., housing developments, industrial sites – during the flight. Along much of the southwest bank of our survey route, built-up regions extend quite close to the river's edge. Thus, although the helicopter could get fairly close to the southeast bank by remaining close to the river surface and shooting across the river, it was not possible to do the same with the northwest bank; this would have brought the helicopter too close to the built-up areas. While surveying the northwest bank, the helicopter had to stay at a significantly higher elevation over the southwest bank to preserve the 500ft buffer zone. As a result, most of the footage of the northwest bank is shot from a greater distance than the footage from the southwest bank. This has several effects on the results of the survey.

First, it altered the temperature difference between the feature and the bank. The greater distance resulted in features appearing warmer than they probably are, which raised the minimum temperature in the photo, which diminished the strength of the temperature anomaly. Thus, numerous features along the northwest bank appear less important as discharge features, relative to the southwest bank, then they should.

Second, shooting from a greater distance along the northwest bank made it more difficult to determine what the feature actually was; bank features appear more homogenized, more smoothed out in the thermal photos. Features with smaller temperature anomalies may be completely obscured.

Third, shooting from different elevations made it difficult to be consistent when grouping features according to size. What appears large relative to the majority of features noted on the southeast bank becomes quite small when viewed from 200ft further away. Thus, the consistency of the size categories between one bank and the other may be questionable.

One stretch of the survey route, the northwest bank directly upstream from Glen Morris, shows numerous canoe surveyed tributary/seeps that were apparently not noticed by the FLIR survey. This is also the result of distance. Figure 4.1, showing the flight path of the helicopter, illustrates the wide berth the helicopter made around Glen Morris. By the time the helicopter had moved close enough to the river again to resume filming, it was already a kilometer or two upstream.

4.4.2 Successes of the FLIR Survey

Despite the previous discussion, the FLIR survey was successful in locating strong groundwater discharge activity that might have gone un-noticed by visual methods. Figure 4.3 illustrates this fact. A large number of discharge features are noted along the northwest bank, downstream of Shep's footbridge (discharge reach one). These features were noted in both the FLIR survey and during the earlier visual conducted by canoe. These features were evident in the canoe survey because, while these discharge features might ultimately be derived from groundwater discharging upslope, by the time the discharge reaches the Grand it had accumulated into medium to large cold-water tributaries with well-defined channels and relatively large volumes of water.

On the other hand, figure 4.3 also highlights three sub-reaches, ranging from several hundred meters to over a kilometer long, along the Grand River with strong seep activity. As individual features, the seeps are fairly small features and were not noticed during the canoe survey. The first sub-reach is located on the southeast bank just upstream from the Glen Morris Bridge, covered by IR photos 1377 to 1383 (See Appendix A). The features are immediately obvious in the infrared photos. The second sub-reach is also on the southeast bank, downstream of the Glen Morris Bridge, and captured in IR photos 1399 to 1410. These features are slightly less obvious then the first sub-reach, and more uncertainty exists as to whether they are actually seeps or runoff whose channels are obscured by dense bank vegetation. Regardless, they show strong temperature anomalies and are most likely groundwater fed. The third and final sub-reach was found at the most southern tip of the IR survey, along the northwest bank. An enormous amount of seepage, relative to the rest of the survey, appears to be discharging from gravel and sand overburden units along a steep cutbank overlooking the Grand River. The features show up strikingly in IR photos 1458 to 1467. Even with such a large area over which discharge is entering the Grand River at this location, this discharge went un-noticed during the visual canoe survey. One can speculate as to the reasons; a large factor is because without the defined channel structures of some of the other discharge features, many slowly seeping features go un-noticed, regardless of the size of the discharge area. There was no iron or manganese oxide staining to draw attention to the discharge. A considerable factor may be that, while conducting the canoe survey, one must also canoe. With two people in the canoe for the survey, both have immediate paddling responsibilities in order to successfully navigate downriver. The search for discharge comes secondary to that responsibility, and it is inevitable that in some reaches, both surveyors will be focused on canoeing and not on locating discharge. In these locations, the banks will not be given the same level of scrutiny as other, more easily navigable reaches, and some discharge will be missed.

The last sub-reach may be one such reach. The water here is moving quickly (with velocities greater than two ms^{-1}) along a cutbank, and both researchers had their attention focused on navigating the river. A third researcher could be employed, whose only responsibility would be to survey for discharge, but this reduces the cost effectiveness of a survey by canoe and, at that third sub-reach, might still have been missed. Arguments could be made both for and against using a third person, and how well such a survey would compare to the IR survey in terms of people hours, cost, and time.

In addition to finding discharge that would have otherwise gone un-noticed, the FLIR survey successfully addressed the presumption that, in areas of strong groundwater discharge, seepage would be found along both sides of the bank, and this discharge might continue below the river channel. These reaches would be the areas in which further, more spatially restricted investigations would take place, with the eventual goal of obtaining groundwater samples directly from the riverbed. The IR survey indicates only one such reach, directly downstream of Glen Morris. This reach has been extensively studied by previous workers (Encalada, 2008; Pastora, 2009; Hererra, 2012), and previously drilled observation wells indicated that overburden sediments extend beneath the riverbed (See Figures 3.1 through 3.5). There were no other reaches where significant groundwater discharged from both banks (Figure 4.3).

The FLIR survey was also successful in determining where seeps should be sampled for chemical and isotope analysis. Because the large area seeps were immediately obvious in both the IR video and IR Photo data, it could be used to target the geochemistry sampling survey well before any in depth analysis on the FLIR photos were completed.

4.5 Conclusions

The FLIR survey was successful in that it identified at least three major groundwater discharge zones along a sub-section of the discharge reach from Cambridge to Brantford. These discharge zones were repeatedly missed during canoe surveys. The canoe surveys were only competent when the input to the Grand had a defined channel structure easily seen by the eye. Numerous areas of groundwater seepage, lacking this structure, were missed. The FLIR survey, on the other hand, clearly picked up the temperature contrasts between these seeps and the surrounding bank features.

The FLIR survey also allowed for a fairly uniform categorization of various features recorded by the camera. One factor that reduced this consistency was that the northwest bank was filmed at a greater distance than the southeast bank, due to flight regulations (see discussion). This reduced the

strength of the temperature contrasts picked up by the camera, and changed the size of the features recorded on the northwest bank relative to those on the southwest bank.

Most of the uncertainty in discharge features, represented by smaller temperature anomalies, occurs on the southeast bank. This could ultimately be a function of distance from the bank the survey was completed in; the closer distance allowed the camera to pick up smaller temperature contrasts, increasing the sensitivity of the survey. Thus there are more features recorded with only mild temperature contrasts with the surrounding bank. These features are not present to the same degree in the northwest bank, because the greater distance dampens the contrasts; only large features with significant contrasts are noted.

One of the main previously-held assumptions regarding groundwater discharge along the Grand River needed to be re-conceptualized after the FLIR survey. It was assumed, prior to the survey, that areas of considerable discharge may have discharge occurring from both banks, and possibly continuing under the riverbed. Three out of the four major seep discharge zones along the surveyed reach were without comparable counterparts on the opposite bank.

Two conclusions were also reached that may improve the FLIR thermography methodology for future research:

1. To produce the best results with a FLIR thermal survey, the survey should be done on a cloudy day during winter, when ambient temperatures are just below zero. This will provide the most uniform ambient temperatures, minimize the effects of solar radiation, and minimize brush cover on the banks.
2. A survey done during mid-day increases the temperature of discharge features, but increases the contrasts between the features and surrounding bank considerably more; thus, it appears this is a more appropriate time to conduct the survey than the morning.

Chapter 5 – Drag-Probe Surveys and Temperature Profiling

5.1 Introduction

One drawback to the FLIR survey is that, because the camera only records radiation emitted by the surface of objects, it can't provide information about temperatures below the river's surface, in the riverbed (Conant, 2008). To detect the thermal trace of groundwater discharging through the riverbed on the surface of the Grand, the flux would need to be very high. With the exception of fractures or other structures that may concentrate flow, groundwater doesn't generally discharge from streambeds at rates that could be thermally detected at a river's surface (Conant, personal communication). Even at locations where discharge is relatively high may not be show any surface temperature expression, depending on stream properties such as flow, volume, and water column depth. To gain information about the streambed, different temperature methods are needed.

Drag-probe surveys were the second temperature method tested to locate groundwater discharge along the Grand River. These surveys have been utilized in various capacities to investigate groundwater and surface-water interactions (Lee et al., 1997; Vaccaro and Maloy, 2006; Bustros-Lussier, 2008; Drake, 2009). These surveys measure temperature, and sometimes electrical conductivity, along the stream-streambed interface.

Temperature profiling was the third temperature method used to locate groundwater discharge in the Grand River. The method is simple; a temperature probe is inserted a pre-determined depth into the riverbed, allowed the thermistor to equilibrate with sub-surface, and record the measurement. Variations on temperature profiling are amoung the most commonly used thermal methods employed in streambeds.

The drag-probe surveys and temperature profiling were employed using a scaling down type approach. The objective of the drag-probe surveys was to find sub-reaches of potential groundwater discharge that could then be temperature profiled. Because the discharge reach is approximately 42km long, it had to be reduced to smaller, more manageable sections to prospect for groundwater. If locations with encouraging temperature anomalies were discovered, they would be profiled to 'map' groundwater discharge and determine specific locations to come back later and sample.

5.2 Methods

5.2.1 Drag Probe Surveys

To conduct a drag probe survey, one or more temperature measuring devices are dragged downstream along the stream-streambed interface. This results in a downstream trace of temperature measurements that can yield useful information about possible locations of groundwater discharge, if several important caveats are considered:

1. As with all groundwater surface-water investigations utilizing temperature, there must be a temperature contrast between the groundwater discharge and overlying surface-water. In southern Ontario, conditions are optimal to conduct the survey during midsummer, when daily water temperatures can reach up to 30°C, or during the winter, when daily water temperatures are slightly above 0°C.
2. The boat floats down the river at the same velocity as the river. Although difficult to achieve in practice, in theory this allows continuous monitoring of a single 'packet' of water as it moves downstream. Along the way, the temperature of this packet of water will be influenced by various heat transfers, from which the influence of groundwater can be extracted (Vaccaro and Maloy, 2006).
3. The magnitude of the groundwater discharge flux is sufficient to cause a temperature change that can be measured. This, in turn, is dependent on stream velocity, size, and mixing properties, as well as the time constant and sensitivity of the temperature probe being used. All of these factors can limit the volume of groundwater in contact with the sensor, and influence the probe's ability to sense temperature changes caused by groundwater.

For this research, two non-vented levelogger gold probes were used; one floating at the river's surface, and the other dragged along the riverbed (Figure 5.1). This was done to investigate vertical temperature contrasts in the water column, and to obtain water depth measurements. As both leveloggers were non-vented, it was necessary to account for atmospheric and water column pressure in order to obtain a water column depth. By using two leveloggers, the water level reading from the surface logger could be subtracted from the riverbed logger to obtain a reasonably accurate depth measurement.

Plastic PVC casings were designed for the probes to minimize damage as the probes were dragged behind the boat. This was more critical for the riverbed probe than the stream surface probe, as the

stream surface probe rarely encountered objects. The casing for the surface probe was simply a cylindrical PVC shell (Figure 5.2). The casing for the riverbed logger was a 27cm long cylinder, with a 5.3cm diameter at the open, upstream end, and a streamlined, bullet-shaped head at the downstream end (Figure 5.2). A small hole was drilled into tapered, downstream end of the casing head, through which 180lb test wire was strung. Inside the casing, this wire was attached to a bolt, which was threaded through the levelogger gold probe cap. Centimeter wide slits were cut lengthwise from the open, upstream end of the casing of approximately 10cm in length. This allowed the probe thermistor to remain in contact with river and groundwater at all times, while allowing any debris caught in the probe to slide out the upstream end as the probe moved downstream. The casing itself consisted of two halves, which could be unscrewed as required to facilitate easier access to the probe. Weights could be strung on the test wire in the head of the casing to achieve the desired buoyancy. If the probe assembly was too heavy, it immediately caught on the cobble bottom, despite the streamlined profile. It also greatly increased the force of impacts as the probe scraped along the riverbed. If the probe assembly was too light, there was not enough contact with the riverbed, and potential discharge locations could be missed.

A layer of 0.5cm I.D. (inner diameter) mini piezometer tubes, approximately 2 inches long, was taped around the body of the levelogger gold probes, followed by neoprene wrapped almost to the diameter of the PVC casing (Figure 5.2). The mini-piezometer tubes allowed water to move freely along the length of the probes, and separated the probes from possible insulating effects of the neoprene. The pocket-filled nature of the neoprene provided shock absorbance as the probe bumped it's way downstream.

The surface probe assembly was hung directly off the boat so that it floated, just covered by the river, approximately 2m behind the boat. The wire lead of the riverbed probe was attached to a thick 10m line, to which a float was attached at the top end. This assembly was not tied to the canoe. In the event that the probe became stuck on the riverbed, the researcher had 10m of line to try to unstick the probe as the canoe continued moving downstream. If this proved futile, the researcher could then toss the line overboard: the float prevented the line from sinking and allowed the team to turn back upstream, locate the float, and retrieve the probe.

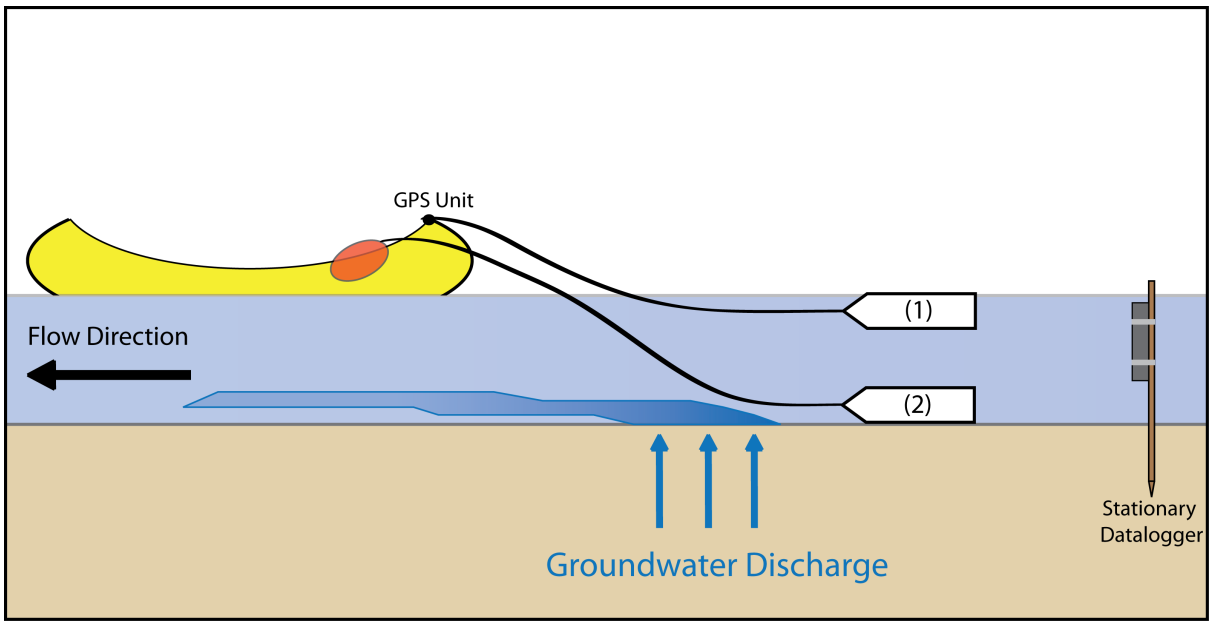

Figure 5.1 Schematic of a the set-up for the drag probe surveys. Two probes record temperatures at the top and bottom of the water column. The riverbed probe is attached to a float (red balloon) so that, in the event the probe is caught on the riverbed, it can be thrown overboard without being lost. The researchers are then able to turn around, retrieve the probe, and continue surveying. Any point during the survey that the probe gets caught will affect the thermal trace that the probe records, as the probe stays stationary and has more time to react to the local temperature conditions than it would otherwise. The surface probe is attached directly to the boat, as there usually isn't much debris in the water column for it to catch on. A GPS unit records the location of the probes at one or two second intervals for the duration of the survey.

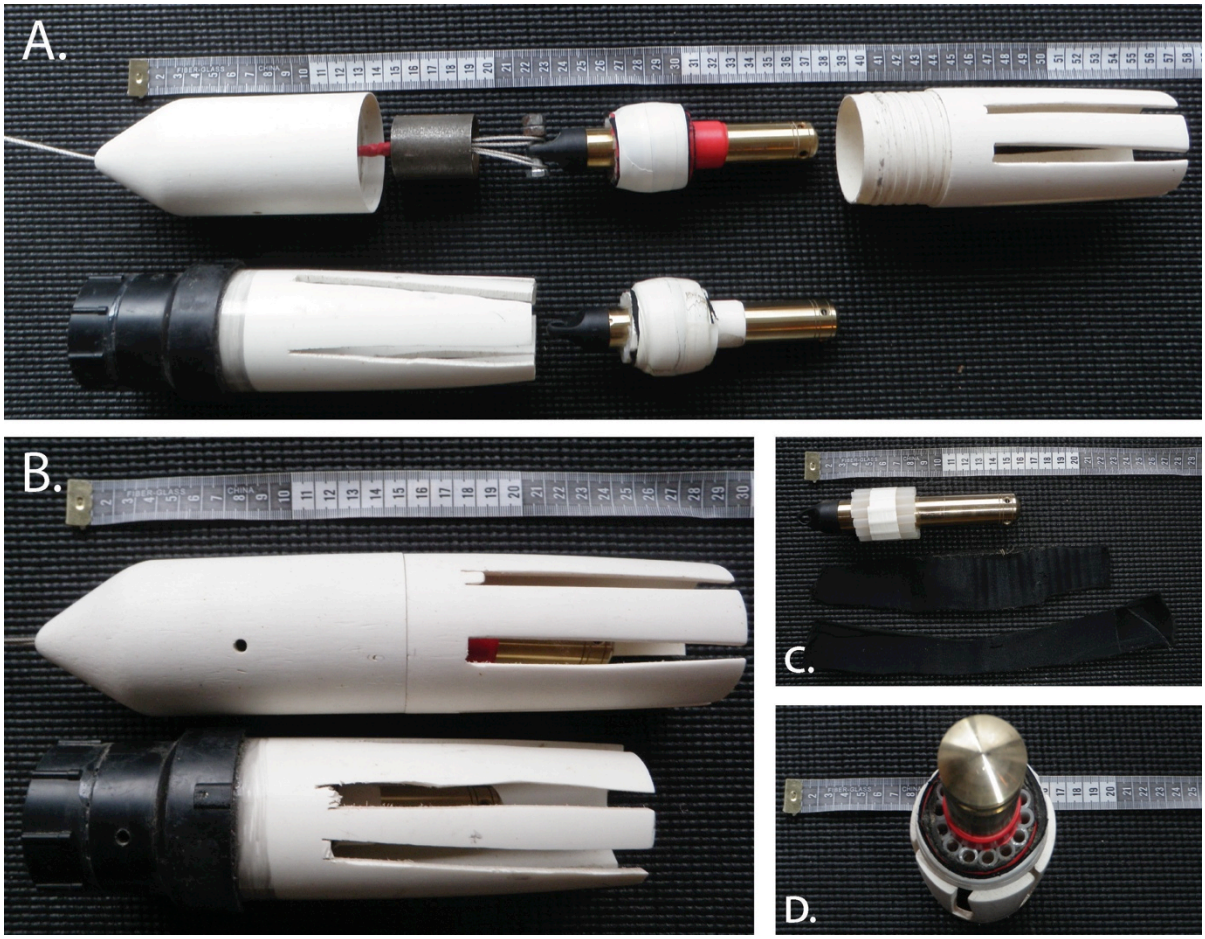

Figure 5.2 Construction of the drag probes. A PVC casing houses a Solinst levelogger thermistor (photo A). 180lb test wire, strung through the tip of the casing, attached to a rope lead, which runs to the boat. The test wire is attached to the cap of the levelogger. Above the cap, weights can be strung on the wire to allow the probe to achieve the desired buoyancy. Slits are cut into the upstream half of the casing, to maximize river flow past the thermistor sensor and to allow debris caught along the sides of the probe to slide out the upstream end. Although the riverbed probe was streamline as much as possible, this was not needed for the river surface probe (photo B). Several layers of material were wrapped around both leveloggers (photo C). The first layer was 0.5cm I.D. polyurethane tubing cut into 5cm lengths. This allowed water movement along the entire length of the probe (photo D). On top of the tubing several layers of neoprene were wrapped, to provide cushioning for the probe as the outside casing scraped along the riverbed.

Other equipment used during the surveys included the Magellan Mobile Mapper handheld device used for the FLIR surveys. This GPS device the recorded time and position of the canoe every one or two seconds during the survey. As with the FLIR surveys, the drag-probe measurements and GPS

datasets were combined though time signatures to yield datasets giving riverbed and river-surface temperatures, water level, and location data at one second intervals down the river.

All of the drag-probe surveys more or less followed the same procedure. Researchers arrived at the launch point between 10:00am and 11:00am. This allowed time for incoming solar radiation to increase the temperature of the river, hopefully increasing the contrast between it and discharging groundwater. The clocks on the probes, wristwatches, and GPS were synched one final time. The probes were activated, and placed in the river while the canoe was set up for the survey. Allowing the probes to equilibrate with the initial river temperature was important, because often they would heat up on route to the launch point. Next, the GPS router was attached at the stern of the canoe, to bring it as close to the probes as possible. Once the GPS was activated, the survey was ready to begin. One researcher sat in the front of the canoe, holding the line to the stream-bed probe. The second researcher sat in the back of the canoe and steered down the river. Paddling was avoided as much as possible to remain at the same velocity of the river, unless speed was needed for steering purposes.

Often, for various reasons, it was impossible to remain at the same velocity as the river. The canoe had to be steered around rocks or submerged deadfall, or the researchers needed to traverse the river to avoid becoming grounded on gravel-bars. Several riffle sections also proved to flow much faster than anticipated. During one survey, while flying down one of these riffle sections, the riverbed probe caught something on the riverbed and yanked the line out of the front researchers hands so forcefully that the canoe almost capsized. After that, the riverbed line was pulled in for fast moving riffle sections, so that the riverbed probe remained just submerged alongside the surface probe. Although the probe did not retain contact with the riverbed for these ripples, this likely did not impact the results of the surveys, as the riverbed and river-surface probes, with a few exceptions, gave the same temperature readings (See results, 5.3)

Once the exit point was reached, the time and location of the survey end was noted and data downloaded from the GPS and leveloggers, via a docking port, to a laptop. Everything was packed up and the team returned to the University of Waterloo.

Two sets of drag-probe surveys were completed down the discharge reach; the first in early July, and the second in mid September. Ideally, the first surveys would have been completed during low-flow conditions, but because the drag-probe surveys were the first step in a series of procedures – temperature profiling and sampling were to follow – they needed to be completed as early in the field season as possible. Throughout June, flow never reached baseflow conditions, and after the first week of July it was judged that the survey would have to be done before true baseflow conditions were

reached, or risk leaving no time in the field season to temperature profile and sample. Thus average flow conditions during the first set of drag probe surveys were 23.41 m^3s^{-1} and 31.37 m^3s^{-1}, or 38% and 39% greater than baseflow at Cambridge and Brantford, respectively.

The June surveys consisted of three separate runs down the discharge reach; one along the northwest bank, the second along the southeast bank, and the third down the middle of the river. This was to provide better spatial coverage of the riverbed. From Cambridge down to Brantford, the Grand River ranges between 50m and 80m wide. If only one survey was conducted down the thalweg of the river channel, groundwater discharge near the banks could be missed, and key sampling opportunities could be lost. By repeating the survey along each bank as well as the middle, it was expected that smaller areas of groundwater discharge could be discovered. It was also expected this would allow for a better comparison with the FLIR survey: seep discharge along the banks of the Grand could indicate where discharge is occurring to the riverbed, but because the river is so wide, this discharge may not extend beneath the entire river. With only one survey down the river, it was thought that discharge that was a riverbed continuation of the bank seeps could be missed.

Remaining in middle of the river for the third July survey proved challenging. At many locations, the Grand River thalweg crosses from one bank to the other, leaving shallow gravel bars in the middle of the river upon which the canoe easy got stuck. To avoid this, the canoe was positioned in the middle of the river when possible, but followed the thalweg when necessary.

The drag probe survey was repeated over September 13th and 14th, 2011. This time, the survey was completed under good baseflow conditions with the Galt and Brantford flow gauges reading 17.74 m^3s^{-1} and 22.14 m^3s^{-1}, or 4.35% and 0.64% greater flow than baseflow as defined for 2011, respectively (See chapter 2.7). The expectation was that, not only would the survey confirm suspected groundwater discharge locations discovered from the procedures that followed the first surveys, but that changes in the downstream temperature traces, due to lower flow conditions, would be observed.

The major difference in the second survey was that only one run, down the thalweg of the river, was completed. This was done for two reasons. First, the river level at base-flow conditions make canoeing large parts of the river impossible, unless the thalweg is followed. Second, analysis of the June surveys suggested that the probes could only pick up large, reach scale temperature trends (See discussion, section 5.4). Although the surveys did not perform as well as had been anticipated, useful data was gained that ultimately helped discover groundwater discharge locations to sample (see results and discussion, sections 5.3 and 5.4).

Temperature and water level data records were obtained from a stationary datalogger installed in the Glen Morris area, to provide a standard against which to compare the downstream Grand River temperature evolution recorded by the drag prove surveys.

5.2.2 Temperature Profiling

The theoretic foundation for the third temperature method has its origins in a branch of research using heat and temperature as a tracer for groundwater (Stallman 1965; Stonestrom and Constantz 2003; Conant 2004; Schmidt et al. 2007). The specific procedure is based loosely on that used by Conant (2004), with changes largely due to the difference in size between the two rivers investigated.

The method involves inserting a temperature probe a set distance into the riverbed, letting the temperature stabilize in the meter, and recording the measurement. The probe is pulled from the riverbed, then moved a set distance and the procedure is repeated; i.e., the temperature in the riverbed is "mapped" along the selected reach. Conant, (2004), developed an empirical relationship between the temperature below the riverbed, measured in this way, and vertical flux measurements ($L \cdot day^{-1}$) obtained through piezometers inserted along a 60m reach of the Pine River, Ontario, Canada. Schmidt et al. (2007), built upon this concept and used an analytical solution to the one-dimensional steady-state heat diffusion-advection equation to determine groundwater fluxes from the measured temperature data:

$$q_z = -\frac{K_{fs}}{\rho_f C_f Z} \ln \frac{T_{(z)} - T_L}{T_O - T_L} \quad (5.1)$$

Where:

q_z = Specific Darcy flux ($m \cdot s^{-1}$)

K_{fs} = Geometric mean of the thermal conductivity of the solid-fluid system ($J \cdot s^{-1} m^{-1} K^{-1}$)

ρ_f = Density of the fluid ($kg \cdot m^{-3}$)

C_f = Heat capacity of the fluid ($J \cdot kg^{-1} K^{-1}$)

z = Depth into the riverbed the probe is driven (m)

$T_{(z)}$ = Temperature at depth (z) (°C)

T_L = Temperature at the aquifer bottom (°C)

T_O = Temperature at the riverbed/river interface (°C)

$$K_{fs} = K_s^{(1-n)} + K_f^n \quad (5.2)$$

Where:

$K_s^{(1-n)}$ = Thermal conductivity of solids ($J \cdot s^{-1} m^{-1} K^{-1}$)

K_f^n = Thermal conductivity of the water ($J \cdot s^{-1} m^{-1} K^{-1}$)

n = porosity of the subsurface (-)

For this study, temperature profiling was used in two capacities. The first was at a site, just south of Glen Morris, where previous workers had noted potential non-WWTP sources of nitrate in the riverbed sediments (Encalada, 2008; Pastora, 2009). Here, during July and August 2010, and again on February 27th, 2011, temperature profiling was used to 'map' out the vertical flux of groundwater over a 60m by 160m area of riverbed. Because of the considerably larger area covered, no grid spacing was used as per the method of Conant (2004), but temperature measurements were taken at approximately 5m to 10m spacing, and GPS locations were recorded for each measurement. The second capacity involved using the temperature probes as a reconnaissance tool, from August 10th 2011 to August 17th 2011. As part of the larger effort to locate riverbed discharge along various locations down the discharge reach, temperature profiling was used along reaches where the drag probe surveys suggested discharge to the riverbed.

Each time the probes were used, solinst dataloggers were used to record surface water temperature and level data for the duration of the profiling. With the exception of February 27th, 2011, all of the profiling was done during the summer, and some diurnal fluctuation in surface water temperature (T_O) is expected. If the twenty-four hour moving average of the surface-water temperatures is essentially constant, then the average of the surface-water temperature over the profiling time period should be a decent estimate of quasi-steady state conditions (Schmidt et al., 2007). Figure 5.3 shows twenty-four hour moving averages for profiling over August 10th to 17th, 2011 for a GRCA datalogger and one installed for this research. The GRCA datalogger shows daily temperature maximums approximately twice the size of the other datalogger, but similar minimum daily values. Both twenty-four hour moving averages behave similarly over time, although the GRCA datalogger shows higher temperature values. It is suggested that the muted daily maximums of the other datalogger could be due to the discharge of cold-water tributaries in the vicinity of the datalogger: the FLIR survey indicates numerous runoff and seep discharge types nearby (Figure 4.1 – Datalogger is installed at the

same location the FLIR camera was tested at. Figure 4.3 – numerous tributaries and seeps along this stretch of the river). Therefore, the GRCA datalogger was used. Although the twenty-four hour moving average shows fluctuations on the order of 2°C, there are no evident long-term trends, and the surface-water conditions are assumed a decent approximation for quasi steady-state conditions. T_O calculations were made for the other profiling surveys as well. For details, see Herrera (2012).

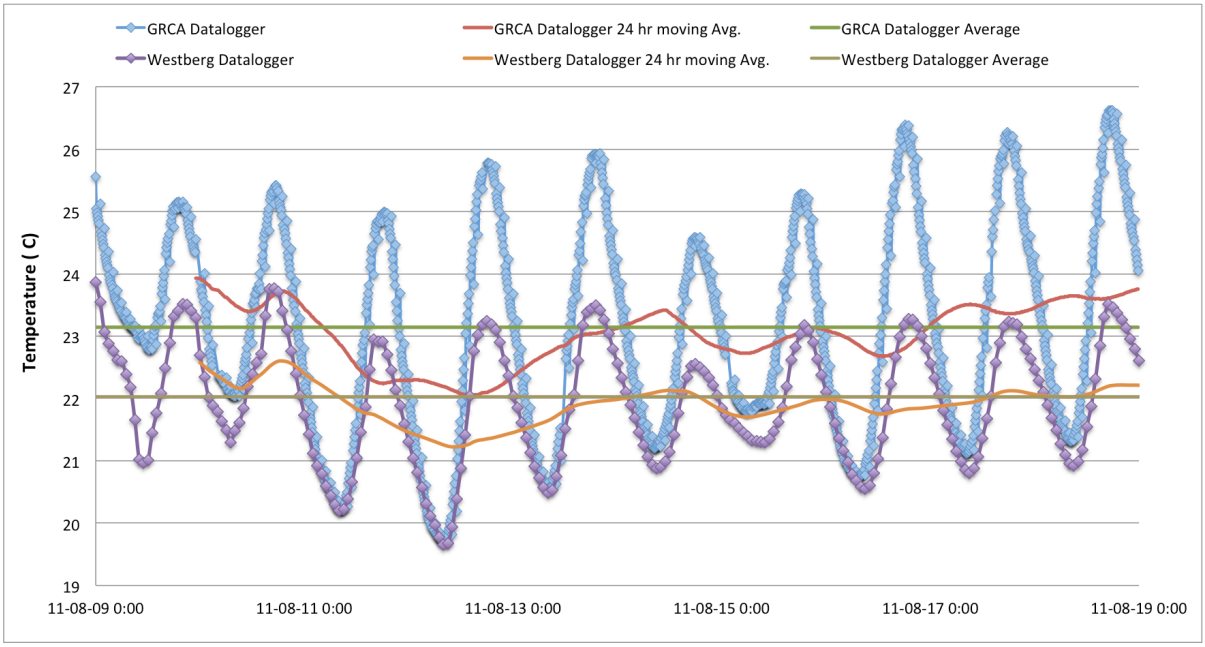

Figure 5.3 Surface-water temperatures during temperature profiling obtained from a GRCA levelogger installed near Glen Morris Bridge and a second installed at the same site that the FLIR camera was tested (see figure 4.1). Although there is some variability in the 24 hr moving averages, there is no obvious long-term trend and it was deemed appropriate to average the diurnal fluctuations from the GRCA datalogger to obtain a value for T_O. Data from the second levelogger was not used, as daily maximums appear dampened relative to the GRCA logger (possibly due to nearby cold-water tributaries).

5.2.3 Temperature Profile Construction

The temperature probes were constructed to minimize internal heat transfer during insertion without compromising durability. Along the discharge reach, the riverbed material alternates between bedrock and modern fluvial deposits derived from the erosion of tills. Considerable force was needed to penetrate this bed material, which the probes had to be designed to withstand.

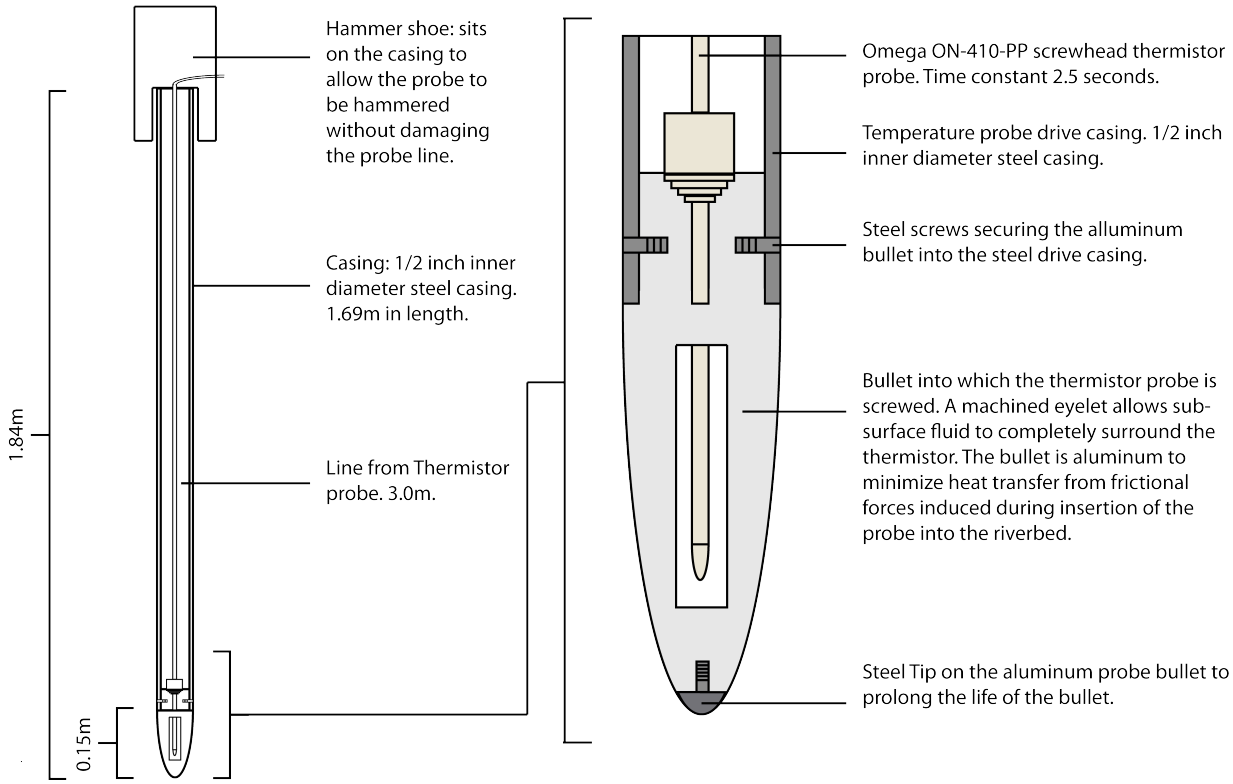

Figure 5.4 Construction of probes used for temperature profiling.

The general construction of the probes is illustrated in figure 5.4. The actual temperature sensor, a 406 series Oakton screw-head thermistor, is screwed into a drive-point head, which is itself set into a rod 1.69m in length. The drive-point head is machined so that most of the thermistor probe is in contact with sediments and pore fluids, not the aluminum casing. The transmission cable travels from the thermistor out the top of the rods to be plugged into a Barnet temperature-recording meter. A cylindrical shoe with an arched cut-out along its bottom edge is slipped over the open, upper end of the rods. This shoe receives the impact from the hammer, and transfers it into the rods and drivepoint head while the probe is being inserted into the riverbed. The cable exits the rods through the cut-out untouched.

Three separate probes were designed. The first was constructed with an aluminum drive-point head and a ¼ inch I.D. aluminum rod through which the cable was routed. It was anticipated that the thinnest probe possible would minimize resistance during insertion into the riverbed, and that the aluminum head would reduce the transfer of heat by friction from the drive-point to the thermistor (personal communication, Dr. Brewster Conant Jr. August 2010). The second probe was constructed

from ½ inch steel casing, in the event that the riverbed proved impermeable to the thinner aluminum probe. Greater force could be applied to insert this probe, force that would bend or otherwise break the more frail aluminum probe. To minimize heat transfer, the ½ inch steel probe also had an aluminum drive-point head; to maximize durability, the drive-point head was capped with a steel insert (Figure 5.4). The final temperature probe was also constructed from ½ inch steel casing, and also had a steel drive-point head. It was the most durable, but also possibly the most influenced by heat, created through frictional forces as the probe moves into the riverbed, being transferred to the thermistor through the steel drive-point head.

5.2.4 Testing the Temperature Probes

The probes were first tested in the Grand River during August 2010. The temperature 20 cm below the riverbed was mapped over an area of approximately 60m x 160m at a site where previous researchers found evidence of groundwater discharge (Figure 5.5). Although the profiling took several days to complete during which ambient temperature conditions varied considerably, areas of significant temperature contrasts were noted within the riverbed which resulted in a wide variety of vertical groundwater flux calculations and a decent understanding of where groundwater discharges to the riverbed along this stretch of the Grand River. To read about this study site in more detail, the reader is referred to Herrera (2012).

During this test run it became apparent that the ¼ inch aluminum probe would not withstand the sledge blows needed to insert the probe any distance into the cobble riverbed. Several times, the rod bent and the thermistor transmission cable split from the temperature sensor after numerous blows from the hammer. The steel probes proved more resilient, but the thermistors still tended to split apart from impact forces from the hammer blows. Finally, a method similar to that of Baxter et al. (2003) for inserting mini-piezometers was adopted. A steel spike was used to create most of the hole, after which the temperature probe was inserted and gently tapped just deep enough to ensure the probe tip was completely inserted into undisturbed sediment. To check the precision of this method, several measurements were made pounding the probe the whole 20cm into the subsurface directly adjacent to measurements made with the steel spike and probe method. Temperatures recorded using the second method were generally within 0.2°C of first, a satisfactory result given the difficulty in taking a duplicate measurement in exactly the same location.

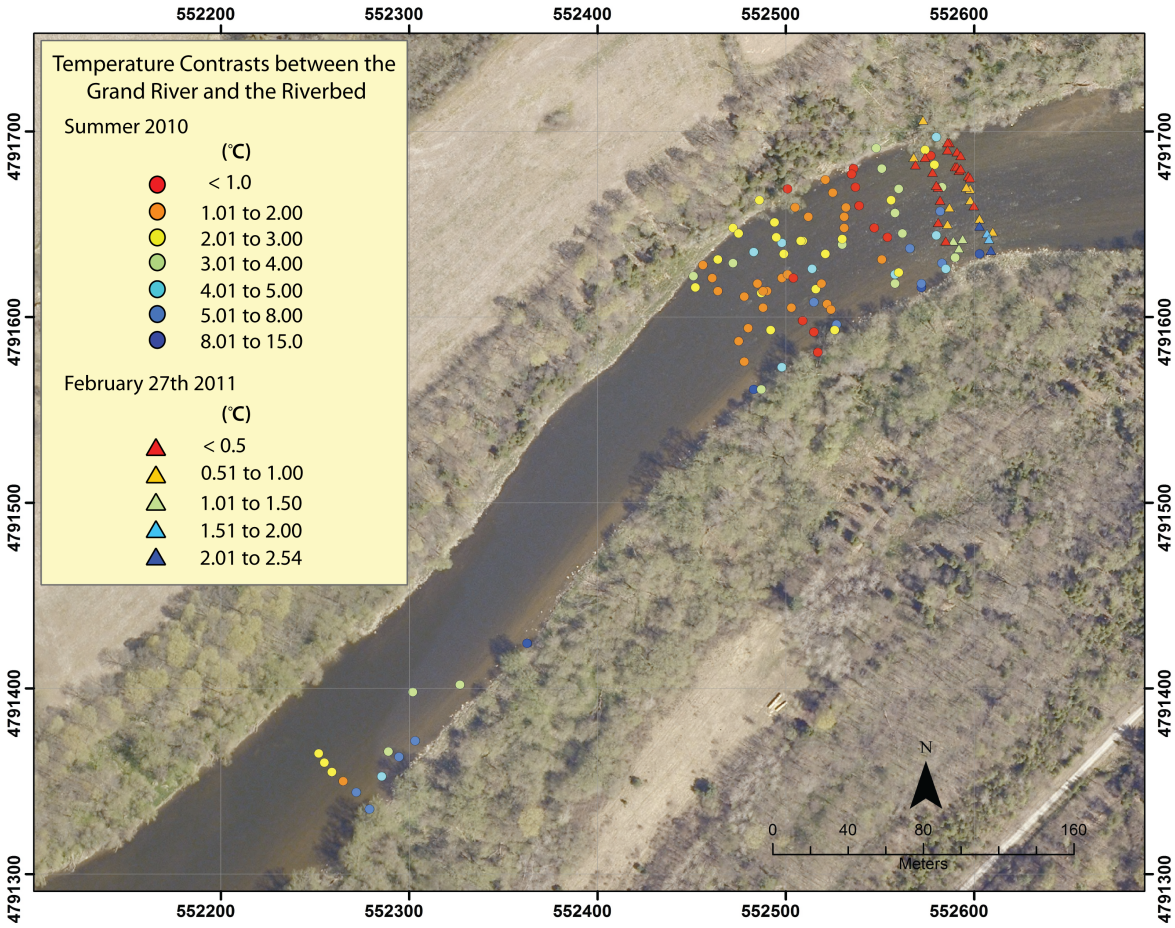

Figure 5.5 Temperature profiling at the Glen Morris study sites. Temperatures are taken approximately 20cm into the riverbed. Profiling was completed over several non-consecutive days during the summer of 2010, under variable ambient temperature conditions. Because this limits the possibility of obtaining a representative T_O value, only temperature contrasts are shown, not vertical flux calculations. In contrast, profiling during February 2011 was completed in one day, with below zero ambient temperatures. Thus, although shown in blue to be consistent with the summer data, the groundwater is warmer than the river and temperatures into the riverbed increase. Contrasts are also lower in magnitude than those recorded during the summer, even in similar locations. This may be due to meter scale discharge flux heterogeneity, or it may be due to differences in river stage.

On February 27th, 2011, the probes were used a second time along the same discharge reach (Figure 5.5). A considerable drawback of the summer profiling was that, because the riverbed area that was mapped was so large, the profiling was completed over several days, some non-consecutive. This results in a poor approximation of the T_O term, which reduces the validity of the quasi steady-state condition necessary to calculate the discharge flux from equation (5.1). For several days around February 27th, 2010, river temperatures stayed a degree or two above zero, resulting a good

approximation of T_O consistent with a quasi steady-state surface temperature boundary. As detailed in chapter three, winter can present optimal conditions under which to utilize the temperature probes as the T_O term in equation (5.1) is essentially constant – i.e., there is no need to calculate an average temperature to condense daily temperature oscillations into one useable value. In addition, as the best method of probe insertion had been determined earlier, the profiling went smoother, more quickly, and no probes were broken.

5.2.5 Temperature Profiling as a Reconnaissance Tool

Further temperature profiling was conducted during July and August of 2011, immediately after the discharge reach was surveyed with the drag probes. While profiling in February was done to test the probes and to determine a vertical groundwater flux along a small reach of the Grand, profiling in July and August 2011 was used as a reconnaissance tool. Sub-reaches where groundwater appeared to be discharging, based on drag probe survey results, were targeted. The intended procedure of the temperature method involved a logical transition – a smooth decrease in scale – from the drag probe surveys to temperature profiling. It had been anticipated that the drag probe surveys would indicate suitable reaches for further investigation; the results, however, only indicated one reach of considerable discharge, and it was approximately six kilometers long; too long to profile at the same sort of resolution as the profiling completed in August 2010 and February 2011.

The indicated reach, therefore, was profiled at approximately 25m intervals. At each point, a temperature measurement and GPS location were recorded. Rather than obtaining a high resolution 'map' of riverbed temperatures, this resulted in data at specific, unrelated points along the reach. This was repeated along several other stretches of the discharge reach. As no other stretch was explicitly suggested for profiling by the drag probe data, other reaches were profiled based on access, and on obtaining a decent distribution of temperature measurements along the discharge reach.

5.3 Results

5.3.1 Drag Probe Survey July 2011

Figures 5.6 to 5.142 illustrate the results of the drag probe surveys completed in July 2011. Figure 5.6 shows both the temperature data from both the surface and the riverbed leveloggers for exemplary purposes. With the exception of three anomalous situations, the two loggers recorded essentially the same temperature during all surveys. The first exception occurred when the probes were taken out of

water. This occurs between Paris and Brantford, where a portage must be taken to circumvent a weir; water evaporated from each logger at different rates, which caused each logger to change temperature differently until they were put back in the river downstream of the weir. Once placed back into the river, they were given 10 to 15 minutes to re-equilibrate with the stream temperature. This portage is seen on figures 5.10 to 5.12 and 5.14, where the depth trace goes to zero, approximately 2/3rds down the Paris to Brantford reach. The second exception when logger temperatures differed is when the riverbed logger got caught on debris on the riverbed, and the researchers needed to canoe back upstream to retrieve it. In this case, the riverbed logger stayed stationary, while the surface logger moved with the canoe as the riverbed logger was recovered. The third exception was when a large cold-water tributary enters the Grand. This would occasionally change the temperature of the riverbed logger to a greater degree than the surface logger.

Figure 5.6 shows that the riverbed logger consistently recorded a 0.2°C higher temperature than the surface levelogger. This is not due to a real difference in temperature between the surface and riverbed, but reflects the accuracy associated with the levelogger temperature measurements. Solinst states they are accurate to approximately 0.2°C (http://www.solinst.com). Because the temperature differences between loggers were minimal and the causes were not groundwater related, the surface trace is removed from subsequent figures to enhance the clarity of the figures.

Table 5.1 Ambient temperature conditions* during drag probe surveys

				Brantford Ambient Daily Temperature Fluctuations (°C)			Kitchener Ambient Daily Temperature Fluctuations (°C)		
Date	Reach	Survey Start	Survey End	Min	Mean	Max	Min	Mean	Max
06-30-11	Cambridge to Paris	10:51am	4:59pm	11	18.5	26	7.1	15.8	24.5
07-01-11	Paris to Brantford	11:11am	5:35pm	9.5	18.5	27.5	6.9	17.2	27.4
07-04-11	Cambridge to Paris	10:56am	5:16pm	16	22	28	12.2	19.1	25.9
07-05-11	Paris to Brantford	10:18am	4:07pm	14	21	28	9.9	19.8	29.6
07-06-11	Cambridge to Paris	11:00am	5:52pm	21.8	21.4	30	14.4	21.1	27.8
07-07-11	Paris to Brantford	10:10am	5:07pm	16.9	21.7	26.5	13.1	19.5	27.8
09-13-11	Cambridge to Paris	11:10am	5:58pm	NA	NA	26.2	7.4	15.5	23.6
09-14-11	Paris to Brantford	10:10am	3:50pm	10.4	15.6	20.8	4.1	12.3	20.4

***Data from National Climate Archives: http://climate.weatheroffice.gc.ca/climateData/canada_e.html)**

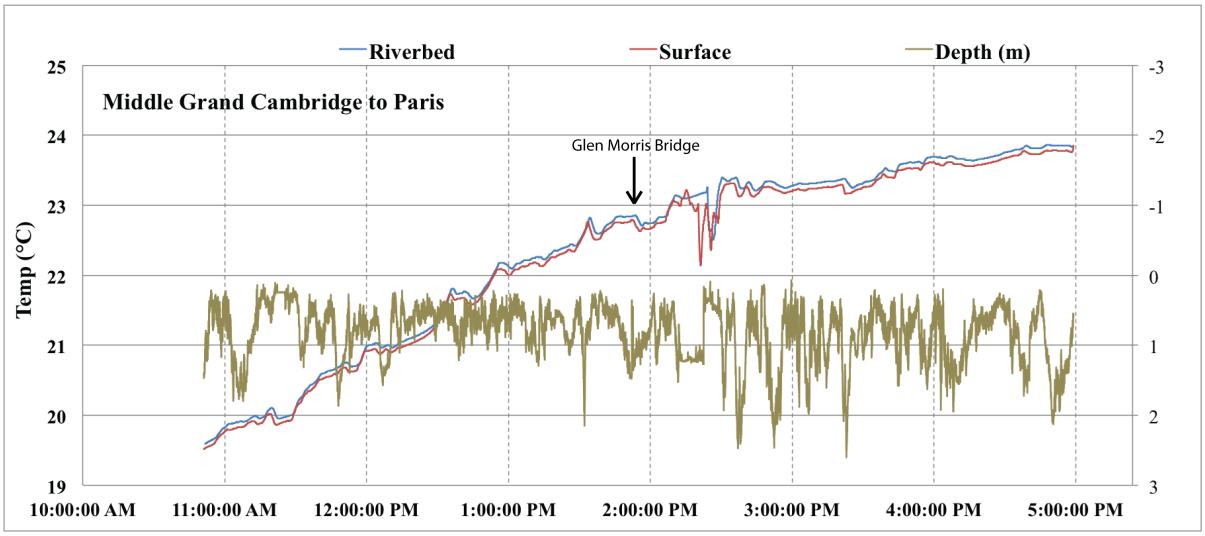

Figure 5.6 Results of the June 2011 drag probe survey from Cambridge to Paris down the middle of the Grand River channel. Both the surface and riverbed loggers are shown in this figure to illustrate how, with a few exceptions, vertical temperature gradients within the Grand are minimal. The deviation between loggers just after the Glen Morris Bridge is because the riverbed logger got stuck, and approximately 15 minutes was spent retrieving it.

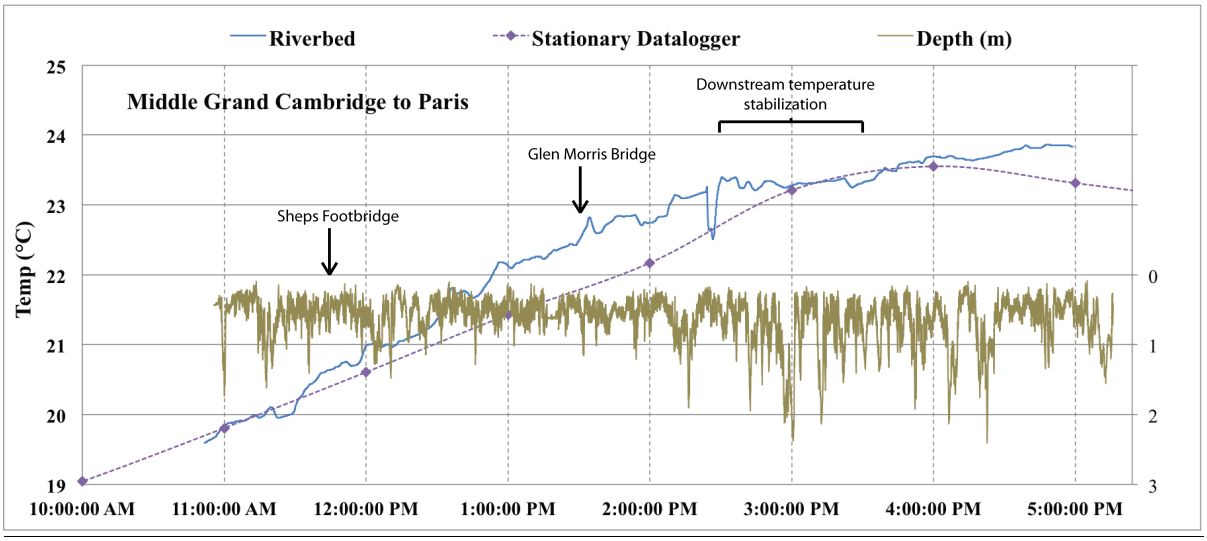

Figure 5.7 Results from the June 2011 drag probe survey from Cambridge to Paris down the middle of the Grand River. Temperatures between the two stationary dataloggers and the riverbed drag probe are in good agreement. A reach several kilometers in length downstream of the Glen Morris Bridge shows stabilizing temperatures while the stationary dataloggers continue to show increasing temperatures.

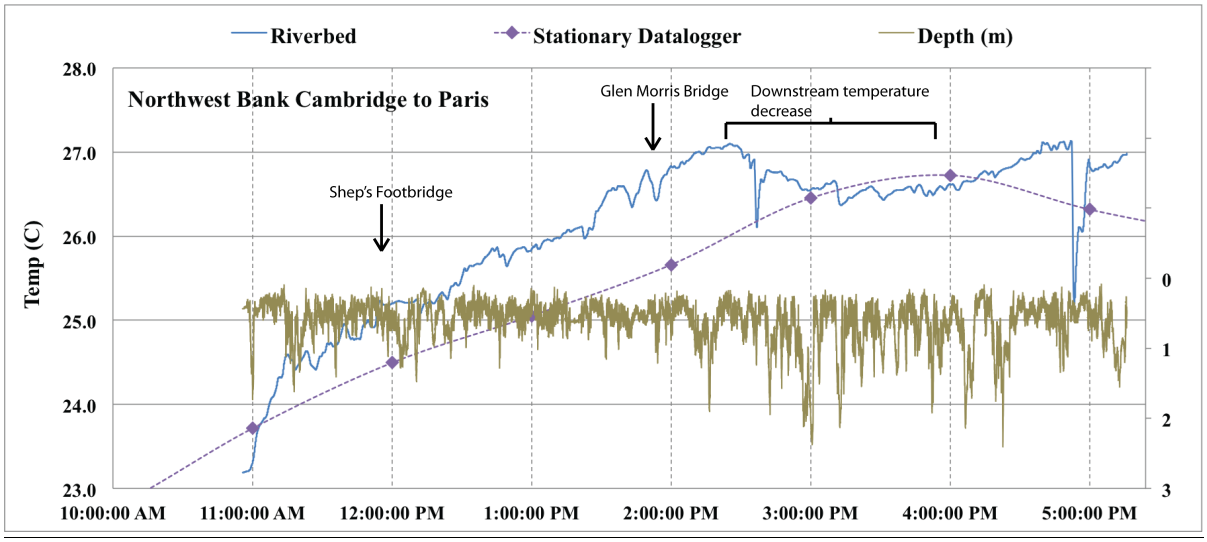

Figure 5.8 Results from the June 2011 drag probe survey from Cambridge to Paris down the northwest bank of the Grand River. The trace shows a similar temperature evolution to the middle trace (Figure 5.7 above) but a larger temperature decrease south of the Glen Morris Bridge is noted. Again, the stationary loggers continue to record increasing temperatures.

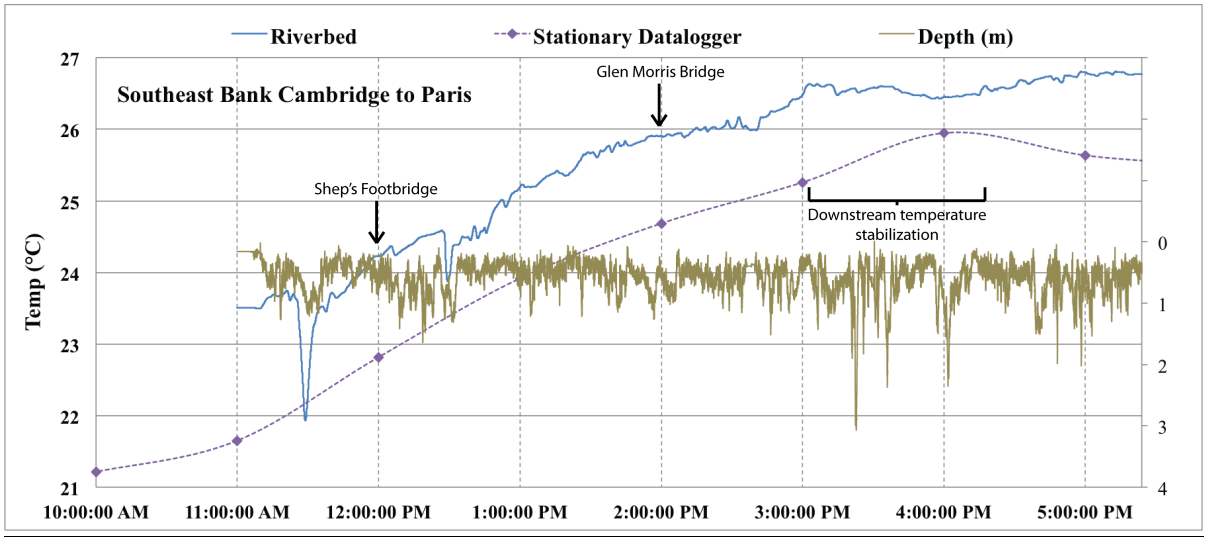

Figure 5.9 Results from the June 2001 drag probe survey from Cambridge to Paris down the southeast bank of the Grand River. Same general trend as the previous Cambridge to Paris figures, although the temperature decrease south of Glen Morris Bridge seen along the northwest bank is missing. Instead, only a short temperature stabilization is noted.

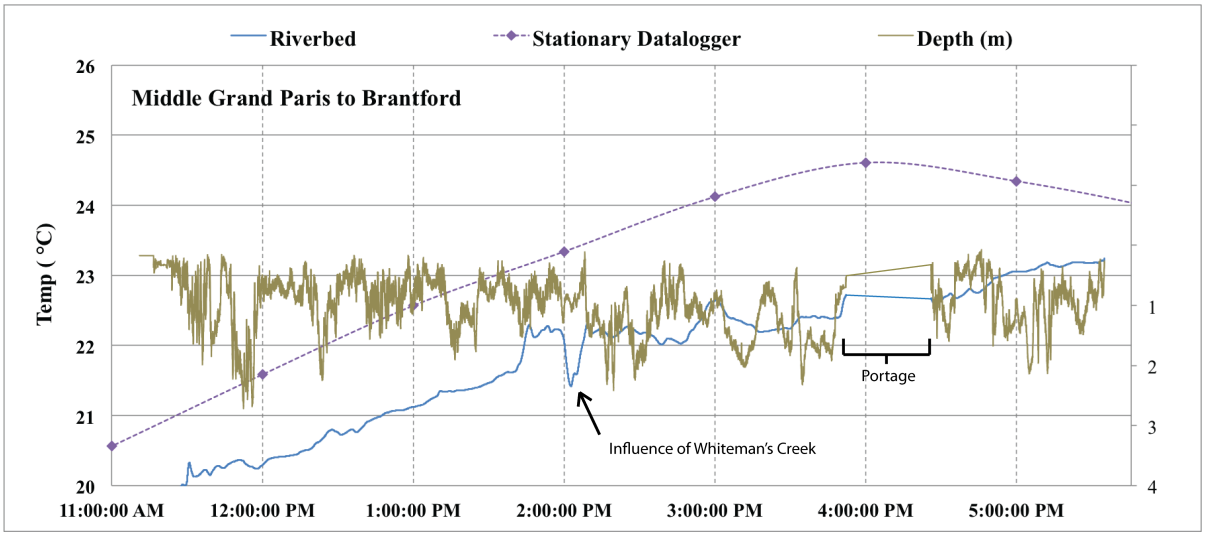

Figure 5.10 Results from the June 2011 drag probe survey from Paris to Brantford down the middle of the Grand River channel. The temperature of the drag probe is below that of the stationary loggers for the entire stretch (loggers are located upstream near Glen Morris). The downstream temperature increases at a slower rate than between Cambridge and Paris. No considerable temperature decreases are apparent.

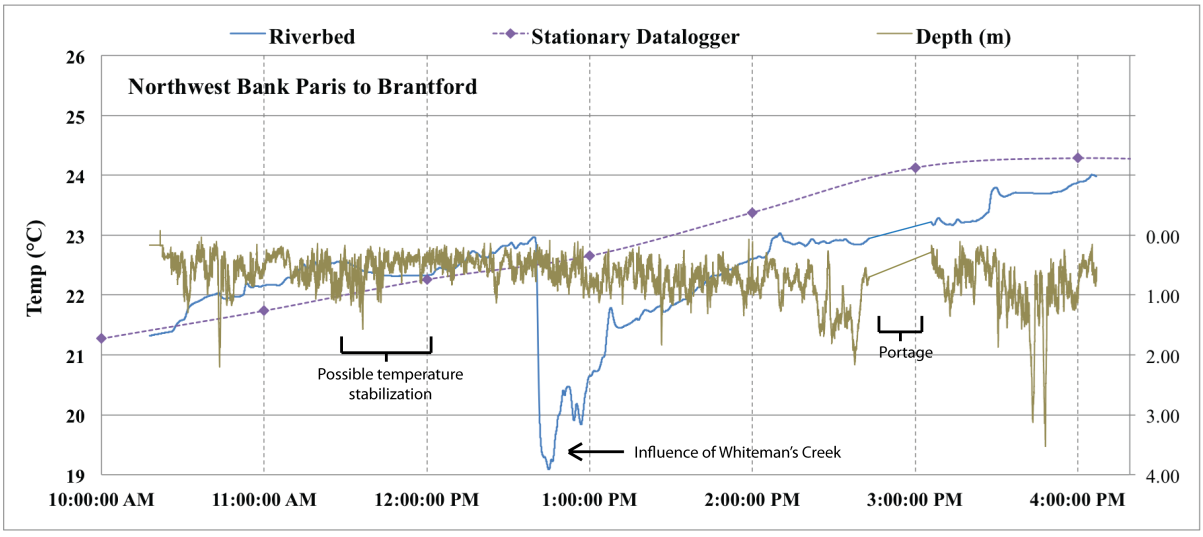

Figure 5.11 Results from the June 2011 drag probe survey from Paris to Brantford down the northwest bank of the Grand River. Similar to the middle trace along this reach, the temperature of the drag probe survey is always lower than that of the stationary leveloggers upstream. Temperatures increase relatively little downstream, with the exception of where Whiteman's Creek converges with the Grand River.

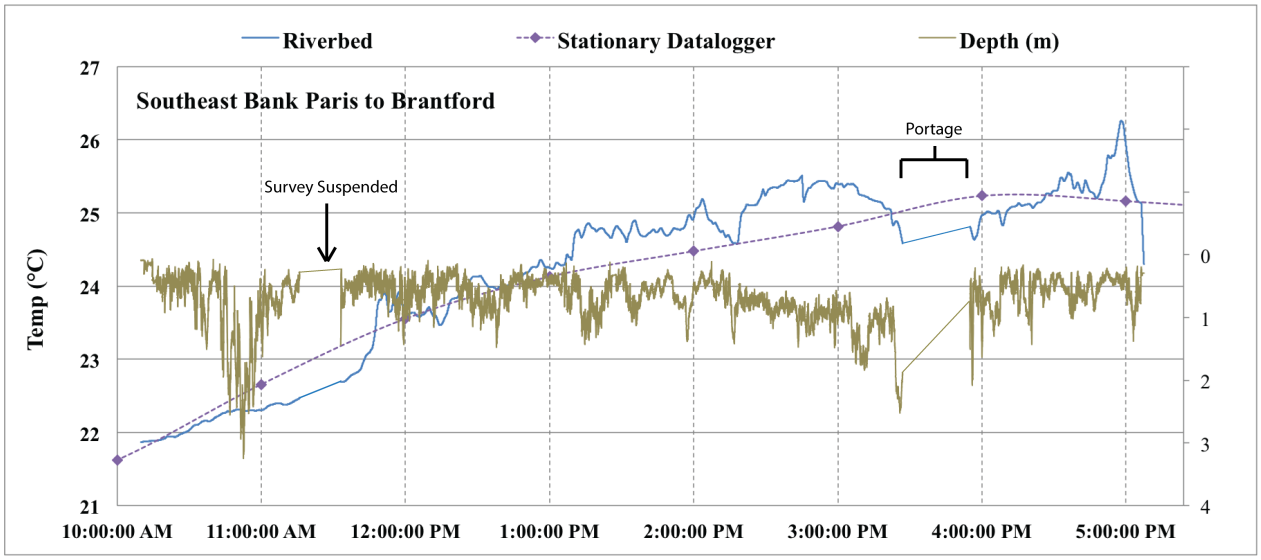

Figure 5.12 Results from the June 2011 drag probe survey from Paris to Brantford down the southeast bank of the Grand River. Temperatures are fairly consistent between the levelogger upstream and the drag probe. The survey was suspended for 10 minutes at 11:30am, during which the probe sat in shallow water clearly warmer than the main river channel.

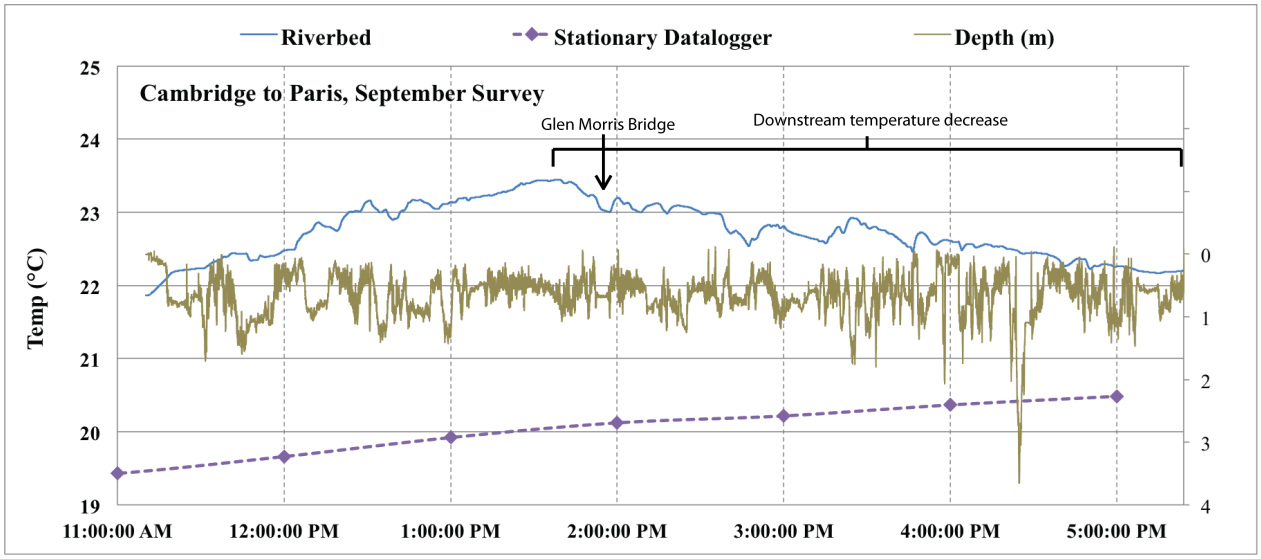

Figure 5.13 Results from the September 2011 drag probe survey from Cambridge to Paris down the thalweg of the Grand River. The temperature of the stationary logger is lower than the drag probe, but continually increases throughout the day. The drag probe shows a considerable decrease in temperature beginning before the Glen Morris Bridge and continuing almost down to Paris.

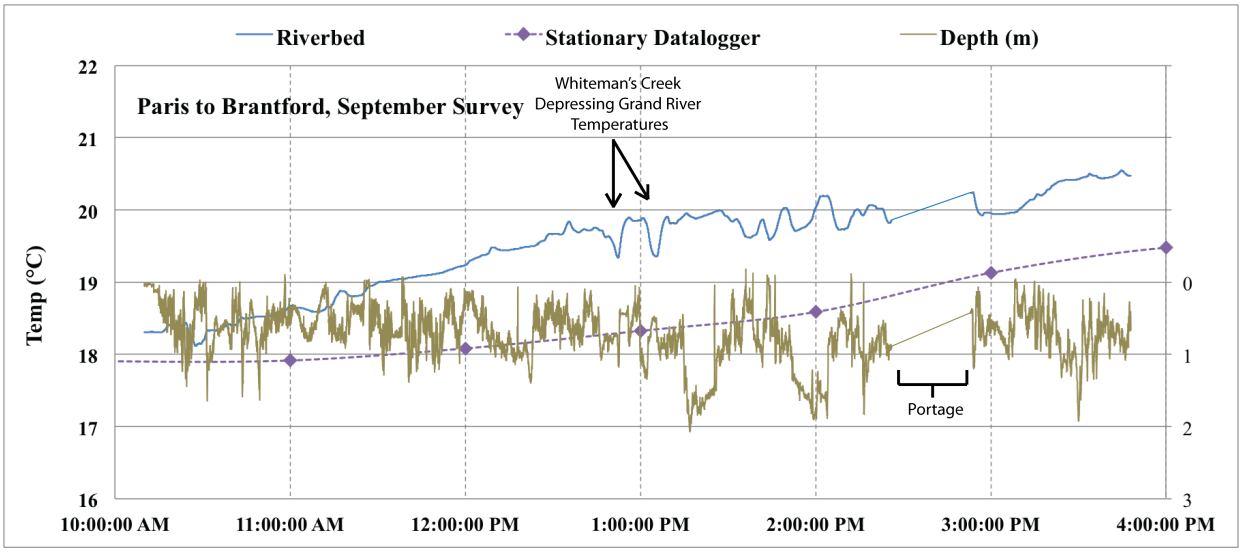

Figure 5.14 Results from the September 2011 drag probe survey from Paris to Brantford down the thalweg of the Grand River. Whiteman's Creek causes two dips in temperature as the canoe moves laterally across the river channel, away and then towards the northwest bank, as the canoe follows the thalweg downstream. No other temperature anomalies due to the influence of groundwater are apparent.

5.3.2 Temperature Profiling

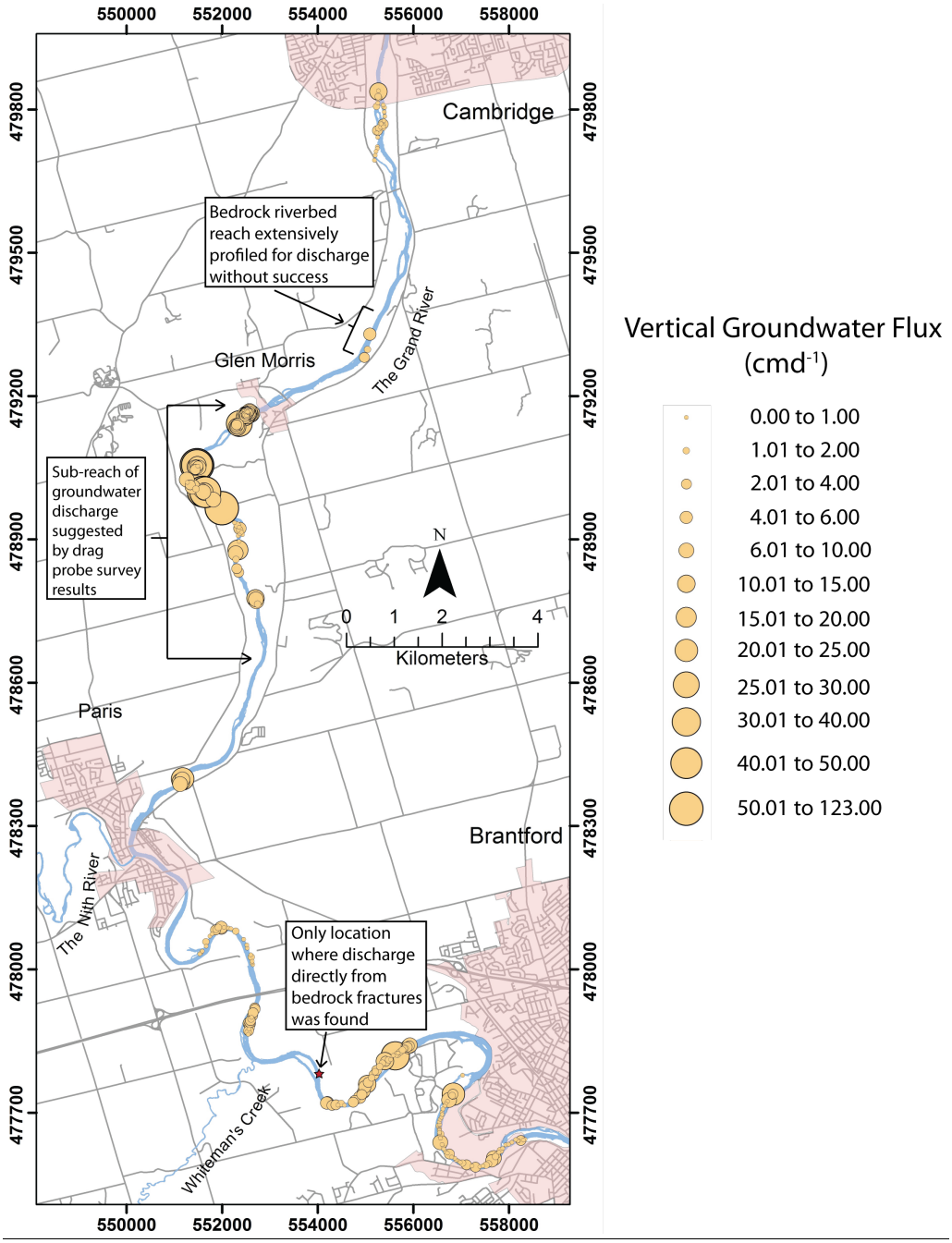

Figure 5.15 Locations where temperature measurements were taken in the riverbed along the discharge reach from February 2011 profiling and summer 2011 reconnaissance profiling. The largest vertical flux calculations were found to be in the same general area as both considerable bank seepage, highlighted by the FLIR survey (discharge reaches three and four on figure 4.3), and the strongest in-stream temperature decreases noted during the June and September drag probe surveys. Other discharge locations were also found, although with lower fluxes.

5.4 Discussion

5.4.1 Drag Probe Surveys

July 2011 Cambridge to Paris

The three downstream temperature traces from Cambridge to Paris display similar large-scale characteristics. All three profiles show a relatively consistent increase in temperature until after the Glen Morris Bridge. After the bridge, temperatures do not increase as strongly, and the degree to which this occurs varies between profiles.

The northwest bank profile shows a temperature decrease of approximately 0.6°C over six kilometers before continuing to increase. There could be several possible causes of this. As the temperatures of both the GRCA and independent dataloggers installed in the Glen Morris region continue to increase as the temperature of the drag probe decreases, the decrease is not likely caused by a drop in ambient temperatures or incoming solar radiation, both of which would affect all three dataloggers. Mixing of cold-water tributaries can also be ruled out. While there is a large cold-water tributary at the beginning of the temperature decrease, there is larger, and considerably colder one, at the end of the northwest bank trace (Figure 5.8). Both these cold-water tributaries cause a sharp drop in temperature, but soon afterwards the temperature trace rebounds, and continues along a normal, increasing daytime trajectory. The temperature decrease downstream of the bridge, therefore, suggests a continuous input of colder water over a longer reach. This interpretation is supported by the FLIR survey; one area of considerable seepage along the northwest bank was identified in this same stretch of the Grand (discharge reach 3, Figure 4.3).

In contrast to the northwest bank temperature trace, there is no strong temperature decrease along the southwest bank profile. Instead, temperatures stabilize just downstream from the Glen Morris Bridge (Figure 5.9). Changing ambient conditions do not appear to be influencing this stabilization, as the independent, stationary datalogger shows a consistent temperature increase (the GRCA datalogger didn't record data for the entire duration of this drag-probe survey). Again, the cause is suggested to be cold-water input from groundwater. Results from the FLIR survey support this conclusion as well; considerable groundwater discharge activity along the southeast bank was also noted just south of Glen Morris Bridge (Figure 4.3).

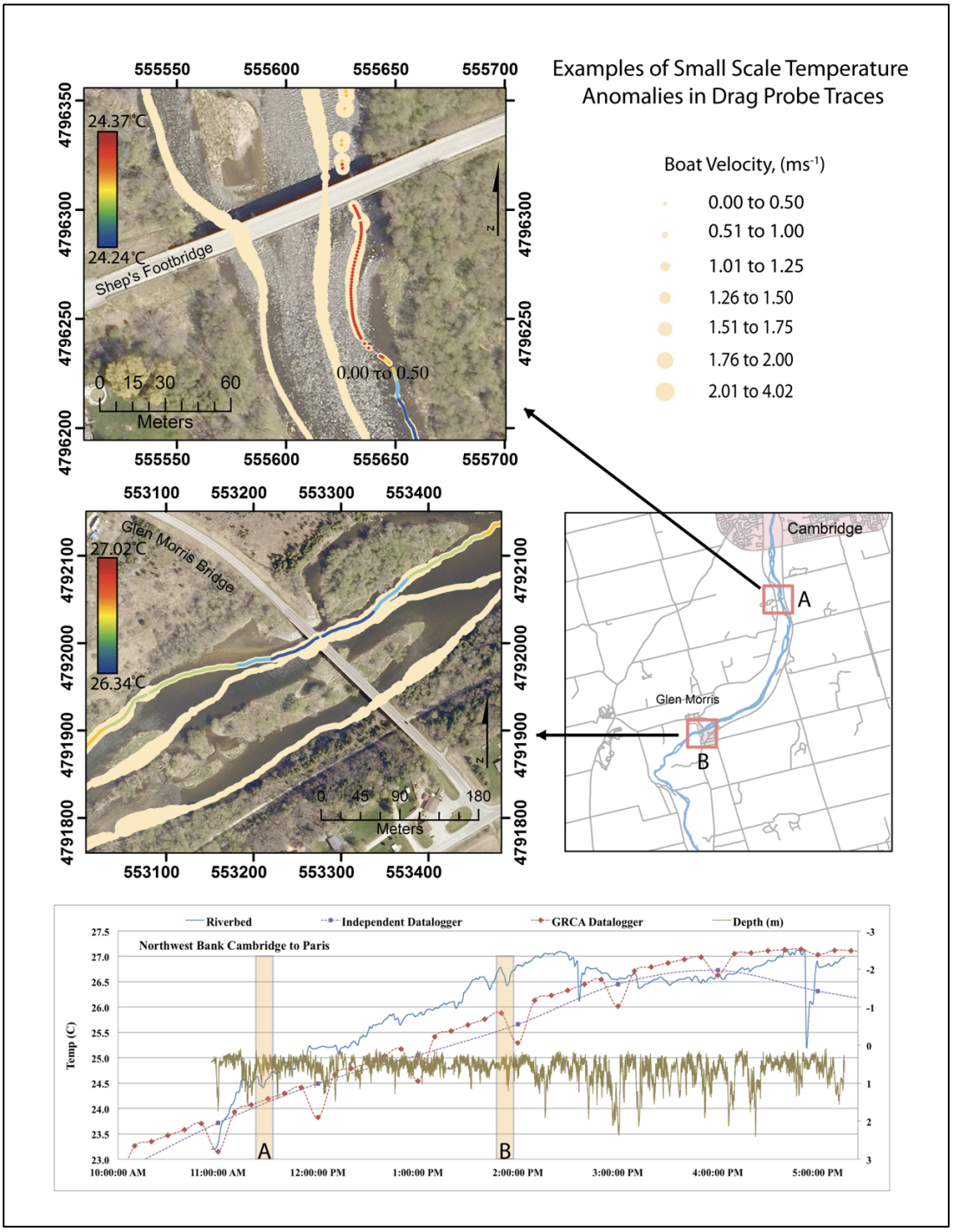

Figure 5.16 Examples of small scale temperature fluctuations in the drag probe traces. Example (A) is a temperature transition from the river thalweg to a more stagnant eddy. Example (B) is unexplained; the temperature decrease starts before the side channel, which may be affected by cold-water inputs, re-joins the main channel; i.e., there must be some other additional temperature influence.

The middle temperature trace shows a small temperature stabilization after the Glen Morris Bridge. This may suggest, again, that cumulative discharge downriver is depressing stream temperatures. If so, discharge may primarily occur along the banks, as the middle stream trace shows the smallest contrast from the standard temperature curve illustrated by the stationary dataloggers.

In addition to large-scale characteristics, there are numerous smaller features within the drag probe traces that elucidate processes occurring within the river. Already mentioned are the cold-water tributaries, which in the temperature traces, are essentially point-source additions of cold water to the Grand River. Most of the tributaries do not affect temperatures for long, although strong initial depressions are clear. These tributaries also do not appear much, or at all, in the other traces. The cold-water tributary at the start of the temperature decrease in the northwest bank trace only shows up slightly in the middle trace, and the larger, colder tributary farther downstream doesn't show up at all. There are also two cold-water tributaries that enter the Grand from the southeast bank that make no impression in either the northwest bank or middle traces.

Other small-scale temperature fluctuations noted within the profiles are difficult to explain. These features don't seem to correlate well with anything: not depth, shading, stream velocity, or known groundwater inputs. It was originally thought that these smaller structures might be indicative of concentrated groundwater discharge areas, but after extensive exploration temperature profiling several of these areas, it was concluded that that was likely not case. Figure 5.16 illustrates two examples of small-scale temperature fluctuations. Example (A) occurs as the southwest bank trace crossed from a fast flowing riffle section into a much slower moving eddy. At the same time, temperature decreases abruptly (abet only slightly). One explanation is that because the riffle section is much more shallow than the eddy, the riverbed absorbs more solar radiation which results in a slightly higher temperature. The eddy could also be shaded. Example (B) presents a second perplexing temperature trend. Two decreases are noted, in quick succession, of which example (B) is the second. The side channel upstream of the Glen Morris Bridge contained input from cold-water tributaries draining adjacent wetlands, which could account for the temperature decrease downstream of the bridge. The decrease, however, begins upstream of the bridge. This may be due to other cold-water additions further upstream, but it remains unclear. This area was carefully profiled for groundwater discharge, but no points of strong vertical discharge were found.

The depth profiles for all three drag-probe surveys are similar. Upstream of Glen Morris, there is a section approximately eight km long that appears to have subdued pool/riffle topography. This correlates well with sections of the stream known to run over bedrock. Before and after this bedrock

section, pool and riffle sequences dominate, with the deepest pools, approximately three meters in depth, occurring along the southeast bank.

Upstream of Glen Morris, all three downstream traces show temperatures elevated relative to the stationary dataloggers. This was not expected, as there are a considerable number of cold-water tributaries, fed from spring discharge higher up the moraines, that enter the Grand along this reach (see Figure 4.3). These elevated temperatures could be due, in part, to the bedrock surface itself. Bedrock presents a more uniform surface than unconsolidated sediments, and may absorb more solar radiation – the uneven surface of unconsolidated sediment tends to scatter incoming radiation.

July 2011 Paris to Brantford

The drag probe profiles from Paris to Brantford all show slowly increasing downstream temperatures, without the type of decrease or stabilization noted in the profiles upstream. The rate at which temperatures increase downstream was lower for all three profiles than between Cambridge and Paris (i.e., the temperature curve was flatter). The northwest bank profile shows a small temperature stabilization and a slight temperature decrease from approximately 11:30am to 12:00pm (Figure 5.11). This is the most significant temperature change, in all three traces, that could possibly be attributed to groundwater discharge.

The northwest bank shows a very sharp, strong decrease in temperature as Whiteman's Creek converges with the Grand River: in contrast with the cold-water tributaries entering the Grand between Cambridge and Paris, Whiteman's Creek has sufficient volume to depress temperatures along the northwest bank for several kilometers (Figure 5.11). There is a smaller, secondary decrease in temperature just after the first initial plunge, which is the result of moving away from the northwest bank laterally across the river. It was not always possible to stay directly adjacent to the northwest bank for the entire survey, and when the research boat moved away from the bank, temperatures increase. When the boat moves towards the bank, temperatures decrease. In a similar fashion, the middle river drag survey profile shows only a slight temperature change due to the addition of Whiteman's Creek. During the stretch of river where the northwest bank trace shows temperatures rebounding after the convergence of Whiteman's Creek, the middle survey shows only a temperature stabilization, which may or may not be related. Whiteman's Creek has no obvious effect on the temperature trace of the southeast bank.

September 2011 Cambridge to Paris

The September survey down the thalweg agreed fairly well with the July surveys in terms of large-scale features. The Cambridge to Paris survey shows the same initial type of temperature increase captured in all three July traces. The subsequent temperature decrease, however, is more pronounced, starts before Glen Morris Bridge rather than after, and continues almost all the way to Paris. The temperature decrease is large enough that the temperature recorded at the end of the survey in Paris is only slightly higher than the temperature recorded at the beginning of the survey, five hours earlier. The stationary dataloggers in Glen Morris plot the expected daily diurnal temperature increase, refuting the possibility that this temperature decrease could be due to environmental conditions rather than groundwater discharge (Figure 5.13).

If the temperature decrease is caused by groundwater discharge, then the more pronounced decrease in the September survey could be a function of the lower streamflow conditions. During the September survey, the flow gauge in Cambridge measured 17.74 m^3s^{-1}, only slightly greater than baseflow. During the June/July surveys, streamflow at Cambridge averaged 23.41 m^3s^{-1}, or 38% greater than baseflow. Groundwater discharge in September would be a greater proportion of streamflow than it would be in June, and this may be in the temperature trace. River stage was also lower in September than it was in June; this would have increased the discharge flux beneath the riverbed, resulting in more groundwater in the Grand in September, and therefore having a greater affect on in-stream temperatures.

The September 2011 Paris to Brantford stream trace is also similar to the profiles completed in June. There is only a small, abrupt, doubled temperature decrease at the convergence of Whiteman's Creek and the Grand. This double dip in temperature is, similar to the Paris to Brantford northwest bank trace, related to lateral movement across the grand (Figure 5.14).

5.4.2 Drag Probe Survey Limitations

The Solinst levelogger gold probes provided only a muted depiction of temperature changes along the Grand. The temperature increase at 11:30am in figure 5.12 provides an example of this. Here, the survey along the southeast bank was suspended for approximately five minutes during which the probe sat in stagnant, shallow water near the bank. When the probe was stationary in one place and had more time to react to the temperature of the water it was immersed in, a much greater temperature change was observed. Although it may also be the case that the shallow water was also considerably

warmer than the main river channel, (which would also increase the temperature change observed) another type of probe with a smaller time constant may be a better choice for a drag probe survey.

The main objective of the drag-probe surveys was to identify specific locations of groundwater discharge that could be temperature profiled and subsequently sampled. In this respect, the surveys only highlighted one sub-reach, from the Glen Morris Bridge to Paris. The reach was, at its shortest definition, several kilometers long – far too long to temperature profile in detail. The fact that no discharge reach was highlighted along the stretch from Paris to Brantford may be due to Whiteman's Creek masking other cold-water additions to the Grand.

5.4.3 Temperature Profiling

Figure 5.19 shows the locations where the temperature probes were used during the summer of 2011. The reach first profiled was the one highlighted by the June drag probe surveys, just south of Glen Morris. Riverbed temperature measurements were taken every 25m or so down the river. At each riverbed temperature measurement, the river temperature was measured and GPS locations recorded. Of 143 measurements taken in the riverbed along this reach, six resulted in vertical groundwater flux calculations greater than 40 $cm \cdot d^{-1}$ (Figure 5.15).

The drag-probe survey results did not strongly suggest any other reaches to profile, so other locations along the discharge reach were chosen based on access, feasibility, and providing acceptable spatial coverage. Although the temperature probes could be used in water up to three meters deep, temperature profiling by boat proved both difficult and time consuming. Thus, reaches were restricted to ones that could be waded. The deepest water profiled was just over 1.3m deep, in pools with low current. In riffle sections with greater current, the maximum profiled depth was considerably less. This also resulted in a profiling survey that at times was concentrated along the banks of the Grand, where the water column was shallower and the current more gentle. In only a few locations was it possible to profile directly in the center of the river channel.

After several days of profiling, trends began to emerge that could help focus researchers in the direction of groundwater discharge. One was that, despite a concerted effort to detect groundwater discharging directly from bedrock fractures, none was found with the exception of one fracture, several kilometers upstream from the Brant Conservation area (Figure 5.15). A significant portion of the bedrock upstream of Glen Morris was also carefully probed for discharge, without success, and without even finding a fracture large enough to insert the probe. This could suggest that conduits for groundwater flow are limited here, and perhaps so is discharge directly from the bedrock. This is

supported by the drag probe survey results, but contradicted by the FLIR survey; all of the drag probe surveys from Cambridge to Paris indicated consistently rising temperatures along the bedrock reaches from Cambridge down to around the Glen Morris Bridge, similar to the diurnal temperature increases recorded by the stationary probes. The FLIR survey highlighted a reach of considerable bank seepage discharging from the flanks of the moraines along the northwest bank (Figure 4.3).

In many cases, groundwater discharge was noted in alcoves, or locations where eddies seem to have eroded away parts of the bank, leaving a pool protected on the upstream side by bank material. In some cases, these were also areas where surface tributaries entered the Grand, and the groundwater discharge directly to the riverbed may be a continuation of the same source under the river. Most discharge was found closer to the banks than the middle of the river, which is at least partly a reflection that the middle of the river channel was more difficult to reach. Many of the reaches that were profiled in the middle of the river were also riffle sections, and no locations profiled along riffles showed large decreases in temperature.

5.5 Conclusions

5.5.1 Drag Probe Surveys

One result of the drag probe surveys was the development of a conceptual interpretation of how cold-water tributaries and reach scale groundwater discharge affect downstream temperature traces (Figure 5.17). This interpretation was established by matching temperature fluctuations to the locations of known cold-water tributaries, and on the absence of any plausible cause of the temperature decrease from Glen Morris to Paris other than the cumulative effects of diffusive groundwater discharge. The interpretation summarizes what was accomplished by the drag probe surveys. The surveys could clearly detect point source discharge from banks. The survey also appears to be able to detect diffuse groundwater discharge on a kilometer scale reach length. The survey was not able to detect distinct groundwater locations short enough to temperature profile in detail.

The drag probe survey results suggest that, if the temperature decrease from Glen Morris to Paris is caused by groundwater discharge, then this stretch of the river may contain one of the largest fluxes of groundwater discharging to the Grand River in the discharge reach. This does not agree with the work by Scott and Imhof (2005), who determined, by means of streamflow gauge mass balance methods, that this particular stretch contributes the least groundwater to the Grand River of the whole discharge reach (Figure 5.18). It is, however, consistent with work done by Holysh et al. (2001),

Graham and Banks (2004), and Calautti (2010), all of whom note a large discharge zone along the eastward turning cutbank south of Glen Morris (Figures 5.19 and 5.20). It is also consistent with the FLIR survey, which noted considerable bank discharge in the same region (Figure 4.3), and to a lesser extent the temperature profiling, which found several points of considerable vertical discharge to the riverbed (Figure 5.15).

The overall quality of the survey has already been discussed, but it is worth mentioning that a survey that includes conductivity may ultimately be more useful than one that only measures temperature. On its own, electrical conductivity may not provide better data than temperature, being subject to its own set of limitations: for example, groundwater of similar conductivity to the river will not be picked up. Combined, however, these two parameters may provide a more complete picture of riverbed discharge.

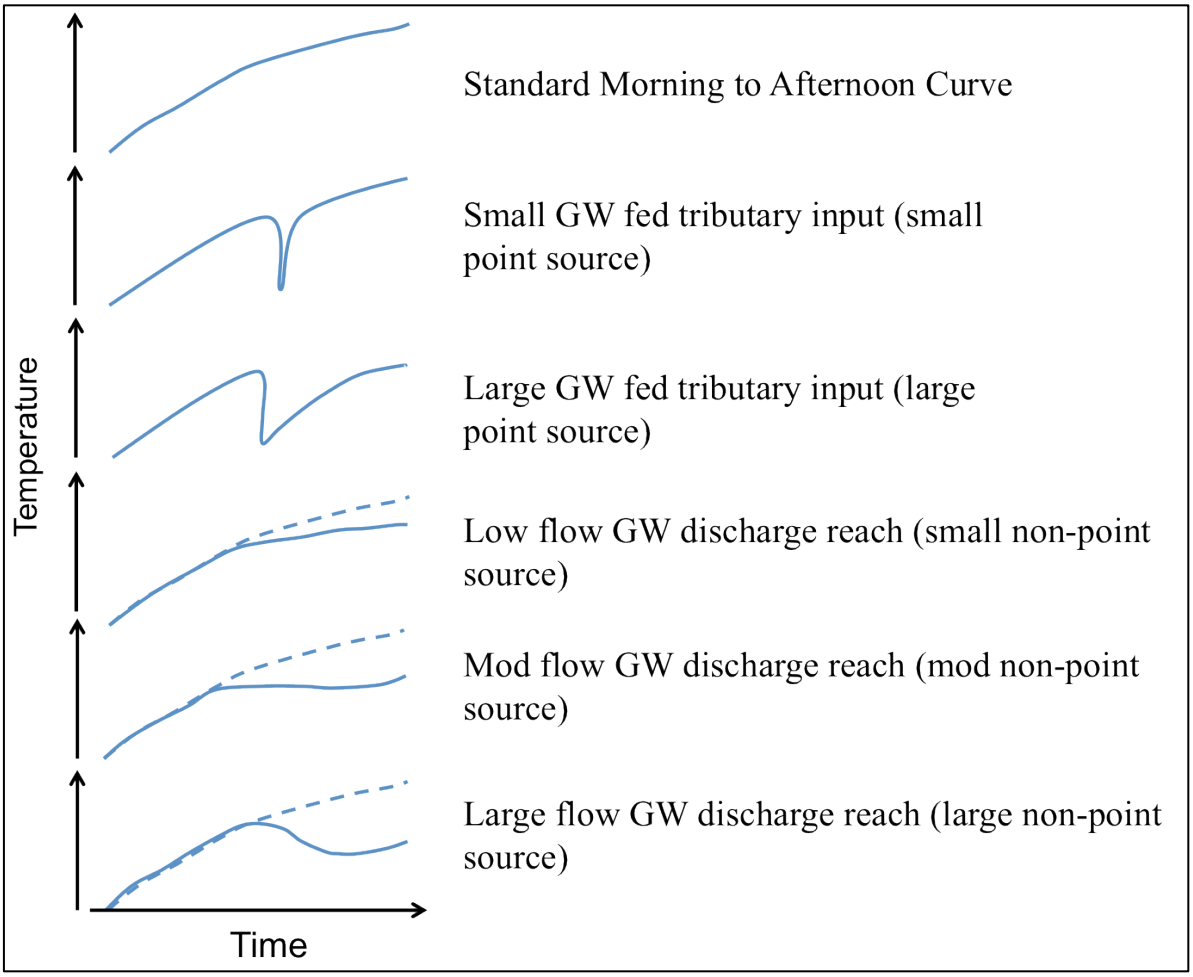

Figure 5.17 A conceptual interpretation of large-scale features highlighted from the drag probe survey results.

5.5.2 Temperature Profiling

Once the steel spike was used to reduce the depth the probes were used to penetrate the ground, the profiling went smoothly and without any major obstructions. Numerous locations were found could be returned to and sampled for groundwater discharge. As a reconnaissance tool, however, the method was poorly matched to the size of the Grand River and potential discharge reaches. To fully utilize the technique of Conant (2004), a greater reduction in scale is needed than was provided by the drag probe surveys. This is a stronger reflection of the failings of the drag probe surveys than of the temperature profiling method.

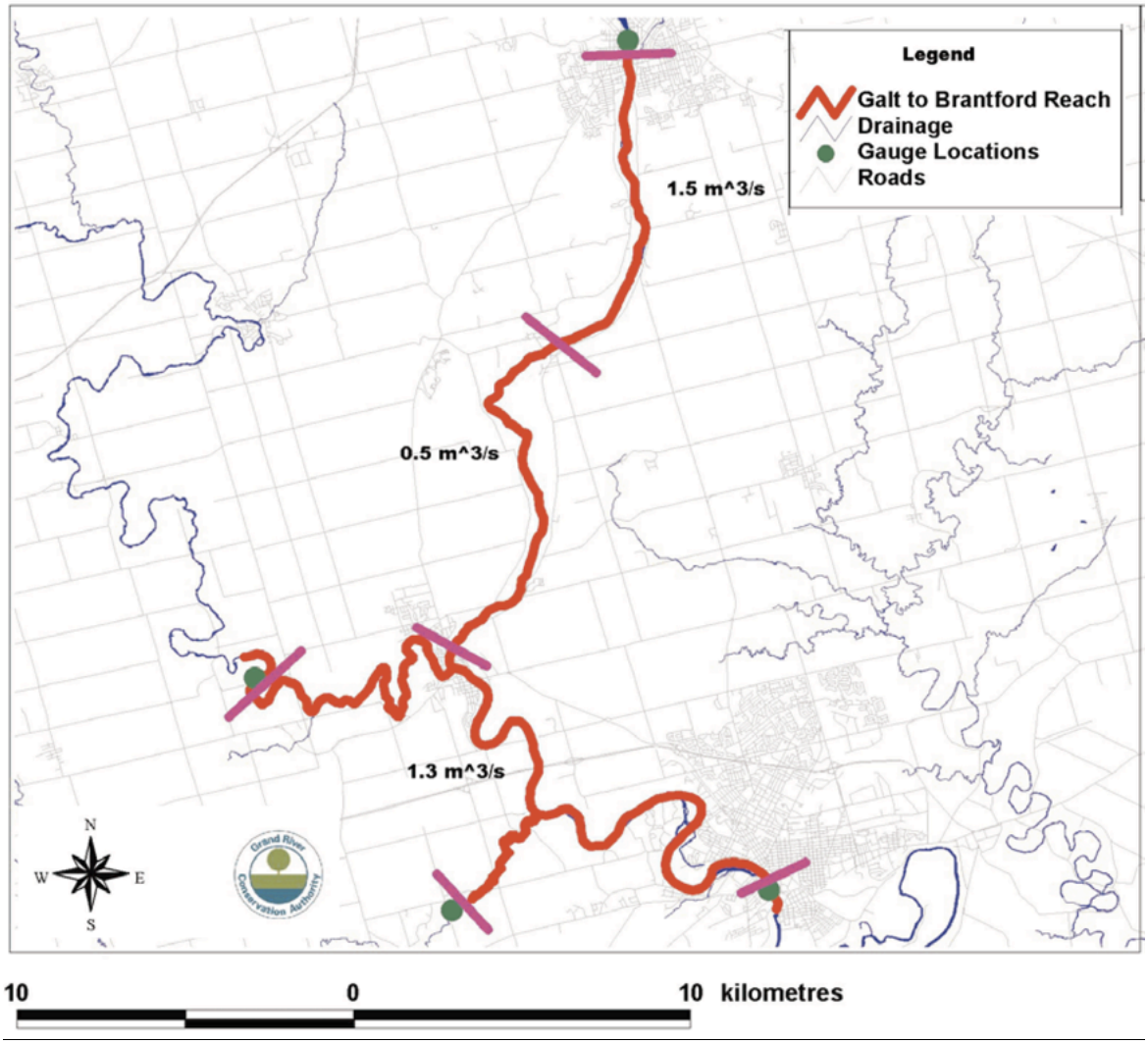

Figure 5.18 Previously estimated groundwater discharge additions along several sub-reaches of the Grand River, the Nith River, and Whiteman's Creek. From Scott and Imhoff (2005).

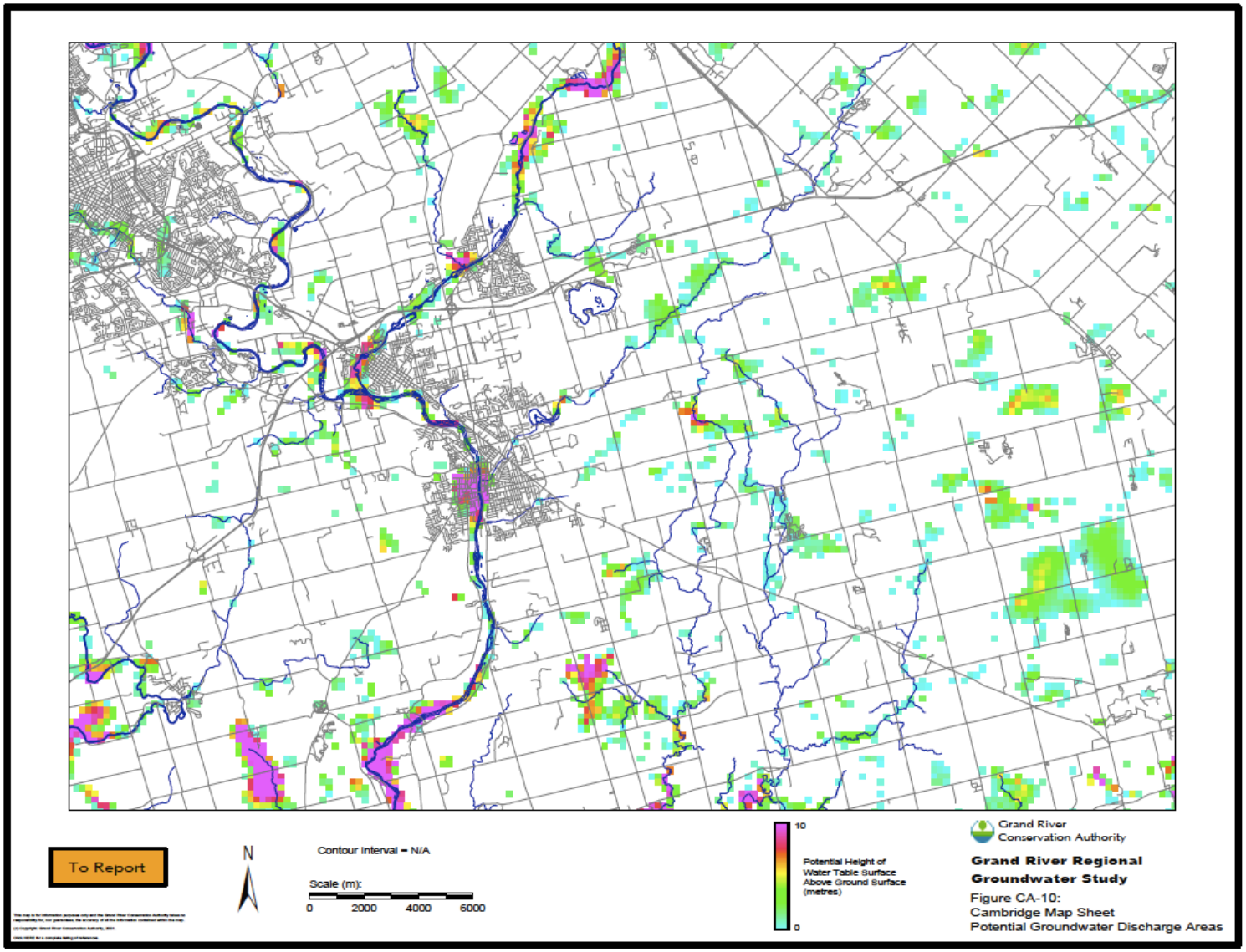

Figure 5.19 Potential groundwater discharge zones, based on the height of the water table surface above ground surface (or river stage). The Glen Morris region shows considerable vertical discharge gradients. From Holysh et al. (2001).

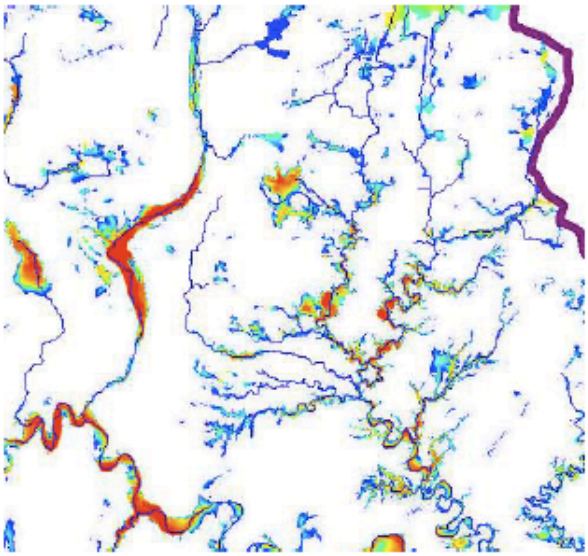

Figure 3.27: Expanded view (see inset of Figure 3.27) of GAWSER-FEFLOW discharge and recharge (after Graham and Banks, 2004). Note similarity of red/orange/yellow (gaining) stream reaches of Figure 3.28.

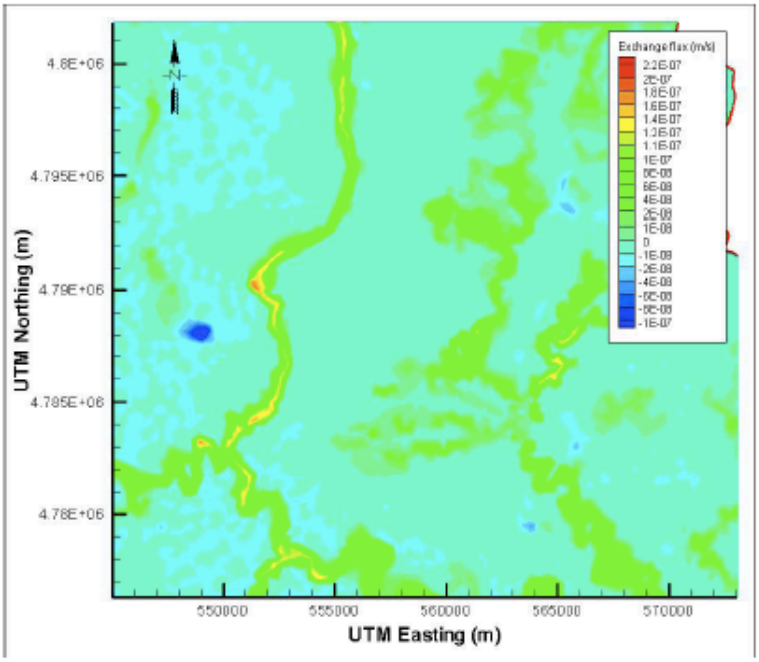

Figures 3.28: Expanded view of HGS-computed exchange flux, base case scenario

Figure 5.20 Modeled discharge from Graham and Banks (2004), *in* Calautti (2010), as well as results from Calautti (2010). Both models show relatively large discharge fluxes south of Glen Morris, in good agreement with the FLIR camera, drag probe survey, and temperature profiling results.

Chapter 6 – Characterization of Regional vs. Local Groundwater Systems and Discharge to the Grand River

6.1 Introduction

In regions with geological units containing distinct sulfur minerals, the isotopes of sulfur and oxygen in dissolved sulfate can be useful tools for tracing the origin, flow-path, and mixing of groundwater discharge to river systems (Gu et al., 2008). The Grand River Watershed, Ontario, Canada, is one such region. The western half of the 6800 km^2 watershed is underlain by the Salina bedrock formation, a unit composed of cyclically deposited carbonates, evaporites, and shales (O'shea et al., 1988). Although the exact origin and depositional history of the Salina formation has been the subject of considerable debate, sulfate evaporites within the formation clearly preserve the $^{34}S/^{32}S$ and $^{18}O/^{16}O$ isotope ratios of the Permian seawater from which they precipitated. From 115 samples of anhydrite in Salina formation core extracted from various locations in Southern Ontario, $\delta^{34}S\text{-}SO_4^{2-}$ values ranged from 21.2‰ to 32.6‰, with a median value of 28.2‰. $\delta^{18}O\text{-}SO_4^{2-}$ values ranged from 11.5‰ to 18.1‰ with a median value of 13.7‰ (compiled from Fritz et al., 1988). Other studies have documented $\delta^{34}S$ and $\delta^{18}O$ values of sulfate dissolved in groundwater that, along with redox conditions and general geochemistry, strongly suggest sulfate derived from the Salina formation (Nowicki, 1976; Woeller, 1982; Stotler et al., 2011). Other geological sources of sulfate likely present in the area have considerably different $\delta^{18}O$ and $\delta^{34}S$ values; sulfate derived from the oxidation of sulfide minerals and organic materials, collectively termed terrestrial sulfates, show $\delta^{34}S\text{-}SO_4^{2-}$ values that range from -15‰ to 5‰, and $\delta^{18}O\text{-}SO_4^{2-}$ values that range from -10‰ to 5‰ (Krouse and Grinenko, 1991). Previous research has noted that sulfides are ubiquitous in low concentrations throughout the overburden units in the Grand River Watershed; therefore, much of the sulfate in these units is ultimately derived from the oxidation of these sulfides (Robertson et al., 1998).

It was predicted that the isotope ratios of sulfate in groundwater discharge to the Grand River would show a clear distinction between discharge that had followed shallower flow-paths through the overburden and discharge that had followed deeper, regional flow-paths through the bedrock units below. The flow-path history of groundwater discharge to the Grand River is important, because the wastewater management strategy in the watershed is, in part, contingent on the assumption that groundwater discharge dilutes and assimilates in-stream nitrate from WWTPs (Holysh et al., 2001; Cooke, 2006; LESPRTT, 2008; Anderson, 2012). Contradictory to this conceptual model are

numerous cases where high nitrate concentrations have been found in shallow aquifers across southern Ontario and the Grand River Watershed as result of agricultural activity and septic tank effluent (Starr et al., 1987; Robertson et al., 1996; Aravena and Robertson, 1998; Vidon and Hill, 2004; Shabaga and Hill, 2010; Stotler et. al., 2011; Senger, 2012). As a result, groundwater from overburden aquifers may contribute nitrate to the Grand River rather than diluting in-stream concentrations. This study focuses on using sulfate, and $^{34}S/^{32}S$ and $^{18}O/^{16}O$ isotopic ratios of sulphur and oxygen in sulfate, to identify discharge from shallow vs. deep flow-systems, and to compare the relative contribution of each system to the Grand River during early summer and later summer flow conditions.

6.2 Study Area

The Grand River runs for 300 km from its headwaters in the Dundalk highlands south to Lake Erie. Previous researchers have identified a forty-two kilometer stretch of the river, between the municipalities of Cambridge and Brantford, as an area where a considerable flux of groundwater discharge to the Grand River occurs. Estimates of the total contribution to streamflow varies, but values as high as 25% of the river flow, during baseflow conditions, have been calculated (Scott and Imhof, 2005). This area of the Grand River is colloquially known as the discharge reach, and is the study area for this research (Figure 6.1).

The climate in the region is temperate continental. Precipitation occurs fairly evenly throughout the year, although a substantial input to the watershed drainage system occurs during the spring snow melt. Two bedrock formations underlie the study area: the Guelph formation in the north, consisting of inter-bedded dolostone and limestones, and the Salina formation in the south, a cyclically deposited series of limestones, shales, and evaporites. Over the bedrock, various sediment types have been deposited by the advance and subsequent retreats of successive quaternary glaciations; the discharge reach is covered by a series of moraines, kame deposits, outwash plains, and other ice contact and glacio-fluvial sediments. Elevation in the region is strongly influenced by the quaternary geology, which has resulted in varied, hummocky topography. This acts to increase groundwater recharge and reduces the size of the sub-catchments through which the Grand River flows, limiting the number of surface-water tributaries entering the Grand River in this part of the watershed (Figure 6.1). However, two main tributaries, the Nith River and Whiteman's Creek, drain into the Grand River in the southern half of the study area. A more detailed description of the discharge reach is given in Chapter Two: Study Area Characterization.

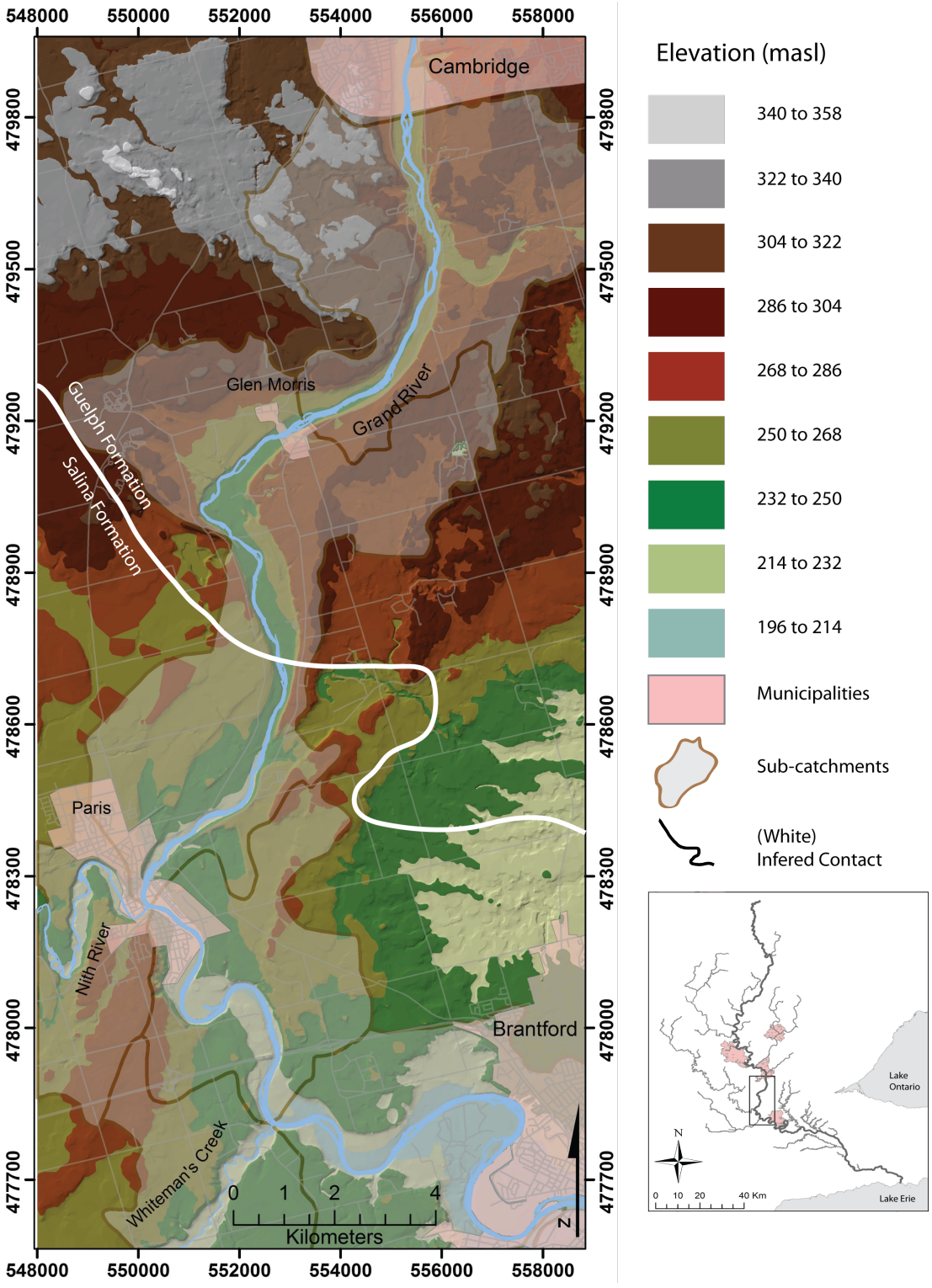

Figure 6.1 The discharge reach.

6.3 Methods

6.3.1 Sample Collection

In order to characterize groundwater and groundwater discharge in the study area, water samples were collected from domestic wells, seeps, tributaries, riverbed sediments, and the Cambridge and Paris WWTPs (Figure 6.2). To characterize the chemistry of the Grand River during early and late summer flow regimes, two sets of river samples were collected; one in early June, 2011, at flow conditions 70% greater than baseflow, and a second set in early September, 2011, at baseflow conditions (Figure 6.3). For all samples, a Hach™ HQ40d dual-input meter and probe assembly was used to measure DO, conductivity, temperature, and pH. All samples collected were analyzed for anions, DOC, and ammonium concentrations, while select samples were analyzed for $^{34}S/^{32}S$ and $^{18}O/^{16}O$ isotopic ratios of sulfate and $^{15}N/^{14}N$ and $^{18}O/^{16}O$ isotopic ratios of nitrate (nitrate to be discussed in chapter seven). Anion, DOC, ammonium, and nitrate isotope samples were passed through Whatman™ 0.45uM field filters into 40mL HDPE containers before being stored at 4°C for transportation back to the University of Waterloo. Ammonium samples were acidified to a pH of 5 using diluted sulphuric acid. Sulfate isotope samples were collected in 1L HDPE Nalgene bottles and passed through 0.45uM filters using vacuum pumps back at the laboratory.

Probe measurements of all samples, with the exception of those collected from the Grand River, were measured in a vertical flow cell to minimize contact with the atmosphere. Probe readings in the river were taken by immersing the probe in the river while the sample was collected. For all samples, probe measurements were not recorded until readings stabilized, after which three measurements were recorded, then averaged for a final value. If one measurement was considerably different from the others it was discarded, and the remaining two values averaged for a final value.

Domestic wells were purged until temperature, pH, and electrical conductivity measurements stabilized before samples were taken. Due to the possibility of aeration during pumping, dissolved oxygen (DO) data from the wells is not regarded as necessarily representing in-situ conditions. Considerable effort was made to collect seep samples as close to the discharge point as possible, and therefore DO values are regarded as representative of in-situ conditions. Water samples were collected from the riverbed using the Waterloo Profiler™, a direct-push sampling device developed at the University of Waterloo (Pitkin et al., 1999). Riverbed samples were taken at 19 locations along the Grand River discharge reach, selected from previously profiled locations to capture a range of

groundwater discharge flux conditions (Figure 6.2). At each location, up to five samples were collected; one in the water column, and then one every 25cm into the riverbed up to a maximum depth of one meter, or as deep as the profiler could be inserted. Although the system minimizes atmospheric contact during sample collection, probe measurements were made in a vertical flow-through cell once the samples were at the surface. Therefore, the temperature measured in the flow through cell is not considered representative of riverbed conditions, as extensive heat transfers can occur on route to the surface. To accurately measure riverbed temperatures, a thermistor probe was inserted 10 cm into the riverbed immediately prior to sample collection. It was important to gain accurate temperature data because inferences can be made regarding the magnitude of the vertical groundwater discharge flux based on the temperature at depth (Stonestrom and Constantz, 2003; Conant, 2004; Anderson, 2005; Schmidt et al., 2007; Constantz, 2008). Equation 6.1 from Schmidt et al. (2007), is the Turcotte an Schubert (1982) analytical solution to the one-dimensional steady-state heat diffusion-advection equation:

$$q_z = -\frac{K_{fs}}{\rho_f C_f Z} \ln \frac{T_{(z)} - T_L}{T_O - T_L} \quad (6.1)$$

Where:

q_z = Specific Darcy flux ($m \cdot s^{-1}$)

K_{fs} = Geometric mean of the thermal conductivity of the solid-fluid system ($J \cdot s^{-1} m^{-1} K^{-1}$)

ρ_f = Density of the fluid ($kg \cdot m^{-3}$)

C_f = Heat capacity of the fluid ($J \cdot kg^{-1} K^{-1}$)

z = Depth into the riverbed the probe is driven (m)

$T_{(z)}$ = Temperature at depth (z) (°C)

T_L = Temperature at the aquifer bottom (°C)

T_O = Temperature at the riverbed/river interface (°C)

$$K_{fs} = K_s^{(1-n)} + K_f^n \quad (6.2)$$

Where:

$K_s^{(1-n)}$ = Thermal conductivity of solids ($J \cdot s^{-1} m^{-1} K^{-1}$)

K_f^n = Thermal conductivity of the water ($J \cdot s^{-1} m^{-1} K^{-1}$)

n = porosity of the subsurface (-)

Using equation 6.1, it is possible to gain estimates of the vertical groundwater flux through the riverbed using only two temperature measurements, $T_{(Z)}$ and $T_{(O)}$. This is based on two assumptions that may not be valid for all discharge locations: 1) flow at depth is at steady-state, and 2) the groundwater flux is entirely vertical. Approximations for T_O can be made by averaging surface-water temperatures during profiling (Schmidt et al., 2007).

6.3.2 Sample Analysis

Anion samples were analyzed in aliquots of 0.5ml using a Dionex ICS-90 Ion Chromatograph. DOC samples were analyzed using a Rosemount Dohrmann DC-190 total carbon analyzer, and ammonium concentrations were determined using a Beckman DV 530 spectrophotometer following the procedure of Solorzano (1969). Samples for sulfate isotopes were concentrated when needed, then washed with HCl to neutralize dissolved carbonates. Samples were placed in a warm bath, then barium chloride added to precipitate barium sulfate. Samples were centrifuged, the supernatant decanted, and the barium sulfate was dried, ground, and baked in a high temperature ceramic oven at 550°C to remove any remaining organics. Finally, the samples were analyzed at the Environmental Isotope Lab at the University of Waterloo for the determination of $\delta^{34}S$ and $\delta^{18}O$ values, given in per mil units (‰) relative to the Vienna Cañon Diablo Troilite (VCDT) and Vienna Mean Standard Ocean Water (VSMOW), respectively. Analytical precision for both $\delta^{34}S$ and $\delta^{18}O$ values is on the order of +/- 1‰. Nitrate isotope samples were freeze-dried, then converted to nitrous oxide using a chemical denitrification method based on that of McIlvin and Altabet (2005). Samples are frozen in 4 mL glass vials then freeze dried and reconstituted with 2 mL of 0.75M sodium chloride. Cadmium is added and the samples are shaken for 24 hours to reduce nitrate to nitrogen dioxide. The samples are filtered, to remove the Cadmium, and then injected into a Helium filled headspace vial. The nitrogen dioxide is further reduced to nitrous oxide by reaction with a buffer solution of 2M sodium azide and 20% glacial acetic acid. After 30 mins on a tilt shaker, the reaction is quenched with 1 mL of 6M sodium hydroxide solution. The headspace vials are then over pressurized with 10 mL of helium gas. Nitrous oxide samples were run by injecting 3 to 6 mL into a GV Trace Gas pre-concentrator system, attached to a trace gas mass spectrometer at the Environmental Isotope Lab at the University of Waterloo for the determination of $\delta^{15}N$ and $\delta^{18}O$ values. Nitrous oxide isotopic ratios were then corrected to yield values of $\delta^{15}N$ and $\delta^{18}O$ of nitrate through

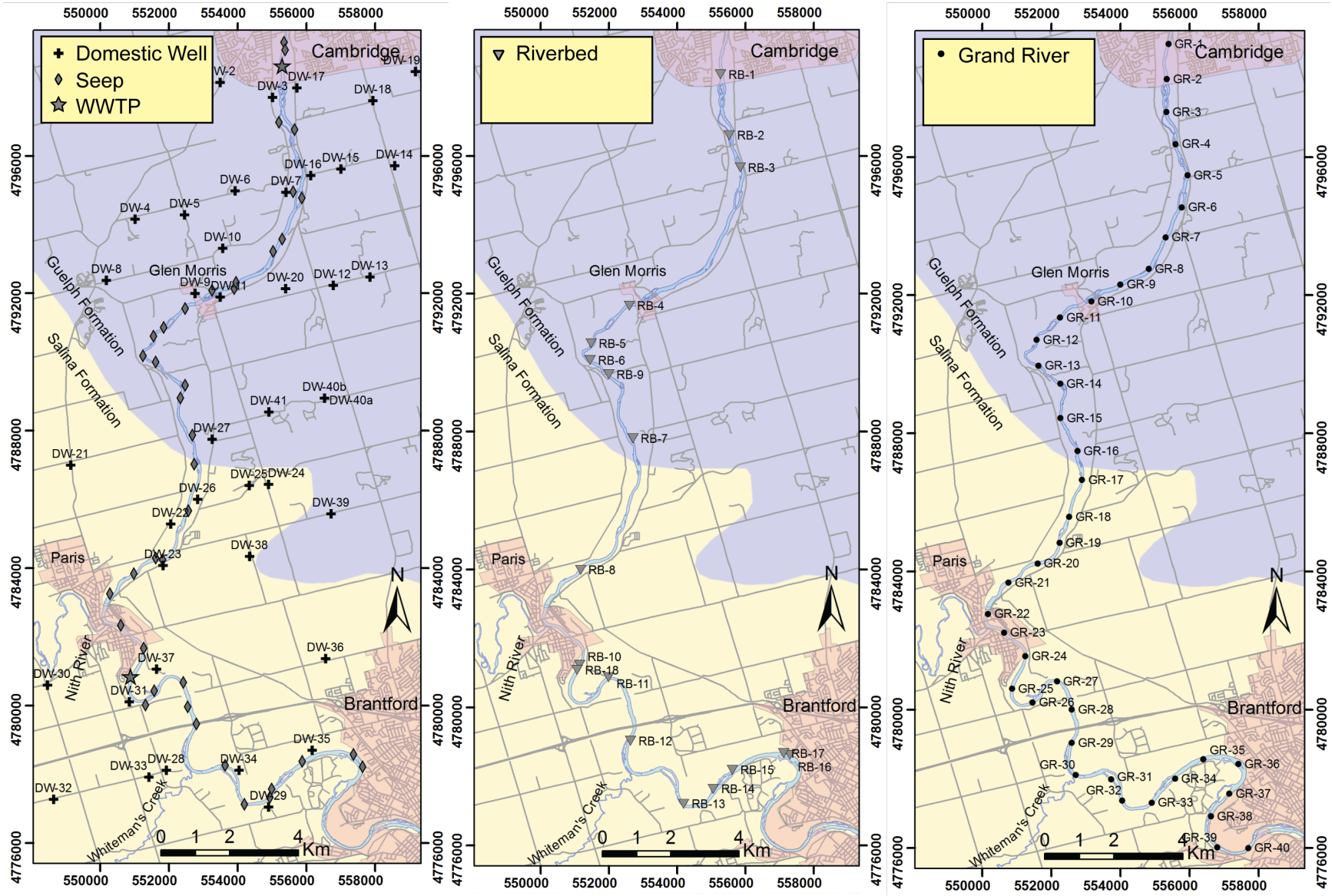

Figure .2 Sampling locations in the study area.

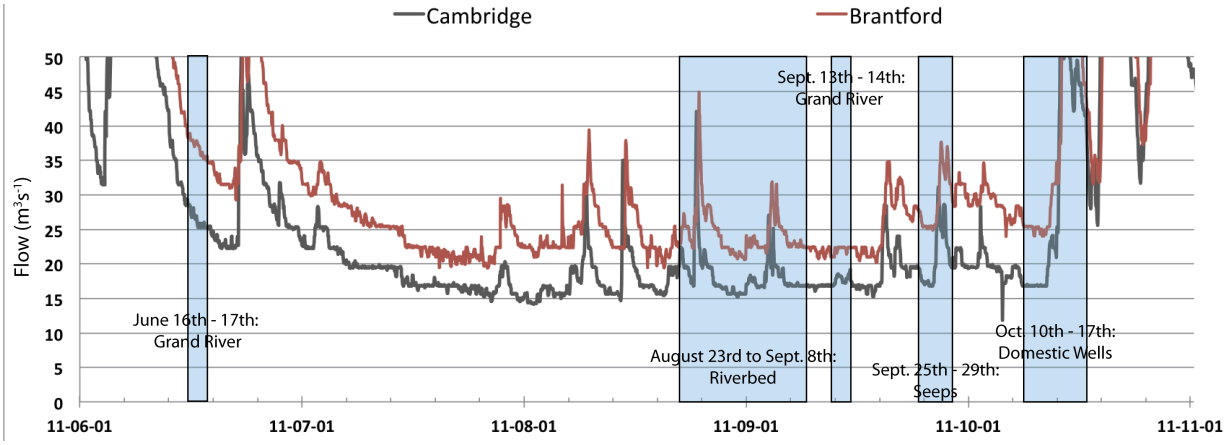

Figure 6.3 Flow conditions in the Grand River during sample collection.

internal standards prepared and run with the samples. $\delta^{15}N$ results are expressed in units of per mil (‰) relative to atmospheric nitrogen (N_2), and $\delta^{18}O$ results are expressed in units of per mil (‰) relative to the Vienna Standard Mean Ocean Water (VSMOW). Analytical precision for both $\delta^{15}N$ and $\delta^{18}O$ results is on the order of +/- 1‰. Nitrate and nitrate isotopes are discussed in detail in Chapter seven.

6.4 Results

6.4.1 Sulfate and Chloride in Groundwater

Sulfate concentrations in the discharge reach varied over several orders of magnitude (Figure 6.4). Sulfate in the domestic wells ranged from 4.4 $mg \cdot L^{-1}$ up to 1182.8 $mg \cdot L^{-1}$, with a median value of 24.0 $mg \cdot L^{-1}$ (n = 42). Only three samples, all from bedrock wells, had concentrations greater than 100 $mg \cdot L^{-1}$, at 117.2, 662.0, and 1182.8 $mg \cdot L^{-1}$, the two highest of which were from wells screened in the Salina formation. In contrast, the highest sulfate in the three samples collected from the Guelph formation was 43.2 $mg \cdot L^{-1}$. Sulfate in overburden wells, throughout the study area, ranged between 14.5 $mg \cdot L^{-1}$ and 82.2 $mg \cdot L^{-1}$ (n = 13). This distribution of sulfate in the domestic wells is consistent with previous samples collected by Singer et al. (2003), who showed that the Salina formation, due to gypsum and anhydrite minerals in its evaporite sequences, can have much greater concentrations of sulfate than either the overburden or the Guelph formation (Figure 2.5).

Sulfate in samples collected from seeps and tributaries ranged from 5.4 $mg \cdot L^{-1}$ to 1253.6 $mg \cdot L^{-1}$, with a median concentration of 32.1 $mg \cdot L^{-1}$ (n = 43). Similar to the domestic wells, the two samples with the highest concentrations, at 1253.6 $mg \cdot L^{-1}$ and 576.8 $mg \cdot L^{-1}$, were both collected from

groundwater discharging directly from Salina bedrock, and the first from a rather unique setting; an artesian spring flowing from an outcrop in the middle of the Grand River, just north of the Salina-Guelph formation contact (Figure 6.4). Considering only seep samples and excluding the two from the Salina formation, sulfate concentrations ranged from 15.0 $mg \cdot L^{-1}$ to 55.3 $mg \cdot L^{-1}$, with a median value of 31.2 $mg \cdot L^{-1}$ (n = 23). Like samples from the overburden wells, these samples were from seeps distributed across the study area, discharging from sediment overlying both the Guelph and Salina bedrock formations. The two largest tributaries in the area, Nith River and Whiteman's Creek, had relatively high sulfate concentrations at 131.4 $mg \cdot L^{-1}$, and 116.9 $mg \cdot L^{-1}$, respectively. Sulfate in samples from the Cambridge and Paris WWTPs were higher, at 214.7 $mg \cdot L^{-1}$ and 159.6 $mg \cdot L^{-1}$, respectively, although not as high as concentrations in groundwater coming directly from the Salina formation.

Samples collected from the riverbed had sulfate concentrations ranging from 13.9 $mg \cdot L^{-1}$ to 952.2 $mg \cdot L^{-1}$. While the domestic well and seep samples clearly represent groundwater, samples collected from the riverbed could include both groundwater and hyporheic river-water components. The first indication regarding which samples would include which water component came from the vertical discharge flux calculations during earlier temperature profiling (see chapter five). It was expected that samples collected from locations with strong vertical fluxes would contain mainly groundwater, while samples from locations with weak vertical fluxes could include a river water component as well. Because the dominant source of chloride in the Grand River was expected to be from upstream WWTPs, it was anticipated that chloride could be used as a tracer for river water in the riverbed, and therefore that the change in chloride concentrations, with depth along the vertical profiles, would geochemically agree with the earlier flux estimates based on temperature. The collected samples confirmed that the WWTPs are the main source of chloride to the Grand River in the study area; there was a clear and consistent difference in chloride concentrations between groundwater, the Grand River, and WWTP samples. Chloride concentrations in all domestic wells ranged from 2.6 $mg \cdot L^{-1}$ to 121.3 $mg \cdot L^{-1}$ with a median value of 31.4 $mg \cdot L^{-1}$ (n = 42). Chloride concentrations in seep samples ranged from 4.3 $mg \cdot L^{-1}$ to 169.2 $mg \cdot L^{-1}$, with a median value of 28.9 $mg \cdot L^{-1}$ (n = 23). Chloride concentrations in the June Grand River samples ranged from 75.5 $mg \cdot L^{-1}$ to 98.1 $mg \cdot L^{-1}$ with a median value of 88.5 $mg \cdot L^{-1}$ (n = 40), and in September, Grand River samples ranged from 79.5 $mg \cdot L^{-1}$ to 115.4 $mg \cdot L^{-1}$ with a median value of 103.3 $mg \cdot L^{-1}$ (n = 40). Chloride concentrations from the Cambridge and Paris WWTP effluent were much higher, at 390.2 $mg \cdot L^{-1}$ and 468.6 $mg \cdot L^{-1}$, respectively.

Figure 6.5 shows examples of sulfate and chloride concentrations (as well as $\delta^{34}S$ values, to be discussed later) in vertical profiles at select riverbed sampling locations. In most cases, there is a clear distinction between chloride and sulfate in the river and the riverbed samples that correlates well with the magnitude of the calculated vertical discharge flux. Locations with high flux estimates have vertically consistent chloride and sulfate, at concentrations distinct from the overlying river water. Locations with lower flux estimates have less consistent concentrations. Riverbed samples indicative of groundwater have lower chloride values than the river, and sulfate concentrations that are either lower or considerably higher, suggesting two distinguishable groundwater types within the riverbed (RB-5, RB-8, and RB-13). Hyporheic river water is defined as water within the riverbed with similar chloride concentrations to that of the overlying Grand River. In one case, RB-18, both chloride and sulfate show an evolution from river type values at the top of the profile towards a second water type assumed to be deeper in the subsurface. This location appears to be indicative of a transitional mixing zone. A final riverbed profile is highlighted at location RB-4. Here, there is clear evidence of river water at least 25cm into the riverbed, but a change in water type occurs between 25cm and 50cm. This abrupt water type change could be caused by either a low-flow boundary or a strong horizontal flow component. This may imply that, at this location, groundwater does not discharge directly upwards, but without more information this becomes somewhat speculative. Due to the uncertainty in discharge flow-paths, sample locations such as these were not considered further in terms of characterizing groundwater discharge to the Grand River.

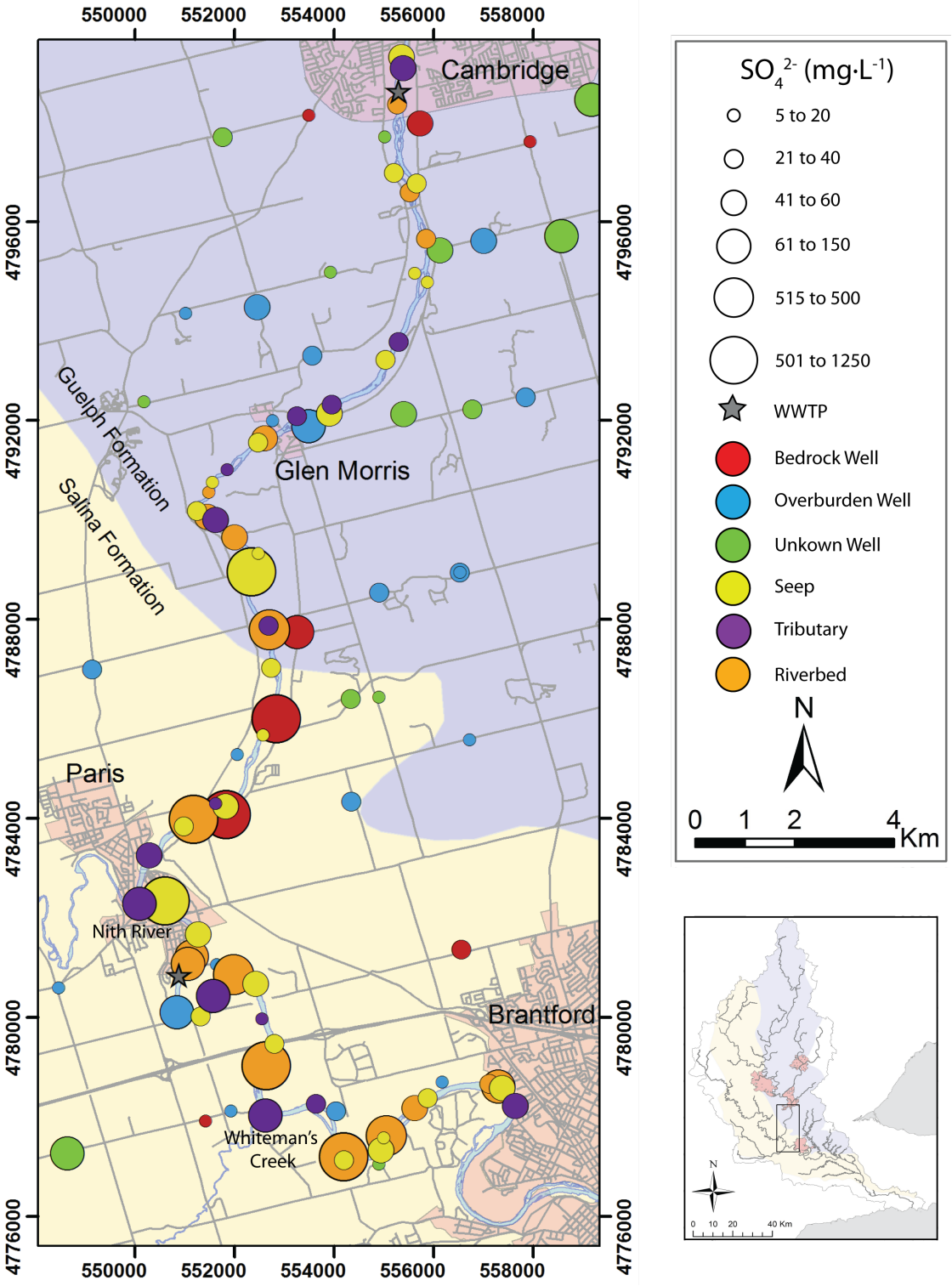

Figure 6.4 Distribution of sulfate in domestic wells, seeps, tributaries, and riverbed porewater along the discharge reach.

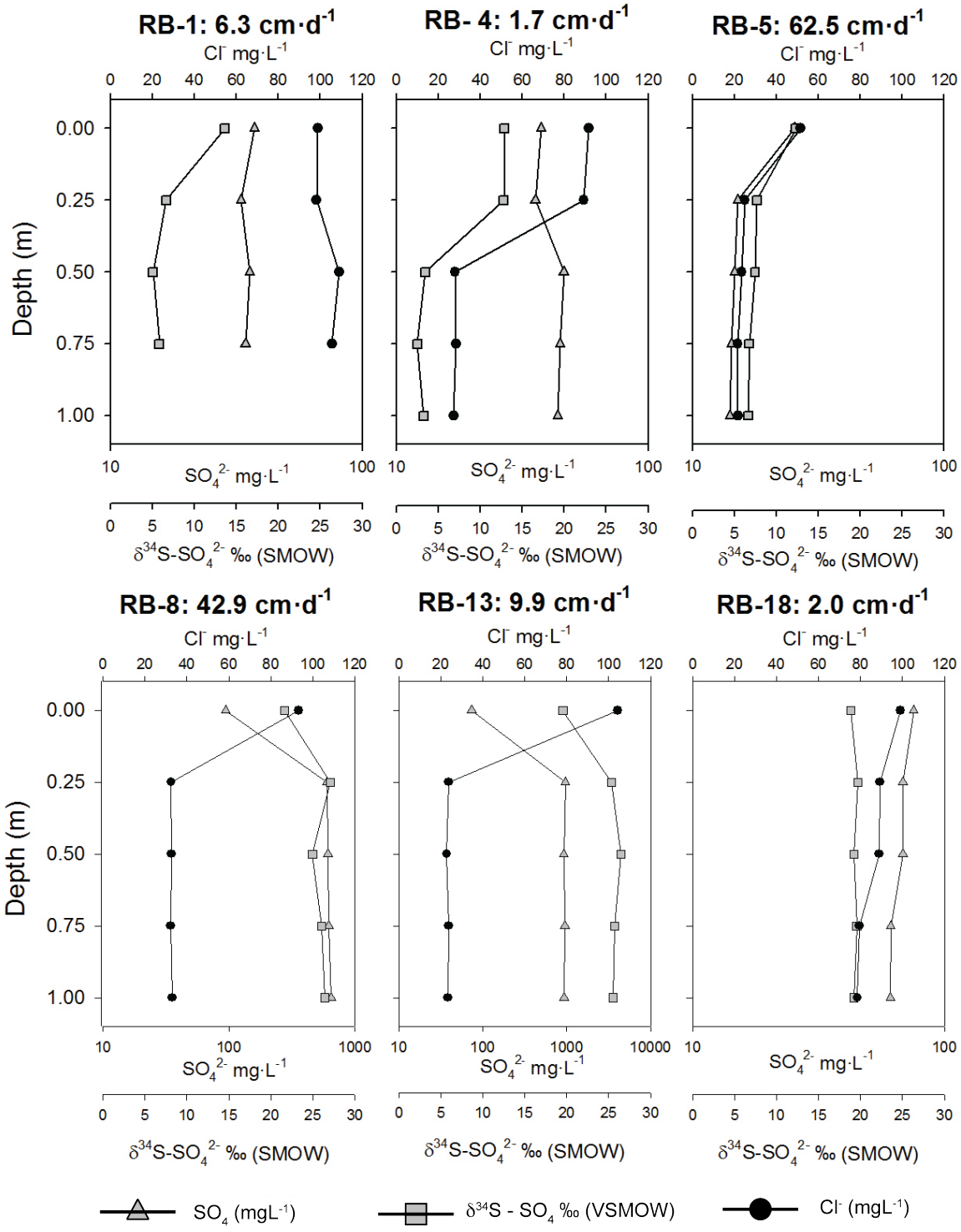

Figure 6.5 Vertical profiles of select riverbed sampling locations, showing chloride, sulfate, and $\delta^{34}S$ values. The sample collected at a depth of 0.00m is the sample taken from the water column. Vertical flux estimates are shown above the profile for each location.

6.4.2 Sulfate Isotopes in Groundwater

Seventeen domestic well samples known to be from the Guelph or Salina formations, or the overburden, were selected for the analysis of $^{34}S/^{32}S$ and $^{18}O/^{16}O$ isotopic ratios in sulfate (Figure 6.6). $\delta^{34}S$ values ranged from -1.4‰ to +33.4‰, and $\delta^{18}O$ values ranged from -5.0‰ to 15.4‰. Higher $\delta^{34}S$ and $\delta^{18}O$ values were generally associated with samples collected from wells screened in the Salina formation, while lower $\delta^{34}S$ and $\delta^{18}O$ values were associated with the Guelph formation and the overburden.

Ten seep samples were analyzed for $^{34}S/^{32}S$ and $^{18}O/^{16}O$ isotopic ratios in sulfate; two discharging directly from the Salina formation, and the other eight from the overburden at various locations throughout the study area (Figure 6.6). The two samples from the Salina formation had $\delta^{34}S$ and $\delta^{18}O$ values of 27.8‰ and 27.3‰, and 12.5‰ and 10.6‰, respectively. The other seep samples were relatively depleted in both ^{34}S and ^{18}O, with $\delta^{34}S$ values ranging from -1.3‰ to 13.4‰, and $\delta^{18}O$ values ranging between -2.4‰ and 5.0‰.

Samples from six riverbed locations were analyzed for $^{34}S/^{32}S$ and $^{18}O/^{16}O$ isotopic ratios in sulfate (Figures 6.5 and 6.6). The sulfate isotopes agreed well with chloride and sulfate concentrations used to separate hyporheic water from groundwater types (Figure 6.5). Sampling locations RB-8 and RB-13, whose sulfate concentrations suggested a Salina groundwater origin, had the most enriched isotopic ratios, with maximum $\delta^{34}S$ values of 27.1‰ and 26.5‰, and maximum $\delta^{18}O$ values of 12.8‰ and 12.6‰, respectively. R19, where chloride indicated mixing between hyporheic river-water and an undetermined groundwater type, showed essentially constant $\delta^{34}S$ and $\delta^{18}O$ values in the riverbed, at approximately 19‰ to 20‰ and 8‰ to 9‰. The remaining riverbed samples, RB-1, RB-4, and RB-5, all had relatively depleted $^{34}S/^{32}S$ and $^{18}O/^{16}O$ isotopic ratios compared to both the Salina type samples and the Grand River samples (depth: 0.00m) taken during the riverbed profiling (Figure 6.5). $\delta^{34}S$ values ranged between 2.5‰ and 7.7‰, and $\delta^{18}O$ values ranged between -1.6‰ and 3.4‰.

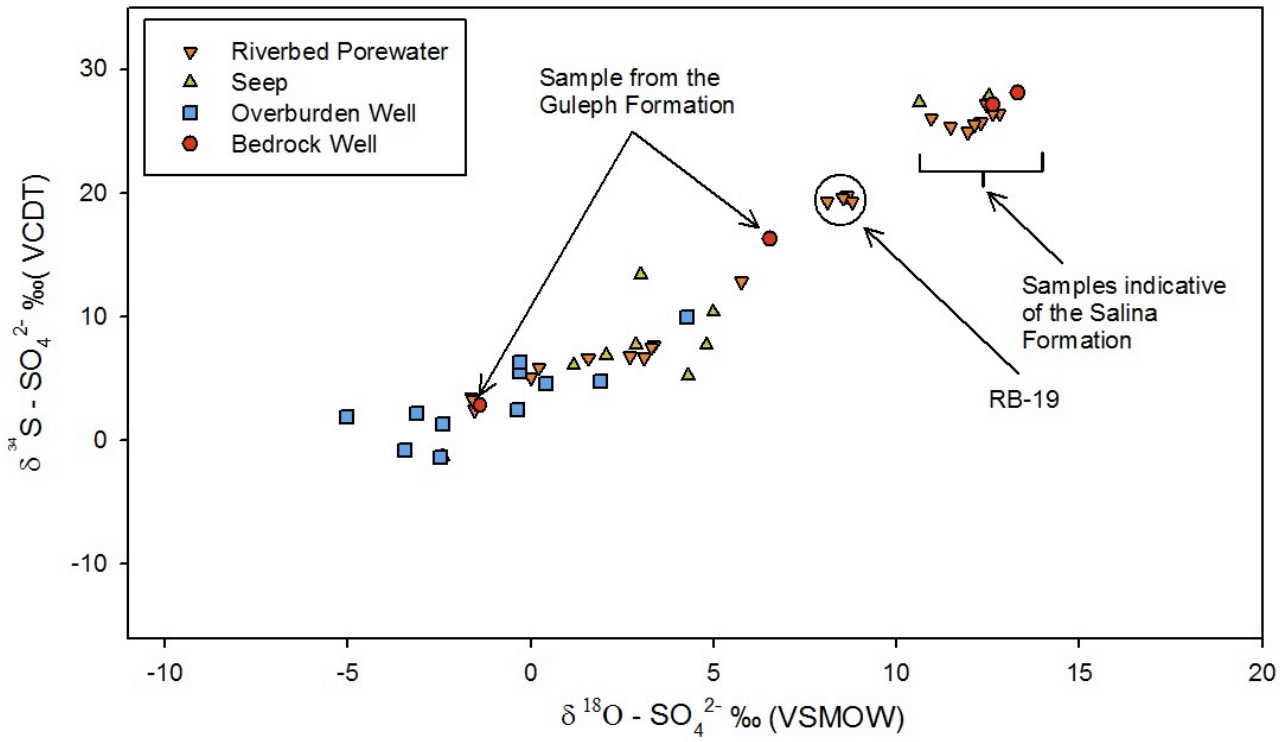

Figure 6.6 $\delta^{34}S$ and $\delta^{18}O$ values of all samples selected for isotopic analysis of sulfate

6.4.3 Sulfate and Chloride in the Grand River

Sulfate concentrations in the Grand River were higher during the September survey than the June survey (Figure 6.7). Between Cambridge and Paris, downstream concentrations along both surveys stay relatively constant; in June, concentrations increase from 31.5 $mg \cdot L^{-1}$ to 33.5 $mg \cdot L^{-1}$, while in September concentrations increase from 36.4 $mg \cdot L^{-1}$ to 44.6 $mg \cdot L^{-1}$. At Paris, the convergence of the Nith River brings a considerable load of sulfate clearly seen in both early and late summer surveys. After Paris, sulfate increases more rapidly in the September survey than the June survey, but an increase is clear in both surveys relative to the consistency of concentrations noted upstream. In June, the Grand River reaches a maximum sulfate concentration of 63.6 $mg \cdot L^{-1}$. In September, the river reaches a maximum concentration of 82.5 $mg \cdot L^{-1}$. The sulfate input of Whiteman's Creek does not register in June, but is just noticeable in September.

Chloride concentrations in the September survey show a sharp increase three kilometers down the discharge reach, followed by a relatively consistent concentration plateau all the way to Paris. The June survey does not show this initial increase, but concentrations are also relatively consistent until

Paris. Chloride concentrations are considerably higher in September than in June. Like sulfate, the convergence of the Nith is clear in the downstream chloride trace; unlike sulfate, the Nith has a much lower chloride concentration than the Grand River. Similarly to sulfate, a greater change is noticed after the Nith than before; rather than increase, however, chloride concentrations drop. Between the Nith River and Whiteman's Creek, chloride concentrations in the September survey drop consistently. After Whiteman's Creek, chloride appears to plateau. In the June survey, chloride concentrations drop almost until Brantford. The convergence of Whiteman's Creek can be seen in both surveys. The maximum chloride concentration upstream of the Nith, in June, is 98.9 $mg \cdot L^{-1}$. The minimum chloride value, after the Nith, is 77.4 $mg \cdot L^{-1}$. In September, the maximum upstream chloride concentration is 115.4 $mg \cdot L^{-1}$: the minimum downstream value is 93.2 $mg \cdot L^{-1}$.

6.4.4 Sulfate Isotopes in the Grand River

Every fourth sample from both the September and June Grand River surveys were analyzed for $^{34}S/^{32}S$ and $^{18}O/^{16}O$ isotopic ratios of sulfate (Figure 6.7). Overall, both $\delta^{34}S$ and $\delta^{18}O$ increase downstream from Cambridge to Brantford. The most noticeable change is a considerable increase in both $\delta^{34}S$ and $\delta^{18}O$, between samples GR-21 and GR-25, as the Nith joins the Grand. In contrast, there is no noticeable shift in $\delta^{34}S$ and $\delta^{18}O$ values where Whiteman's Creek joins the Grand River.

$\delta^{34}S$ values generally increase downstream in the September survey, with only GR-13 showing a decrease, of 0.4‰, relative to the samples taken before it (Figure 6.11). $\delta^{34}S$ values increase 1.5‰ from Cambridge to the mouth of the Nith, with downstream $\delta^{34}S$ values essentially constant until sample GR-13, and a 1.4‰ increase between GR-13 and GR-21. This latter enrichment in ^{34}S roughly coincides with where the Grand River crosses the contact between the Guelph and Salina formations. Between the two samples immediately up and downstream of the Nith, GR-21 and GR-25, $\delta^{34}S$ values in the Grand River increase 3.5‰. After GR-25, $\delta^{34}S$ values increase another 1.2‰ to Brantford.

There are no clear downstream trends in the $\delta^{18}O$ values of the September survey, with the exception of a 2.1‰ increase between the two Grand samples immediately upstream and downstream of the Nith. Trends are also weaker in both $\delta^{34}S$ and $\delta^{18}O$ values in the June survey. There are net increases in $\delta^{34}S$ values of only 0.2‰ and 0.7‰ upstream and downstream of the Nith, respectively, and no clear trend in $\delta^{18}O$ values other than the Nith's input. This remains an obvious influence, causing an increase in $\delta^{34}S$ and $\delta^{18}O$ values of 4.0‰ and 2.6‰, respectively.

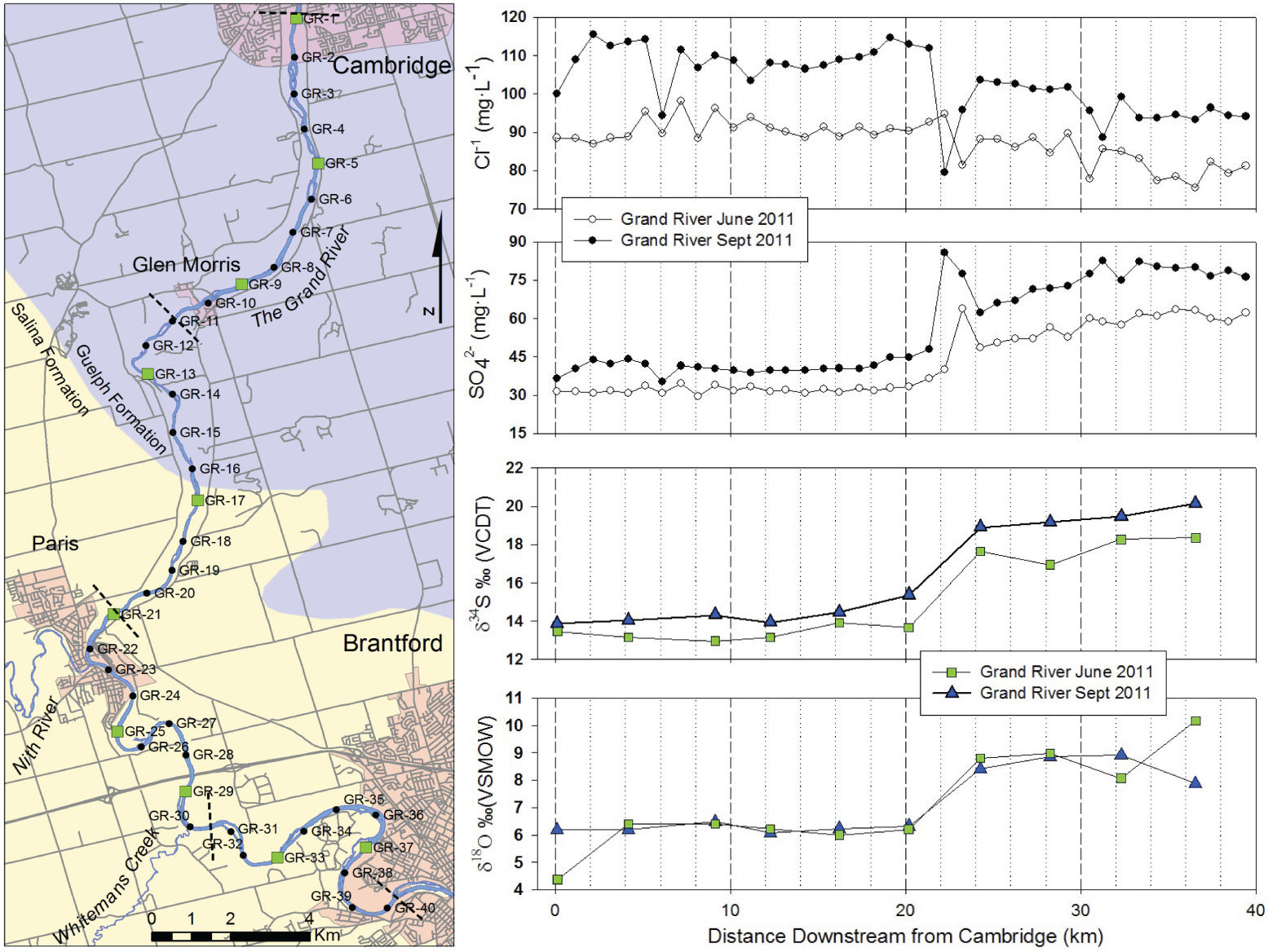

Figure 6.7 Downstream continuum plots of anions and $\delta^{34}S$ and $\delta^{18}O$ values of sulfate.

6.5 Discussion

6.5.1 Aquifer Characterization

The range of $\delta^{34}S$ and $\delta^{18}O$ values from domestic well samples were plotted against anticipated sulfate source values from the literature (Figure 6.8). Most samples plot as expected; samples from wells screened in the overburden plot near the terrestrial sulfate end-member (as defined by Kendall and Macdonnell, 1998), while samples obtained from wells screened in the Salina formation fall within a dual box-plot summary of $\delta^{34}S$ and $\delta^{18}O$ values found in Salina anhydrite from Fritz et al. (1988). Only two wells screened in the Guelph formation were sampled: one plots within the terrestrial sulfate end-member, and the other plots intermediate between the terrestrial and Salina formation sulfates. No samples appear influenced by sulfate from either fertilizer or precipitation. Some terrestrial sulfate samples, however, appear to plot along a line that could be extended through the Salina formation summary; DW-8 (domestic well eight) in particular. This apparent trend can be explained either through mixing relationships between isotopic end-members, or by fractionations induced by the reduction of terrestrial sulfates. A sulfate reduction area, showing the expected co-evolution of $\delta^{34}S$ and $\delta^{18}O$ values as sulfate is reduced, has been defined for samples containing terrestrial sulfate (Figure 6.8). As shown by Fritz et al. (1989) - and subsequently others - the behaviour of $\delta^{34}S$ values is considerably different than that of $\delta^{18}O$ values during sulfate reduction. $\delta^{34}S$ values increase along a Rayleigh-type fractionation curve for closed-system, kinetic isotope fractionation reactions (Kendall and Mcdonell, 1998). $\delta^{18}O$ doesn't necessarily increase, but approaches, from whatever initial delta value reduction began at, a value approximately 30‰ greater than the average $\delta^{18}O$-H_2O of groundwater in the region (Fritz et al., 1989; Berner et al., 2002; Schiff et al., 2005). Encalada (2008) and Pastora (2009) found groundwater $\delta^{18}O$-H_2O values in the Glen Morris region to be -10‰ VSMOW, and therefore the expected $\delta^{18}O$ reduction trajectory asymptotically approaches 20‰ on the $\delta^{18}O$-SO_4^{2-} axis (Figure 6.8).

On the plot of $\delta^{34}S$ vs. $\delta^{18}O$ values, the area that defines possible terrestrial sulfate reduction trajectories overlaps the mixing trend between the terrestrial sulfate and Salina sulfate isotopic end-members. The two were separated, however, by plotting sulfate concentration against $\delta^{34}S$ values (Figure 6.9). From this plot, two samples appear anomalous. DW-8 shows a much higher $\delta^{34}S$ value than any other sample from wells screened in the overburden. This may mean a small concentration of Salina sulfate is present in the sample, or it may suggest that the sample has been affected by sulfate reduction. Low concentrations of Salina sulfate could be present in overburden material, as

bedrock fragments picked up by advancing glaciers are commonly present as clasts in the overburden material (Karrow, 1987; Robertson et al., 1996). On the other hand, a low nitrate concentration (0.2 $mg \cdot L^{-1}$) and the presence of ammonium (0.2 $mg \cdot L^{-1}$) suggest redox conditions may also be suitable for sulfate reduction (DO is not used as the sample may have artificially high concentrations from aeration during pumping). DW-36, screened in the Salina formation, has a more complicated history that remains unclear. A nitrate concentration of 0.2 $mg \cdot L^{-1}$ and ammonium concentration of 0.3 $mg \cdot L^{-1}$ suggest redox conditions where sulfate reduction may also occur. The $\delta^{34}S$ value, however, is not high enough to suggest reduction beginning from common Salina sulfate concentrations or $\delta^{34}S$ values. If sulfate at DW-36 originates from the Salina formation and is unaffected by reduction, its concentration, at 24.9 $mg \cdot L^{-1}$, plots below the 10^{th} percentile value of the formation (Singer et al., 2003). An alternative explanation for the low concentration and/or the anomalous $\delta^{34}S$ value is that pumping has caused the drawdown of overburden groundwater into the bedrock formation. Upon reduction, the sulfate from this groundwater has concentrations and an enrichment in ^{34}S as expected from the overburden material, despite coming from a deeper well screened in the Salina formation.

The other domestic well overburden samples do not appear to be affected by sulfate reduction (Figure 6.9). To lie on a reduction trajectory, they would have had to begin reduction with higher sulfate concentrations than generally found in overburden materials (Figure 2.5), and lower $\delta^{34}S$ values than generally found in the Salina formation. Without evidence that sulfate with these characteristics is present in the study area, these samples are more simply described as having a range of sulfate concentrations unaffected by reduction. DW-27, from the Guelph formation, is more simply described as the result of mixing between sulfate defined by two isotopic end-members. Sulfate reduction, however, may have occurred in the Salina formation samples. If concentrations are high enough, fractionation effects can be obscured (see section 3.3.1). In these cases, sulfate reduction does not reduce the effectiveness of using the isotope ratios to label where the groundwater came from. Therefore, if DW-8 and DW-36 are disregarded, along with the sulfate reduction area, figure 6.8 yields a decent characterization of groundwater in the Salina formation and the overburden based on sulfate isotopes.

While the overburden material and Salina formation are isotopically well defined, the Guelph formation does not appear to have a unique $\delta^{34}S$ or $\delta^{18}O$ signature. Literature data suggested that the Guelph formation generally has lower sulfate concentrations than the overburden (Figure 2.5), and it was on this basis that it was originally expected the two could be separated. Sample concentrations,

however, did not match the literature data; numerous samples from the overburden had lower sulfate concentrations than expected, leaving them indistinguishable from the Guelph formation.

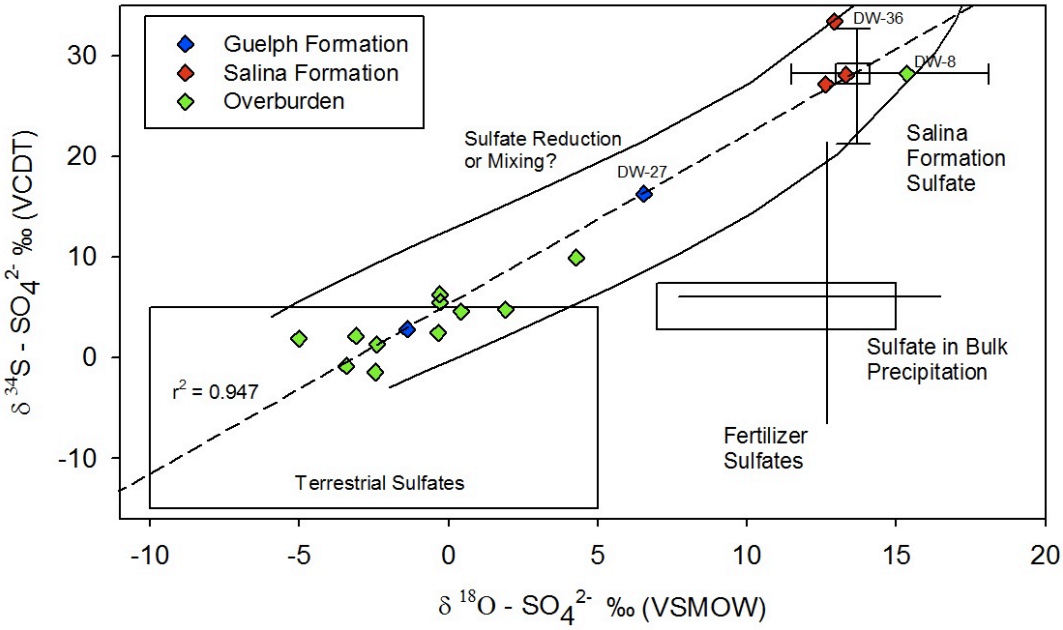

Figure 6.8 Domestic wells sulfate isotope samples compared to literature values of potential sources.

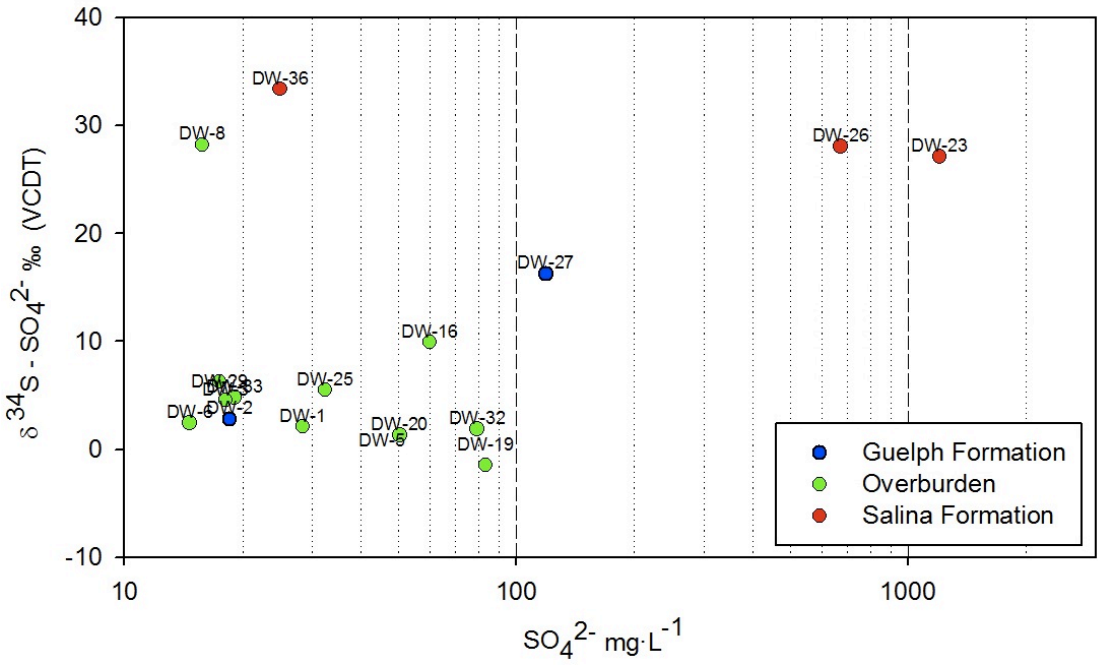

Figure 6.9 $\delta^{34}S$ (‰ VCDT) vs. SO_4^{2-} ($mg \cdot L^{-1}$) plot to compare end-member mixing or sulfate reduction trends.

6.5.2 Shallow vs. Deep flow systems in Groundwater Discharge

None of the seep samples had sulfate concentrations and/or $\delta^{34}S$ values that suggest the influence of sulfate reduction (Figure 6.10). On a $\delta^{34}S$ vs. $\delta^{18}O$ plot, the seep samples appear consistent with both the literature end-members and the mixing trend developed from the domestic well samples (Figure 6.11). With the exception of two samples, sulfate in seep discharge also plots close to the terrestrial sulfates end-member found in either overburden or Guelph formation wells. Both anomalous seep samples discharge directly from the Salina formation, one an artesian spring bubbling up from a bedrock outcrop in the centre of the river channel. It is suggested, therefore, that unless flowing directly from outcrops of the Salina or Guelph formations, seep samples are indicative of shallow, overburden groundwater flow systems.

Similar to the seep samples, the isotopic ratios of the riverbed samples appear unaffected by sulfate reduction (Figure 6.10), although reduction may still be occurring at some locations. Dissolved oxygen, nitrate, ammonium, and sulfate concentrations at riverbed sampling locations R8 and R13 imply redox conditions are optimal for sulfate reduction, but, if occurring, the isotopic effects are obscured by high sulfate concentrations. Thus, these samples also appear consistent with literature isotopic end-members and the mixing trend developed from the domestic well samples (Figure 6.11).

Where along the mixing trend the riverbed samples plot depends on where the sample was collected relative to the bedrock units, as well as the extent to which the sample is composed of groundwater or hyporheic-zone stream water. R1, R4, and R18 all have hyporheic stream water components. R5, located north of the Salina-Guelph contact, is groundwater from either the Guelph formation or the overburden. R8 and R13, both south of the contact, are clear examples of Salina formation groundwater discharging to the Grand River (Figure 6.12).

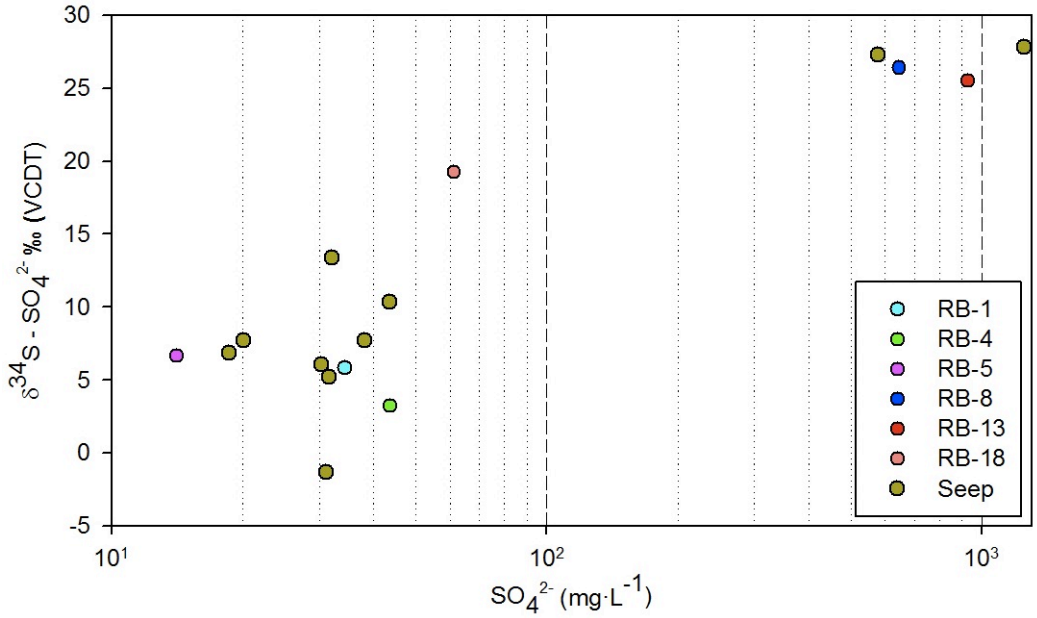

Figure 6.10 $\delta^{34}S$ (‰ VCDT) vs. SO_4^{2-} (mg·L^{-1}) plot of seep and riverbed discharge samples. At each riverbed sampling site, the sample retrieved from the greatest depth in the riverbed was analyzed for $\delta^{34}S$ and $\delta^{18}O$ values. No samples appear significantly affected by sulfate reduction, despite optimal conditions in some riverbed environments.

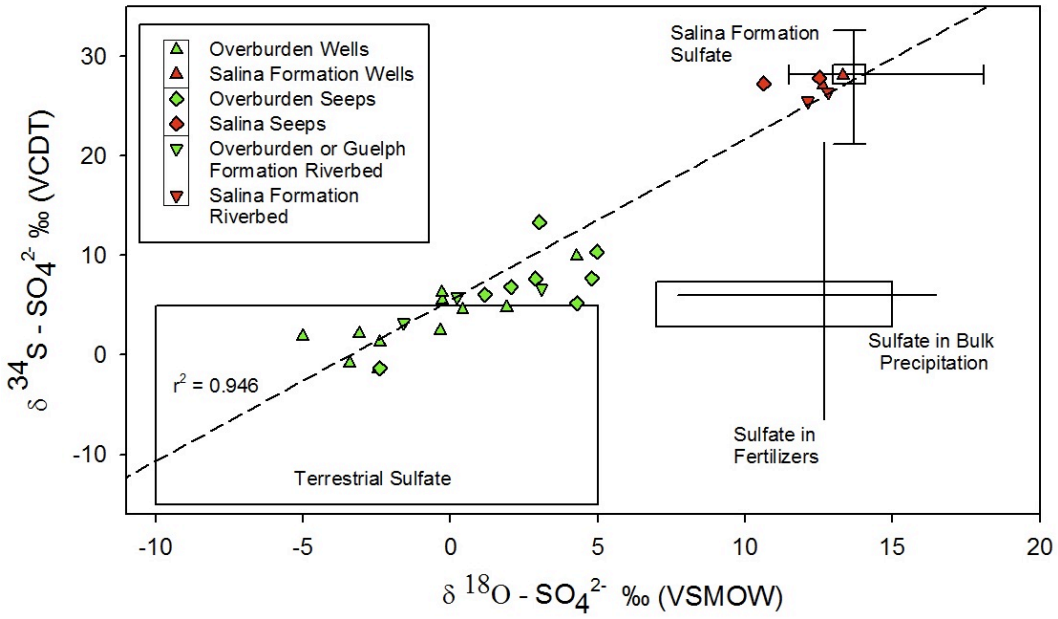

Figure 6.11 Seep and riverbed samples plotted against literature isotopic end-members.

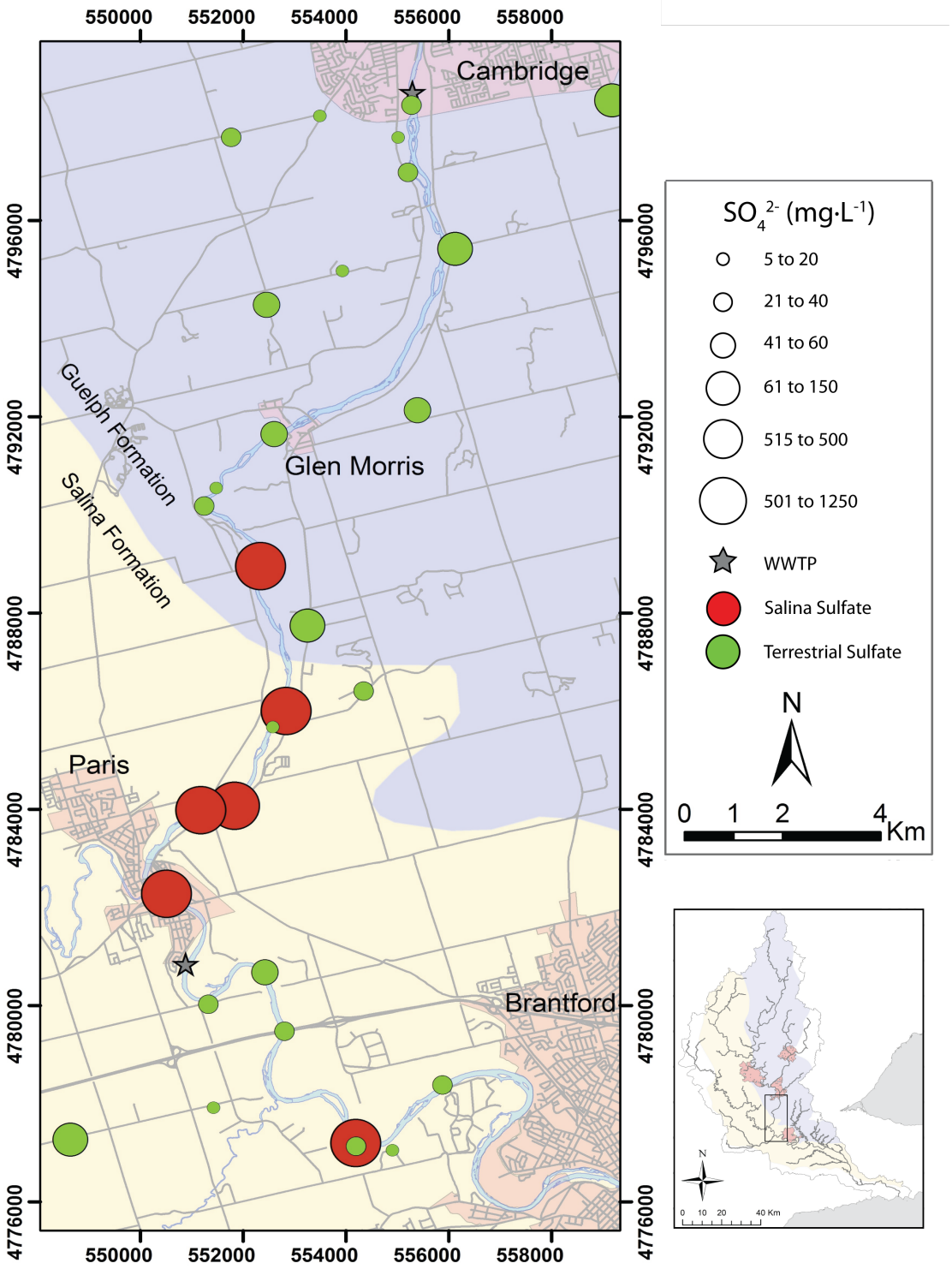

Figure 6.12 Salina formation and terrestrial sulfate distribution in the study area. The one Salina labeled seep north of the Guelph-Salina contact is an artesian spring from a bedrock outcrop in the middle of the Grand River.

6.5.3 Groundwater Discharge in the Grand River

Thus-far, chapter six has illustrated how the Salina formation groundwater can be clearly distinguished from the overburden and the Guelph formation by high sulfate concentrations and $\delta^{34}S\text{-}SO_4^{2-}$ values, and how groundwater discharge to the Grand River can be characterized in a similar manner. Using this distinction, it is suggested that portions of the downstream geochemical trends, from Cambridge to Brantford in the June and September Grand River surveys, show evidence of discharge from the Salina formation. Differences between the surveys appear to be predominately due to a greater WWTP flow component in the river in September than in June, rather than the input of groundwater along the discharge reach.

In June, flow rate in the Grand River is 70% greater than baseflow. The consistent concentrations of chloride and sulfate upstream of the Nith River imply that, relative to the riverflow, minimal groundwater discharge is entering the Grand River. Were considerable volumes of discharge entering the Grand, a steady decrease in chloride would be expected as cumulatively increasing amounts of groundwater from the overburden and Guelph formations enter the river, both of which have lower chloride and concentrations than the Grand River (groundwater was sampled only in September, but concentrations in June are assumed to be similar). Sulfate is only slightly lower in groundwater discharge – upstream of the Guelph/Salina formation contact – than the Grand River, so the same sort of cumulative input of groundwater along the upper portion of the discharge reach would be less clear in the sulfate trends than in the chloride trends.

In September, at baseflow, a slight dilution in chloride, and arguably one in sulfate, is observed between kilometers three and fourteen (twelve for sulfate) that may indicate groundwater discharge (figure 6.7). There is also a large decrease in chloride at kilometer six without a clear input, and after kilometer fourteen, slowly increasing chloride concentrations. Overall, the trends are similar to the June survey; no clear indication of a large, cumulative groundwater input between Cambridge and Paris. If groundwater input is minimal along the discharge reach, at least above Paris, then the seasonal changes in chloride and sulfate in the Grand River surveys must be coming from upstream.

Downstream of Paris, in both the June and September surveys, there is a cumulative decrease in chloride and concurrent increase in sulfate that may suggest groundwater input. The change in both chloride and sulfate is greater in September, at baseflow, then in June. The increase in sulfate clearly implicates the Salina formation as the origin of the groundwater.

In addition to lower chloride and sulfate concentrations, in June, sulfate in the Grand River has a lower $\delta^{34}S$ value relative to September, although the difference between surveys is small compared to the difference in $\delta^{34}S$ vales upstream and downstream of the Nith River's input. Lower $\delta^{34}S$ values in June indicate that the Salina formation sulfate makes up a smaller proportion of the in-stream sulfate, although it is not immediately clear what other sulfate inputs would make up the rest of the sulfate. It is clear, however, that the sulfate must be coming in from upstream of the discharge reach. If it were sulfate in shallow system groundwater along the discharge reach, a cumulative decrease in $\delta^{34}S$ values would be expected downstream, as more and more discharge enters the Grand River. This may be occurring from GR-1 to GR-9, before the river crosses the Salina-Guelph contact, but if so, the depletion is minimal (Figure 6.7). If the sulfate has come in upstream of the discharge reach, from WWTPs, tributaries, or other groundwater discharge areas, the input would result in a consistent separation in $\delta^{34}S$ values between the June and September surveys. This conclusion seems reasonable, given the minimal changes in $\delta^{34}S$ values of both surveys before the Nith River, similar to the behaviour of chloride and sulfate. This is also consistent with the underlying bedrock geology of the area; most of the river channel, upstream of the Nith, flows over Guelph formation bedrock rather than Salina formation. Beginning near the Guelph-Salina conctact just upstream of the Nith, $\delta^{34}S$ values increase and continue to increase until Brantford, even disregarding the Nith's input. This is most clear immediately downstream of the Nith River, where a cumulatively increasing $\delta^{34}S$ suggests a continual input of a high $\delta^{34}S$ sulfate source; e.g., the Salina formation, in good agreement with increasing sulfate concentrations along the same part of the discharge reach. This also agrees with specific capacity summaries of the Guelph and Salina formations, which imply that the Salina formation may have a transmissivity twice that of the Guelph formation (see section 2.5). Like the sulfate concentrations, however, the increase in $\delta^{34}S$ appears minimal, implying that the groundwater discharge along this portion of the Grand River may be a relatively small component of the overall Grand River flow. This contradicts groundwater discharge estimates made by other, such as Scott and Imhoff (2005) who suggest that up to 25% of the flow in the Grand River comes from groundwater. This is in good agreement, however, with streamflow data obtained from GRCA dataloggers, which suggest that, with all other flow components accounted for, only 6% to 7% of the Grand River at Brantford could be due to groundwater input at the time the September river samples were collected (assumed here to be a net quantity).

6.6 Conclusions

A detailed sampling campaign was conducted along a 42-km stretch of the Grand River in the lower central Grand River Watershed, Ontario, Canada. It was expected that unique $^{34}S/^{32}S$ and $^{18}O/^{16}O$ isotope ratios and concentrations of sulfate from several geological sources would help characterize the origin and flow-path of groundwater discharging to the Grand River.

Sulfate concentrations and $^{34}S/^{32}S$ isotope ratios in groundwater samples from domestic wells showed a clear distinction between groundwater from the Salina formation and groundwater from the Guelph formation and overlying quaternary sediments. This distinction was also clear in seep and riverbed discharge samples, and it was therefore possible to identify groundwater coming from the Salina bedrock formation vs. the other two groundwater sources. It was not possible to make a similar distinction between discharge from the overburden material and Guelph formation. Further work is needed to determine a geochemical parameter that can differentiate between groundwater from the overburden and the Guelph formation.

For some discharge samples it was possible to distinguish between groundwater from the overburden and Guelph formation based on the location of the discharge. Due to the thick package of overburden sediments covering the discharge reach, samples from bank seepage that contained sulfate from terrestrial sources are suggested to be from the overburden rather than the Guelph formation below. Groundwater discharge from the riverbed was more variable, and examples of both Salina discharge and overburden or Guelph formation discharge were found. The original conceptual model of seeps discharging from shorter, local flow-paths and riverbed discharge coming from deeper, regional flow-paths is in good agreement with these findings, but this could be improved upon if a parameter could be found to distinguish the Guelph formation from overburden sediments.

Chloride was a good tracer to identify groundwater from hyporheic-zone river water, as the most concentrated input of chloride to the river was from WWTPs (Figure 6.2) and groundwater generally had considerably lower concentrations. Conclusions drawn from geochemical profiles in the riverbed were supported by vertical flux estimates calculated using an analytical solution to the one dimensional heat-diffusion-advection equation developed by Schmidt et al. (2007). Fluxes calculated were variable, but several locations appear to be in areas of much greater discharge than has been previously been found in the Grand River discharge reach (Encalada, 2008; Pastora, 2009; Herrera, 2012).

A refined conceptual model of groundwater discharge was suggested. Discharge is proposed to come from either shallow flow-systems identified in the overburden domestic wells and seep samples, or from a deeper regional flow-system, evidence of which was found in wells screened in the Salina bedrock formation, two seeps, and Salina formation discharge directly to the riverbed. In the Grand River, convincing evidence for significant groundwater discharge, relative to the river flow, could only be seen downstream of Paris. Upstream of Paris, the consistency of geochemical parameters in both Grand River surveys suggest that discharge from either system is minimal, in contrast what the results of the FLIR and drag probe surveys indicated (see Chapters four and five). Overall, geochemical differences in the June and September Grand River surveys appear to be caused by inputs upstream of the discharge reach, contradictory to the results of previous work done in the area. The implications this has on the effect of groundwater on nitrate concentrations in the Grand River along the discharge reach are discussed in the next chapter.

Chapter 7 - Evaluation of NO_3 Input to the Grand River: WWTP Effluent vs. Shallow and Deep Groundwater Systems

7.1 Introduction

The Grand River Watershed, southern Ontario, Canada, is home to approximately 900,000 people and has one of the fastest growing populations in Canada (Bellamy and Boyd, 2005). This growth strains the watershed in terms of supplying both adequate water resources to this population and managing wastewater treatment plant (WWTP) effluent from it. This strain is most clearly illustrated in the lower central portion of the watershed; 42-km upstream of the town of Brantford, which takes its entire municipal water supply directly from the Grand River, the urbanized areas of Kitchener, Waterloo, Cambridge, and Guelph release 77% of all the effluent discharge in the watershed directly to the Grand (based on data from Anderson, 2012). Although Brantford treats it water supply, it also relies, in part, on groundwater discharge along the 42-km reach to assimilate and dilute nutrients such as nitrate from upstream WWTPs, reducing the river's nitrate load before the municipal water intake.

This conceptual model, however, may be an oversimplification of the relationship between groundwater discharge and water quality of the Grand River downstream of Cambridge. Elevated nitrate has been found in groundwater in riverbed sediments below the Grand, suggesting that some groundwater inputs may increase nitrate concentrations in the Grand River rather then diluting them (Loreto, 2008; Pastora, 2009). There may also be a temporal element to the relationship between inputs, groundwater or otherwise, along the discharge reach, and nitrate concentrations in the Grand River; at various times during the year, nitrate has been documented both increasing and decreasing downstream from Cambridge to Brantford (Rosamond, 2009).

In the previous chapter, it was shown how groundwater discharge from the Salina bedrock formation could be identified and distinguished from other discharge sources using sulfate concentrations and $^{34}S/^{32}S$ and $^{18}O/^{16}O$ isotopic ratios of sulfate, and how this led to the distinction between shallow and deep groundwater flow-system discharge to the Grand River. It was suggested that the only area of considerable groundwater input along the discharge reach, as indicated by the geochemical surveys, is immediately downstream of Paris, where sulfate concentration $\delta^{34}S$ trends suggest groundwater discharge from the Salina formation. In this chapter the effects of these conclusions, on the conceptual model of how groundwater affects in-stream nitrate concentrations in the Grand River, are discussed.

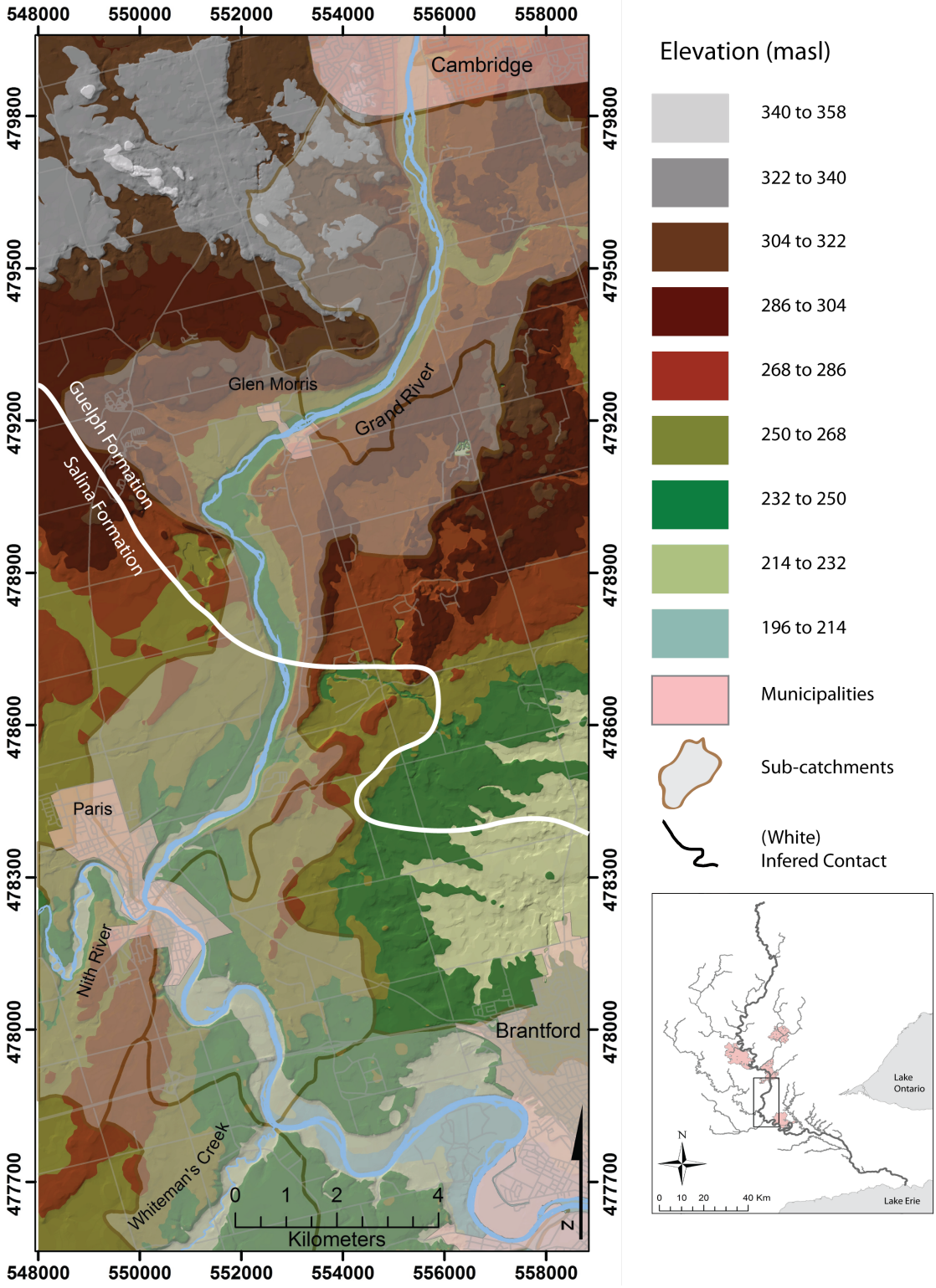

Figure 7.1 The discharge reach.

7.2 The Grand River Discharge Reach

The Grand River discharge reach extends 42 kilometers from the lower municipal boundary of Cambridge down to Brantford (Figure 7.1). Two main bedrock units underlie the area: the Guelph formation, composed primarily of dolostone and limestone in the northern half, and the Salina formation, composed of a cyclically deposited assemblage of shales, dolostones, and evaporites in the southern half. Deposited over the bedrock is a complicated stratigraphy of quaternary sediments: moraines, kame deposits, outwash deposits and spillways, all deposited by the advance, stagnation, and retreat of successive glaciations. Throughout the study area, the thickness of this overburden material increases considerably to the south and west (Holysh et al., 2001). Along some stretches, the Grand River has incised completely through the sediment and flows directly over bedrock. Along others, more recent fluvial sediments have been deposited over the bedrock units or some quaternary sediment remains.

Two main tributaries enter the Grand along the discharge reach: the Nith River, which enters at Paris, and Whiteman's Creek, which enters several kilometers to the south (Figure 7.1). The sub-watersheds through which the Grand flows in this area are fairly narrow, and this restricts the number of other, smaller tributaries entering the Grand between Cambridge and Brantford. Precipitation is fairly consistent on a month-to-month basis, with baseflow conditions occurring in both the winter and summer. A more detailed description of the discharge reach is given in Chapter Two: Study Area Characterization.

7.3 Methods

Groundwater samples were collected from domestic wells screened in overburden and bedrock geological units throughout the study area. Samples were also collected from bank seeps, tributaries, porewater within the riverbed, and from the Grand River. Grand River samples were collected twice; first in mid June, and then in early September, 2011. During the collection of all samples, a Hach™ HQ40d dual-input meter and probe assembly was used to measure DO, conductivity, temperature, and pH. Samples were collected for anions, ammonium, DOC, $^{34}S/^{32}S$ and $^{18}O/^{16}O$ isotopic ratios of sulfate, and $^{15}N/^{14}N$ and $^{18}O/^{16}O$ isotopic ratios of nitrate. The reader is referred to chapter six, section three, for a more detailed description on sample collection and analysis methods.

7.4 Results

7.4.1 Nitrate Concentrations in Groundwater and WWTP inputs to the Grand River

Nitrate concentrations across the study area are shown in figure 7.2. Nitrate in samples from domestic wells range from 0.2 mg $N \cdot L^{-1}$ to 11.0 mg $N \cdot L^{-1}$, with a median value of 2.2 mg $N \cdot L^{-1}$ (n = 42). Three domestic well samples near the Cambridge municipal line have nitrate concentrations over 10 mg $N \cdot L^{-1}$; two are screened in the overburden and one is screened in the Guelph formation. With the exception of this Guelph formation well and one other, bedrock wells tend to be screened at greater depths and have lower nitrate concentrations than overburden wells (Figure 7.3). Of forty-two wells sampled, nine were known to be screened in bedrock formations. Of these nine, only two wells have nitrate concentrations greater than 0.3 mg $N \cdot L^{-1}$, at 4.8 mg $N \cdot L^{-1}$ and 8.7 mg $N \cdot L^{-1}$. In the thirteen overburden wells sampled in the discharge reach, nitrate ranges from 0.2 mg $N \cdot L^{-1}$ to 11.0 mg $N \cdot L^{-1}$ with a median value of 0.6 mg $N \cdot L^{-1}$. The remaining twenty wells, screened in unknown formations, have nitrate concentrations ranging from 0.2 mg $N \cdot L^{-1}$ to 6.1 mg $N \cdot L^{-1}$ with a median concentration of 0.9 mg $N \cdot L^{-1}$.

Nitrate in groundwater discharge samples show a concentration range similar to the domestic wells. Seep samples across the study area rang from 0.2 mg $N \cdot L^{-1}$ to 14.1 mg $N \cdot L^{-1}$, but with a higher median nitrate concentration of 3.8 mg $N \cdot L^{-1}$ (n = 25) than observed in the domestic wells. Riverbed samples rang from below detection limit to 5.0 mg $N \cdot L^{-1}$, with a median value of 0.8 mg $N \cdot L^{-1}$ (n = 62). No spatial pattern was discernible other than the fact that riverbed porewater samples generally show lower nitrate concentrations than the seep samples.

The highest sampled concentration input of nitrate to the Grand River came from the Galt waste-water treatment plant at 27.7 mg $N \cdot L^{-1}$. This was slightly higher than the range of nitrate concentrations the treatment plant discharged between 2003 and 2008 (min = 0.5, median = 18.0, max = 24.6 mg $N \cdot L^{-1}$; Anderson, 2012).

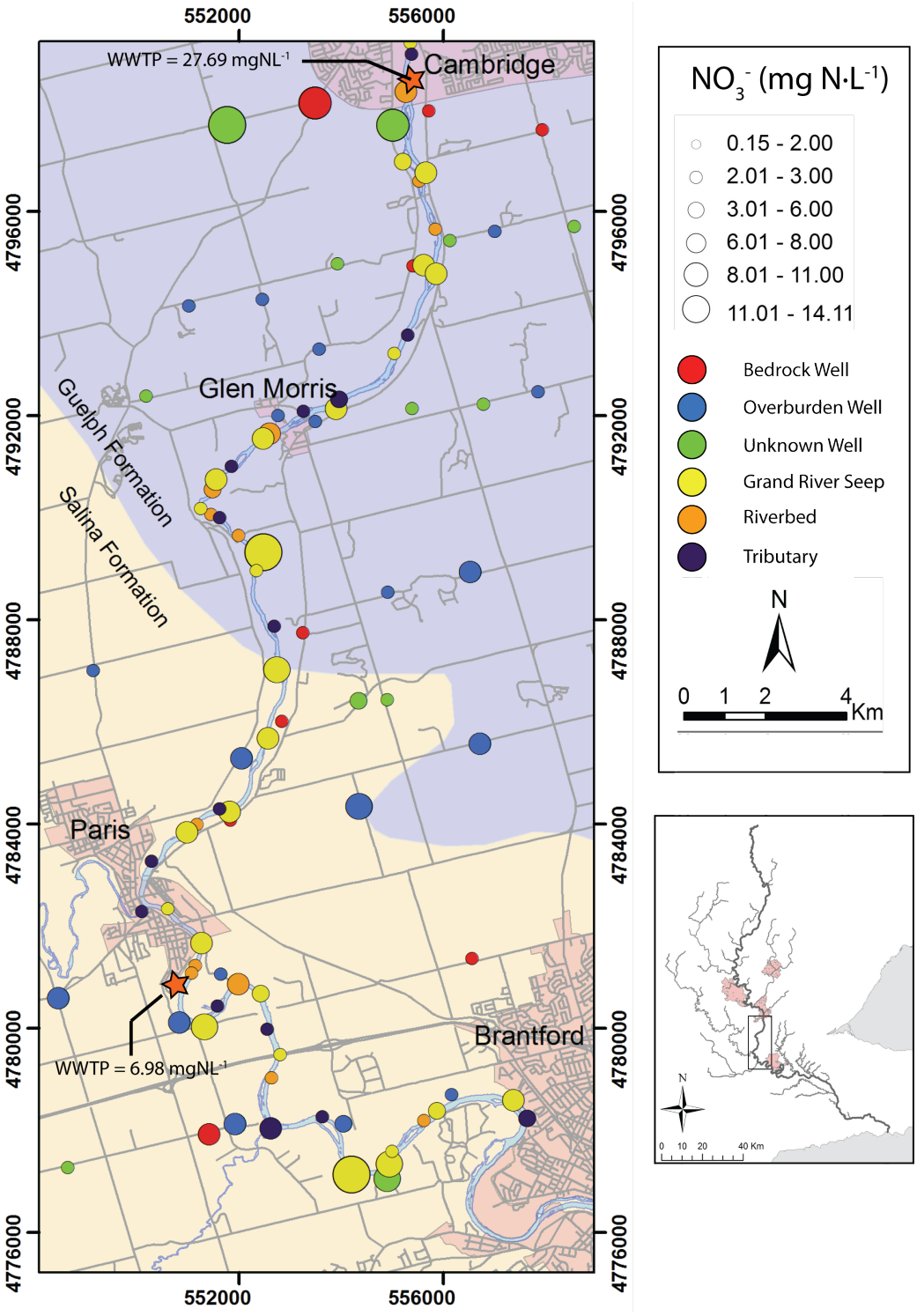

Figure 7.2 Nitrate concentrations in domestic wells, seeps, tributaries, and the riverbed across the discharge area.

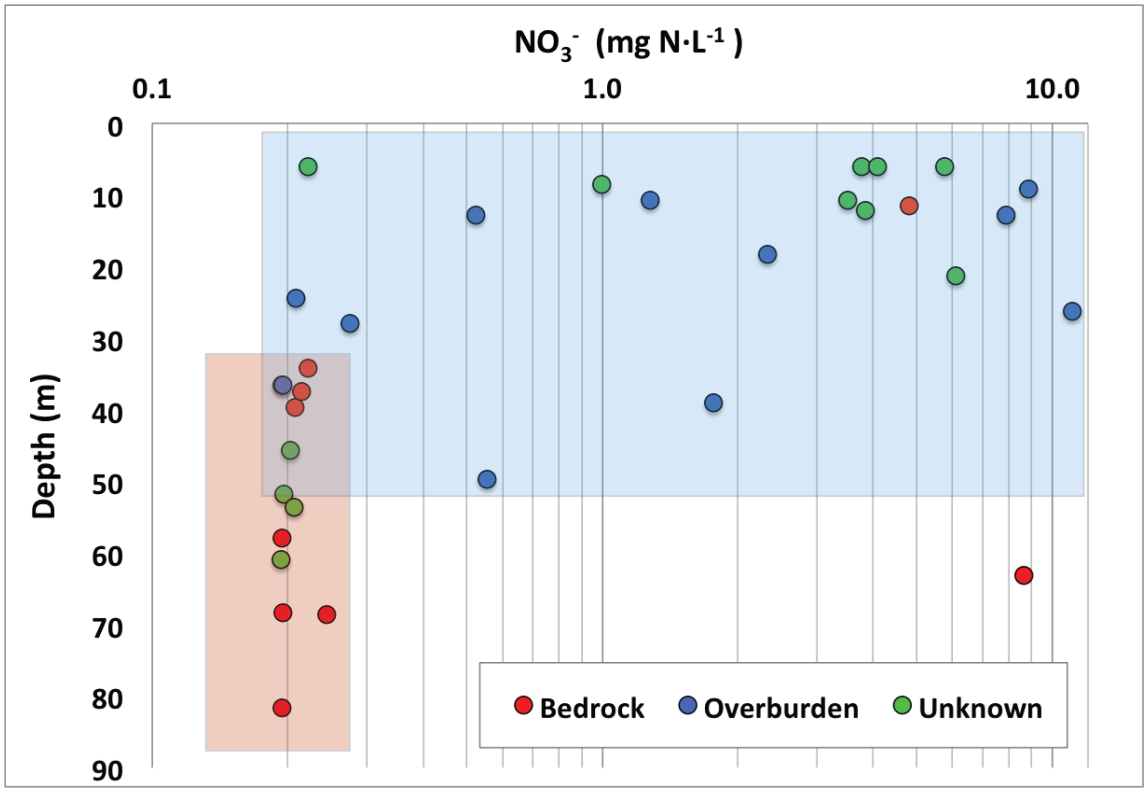

Figure 7.3 Relationship between depth and nitrate concentrations in bedrock and overburden wells

7.4.2 Nitrate Isotopes in Groundwater Across the Discharge Reach

Select samples from the domestic wells, seeps, the riverbed, and the Grand River were analyzed for nitrate isotopes, with the intent of determining both possible sources of nitrate to the Grand River and the extent to which denitrification removes nitrate in discharge from the overburden and bedrock formations.

Four domestic well samples were analyzed for nitrate isotopes. Two, DW-23 and DW-26, were previously used to define Salina formation groundwater. The other two, DW-2 and DW-3, near the Cambridge municipality border, show high nitrate concentrations relative to other domestic wells in the region (Figure 7.2). DW-23 and DW-26 are both anoxic with low nitrate concentrations of 0.2 mg $N \cdot L^{-1}$ and 0.2 mg $N \cdot L^{-1}$, $\delta^{15}N$ values of 27.3‰ and 16.3‰, and $\delta^{18}O$ values of 21.6‰ and 2.7‰, respectively. DW-2 and DW-3 both have oxic levels of DO and higher nitrate concentrations of 8.7 and 8.8 mg $N \cdot L^{-1}$, $\delta^{15}N$ values of 3.6‰ and 4.1‰, and $\delta^{18}O$ values of -0.6‰ and -1.0‰ (Figure 7.4).

Fourteen seep samples were analyzed for $^{15}N/^{14}N$ and $^{18}O/^{16}O$ isotopic ratios of nitrate. Of these fourteen samples, nine had been previously analyzed for $^{34}S/^{32}S$ and $^{18}O/^{16}O$ isotopic ratios of sulfate; eight of these samples were classified as containing sulfate from the overburden material, and one contained Salina formation sulfate (and discharged directly from a bedrock outcrop). Seven of the overburden seeps have $\delta^{15}N$ and $\delta^{18}O$ values that are similar to nitrate derived from ammonium fertilizers or soil nitrogen compounds; $\delta^{15}N$ values range from 1.9‰ to 4.5‰, and $\delta^{18}O$ values range from -2.3‰ to 2.2‰. The eighth overburden seep is more enriched, with $\delta^{15}N$ value of 12.1‰ and a $\delta^{18}O$ value of 4.0‰, plotting within the literature range that corresponds to a septic waste or manure nitrogen source (Figure 7.4). The Salina formation seep has $\delta^{15}N$ and $\delta^{18}O$ values intermediate between the soil nitrogen seeps and the septic or manure nitrogen seep, at 9.9‰ and -0.3‰. As all seeps sampled have relatively high concentrations of DO, it is suggested that the enriched sample is indicative of a different source rather than denitrification. The Salina bedrock seep referred to above has a nitrate concentration of 1.3 mg $N \cdot L^{-1}$, and is oxic (DO = 4.2 mg $\cdot L^{-1}$). Of the five other seep samples analyzed for $^{15}N/^{14}N$ and $^{18}O/^{16}O$ isotopic ratios of nitrate, samples that were not analyzed for sulfate isotopes, three plot within the soil nitrogen literature range, and two appear to be from septic system or manure sources (Figure 7.4).

At the riverbed locations R4, R5, R8, R13, and R18, the sample at 1m depth was analyzed for $^{15}N/^{14}N$ and $^{18}O/^{16}O$ isotopic ratios of nitrate. The origin of the water in all five samples had previously been characterized using sulfate isotopes (see chapter six). R8 and R13 are examples of locations where Salina formation discharges directly to the riverbed. R8 and R13 have $\delta^{15}N$ values of 17.2‰ and 16.9‰, and $\delta^{18}O$ values of 7.7‰ and 9.1‰. When considered with these samples low DO and low nitrate concentrations (0.5 mg $N \cdot L^{-1}$ and 0.8 mg $N \cdot L^{-1}$ for R8 and R13), the relatively high delta values may imply denitrification is occurring. In contrast, R4 and R5 both have more depleted $\delta^{15}N$ and $\delta^{18}O$ values of 3.3‰ and 5.0‰, and -2.1‰ and -0.4‰, respectively, along with oxic conditions consistent with the overburden seep samples. R18, previously identified as hyporheic river-water, plots intermediate between the depleted values of R4 and R5 and the more enriched values of R8 and R13, with $\delta^{15}N$ and $\delta^{18}O$ values of 8.9‰ and -2.2‰, respectively (Figure 7.4).

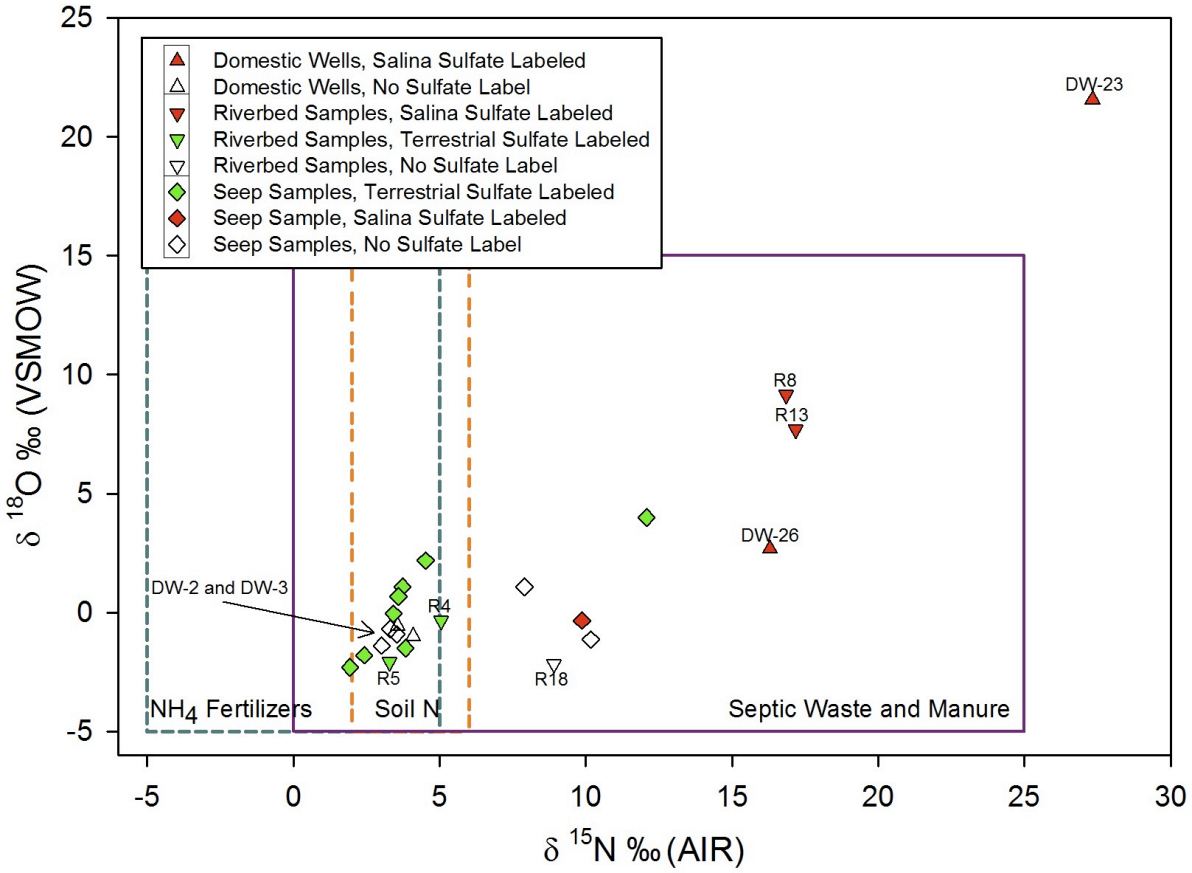

Figure 7.4 Distribution of nitrate isotopes in groundwater in the discharge reach

7.4.3 Nitrate Concentrations in the Grand River

Nitrate concentrations are slightly lower in the Grand River in September than in June (Figure 7.5). This is a clear contrast with other anions in the Grand River, all of which have higher concentrations during baseflow conditions in September than during the higher flow conditions in June. There is considerable variability in the nitrate concentrations below Cambridge, especially in the September survey. As with other anions in the Grand River, the convergence of the Nith River is clear in the September survey; however, it is not all that evident in the June survey. After the Nith River, the September survey, overall, shows decreasing nitrate concentrations downstream, while concentrations during the June survey stay relatively constant.

7.4.4 Nitrate isotopes in the Grand River

$\delta^{15}N$ values are generally slightly enriched in the Grand River in September relative to June (Figure 7.5). One September sample, collected just where the Grand River crosses the Guelph-Salina contact, had a relatively depleted $\delta^{15}N$ value more consistent with the June survey $\delta^{15}N$ values. After this point, $\delta^{15}N$ values gradually became more enriched down the discharge reach. In June, a gradual depletion in $\delta^{15}N$ values is noted down the discharge reach. In both surveys, $\delta^{18}O$ values are fairly consistent downstream, ranging between approximately -2‰ and 1‰. No discernable pattern was evident.

7.5 Discussion

7.5.1 Nitrate in samples containing Terrestrial vs. Salina Formation Sulfate

Samples containing terrestrial sulfate showed a greater range in nitrate concentrations and contained significantly higher concentrations of nitrate than samples containing Salina sulfate isotopic ranges (Rank-Sum Test: $p = 0.0014$, figure 7.6). This may be due to older water generally lacking a source of nitrate in the deeper aquifer, or it may be the result of a greater potential for denitrification in the Salina formation due to more consistently anoxic conditions. Because of the technique employed to sample the domestic wells (from outdoor faucets), recorded DO values may not be representative of in-situ conditions. There are numerous opportunities for oxygen to enter the system as groundwater flows through the house plumbing, so high values of dissolved oxygen do not necessarily indicate an oxic subsurface environment. If, on the other hand, DO values were low (< 2 $mg \cdot L^{-1}$), it was taken as indicative of the redox environment within the well. Of the forty-two domestic wells sampled, eighteen contained dissolved oxygen less than 2 $mg \cdot L^{-1}$; of these eighteen wells, fifteen had nitrate concentrations less than 0.2 mg $N \cdot L^{-1}$, and the other three were 0.8 mg $N \cdot L^{-1}$, 1.3 mg $N \cdot L^{-1}$, and 4.1 mg $N \cdot L^{-1}$, respectively. Of the other twenty-four wells with DO concentrations greater than 2 mg $N \cdot L^{-1}$, nitrate ranged from < 0.2 mg $N \cdot L^{-1}$ to 11.1 mg $N \cdot L^{-1}$. The best example of a DO measurement that does not reflect subsurface conditions is at DW-8, where nitrate and sulfate concentrations are low (0.2 mg $N \cdot L^{-1}$ and 15.8 $mg \cdot L^{-1}$, respectively), and where $\delta^{34}S$ values indicate sulfate reduction – i.e., clearly an anoxic environment, but measured DO was 9.4 $mg \cdot L^{-1}$. Of the two wells indicative of Salina formation groundwater, DW-23 and DW-26, DW-23 showed anoxic conditions and low nitrate concentrations (0.2 $mg \cdot L^{-1}$ and 0.2 mg $N \cdot L^{-1}$) while DW-26 may have been contaminated with atmospheric oxygen (DO = 6.8 mg $N \cdot L^{-1}$, nitrate = 0.2 mg $N \cdot L^{-1}$).

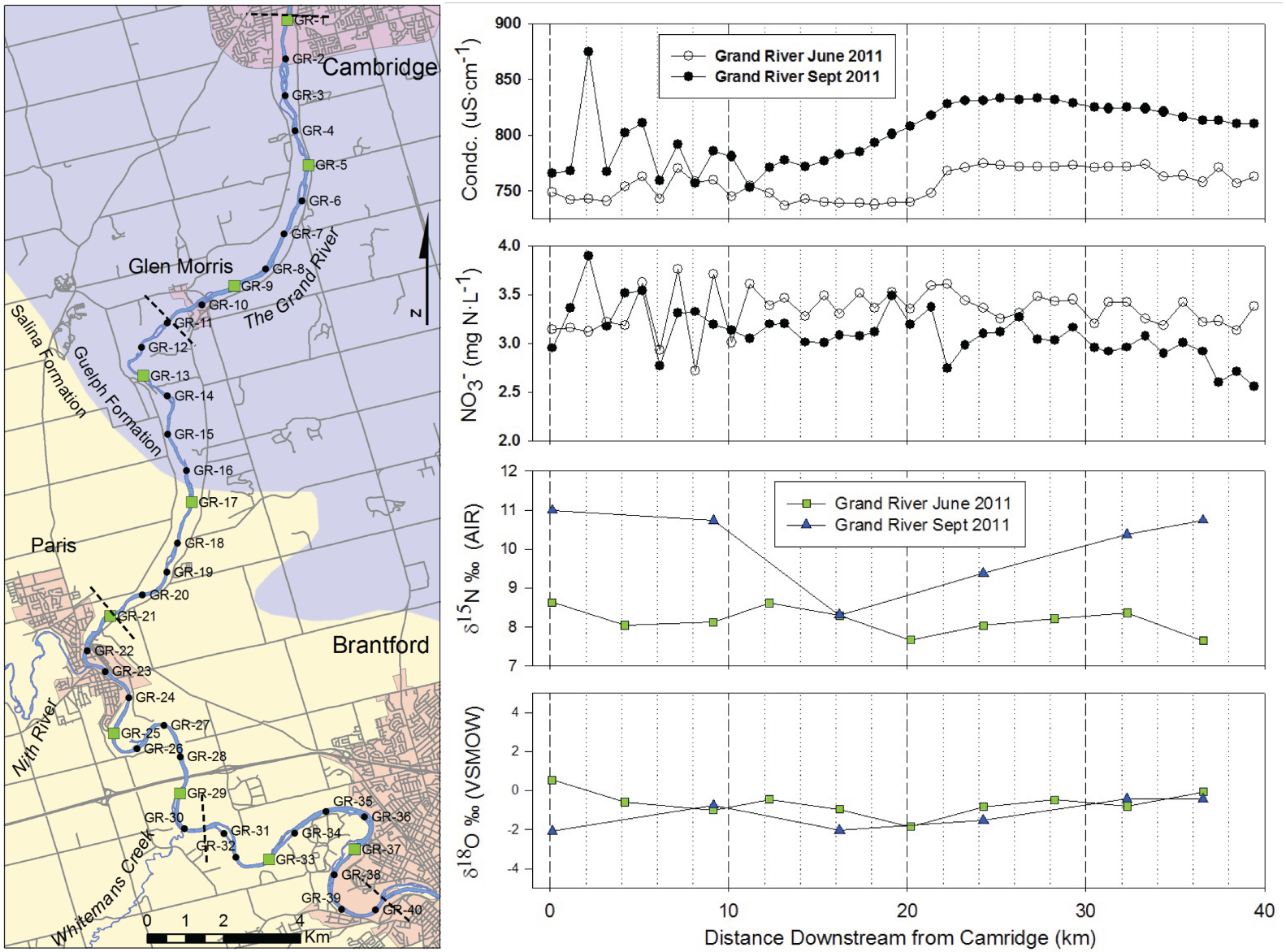

Figure 7.5 Conductivity and nitrate concentrations and isotopes down the discharge reach.

Seep sample DO values may be more representative of shallow groundwater redox conditions. Only one seep value was found below 2 mg·L^{-1} DO; GRS-10 at 0.1 mg·L^{-1}, a seep from an artesian spring flowing from a bedrock outcrop in the centre of the Grand River. This was one of two seeps clearly identified as from the Salina formation through high sulfate concentrations and enriched $\delta^{34}S$ and $\delta^{18}O$ values. In addition to DO values, nitrate and ammonium concentrations suggested reducing conditions at GRS-10, at 0.2 mg N·L^{-1} and 0.2 mg·L^{-1}, respectively. The other seep from the Salina formation indicated oxic conditions, with 4.1 mg·L^{-1} and 1.3 mg·L^{-1} for DO and nitrate. Similarly, all other seeps had oxic DO concentrations, and showed no signs that could indicate a change in redox conditions, such as iron or manganese oxide staining.

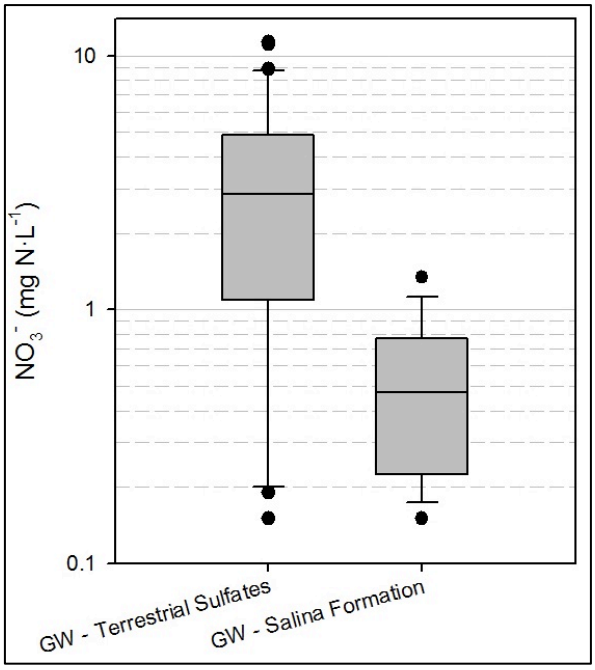

Figure 7.6 Higher nitrate concentrations in groundwater containing terrestrial sulfates than in groundwater containing Salina formation sulfates (Rank-Sum Test: Terrestrial sulfates n = 34, Salina formation sulfates n = 13. p = 0.0014).

Dissolved oxygen concentrations in riverbed samples could be confidently measured, as the waterloo profiler provides an airtight route from the subsurface to the collection container. On route, the sample passes through a clear scintillation vial, and it is easy to see, via bubbles, if there are any leaks in the system. If a leak was found during sampling, connections were tightened and the sample was collected a second time. Of the riverbed locations where groundwater was found discharging from the Salina formation, R8 and R13, DO was < 1.0 mg·L^{-1} and between 2.0 and 3.0 mg·L^{-1}, respectively. Both locations showed nitrate concentrations below 1.0 mg N·L^{-1}. RB-5, which showed

strong groundwater discharge with a terrestrial sulfate signature, had DO above 5 $mg \cdot L^{-1}$ and nitrate concentrations of 2.8 to 2.9 mg $N \cdot L^{-1}$.

Thus, despite some variation - both natural and as a result of the domestic well sampling method - dissolved oxygen levels tended to be lower in samples from the Salina formation than in samples identified with terrestrial sulfate. This, along with nitrate concentrations, may suggest that optimal redox conditions for denitrification may be more widespread in the deeper aquifer than in the shallower aquifer, which is consistent with the $\delta^{15}N$ and $\delta^{18}O$ values shown in figure 7.4.

7.5.2 The Nitrate Contribution to the Grand River From Deep vs. Shallow Groundwater Systems

Figure 7.7 displays $\delta^{15}N$ values vs. nitrate concentrations of all the samples analyzed for nitrate isotopes. The samples identified by terrestrial sulfate isotopes and low sulfate concentrations contain a range of nitrate, and some have higher nitrate concentrations than the Grand River. All of these samples have depleted $\delta^{15}N$ values relative to samples from the Grand River and the Salina formation. The Salina formation samples, with one exception, have considerably enriched $\delta^{15}N$ values and nitrate concentrations below 1 mg $N \cdot L^{-1}$.

It is suggested that the relative enrichment in $\delta^{15}N$ values of the September river samples supports the conclusion arrived at via the sulfate isotope results; that the proportion of baseflow contributed by the Salina formation is greater in September than June (see chapter six). With a greater proportion of flow in the river supplied by the Salina formation with lower concentrations of nitrate than the overburden, a greater proportion of the nitrate present is from the Cambridge and other WWTPs; the Cambridge WWTP sample yielded $\delta^{15}N$ vs. $\delta^{18}O$ values of 11.4‰ and -1.5‰, respectively, slightly more enriched in ^{15}N than the September survey (Figure 7.7). Conversely, in June, the contribution from other upstream inputs is greater –a hypothesis supported by consistent downstream anion concentrations and sulfate isotopes – which results in a lower proportion of nitrate in the Grand coming directly from the WWTPs. Thus the $\delta^{15}N$ of river samples is slightly lower, shifting towards the relatively depleted $^{15}N/^{14}N$ ratios in samples from the overburden aquifers (Figure 7.7).

Downstream $\delta^{15}N$ may also support this hypothesis. As with the $\delta^{34}S$ values, cumulative downstream input from the shallow overburden discharge would result in a gradual decrease in $\delta^{15}N$ values. While this was tenuous at best with $\delta^{34}S$ values, $\delta^{15}N$ values in September do appear to decrease downstream over the upper half of the discharge reach. The subsequent enrichment in the

latter half of the discharge reach could be explained by the input of the Paris WWTP, which, although not selected for nitrate isotope analysis, would be expected to have similar $\delta^{15}N$ and $\delta^{18}O$ values of upstream WWTPs. This may not be reasonable, as the flow input from the Paris WWTP is considerably smaller than the upstream WWTPs. Additionally, the downstream increase appears to be from a cumulative type source rather than a point source like a WWTP. Otherwise, the downstream enrichment in September is difficult to explain through groundwater inputs. It seems unlikely that it would be from the Salina formation, which has enriched $\delta^{15}N$ values but very low concentrations.

$\delta^{15}N$ values in June show a gradual depletion along the entire discharge reach. This is consistent with a cumulative input from shallow overburden groundwater. Thus, the rebound in $\delta^{15}N$ values noted around Paris in the September survey is absent, as the increased input from shallow systems in June obscures other, smaller nitrate inputs to the Grand River.

7.5.3 Nitrate Cycling in the Grand River

Thus-far, this discussion has focused on how nitrate in the Grand River is affected by groundwater inputs. Downstream anion and sulfate isotopic trends, however, suggest that groundwater input along the discharge reach is minimal, with geochemical trends only highlighting one sub-reach, directly downstream of Paris, where the geochemical trace of Salina formation groundwater can be seen coming into the Grand. Thus, the impact of in-stream nitrate cycling processes must be considered as well, as it may have a considerable impact relative to that of groundwater discharge.

In river systems, nitrate is removed by plant uptake, and, during anoxic spells caused by oxygen consumption, denitrification (Kellman and Hillare-Marcel, 1998). Either process would result in decreasing concentrations of nitrate downstream, along with increasing $\delta^{15}N$ values as lighter nitrogen is preferentially consumed in the case of denitrification, and constant $\delta^{15}N$ values if plant uptake is relatively more important, as biological assimilation is a non-fractionating process (Mariotti, 1988).

In the June survey, nitrate concentrations remain relatively consistent while $\delta^{15}N$ values decrease, slightly but consistently, down the discharge reach. This suggests that either A), the removal processes are minimal in June, or B), that fractionation effects are being masked by the input of other, more depleted ^{15}N sources downstream. The second suggestion seems unlikely, as neither anion or sulfate isotope downstream data imply considerable input from source that would lower $\delta^{15}N$ values. The first suggestion may be more reasonable; in June, at 70% greater flow than baseflow, the river is

deeper and flowing quickly. This limits the timeframe in which both processes have to occur, which would minimize fractionations caused by them.

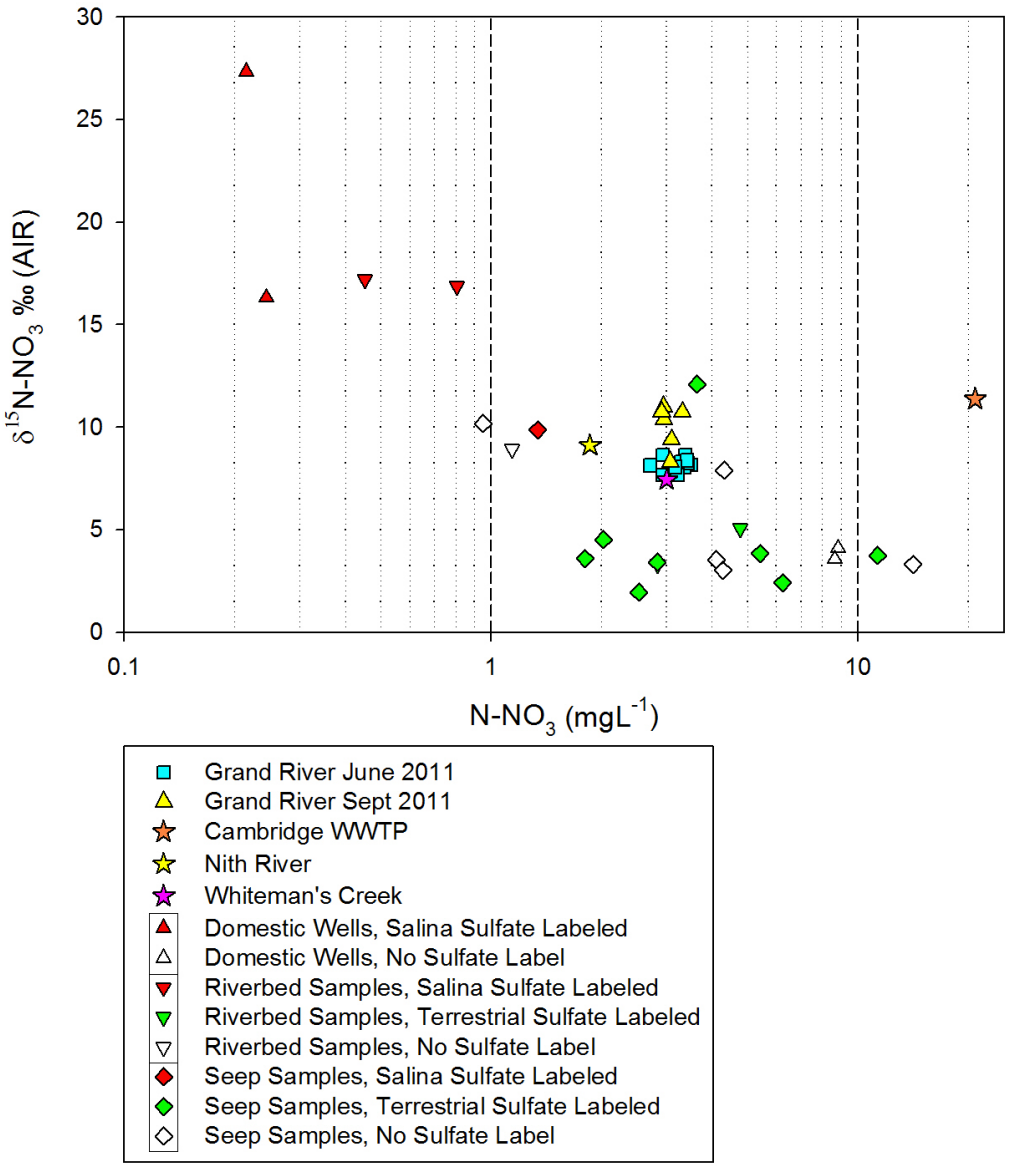

Figure 7.7 $\delta^{15}N$ vs. Nitrate concentrations in the discharge reach

In the September survey, nitrate concentrations stay relatively constant along the upper portion of the discharge reach and then decrease along the lower, while $\delta^{15}N$ values first decrease until approximately the Guelph and Salina formations contact, where $\delta^{15}N$ increases until Brantford (Figure 7.5). The initial decrease in $\delta^{15}N$ is difficult to explain, and could be a result of an

anomalously low $\delta^{15}N$ value sampled at GR-17. The subsequent increase in $\delta^{15}N$ could be consistent with an increased importance of plant uptake and denitrification occurring in-stream, but could also be consistent Salina formation groundwater entering the Grand south of Paris. In September, daytime temperature are considerably greater than in June, and anoxic occurrences much more likely to happen. Additionally, the river is at baseflow and therefore much more shallow and slower flowing, which may increase the impact of in-stream nitrate removal (CITATION NEEDED). Salina formation groundwater input would also lower nitrate concentrations, as well as increase $\delta^{15}N$ values, as Salina formation groundwater tends to be low in nitrate and have elevated $\delta^{15}N$ values due to denitrification. Were nitrogen uptake processes to have a considerably greater impact in the September survey than the June, it would be expected that nitrate concentrations would decrease and $\delta^{15}N$ values would increase over the entire discharge reach. At this point, there isn't much information to expect nitrate removal processes to be greater below Paris than above, with the exception of the channel gradient. Above Paris, the Gradient is considerably steeper than below, which increases river velocity and reduces the timeframe in which removal processes have to affect in-stream nitrate. Geochemical trends, however, suggest that the main groundwater input is Salina formation groundwater just south of Paris, which does agree with nitrate concentration and $\delta^{15}N$ downstream trends.

7.6 Conclusions

Groundwater labeled with Salina formation sulfate tends to have lower concentrations of nitrate than groundwater labeled by terrestrial sulfates. Dissolved oxygen and nitrate concentrations give a general redox interpretation of sample types in the area, with repercussions on the cycling of nitrate within the region. Groundwater samples from domestic wells screened in all formations have the potential to be anoxic, but the sampling method restricts any attempt to be more specific. Seep samples tend to be oxic with a range of nitrate concentrations. Samples of riverbed discharge reveal a range of redox conditions; the Salina formation discharge locations tend to be anoxic and low in nitrate, while overburden or Guelph discharge locations tend to be oxic with a range of nitrate concentrations.

Samples labeled as overburden by terrestrial sulfate isotope ranges tend to show more depleted $\delta^{15}N$ values than the river samples, which appear strongly influenced by upstream WWTPs, and more depleted $\delta^{15}N$ values than the nitrate in Salina formation groundwater, which generally appears to have undergone denitrification (Figure 7.7). Additionally, September river samples had slightly lower nitrate concentrations than the June river samples, a situation somewhat reversed from the rest of the

geochemical parameters measured during the surveys. It is suggested that the downstream decrease in nitrate shown by the September survey is due to dilution, as opposed to in-stream nitrate removal processes, as increasing amounts of Salina formation groundwater enters the Grand River down the discharge reach downstream of the Nith River.

It is proposed that the overall increase in $\delta^{15}N$ values of the September river samples supports the conclusion arrived at via the sulfate isotope results; that the proportion of baseflow contributed by the Salina formation is relatively greater in September than June. Soil nitrogen or ammonium fertilizer based nitrate load is lower in September, so $\delta^{15}N$ values shift towards the isotopic ratios of the other main source of nitrate in the Grand River; in-stream nitrate from upstream WWTPs (Figure 7.7).

Even though the deeper flow system acts to dilute in-stream nitrate, concentrations in the Grand River appear mainly dictated by the upstream WWTPs. Overburden systems do not appear to contribute a considerable groundwater volume to the river, although what contribution is there may not contribute to diluting nitrate from upstream WWTPs. Nitrate in the overburden system appears to be generally as high or higher than in-stream concentrations, although it is unknown how this may change on an annual timescale. The importance of in-stream removal is not clear from the results of this research, but, due to the small amount of groundwater that appears to discharge, may be relatively significant.

Chapter 8 – Conclusions and Recommendations for Further Work

The two methods used to characterize groundwater surface-water interactions along the Grand River discharge reach were in many ways complementary to one another, offering unique evidence in support of, or against, the conclusions of the other. The first section of this chapter summarizes the individual conclusions arrived at from each methodology: the FLIR survey, the drag probe surveys and temperature profiling, using sulfate isotopes as tracers for shallow and deep groundwater systems, and nitrate inputs in the Grand River discharge reach. The second section of this chapter summarizes the broader conclusions that address the main research objectives introduced in chapter one. Finally, recommendations for further research are discussed, in terms of what can be done to more completely understand the original objectives, and in terms of other questions that arose as a result of this research.

8.1 Conclusions and Recommendations on Individual Methods

8.1.1 FLIR Survey

The main deliverable from the FLIR survey was a map of bank discharge along the upper third of the discharge reach (Figure 4.3). This map not only illustrates the distribution of seeps and tributaries along the discharge reach, but also the magnitude of the temperature contrast between each feature and the surrounding bank, and the relative size of each discharge feature. Three large areas of bank seep discharge were highlighted. A fourth discharge area was also indicated, described as a collection of tributaries formed from the accumulation of seeps discharging from higher elevations. This resulted in a considerably clearer understanding of bank discharge along this stretch of the discharge reach, which was previously mapped via visual surveys conducted by canoe. During these previous surveys, only seeps with visible channel structures were noticed, and no distinction could be made between tributaries draining groundwater vs. surface water sources.

Prior to the FLIR survey, it was expected that, in some localized areas, considerable groundwater would be found discharging from both banks. It was hypothesized that, in these locations, discharge might extend beneath the river to discharge directly to the riverbed. If this discharge was found to occur, these areas could then be used to help identify sections of the river where direct riverbed discharge was occurring. The FLIR survey discharge map, however, shows only one location where discharge occurs simultaneously from both sides of the river (Figure 4.3, discharge reach two). This is

a reach just south of Glen Morris, approximately two kilometers long, where extensive work in the riverbed has already been completed (Encalada, 2008; Pastora, 2009; Herrera, 2012). Here, a topographic and bedrock surface cross section indicated, along with monitoring wells installed during the fieldwork of Herrera (2012), that overburden material does extend beneath the riverbed (Figures 3.1, 3.3, and 3.4). Over the rest of the discharge reach surveyed with the FLIR camera, it is difficult to see any spatial correlation between discharge from one side of the river and discharge from the other. Most of the stronger temperature anomalies are found along the northwest bank. This may be due to a sharper drop in elevation, from adjacent uplands to the river, along the north bank than the along south.

Although the survey was able to competently locate groundwater discharge of varying types, several improvements to the method could be made. A survey conducted in winter would likely produce clearer, more consistent results. Temperature fluctuations due to diurnal cycles would be minimal, and reduced bank foliage would make it easier to identify and categorize bank discharge features. For future surveys done by helicopter, talking out the exact details of the flight with the pilot is an absolute necessity. During this survey the pilot informed the researchers that, along several stretches of the discharge reach, he was unable to move closer to the target bank due of a bylaw stating that because the appropriate permit had not been obtained, he was required to stay at least 500ft from urbanized landcover. This came as a surprise, as the pilot had made no previous mention of this bylaw, even though the general procedure of the survey had been discussed in detail. As a result, survey coverage along the north bank upstream of Glen Morris suffered (Figure 4.3).

8.1.2 Drag Probe Surveys

The drag probe surveys resulted in a fairly detailed thermal characterization of the Grand River discharge reach. Only minimal temperature differences were noticed between the riverbed and the river surface. Several significant temperature differences across the river channel were noted. The most obvious example occurs where Whiteman's Creek enters the Grand; a very large temperature decrease and slow, subsequent rebound was noted down the west bank of the river, but only a moderate change and almost imperceptible change was noted down the middle and east bank, respectively.

A conceptual model relating the downstream thermal traces to various input types was constructed. The discharge types conceptualized in the thermal traces were categorized as small and large groundwater fed tributaries, or point source discharge, and reaches of low, moderate, and strong

groundwater input, or diffusive discharge. Using this conceptual model, the June surveys highlighted one six kilometer stretch of the river, beginning just south of the Glen Morris Bridge, that appeared to be a reach of relatively strong diffusive groundwater discharge. This was in good agreement with the FLIR survey results; this is the same section of river where several large stretches of bank seepage were noted. During the September drag probe survey, the same temperature trends were noted in the same locations, but to a greater degree; a larger temperature decrease over a much longer reach of the river was observed. This increased temperature depression was consistent with the conceptual model that a greater portion of riverflow comes from groundwater during low flow conditions.

This reach was successfully temperature profiled, and numerous locations with a strong vertical groundwater flux were found. It is difficult to conclude that the use of the drag probe surveys led to this success, however, as other locations not highlighted by the drag probe surveys as probable discharge areas also proved to have moderate to strong vertical groundwater fluxes. As well, the reach proved too long to temperature probe in any detail; taking temperature measurements approximately every 50m leaves a considerable element of chance to the success of the profiling method. This highlights several limitations in the drag probe surveys that should not be overlooked. The most significant is that the surveys failed to resolve the discharge reach into lengths short enough to be profiled in detail. This may or may not have been a function of the probe type used; using probes with smaller time constants may have resulted in better resolution of temperature changes. It is also strongly recommended that a probe capable of measuring electrical conductivity along with temperature be employed for subsequent surveys. For this research, this may have allowed for the distinction between overburden discharge (possibly lower conductivity than the river) and discharge from the Salina formation (generally higher conductivity than river water).

The river itself may have simply been flowing too fast for a drag probe survey to work. Previous researchers have suggested the surveys produce the best results in rivers flowing at speeds less then 0.21 $m \cdot s^{-1}$ (Vaccarro and Maloy, 2005). The Grand River, along some of the faster riffle sections, flowed at speeds more than two $m \cdot s^{-1}$. This may also imply a decrease in survey effectiveness between the riffle sections and the slower flowing pools.

8.1.3 Temperature Profiling

Overall, the temperature probes proved invaluable as a reconnaissance tool for locating specific points of groundwater discharge from the riverbed to sample. One contribution of this research was the construction of a robust temperature probe; designs by previous researchers, constructed to be

inserted into sand and loose gravel streambeds, proved unable to withstand the considerable force needed to insert the temperature probes into the Grand River riverbed. Sturdier probes, and an insertion method similar to that of Becker et al. (2003), for the insertion of mini-piezometers, greatly increased the lifespan of the temperature probes used in this research.

As stated in the section above, the scaling down approach from drag probe surveys to temperature profiling produced results in only one stretch of the discharge reach. Further temperature profiling along the Grand was essentially random, and locations were chosen for accessibility rather than discharge possibility. Therefore, despite the success in finding further discharge locations, the use of profiling in large rivers is still questionable, unless it is used for specific site characterizations. As a reconnaissance tool in large rivers, it may be too time consuming and labour intensive to be cost effective.

The greatest utility of the temperature method comes from the fact that a useful estimate of vertical groundwater discharge, subject to several assumptions that must be carefully considered, can be gained from a single subsurface temperature measurement (Schmidt et al., 2007). The temperature probes did prove useful in making predictions of the relative magnitude of groundwater discharge, even without the context provided by a "grid" of measurements utilized by researchers such as Conant (2004). These predictions were later compared against geochemical trends in the riverbed profiles. Geochemical consistency within the riverbed was clearly associated with moderate or strong discharge predictions from temperature profiling. Locations were also found with much stronger vertical groundwater fluxes than locations found by previous researchers using other methods (Encalada, 2008; Pastora, 2009). Geochemical trends within the riverbed indicated changes in water types and/or mixing and were consistent with locations of either minimal or low vertical groundwater fluxes. Temperature profiling, however, could not provide any information on horizontal components of groundwater discharge. Additionally, the temperature profiling done in the winter yielded more consistent, comparable results than the profiling done in the summer, due to more consistent surface water temperatures and therefore a more realistic estimate of T_O.

8.1.4 Sulfate Isotopic Characterization

Analysis of domestic wells for sulfate isotopes resulted in a clear distinction between sulfate that originated from the Salina formation and sulfate that originated from the overburden, in good agreement with literature values. In contrast, the Guelph formation was not well characterized, and further work is needed to identify a parameter that can trace groundwater discharge from this bedrock

formation. This could be due, at least in part, to the fact that only two of the domestic wells that were sampled were definitively known to be screened in the Guelph formation. More samples may have resulted in a better characterization.

Seeps, with no flow path information available per individual sample, were assumed to have isotopic ratios unaffected by sulfate reduction as long as sulfate concentrations and $\delta^{34}S$ and $\delta^{18}O$ values remained similar to literature values. This was further supported by moderate to high levels of dissolved oxygen found in almost all seep samples. The isotopic ratios of riverbed samples, with more varied redox conditions, were assumed unaffected by sulfate reduction if chloride and sulfate concentrations, as well as $\delta^{34}S$ values of sulfate, remained consistent. Thus, cases could be determined where sulfate acted as a conservative tracer and could be used to trace groundwater discharge from the Salina formation bedrock aquifer.

Seep samples contained predominately terrestrial sulfate, with two exceptions discharging directly from low-lying Salina formation outcrops along the Grand. Riverbed samples contained Salina formation groundwater, overburden or Guelph formation groundwater, or hyporheic-zone river water. The presence of hyporheic stream water could be predicted on the basis of subsurface temperature measurements, and was confirmed by vertical profiles of chloride concentrations. The groundwater type within the river could also be predicted, by observing where the sample was taken within the discharge reach. Only one sample indicative of Salina formation groundwater was found north of the Guelph-Salina contact. Because the contact is not observed anywhere within southern Ontario (Thurson et al., 1992), this may suggest that, in this specific location, the inferred contact should be moved slightly to the north.

No other obvious form of sulfate appeared to be a major component of any water type sampled within the discharge reach.

The Nith River, because of its relatively large volume, has a considerable impact on the general chemistry of the Grand River, and on sulfate concentrations and isotopes in particular. This may reduce the utility of a sulfate isotopic mass balance to determine a Salina groundwater flux to the Grand, as the overall groundwater addition is obscured by the contribution from the Nith. There were both upstream and downstream increases in $\delta^{34}S$, during the September survey and not associated with the Nith, but even combined, they were not as large as the increase associated with the Nith River (see chapter six). In the June survey, the upstream and downstream increases in $\delta^{34}S$ were almost negligible compared to the input from the Nith River.

Given its apparent impact on the Grand, more work needs to be completed on the Nith river. Topics that could focus future research might include:

1) How significant is the Salina formation groundwater component in Nith River flow? The Nith River has elevated concentrations of sulfate and enriched isotopic ratios relative to the Grand or Whiteman's Creek, but, during summer, does not have the cold water temperature trace apparent in other tributaries such as Whiteman's Creek, and that is generally associated with a groundwater-fed tributary.

2) How significant is the role of the Nith River in improving Grand River water quality? Anion data from this study showed chloride concentrations, generally indicative of WWTPs upstream, decreasing significantly after the Nith's convergence with the Grand. Nitrate showed a small but noticeable decrease as well. Literature data, however, suggests that the Nith usually has a greater median and more variable nitrate concentration than the Grand River (Figure 2.6A, from Cooke, 2006).

8.1.5 Nitrate Inputs along the Discharge Reach

Nitrate concentrations in the Grand River in June were slightly higher than nitrate concentrations in the Grand River in September. A comparison of the nitrate concentrations between groups labelled by Salina sulfate and terrestrial sulfate isotopes found a significant difference (Rank-Sum Test: Salina sulfates n = 13, terrestrial sulfates n = 34. p = 0.0014). The group characterized by Salina sulfate showed significantly lower nitrate concentrations than other groundwater samples labeled by terrestrial sulfate. The Salina sulfate sample group also showed a greater potential for denitrification than samples labeled by terrestrial sulfates. Although the sampling methodology did not allow for accurate measurements of DO in all domestic wells, the domestic well samples run for nitrate isotopes showed an enrichment in both $^{15}N/^{14}N$ and $^{18}O/^{16}O$ ratios consistent with bacterially mediated denitrification. Riverbed porewater sample showed this as well, with the added evidence of reliable DO measurements to indicate redox conditions. Only one of the seep samples from the Salina formation was analyzed for nitrate isotopes, as the other (GRS-10) did not contain enough nitrate to analyze. The seep sample that was run had fairly low nitrate and $\delta^{15}N$ and $\delta^{18}O$ values more closely associated with the other Salina nitrate isotopes than the soil nitrogen source suggested by nitrate isotopes of the other seeps.

Samples labeled by terrestrial sulfates, on the other hand, tended to show $^{15}N/^{14}N$ and $^{18}O/^{16}O$ isotope ratios consistent with literature values associated with either nitrogen fertilizers or soil nitrogen (Figure 7.7). These seep samples, with one exception, contained oxic levels of DO, providing further evidence that the samples remained unaffected by denitrification.

The Cambridge WWTP had slightly enriched $^{15}N/^{14}N$ isotope ratios compared to either river survey or the major tributaries (Figure 7.7). The Nith River and Whiteman's Creek both plotted towards the soil nitrogen literature values, although with more enriched $^{18}O/^{16}O$ ratios than most other samples not affected by denitrification.

8.2 Refined Groundwater Discharge Conceptual Model

This thesis puts forth evidence for a refined conceptual model for groundwater discharge to the Grand River along the 40-km reach from the lower municipal boundary in Cambridge down to the Brantford municipal water intake. Based only on a flow mass balance along the discharge reach, the maximum flow available for net groundwater input to the Grand River, at baseflow conditions in September 2011, was 1.41 $m \cdot s^{-1}$, or 6.4% of total flow at Brantford. This is lower than other input estimates, the highest of which, from Scott and Imhoff (2005), suggested up to 25% of flow at Brantford during baseflow conditions could be from groundwater discharge. As a result, the impact groundwater has on in-stream nitrate may be less significant than currently thought, and may suggest that more focus needs to be placed on in-stream nitrate removal from plant uptake and, under specific environmental conditions, denitrification.

The discharge that does enter the Grand River, however, does not always dilute in-stream nitrate from upstream wastewater treatment plants. Two distinct groundwater sources were labeled by sulfate isotopes; Salina formation groundwater, and a combined category consisting of overburden and Guelph formation groundwater, which can be somewhat separated by discharge location; overburden groundwater discharges to the Grand mostly through bank seeps, while both the overburden and Guelph formation groundwater may discharge directly to the riverbed. Salina formation groundwater predominately discharges directly to the riverbed, with one or two exceptions. The Nith River has considerable concentrations of sulfate from the Salina formation, although the Salina groundwater contribution to its overall flow is unknown.

Discharge rates from each groundwater type are not constant throughout the year. In spring, during snowmelt conditions when the river stage is high, contributions from shallow aquifers, interflow and

runoff may dominate inputs to the Grand, although this is speculative and outside the temporal scope of this thesis. During early summer, melt induced runoff has abated, but due to favourable recharge conditions throughout the middle portion of the Grand River watershed, shallow aquifer water tables are high and strong discharge occurs from shallow aquifers (Figure 8.1). Although the FLIR survey highlighted numerous reaches where it appeared that considerable amounts of groundwater was discharging to the Grand River, none of this discharge was discernable in the geochemical trends above Paris. This suggests that, relative to the river flow, discharge from the overburden may be small. Although the following is based on samples collected only during late summer, it is suggested that this overburden discharge is oxic with a low potential for denitrification. As a result, at least some nitrate may bypass riparian zones and end up in the Grand River, as evidenced by varying nitrate concentrations found in seep samples. Most of this nitrate appears to be derived from soil nitrogen compound or ammonium fertilizers. Groundwater discharge from this shallow flow-system does not necessarily dilute in-stream nitrate from upstream WWTPs.

As the summer progresses, water tables fall and discharge from shallow aquifers decreases, causing the river stage to lower. This causes the proportion of discharge from deeper flow-systems to increase, although the actual discharge flux, determined by regional hydraulic gradients, likely remains constant over annual timescales (Figure 8.2). Downstream geochemical surveys did not detect considerable groundwater, from either the Guelph formation or overburden, discharging upstream of Paris, but did suggest Salina formation groundwater was discharging downstream of Paris. This is consistent with specific capacity data summarized by Singer et al. (2003), who noted that the Salina formation has a geometric mean specific capacity approximately twice as large as the Guelph formation. Discharge from the Salina formation tends to be anoxic and has isotopic ratios of $^{15}N/^{14}N$ and $^{18}O/^{16}O$ of nitrate that provides evidence that denitrification does occur. Considered as an individual input, this groundwater discharge does dilute in-stream nitrate from upstream WWTPs.

The effect of groundwater discharge on nitrate concentrations in the Grand River is summarized as follows. Discharge from the deeper system appears to dilute in-stream nitrate, while discharge from the shallower system does not appear to dilute in-stream nitrate and may add more nitrate to the river load. As regional discharge tends to be consistent on annual timescales, any sort of temporal fluctuations in Grand River nitrate concentrations (e.g., figure 1.5), due to groundwater discharge, must come from changing flux and/or nitrate concentrations in the shallow system discharge, although the latter is not addressed in this research. Because the overall groundwater input may not be

all that large, however, temporal fluctuations in nitrate (e.g., Figure 1.5) along the discharge reach may be more strongly related to in-stream cycling processes and the variables that control the rates of these processes – stream depth, velocity, and temperature. Because the overall groundwater input along the discharge reach may be smaller than previously considered, the relevance of these in-stream nitrate removal processes may be greater.

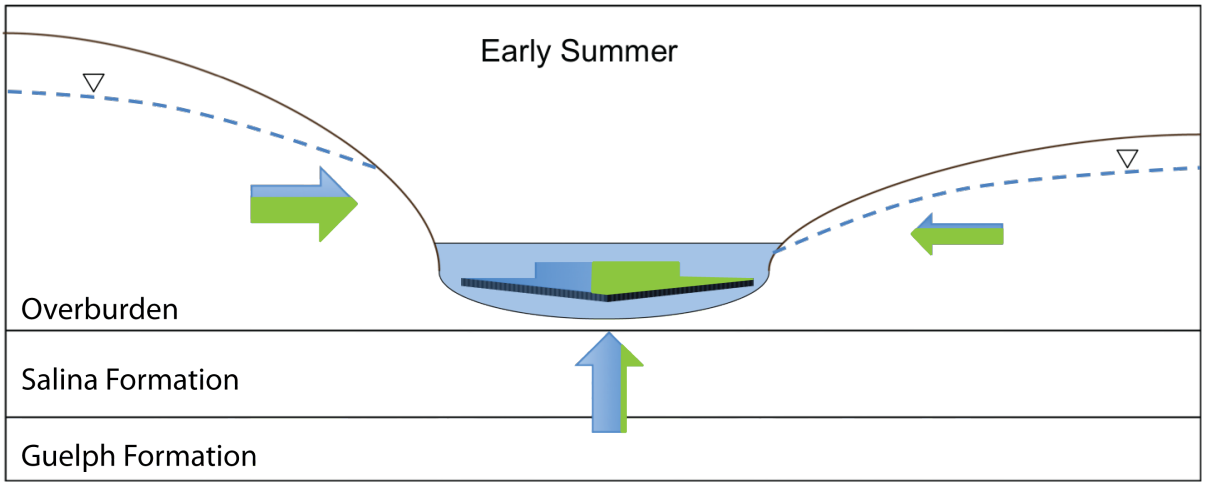

Figure 8.1 Early summer groundwater discharge conceptual model. The arrow size designates flow rate and the proportion of arrow coloured green indicates relative nitrate concentrations. Nitrate in shallow system is not well constrained during early summer conditions, but likely greater than nitrate concentrations in deep system discharge, which is unlikely to vary from early to late summer conditions. The combined groundwater input from both shallow and deep flow systems is small relative to the flow of the Grand River.

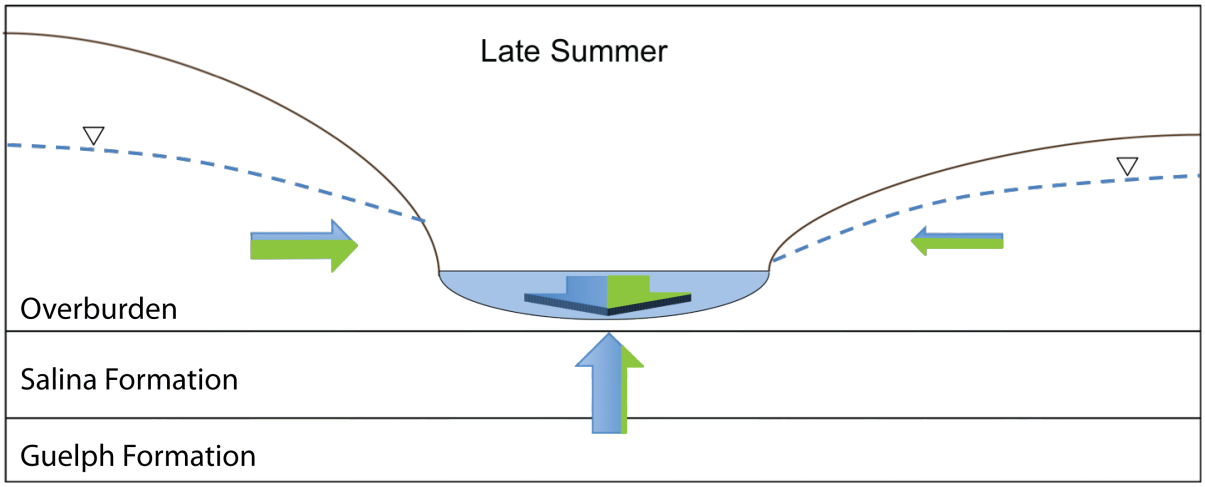

Figure 8.2 Late summer groundwater discharge conceptual model. The arrow size designates flow rate and the proportion of the arrow coloured green indicates relative nitrate concentrations. Compared to early summer conditions, discharge from shallow flow systems is reduced as water tables fall over the summer. Discharge from deeper, regional flow systems remains relatively constant, and nitrate concentrations in the deep discharge remain low. The river flow decreases and in-stream nitrate concentrations fall, abeit only slightly.

8.3 Further Research Directions

The discharge model above is conceptual and more research needs to be done to validate the refinements. Below are the author's suggestions for research that could be done to further enhance understanding of the temporal and spatial aspects of discharge to the Grand River:

1) The FLIR survey could be done again, in winter, down the entire discharge reach to map all seep samples discharging to the Grand.

2) Only two "snapshots" of river conditions are taken for this study; one during early summer, and the other during late summer. The temporal variation of groundwater discharge could be better understood by taking samples in the Grand at Cambridge, Brantford, and in Whiteman's Creek and the Nith River at monthly or bi-weekly intervals throughout year. This would allow seasonal variations in sulfate concentrations, isotope ratios, nitrate concentrations, and nitrate ratios to be observed, related to river stage, and ultimately to discharge patterns.

3) Another parameter needs to be found to separate out Guelph formation discharge from overburden. Which type is discharging where can be inferred because the Grand River has cut through most of the overburden – i.e., overburden groundwater discharges from seeps, the

Guelph formation directly to the riverbed – but a more definitive assumption capacity is desired.

4) This research has, essentially, ignored the effects that river recharge to adjacent aquifers may have on nutrient cycling in the Grand River. River input to adjacent aquifers could be evaluated by tracing river water based on chloride concentrations and boron isotopes in near-by domestic wells.

5) The Nith River needs to be studied in greater detail, given it's apparent impact on Grand River water quality.

6) Further research could be done on the locations where strong vertical groundwater fluxes were calculated to examine spatial extent and variability, as well as to calculate flux measurements integrate over a larger area.

7) The temporal variability of nitrate concentrations in discharge from the shallow groundwater system should be better constrained. This would allow for a more confident appraisal of whether this groundwater discharge adds to, dilutes, or has little affect on in-stream nitrate concentrations over annual timescales.

8) The efficiency of in-stream nitrate removal needs to be better quantified along the Grand River discharge reach.

References

Anderson, M., P. 2005. Heat as a ground water tracer. Ground Water 43(6): 951 – 968.

Anderson, M. 2012. "Assessment of Future Water Quality Conditions in the Grand and Speed Rivers". Waste Management Plan Assimilative Capacity Working Group. Ontario, Canada.

AquaResource Inc. 2009. "Integrated Water Budget Report, Final Report June 2009". Grand River Conservation Authority. Ontario, Canada.

Aravena, R., Evans, M., L., Cherry, J., A. 1993. Stable isotopes of oxygen and nitrogen in source identification of nitrate from septic systems. Ground Water 31(2): 180 – 186.

Aravena, R., Robertson, W.D. 1998. Use of multiple isotope tracers to evaluate denitrification in ground water: study of nitrate from a large-flux septic system plume. Ground Water 36, no. 6: xx-xxx.

Baxter, C., Hauer, F., R., Woessner, W., W. 2003. Measuring groundwater-stream water exchange: new techniques for installing minipiezometers and estimating hydraulic conductivity. Transactions of the American Fisheries Society 132: 493 – 502.

Becker, M., W., Georgian, T., Ambrose, H., Siniscalchi, J., Fredrick, K. 2004. Estimating flow and flux of ground water discharge using water temperature and velocity. Journal of Hydrology 296: 221 – 233.

Bellamy, S., Boyd, D. 2005. "Water Use in the Grand River Watershed". Grand River Conservation Authority, Ontario, Canada.

Berner, Z., A., Stuben, d., Leosson, M., A., Klinge, H. 2002. Applied Geochemistry 17: 1515 – 1528.

Blackport Hydrogeology, Inc., Blackport and Associates Ltd., AquaResource Inc. Review of the State of Knowledge for the Waterloo and Paris/Galt Moraines. Prepared for: Land and Water Policy Branch, Ministry of Environment. Ontario, Canada.

Brown and Rainbow trout populations in the Grand River. Accessed on October 16th 2012. http://www.grandriver.ca/index/document.cfm?sec=31&sub1=9&sub2=0.

Bencala, K., E. 2000. Hyporheic zone hydrological processes. Hydrological processes 14: 2797 – 2798.

Blasch, K., W., Constantz, J., Stonestrom, D., A. DATE. USGS Professional Paper 1703. Ground-water
recharge in the arid and semiarid southwester United States, appendix – 1.

Boulton, A., J., Findlay, S., Marmonier, P., Stanley, E., H., Maurice Valett, H. 1998. The functional significance of the hyporheic zone in streams and rivers. Annual Review Ecological Systems 29: 59-81.

Brabec, M., Y., Lyons, T., W., Mandernack, K., W. 2012. Oxygen and sulphur isotope fractionation during sulfide oxidation by anoxygenic phototrophic bacteria. Geochimica et Cosmochimica Acta 83: 234 – 251.

Brunke, M., Gonser, T. 1997. The ecological significance of exchange processes between rivers and groundwater, Special Review. Freshwater Biology 37: 1-33.

Burgin, A., J., Hamilton, S., K. 2007. Have we overemphasized the role of denitrification in aquatic ecosystems? A review of nitrate removal pathways. Frontiers in Ecological Environment 5(2): 89 – 96.

Bustros-Lussier, E. 2008. Identifying deep groundwater discharge in rivers of eastern Ontario. M.Sc. Thesis, Department of Earth Sciences, University of Ottawa, Ottawa, Ontario.

Canfield, D., E. 2001. Biogeochemistry of Sulfur Isotopes. In J. W. Valley and D. R. Cole (Eds.), Stable Isotope Geochemistry. Rev. Mineral, Geochem, Vol 43: 607 – 636. Mineralogical Society of America, Geochemical Society, Blacksburg, Virginia.

Clark, I., D., Fritz, P. 1997. Environmental isotopes in hydrogeology. Lewis, New York.

Colautti, D. 2010. Modelling the effects of climate change on the surface and subsurface hydrology of the Grand River Watershed. P.hD Thesis, University of Waterloo, Waterloo, Ontario, Canada.

Conant Jr., B. 2004. Delineating and quantifying ground water discharge zones using streambed temperatures. Ground Water 42(2): 243 – 257.

Conant, Jr., B. 2008. Thermal Methods for Detecting Groundwater Discharge. Department of Earth and Environmental Sciences, University of Waterloo. Groundwater Forum Business Meeting, Portland, Oregon.

Constantz, J. 2008. Heat as a tracer to determine streambed water exchanges. Water Resources Research 44(10): 10 – 29.

Cooke, S. 2006. "Water Quality in the Grand River: A Summary of Current Conditions (2000 – 2004) and Long Term Trends". Grand River Conservation Authority. Ontario, Canada.

Devito, K., J., Fitzgerald, D., Hill, A., R., Aravena, R. 2000. Nitrate Dynamics in Relation to Lithology and Hydrologic Flow Path in a River Riparian Zone. Journal of Environmental Quality 29: 1075 – 1084.

Drake, J., A., P. 2009. Identifying and evaluating groundwater discharge within surface water systems through temperature measurements. M.ASc. Thesis, University of Guelph, Guelph, Ontario.

Encalada, M., L. 2008. Inputs of DO into the Grand River in the Glen Morris Area: The role of groundwater and riparian zones. M.Sc. Thesis, Department of Earth and Environmental Science, University of Waterloo, Waterloo, Ontario, Canada.

Faure, G., Mensing, T., M. 2005. Isotopes, principles and applications, 3rd edition. John Wiley and Sons, Inc., Hoboken, New Jersey.

Freeze, R.A., and Whitherspoon, P., A.1967. Theoretical analysis of regional groundwater flow: 2. Effect of water-table configuration and subsurface permeability variation. Water Resources Research 3: 623-634.

Fritz, P., Lapcevic, P., A., Miles, M., Frape, S., K., Lawson, D., E., O'Shea, K., J. 1988. Stable isotopes in sulphate minerals from the Salina formation in southwestern Ontario. Canadian Journal of Earth Sciences 25: 195 – 205.

Fritz, P., Basharmal, G., M., Drimmie, R,. J., Ibsen, J., Qureshi, R., M. 1989. Chemical Geology 79: 99-105.

Graham, J., E., Banks, W., D. 2004. Grand River watershed geological and hydrogeological model project. Waterloo Hydrogeologic, Inc., Waterloo, Ontario.

Gu, A., Gray, F., Eastoe, C., J., Norman, L., M., Duarte, O., Long, A. Ground Water 46(3): 502 – 509.

Harvey, J., W, Bencala, K., E. 1993. The effect of streambed topography on surface-subsurface water exchange in mountain catchments. Water Resources Research 29(1): 89 – 98.

Harvey, J., W., Wagner, B., J. 2000. Quantifying hydrologic interactions between streams and their subsurface hyporheic zones, in: Streams and Groundwaters, edted by: Jones, J., B. and Mulholland, P., J., Academic Press, San Diego. 9-10.

Herrera, R., A. 2012. Conservative solute mass fluxes into the Grand River at Glen Morris, Ontario. M.Sc. Thesis, University of Waterloo, Waterloo, Ontario, Canada.

Hill, A., R., Devito, K., J., Campagnolo, S., Sanmugadas, K. 2000. Subsurface denitrification in a forest riparian zone: interactions between hydrology and supplies of nitrate and organic carbon. Biogeochemistry 51: 193 – 223.

Holysh, S., Pitcher, J., Boyd, D. 2001. "Grand River regional groundwater study". Grand River Conservation Authority. Ontario, Canada.

Karrow, P., F. 1987. Quaternary Geology of the Hamilton-Cambridge Area, Southern Ontario. Mines and Minerals Division, Ontario Geological Survey Report 255. Ontario, Canada.

Lee, D., R., Geist, D., R., Saldi, K., Hartwig, D., Cooper, T. 1997. Locating groundwater discharge in the Hanford reach of the Columbia River. Prepared for the U.S. department of energy, Atomic energy of Canada, Ltd, Chalk River Labratories, Ontario, Canada.

Kellman, L., Hillaire-Marcel, C. 1998. Nitrate cycling in streams: using natural abundances of NO_3^- - $\delta^{15}N$ to measure in-situe denitrification. Biogochemistry 43: 273 – 292.

Kendall, C., MacDonnell, J. 1998. Isotope tracers in catchment hydrology, 1st edition. Elsevier Science,
B. V.

Krouse, H., R., Grinenko, V., A. 1991. Stable isotopes in the assessment of natural and anthropogenic sulphur in the environment. Scope 43, Published by John Wiley and Sons, Ltd.

Lake Erie Source Protection Region Technical Team. 2008. Grand River Watershed Characterization Report. Grand River Conservation Authority. Ontario, Canada.

Larkin, R., G., Sharp, J., M. 1992. On the relationship between river-basin geomorphology, aquifer hydraulics, and ground-water flow direction in alluvial aquifers. Geological Society of America Bulletin, 104: 1608 – 1620.

Lloyd, R., M. 1967. Oxygen-18 composition of oceanic sulphate. Science 156: 1228 – 1231.

Loheide, S., P., Gorelick, S., M. 2006. Quantifying stream-aquifer interactions through the analysis of remotely sensed thermographic profiles and in situ temperature histories. Environmental Science & Technology 40(10): 3336 – 3341.

Maitre, V., Cosandey, A-C., Desagher, E., Parriaux, A. 2003. Effectiveness of groundwater nitrate removal in a river riparian area: the importance of hydrogeological conditions. Journal of Hydrology 278: 76 – 93.

Mariotti, A., Landreau, A., Simon, B. 1988. ^{15}N isotope biogeochemistry and natural denitrification processes in groundwater: Application to the chalk aquifer of northern France. Geochim. Cosmochim. Acta 52: 1869 – 1878.

Mcllvin, M., R., Altabet, M., A. 2005. Chemical conversion of nitrate and nitrite to nitrous oxide for nitrogen and oxygen isotopic analysis in freshwater and seawater. Analytical Chemistry 77(17): 5589 – 5595.

Mengis, M., Schiff, S., L., Harris, M., English, M., C., Aravena, R., Elgood, R., J., MacLean, A. 1999. Mulitiple geochemical and isotopic approaches for assessing ground water NO_3^- elimination in a riparian zone. Ground Water 37(3): 448 – 457.

National Climate Archives: http://climate.weatheroffice.gc.ca/climateData/canada_e.html)

Nowicki, V. 1976. An investigation of the Kitchener aquifer system using the stable isotopes ^{34}S and ^{18}O. M.Sc. thesis, Department of Earth and Environmental Science, University of Waterloo, Ontario, Canada. 116p.

Nriagu, J., O. 1975. Sulfur isotopic variations in relation to sulphur pollution of Lake Erie. In:

Isotope Ratios as Pollutant source and Behavior Indicators. IAEA, Vienna, pp 77 – 93.

Nriagu, J., O., Coker, R., D. 1978. Isotopic composition of sulphur in precipitation within the great lakes basin. TELLUS 30: 365 – 375.

O'Shea, K., J., Miles, M., C., Fritz, P., Frape, S., K., Lawson, D., E. 1988. Canadian Journal of Earth Science 25: 182 – 194.

Pastora, E., M. 2009. Use of Geochemical and Isotope Tracers for Evaluating the Interaction between Shallow and Deep Groundwater Flow Systems and the Grand River in the Glen Morris Area. M.Sc. Thesis, Department of Earth and Environmental Sciences, University of Waterloo, Waterloo, Canada.

Pitkin, S., E., Cherry, J., A., Ingleton, R., A., Broholm, M. 1999. Field demonstrations using the Waterloo ground water profiler. GWMR: 122-131.

Robertson, W., D., Cherry, J., A., Sudicky, E., A. 1991. Ground-water contamination from two small septic systems on sand aquifers. Ground Water 29(1): 82 – 92.

Robertson, W.D., Russell, B.M., Cherry, J.A. 1996. Attenuation of nitrate in aquitard sediments of southern Ontario. Journal of Hydrology 180: 267-281.

Robertson, W.D., Moore, T., Spoelstra, J., Li, L., Elgood, R., Clark, I., D., Schiff, S., D., Aravena, R., Neufeld, F., D. 2012. Natural attenuation of septic system nitrogen by anammox. Ground Water 50 (4): 541 – 553.

Rosemond, M., Thuss, S., Schiff, S., Elgood, R., Anderson, M. 2009. "Determining N sources and processes in the Grand River, Ontario, Canada". Grand River Project Report, University of Waterloo, Waterloo Canada.

Schmidt, C., Conant Jr., B., Bayer-Raich, M., Schirmer, M. 2007. Evaluation and field-scale

application of an analytical method to quantify groundwater discharge using mapped streambed temperatures. Journal of Hydrology 347: 292 – 307.

Scott, R., Imhof, J. 2005. "Exceptional waters: state of the resource report". Fisheries Management Plan, Grand River Conservation Authority. Ontario, Canada.

Senger, N.D. 2012. A multi-decade comparison of groundwater nitrate in the southern Nottawasaga River Watershed. M.Sc. Thesis in progress, Department of Earth and Environmental Sciences, University of Waterloo, Waterloo, Canada.

Shabaga, J.A., Hill, A.R. 2010. Groundwater-fed surface flow path hydrodynamics and nitrate removal in three riparian zones in southern Ontario, Canada. Journal of Hydrology

Shiff, S., L., Spoelstra, J., Semkin, R., G., Jeffries, D., S. 2005. Drought induced pulses of SO_4^{2-} from a Canadian shield wetland: use of $\delta^{34}S$ and $\delta^{18}O$ in SO_4^{2-} to determine sources of sulphur. Applied Geochemistry 20: 691 – 700.

Singer, S., N., Cheng, C., K., Scafe, M., G. 2003. Hydrogeology of southern Ontario, 2nd edition. Environmental Monitoring and Reporting Branch, Ministry of the Environment, Toronto, Ontario.

Sophocleous, M. 2002. Interactions between groundwater and surface water: the state of the science. Hydrogeology Journal, 10: 52 – 67.

Solorzano, L. 1969. Determination of ammonia in natural waters by the phenolhypochlorite method. Limnology and Oceanography 14(5): 799 – 801.

Stallman, R., W. 1963. Computation of ground-water velocity from temperature data.

Starr, R.C., Gilham, R.W., Akindunni, F.F., Miller, D.F. 1987. Studies of nitrate distributions and

nitrogen transormations in shallow sandy aquifers. Final Report, Institute for Groundwater Research for Ontario Ministry of Environment. Ontario, Canada.

Stonestrom, D., A., Constantz, J. 2003. Heat as a tool for studying the movement of ground water near streams. USGS Circular 1260, U.S. Geological Survey, Reston, Virginia.

Story, R., G., Howard, K., W., F., Williams, D., D. 2003. Factors controlling riffle-scale hyporheic exchange flows and their seasonal changes in a gaining stream: A three-dimensional groundwater flow model. Water Resources Research 39(2):

Stotler, R., L., Frape, S., K., Mugammar, H., T., Johnston, C., Judd-Henrey, I., Harvey, F., E., Drimmie, R., Paul-Jones, J. 2011. Geochemical heterogeneity in a small, stratigraphically complex moraine aquifer system (Ontario, Canada): interpretation of flow and recharge using multiple geochemical parameters. Hydrogeology Journal 19: 101 – 115

Suzuki, S. Percolation measurements based on heat flow though soil with special reference to paddy-field.

Taylor, B., E., Wheeler, M., C., Nordstrom, D., K. 1984. Isotope composition of sulfate in acid mine drainage as measure of bacterial oxidation. Nature 308(59): 538 – 541.

Thurston, P., C., Williams, H., R., Sutcliffe, R., H., Stott, G., M. Geology of Ontario. Ontario Geological Survey, Special Volume 4, Part 2. Ministry of Northern Development and Mines, Ontario, Canada.

Trust, B., A., Fry, B. 1992. Sulphur isotopes in plants: a review. Plant, Cell, and Environment 15: 1105-1110.

Turcotte, D., L., Schubert, G. 1982. Geodynamics: applications of continuum physics to geological problems. John Wiley and Sons, New York, USA.

White, D., S. 1993. Perspectives on defining and delineating hyporheic zones. Journal of the North American Benthological Society 12(1): 61 – 69.

White, W., M. 2005. Geochemistry. Accessed at http://www.imwa.info/white-geochemistry.html.

Woeller, R., M. 1982. Greenbrook well field management study 1981 – 1982. M.Sc. Thesis, Department of Earth and Environmental Sciences. University of Waterloo, Waterloo, Ontario.

Woessner, W., W. 2000. Streem and fluvial plain ground water interactions: rescaling hydrogeologic thought. Ground Water 38(3): 423 – 429.

Xue, D., Botte, J., De Baets, B., Accoe, F., Nestler, A., Taylor, P., Van Cleemput, O., Berglund, M., Boeckx, P. 2009. Present limitations and future prospects of stable isotope methods for nitrate source identification in surface – and groundwater. Water Research 43: 1159 – 1170.

Vaccaro, J., J., Maly, K., J. 2006. A thermal profile method to identify potential groundwater discharge areas and preferred salmonid habitats for long river reaches. Scientific Investigations Report 2006 – 5136, U. S. Geological Survey, Reston, Virginia.

Van Everdingen, R., O., Krouse, H., R. 1985. The isotope composition of sulphate generated by bacterial and abiological oxidation. Nature 315: 395-396.

Vidon, P., Hill, A.R. 2004. Denitrification and patterns of electron donors and acceptors in eight riparian zones with contrasting hydrogeology. Biogeochemistry 71: 259-283.

Vitoria, L., Otero, N., Soler, A., Canals, A. 2004. Fertilizer characterization: isotopic data (N, S, C, and Sr). Environmental Science and Technology 38: 3254 – 3262.

Appendix A - Temperature Profiling Data

Sample Location	depth (m)	T_z (°C)	T_L (°C)	T_O (°C)	$T_z - T_L$	$T_O - T_L$	Tau	q_z $L \cdot m^{-2} d^{-1}$	q_z $cm \cdot d^{-1}$
RB-1	0.10	21.45	8.3	21.87	13.15	13.57	0.97	12.97	4.99
RB-2	0.10	18.15	8.3	21.87	9.85	13.57	0.73	132.13	16.90
RB-3	0.10	17.95	8.3	21.87	9.65	13.57	0.71	140.59	17.75
RB-4	0.10	21.05	8.3	21.87	12.75	13.57	0.94	25.71	6.26
RB-5	0.04	16.50	8.3	21.87	8.20	13.57	0.60	519.36	61.16
RB-6	0.11	13.33	8.3	21.87	5.03	13.57	0.37	372.08	40.56
RB-7	0.10	13.13	8.3	21.87	4.83	13.57	0.36	426.03	46.29
RB-8	0.10	13.28	8.3	21.87	4.98	13.57	0.37	413.41	45.03
RB-9	0.10	14.62	8.3	21.87	6.32	13.57	0.47	315.14	35.20
RB-10	0.10	*NA*	8.3	21.87	-8.30	13.57	*NA*	*NA*	*NA*
RB-11	0.10	20.81	8.3	21.87	12.51	13.57	0.92	33.54	7.04
RB-12	0.10	21.75	8.3	21.87	13.45	13.57	0.99	3.66	4.06
RB-13	0.10	21.52	8.3	21.87	13.22	13.57	0.97	10.78	4.77
RB-14	0.20	22.83	8.3	21.87	14.53	13.57	1.07	-14.09	0.44
RB-15	*NA*	*NA*	8.3	21.87	-8.30	13.57	*NA*	*NA*	*NA*
RB-16	*NA*	*NA*	8.3	21.87	-8.30	13.57	*NA*	*NA*	*NA*
RB-17	0.10	19.09	8.3	21.87	10.79	13.57	0.80	94.54	13.14
RB-18	0.10	18.76	8.3	21.87	10.46	13.57	0.77	107.35	14.42
Sum 2011-1	0.40	12.42	8.3	23.14	4.12	14.84	0.28	132.12	13.21
Sum 2011-2	0.20	20.39	8.3	23.14	12.09	14.84	0.81	42.26	4.23
Sum 2011-3	0.20	22.41	8.3	23.14	14.11	14.84	0.95	10.40	1.04
Sum 2011-4	0.05	21.60	8.3	23.14	13.30	14.84	0.90	90.37	9.04
Sum 2011-5	0.02	16.50	8.3	23.14	8.20	14.84	0.55	1223.19	122.32
Sum 2011-6	0.03	15.50	8.3	23.14	7.20	14.84	0.49	994.25	99.42
Sum 2011-7	0.10	16.91	8.3	23.14	8.61	14.84	0.58	224.52	22.45
Sum 2011-8	0.05	16.20	8.3	23.14	7.90	14.84	0.53	520.02	52.00
Sum 2011-9	0.10	20.66	8.3	23.14	12.36	14.84	0.83	75.41	7.54
Sum 2011-10	0.10	18.25	8.3	23.14	9.95	14.84	0.67	164.86	16.49
Sum 2011-11	0.10	20.06	8.3	23.14	11.76	14.84	0.79	95.94	9.59
Sum 2011-12	0.10	21.60	8.3	23.14	13.30	14.84	0.90	45.18	4.52
Sum 2011-13	0.10	22.10	8.3	23.14	13.80	14.84	0.93	29.96	3.00
Sum 2011-14	0.05	21.85	8.3	23.14	13.55	14.84	0.91	75.01	7.50
Sum 2011-15	0.10	22.95	8.3	23.14	14.65	14.84	0.99	5.31	0.53
Sum 2011-16	0.05	22.70	8.3	23.14	14.40	14.84	0.97	24.83	2.48
Sum 2011-17	0.02	22.95	8.3	23.14	14.65	14.84	0.99	26.57	2.66

Sum 2011-18	0.10	23.13	8.3	23.14	14.83	14.84	1.00	0.28	0.03
Sum 2011-19	0.12	20.75	8.3	23.14	12.45	14.84	0.84	60.35	6.04
Sum 2011-20	0.11	13.33	8.3	23.14	5.03	14.84	0.34	405.63	40.56
Sum 2011-21	0.10	21.32	8.3	23.14	13.02	14.84	0.88	53.96	5.40
Sum 2011-22	0.10	14.00	8.3	23.14	5.70	14.84	0.38	394.62	39.46
Sum 2011-23	0.10	21.15	8.3	23.14	12.85	14.84	0.87	59.38	5.94
Sum 2011-24	0.12	20.50	8.3	23.14	12.20	14.84	0.82	67.32	6.73
Sum 2011-25	0.05	14.50	8.3	23.14	6.20	14.84	0.42	719.88	71.99
Sum 2011-26	*NA*	*NA*	*NA*	23.14	*NA*	*NA*	*NA*	*NA*	*NA*
Sum 2011-27	0.15	21.94	8.3	23.14	13.64	14.84	0.92	23.18	2.32
Sum 2011-28	0.02	24.77	8.3	23.14	16.47	14.84	1.11	-214.90	-21.49
Sum 2011-29	0.40	22.00	8.3	23.14	13.70	14.84	0.92	8.24	0.82
Sum 2011-30	0.15	21.33	8.3	23.14	13.03	14.84	0.88	35.76	3.58
Sum 2011-31	0.08	21.88	8.3	23.14	13.58	14.84	0.92	45.74	4.57
Sum 2011-32	0.06	22.09	8.3	23.14	13.79	14.84	0.93	50.44	5.04
Sum 2011-33	0.02	22.41	8.3	23.14	14.11	14.84	0.95	104.02	10.40
Sum 2011-34	0.02	22.21	8.3	23.14	13.91	14.84	0.94	133.45	13.35
Sum 2011-35	0.08	22.14	8.3	23.14	13.84	14.84	0.93	35.96	3.60
Sum 2011-36	0.03	23.04	8.3	23.14	14.74	14.84	0.99	9.29	0.93
Sum 2011-37	0.00	22.30	8.3	23.14	14.00	14.84	0.94	*NA*	*NA*
Sum 2011-38	0.10	22.17	8.3	23.14	13.87	14.84	0.93	27.88	2.79
Sum 2011-39	0.00	10.91	8.3	23.14	2.61	14.84	0.18	*NA*	*NA*
Sum 2011-40	*NA*	*NA*	*NA*	23.14	*NA*	*NA*	*NA*	*NA*	*NA*
Sum 2011-41	0.03	20.84	8.3	23.14	12.54	14.84	0.85	231.50	23.15
Sum 2011-42	0.15	22.14	8.3	23.14	13.84	14.84	0.93	19.18	1.92
Sum 2011-43	0.10	22.20	8.3	23.14	13.90	14.84	0.94	26.99	2.70
Sum 2011-44	0.04	22.80	8.3	23.14	14.50	14.84	0.98	23.90	2.39
Sum 2011-45	0.30	22.35	8.3	23.14	14.05	14.84	0.95	7.52	0.75
Sum 2011-46	0.07	18.34	8.3	23.14	10.04	14.84	0.68	230.21	23.02
Sum 2011-47	0.20	15.16	8.3	23.14	6.86	14.84	0.46	159.11	15.91
Sum 2011-48	0.15	15.35	8.3	23.14	7.05	14.84	0.48	204.64	20.46
Sum 2011-49	0.20	19.80	8.3	23.14	11.50	14.84	0.77	52.58	5.26
Sum 2011-50	0.10	19.25	8.3	23.14	10.95	14.84	0.74	125.37	12.54
Sum 2011-51	0.10	21.50	8.3	23.14	13.20	14.84	0.89	48.30	4.83
Sum 2011-52	0.10	16.90	8.3	23.14	8.60	14.84	0.58	225.00	22.50
Sum 2011-53	0.10	19.42	8.3	23.14	11.12	14.84	0.75	119.01	11.90
Sum 2011-54	0.09	20.38	8.3	23.14	12.08	14.84	0.81	94.29	9.43
Sum 2011-55	0.03	21.48	8.3	23.14	13.18	14.84	0.89	163.07	16.31
Sum 2011-56	0.12	20.31	8.3	23.14	12.01	14.84	0.81	72.72	7.27

Sum 2011-57	0.10	21.78	8.3	23.14	13.48	14.84	0.91	39.64	3.96
Sum 2011-58	0.05	23.18	8.3	23.14	14.88	14.84	1.00	-2.22	-0.22
Sum 2011-59	0.09	22.83	8.3	23.14	14.53	14.84	0.98	9.67	0.97
Sum 2011-60	0.10	22.16	8.3	23.14	13.86	14.84	0.93	28.18	2.82
Sum 2011-61	0.10	22.63	8.3	23.14	14.33	14.84	0.97	14.42	1.44
Sum 2011-62	0.10	22.49	8.3	23.14	14.19	14.84	0.96	18.47	1.85
Sum 2011-63	0.10	22.33	8.3	23.14	14.03	14.84	0.95	23.15	2.31
Sum 2011-64	0.12	22.14	8.3	23.14	13.84	14.84	0.93	23.98	2.40
Sum 2011-65	0.09	22.23	8.3	23.14	13.93	14.84	0.94	29.00	2.90
Sum 2011-66	0.09	22.23	8.3	23.14	13.93	14.84	0.94	29.00	2.90
Sum 2011-67	0.07	20.32	8.3	23.14	12.02	14.84	0.81	124.17	12.42
Sum 2011-68	0.05	22.23	8.3	23.14	13.93	14.84	0.94	52.20	5.22
Sum 2011-69	0.10	22.23	8.3	23.14	13.93	14.84	0.94	26.10	2.61
Sum 2011-70	0.09	22.47	8.3	23.14	14.17	14.84	0.95	21.17	2.12
Sum 2011-71	0.45	21.68	8.3	23.14	13.38	14.84	0.90	9.49	0.95
Sum 2011-72	0.10	21.97	8.3	23.14	13.67	14.84	0.92	33.87	3.39
Sum 2011-73	0.08	22.59	8.3	23.14	14.29	14.84	0.96	19.47	1.95
Sum 2011-74	0.05	22.73	8.3	23.14	14.43	14.84	0.97	23.11	2.31
Sum 2011-75	0.09	23.69	8.3	23.14	15.39	14.84	1.04	-16.68	-1.67
Sum 2011-76	0.00	23.32	8.3	23.14	15.02	14.84	1.01	*NA*	*NA*
Sum 2011-77	0.05	21.45	8.3	23.14	13.15	14.84	0.89	99.72	9.97
Sum 2011-78	0.10	23.33	8.3	23.14	15.03	14.84	1.01	-5.25	-0.52
Sum 2011-79	0.18	22.97	8.3	23.14	14.67	14.84	0.99	2.64	0.26
Sum 2011-80	0.10	22.06	8.3	23.14	13.76	14.84	0.93	31.16	3.12
Sum 2011-81	0.10	22.16	8.3	23.14	13.86	14.84	0.93	28.18	2.82
Sum 2011-82	0.10	22.03	8.3	23.14	13.73	14.84	0.93	32.06	3.21
Sum 2011-83	0.09	21.53	8.3	23.14	13.23	14.84	0.89	52.62	5.26
Sum 2011-84	0.10	22.02	8.3	23.14	13.72	14.84	0.92	32.36	3.24
Sum 2011-85	0.08	22.16	8.3	23.14	13.86	14.84	0.93	35.22	3.52
Sum 2011-86	0.08	22.26	8.3	23.14	13.96	14.84	0.94	31.51	3.15
Sum 2011-87	*NA*	*NA*	*NA*	23.14	*NA*	*NA*	*NA*	*NA*	*NA*
Sum 2011-88	0.10	22.02	8.3	23.14	13.72	14.84	0.92	32.36	3.24
Sum 2011-89	*NA*	*NA*	*NA*	23.14	*NA*	*NA*	*NA*	*NA*	*NA*
Sum 2011-90	0.10	22.49	8.3	23.14	14.19	14.84	0.96	18.47	1.85
Sum 2011-91	0.08	23.01	8.3	23.14	14.71	14.84	0.99	4.54	0.45
Sum 2011-92	0.09	22.77	8.3	23.14	14.47	14.84	0.98	11.57	1.16
Sum 2011-93	0.04	22.99	8.3	23.14	14.69	14.84	0.99	10.47	1.05
Sum 2011-94	0.08	22.10	8.3	23.14	13.80	14.84	0.93	37.46	3.75
Sum 2011-95	0.10	21.70	8.3	23.14	13.40	14.84	0.90	42.10	4.21

Sum 2011-96	0.08	22.87	8.3	23.14	14.57	14.84	0.98	9.47	0.95
Sum 2011-97	0.10	22.60	8.3	23.14	14.30	14.84	0.96	15.29	1.53
Sum 2011-98	0.10	21.15	8.3	23.14	12.85	14.84	0.87	59.38	5.94
Sum 2011-99	0.10	23.10	8.3	23.14	14.80	14.84	1.00	1.11	0.11
Sum 2011-100	0.10	22.70	8.3	23.14	14.40	14.84	0.97	12.41	1.24
Sum 2011-101	0.15	22.41	8.3	23.14	14.11	14.84	0.95	13.87	1.39
Sum 2011-102	0.08	23.18	8.3	23.14	14.88	14.84	1.00	-1.39	-0.14
Sum 2011-103	0.10	23.05	8.3	23.14	14.75	14.84	0.99	2.51	0.25
Sum 2011-104	0.10	22.90	8.3	23.14	14.60	14.84	0.98	6.72	0.67
Sum 2011-105	0.08	23.06	8.3	23.14	14.76	14.84	0.99	2.79	0.28
Sum 2011-106	0.07	24.35	8.3	23.14	16.05	14.84	1.08	-46.18	-4.62
Sum 2011-107	0.30	22.90	8.3	23.14	14.60	14.84	0.98	2.24	0.22
Sum 2011-108	0.10	23.63	8.3	23.14	15.33	14.84	1.03	-13.40	-1.34
Sum 2011-109	0.10	24.57	8.3	23.14	16.27	14.84	1.10	-37.94	-3.79
Sum 2011-110	0.14	23.08	8.3	23.14	14.78	14.84	1.00	1.19	0.12
Sum 2011-111	0.04	24.28	8.3	23.14	15.98	14.84	1.08	-76.31	-7.63
Sum 2011-112	0.10	23.32	8.3	23.14	15.02	14.84	1.01	-4.97	-0.50
Sum 2011-113	0.10	23.92	8.3	23.14	15.62	14.84	1.05	-21.13	-2.11
Sum 2011-114	0.09	24.32	8.3	23.14	16.02	14.84	1.08	-35.06	-3.51
Sum 2011-115	0.09	24.71	8.3	23.14	16.41	14.84	1.11	-46.08	-4.61
Sum 2011-116	0.04	25.12	8.3	23.14	16.82	14.84	1.13	-129.13	-12.91
Sum 2011-117	0.20	22.61	8.3	23.14	14.31	14.84	0.96	7.50	0.75
Sum 2011-118	0.15	23.25	8.3	23.14	14.95	14.84	1.01	-2.03	-0.20
Sum 2011-119	0.08	24.72	8.3	23.14	16.42	14.84	1.11	-52.16	-5.22
Sum 2011-120	0.20	23.15	8.3	23.14	14.85	14.84	1.00	-0.14	-0.01
Sum 2011-121	0.10	24.35	8.3	23.14	16.05	14.84	1.08	-32.33	-3.23
Sum 2011-122	0.10	19.90	8.3	23.14	11.60	14.84	0.78	101.59	10.16
Sum 2011-123	0.20	19.98	8.3	23.14	11.68	14.84	0.79	49.38	4.94
Sum 2011-124	0.10	20.15	8.3	23.14	11.85	14.84	0.80	92.79	9.28
Sum 2011-125	0.10	22.00	8.3	23.14	13.70	14.84	0.92	32.96	3.30
Sum 2011-126	0.10	23.01	8.3	23.14	14.71	14.84	0.99	3.63	0.36
Sum 2011-127	0.12	23.02	8.3	23.14	14.72	14.84	0.99	2.79	0.28
Sum 2011-128	0.10	23.15	8.3	23.14	14.85	14.84	1.00	-0.28	-0.03
Sum 2011-129	0.10	22.85	8.3	23.14	14.55	14.84	0.98	8.14	0.81
Sum 2011-130	0.06	23.47	8.3	23.14	15.17	14.84	1.02	-15.12	-1.51
Sum 2011-131	0.20	22.30	8.3	23.14	14.00	14.84	0.94	12.02	1.20
Sum 2011-132	0.10	22.95	8.3	23.14	14.65	14.84	0.99	5.31	0.53
Sum 2011-133	0.10	14.02	8.3	23.14	5.72	14.84	0.39	393.17	39.32
Sum 2011-134	0.10	23.12	8.3	23.14	14.82	14.84	1.00	0.56	0.06

Sum 2011-135	0.10	23.22	8.3	23.14	14.92	14.84	1.01	-2.22	-0.22
Sum 2011-136	0.05	23.10	8.3	23.14	14.80	14.84	1.00	2.23	0.22
Sum 2011-137	0.09	22.35	8.3	23.14	14.05	14.84	0.95	25.07	2.51
Sum 2011-138	0.12	18.31	8.3	23.14	10.01	14.84	0.67	135.32	13.53
Sum 2011-139	0.20	22.00	8.3	23.14	13.70	14.84	0.92	16.48	1.65
Sum 2011-140	0.06	23.43	8.3	23.14	15.13	14.84	1.02	-13.30	-1.33
Sum 2011-141	0.10	22.92	8.3	23.14	14.62	14.84	0.99	6.16	0.62
Sum 2011-142	0.10	23.15	8.3	23.14	14.85	14.84	1.00	-0.28	-0.03
Sum 2011-143	0.10	22.75	8.3	23.14	14.45	14.84	0.97	10.98	1.10
Sum 2011-144	0.10	23.33	8.3	23.14	15.03	14.84	1.01	-5.25	-0.52
Sum 2011-145	0.10	23.15	8.3	23.14	14.85	14.84	1.00	-0.28	-0.03
Sum 2011-146	0.10	20.50	8.3	23.14	12.20	14.84	0.82	80.79	8.08
Sum 2011-147	0.20	22.00	8.3	23.14	13.70	14.84	0.92	16.48	1.65
Sum 2011-148	0.09	23.30	8.3	23.14	15.00	14.84	1.01	-4.91	-0.49
Sum 2011-149	0.10	22.83	8.3	23.14	14.53	14.84	0.98	8.71	0.87
Sum 2011-150	0.20	22.52	8.3	23.14	14.22	14.84	0.96	8.80	0.88
Sum 2011-151	0.10	22.76	8.3	23.14	14.46	14.84	0.97	10.70	1.07
Sum 2011-152	0.10	23.89	8.3	23.14	15.59	14.84	1.05	-20.33	-2.03
Sum 2011-153	0.12	23.45	8.3	23.14	15.15	14.84	1.02	-7.11	-0.71
Sum 2011-154	0.09	23.70	8.3	23.14	15.40	14.84	1.04	-16.97	-1.70
Sum 2011-155	0.10	24.01	8.3	23.14	15.71	14.84	1.06	-23.50	-2.35
Sum 2011-156	0.08	24.63	8.3	23.14	16.33	14.84	1.10	-49.32	-4.93
Sum 2011-157	0.20	22.35	8.3	23.14	14.05	14.84	0.95	11.28	1.13
Sum 2011-158	0.20	22.25	8.3	23.14	13.95	14.84	0.94	12.75	1.28
Sum 2011-159	0.20	21.10	8.3	23.14	12.80	14.84	0.86	30.49	3.05
Sum 2011-160	0.20	21.45	8.3	23.14	13.15	14.84	0.89	24.93	2.49
Sum 2011-161	0.20	21.60	8.3	23.14	13.30	14.84	0.90	22.59	2.26
Sum 2011-162	0.11	23.02	8.3	23.14	14.72	14.84	0.99	3.04	0.30
Sum 2011-163	0.10	22.87	8.3	23.14	14.57	14.84	0.98	7.57	0.76
Sum 2011-164	0.07	20.85	8.3	23.14	12.55	14.84	0.85	98.75	9.87
Sum 2011-165	0.10	21.42	8.3	23.14	13.12	14.84	0.88	50.80	5.08
Sum 2011-166	0.10	20.76	8.3	23.14	12.46	14.84	0.84	72.09	7.21
Sum 2011-167	0.10	23.00	8.3	23.14	14.70	14.84	0.99	3.91	0.39
Sum 2011-168	0.08	22.84	8.3	23.14	14.54	14.84	0.98	10.53	1.05
Sum 2011-169	0.10	23.16	8.3	23.14	14.86	14.84	1.00	-0.56	-0.06
Sum 2011-170	0.10	23.48	8.3	23.14	15.18	14.84	1.02	-9.34	-0.93
Sum 2011-171	0.03	24.06	8.3	23.14	15.76	14.84	1.06	-82.69	-8.27
Sum 2011-172	0.10	23.50	8.3	23.14	15.20	14.84	1.02	-9.89	-0.99
Sum 2011-173	0.10	23.63	8.3	23.14	15.33	14.84	1.03	-13.40	-1.34

Sum 2011-174	0.04	23.95	8.3	23.14	15.65	14.84	1.05	-54.79	-5.48
Sum 2011-175	0.10	23.63	8.3	23.14	15.33	14.84	1.03	-13.40	-1.34
Sum 2011-176	0.07	22.85	8.3	23.14	14.55	14.84	0.98	11.63	1.16
Sum 2011-177	0.10	22.95	8.3	23.14	14.65	14.84	0.99	5.31	0.53
Sum 2011-178	0.09	23.78	8.3	23.14	15.48	14.84	1.04	-19.35	-1.93
Sum 2011-179	0.10	23.50	8.3	23.14	15.20	14.84	1.02	-9.89	-0.99
Sum 2011-180	0.06	23.88	8.3	23.14	15.58	14.84	1.05	-33.45	-3.34
Sum 2011-181	0.10	23.62	8.3	23.14	15.32	14.84	1.03	-13.13	-1.31
Sum 2011-182	0.06	23.60	8.3	23.14	15.30	14.84	1.03	-20.98	-2.10
Sum 2011-183	0.07	24.35	8.3	23.14	16.05	14.84	1.08	-46.18	-4.62
Sum 2011-184	0.06	24.60	8.3	23.14	16.30	14.84	1.10	-64.50	-6.45
Sum 2011-185	0.11	24.51	8.3	23.14	16.21	14.84	1.09	-33.11	-3.31
Sum 2011-186	0.08	24.01	8.3	23.14	15.71	14.84	1.06	-29.37	-2.94
Sum 2011-187	0.06	24.25	8.3	23.14	15.95	14.84	1.07	-49.58	-4.96
Sum 2011-188	0.11	24.50	8.3	23.14	16.20	14.84	1.09	-32.87	-3.29
Sum 2011-189	0.09	27.55	8.3	23.14	19.25	14.84	1.30	-119.23	-11.92
Sum 2011-190	0.03	24.25	8.3	23.14	15.95	14.84	1.07	-99.16	-9.92
Sum 2011-191	0.09	24.68	8.3	23.14	16.38	14.84	1.10	-45.24	-4.52
Sum 2011-192	0.09	24.14	8.3	23.14	15.84	14.84	1.07	-29.88	-2.99
Sum 2011-193	0.08	24.19	8.3	23.14	15.89	14.84	1.07	-35.24	-3.52
Sum 2011-194	0.07	24.06	8.3	23.14	15.76	14.84	1.06	-35.44	-3.54
Sum 2011-195	0.10	24.27	8.3	23.14	15.97	14.84	1.08	-30.27	-3.03
Sum 2011-196	0.04	24.53	8.3	23.14	16.23	14.84	1.09	-92.31	-9.23
Sum 2011-197	0.10	21.29	8.3	23.14	12.99	14.84	0.88	54.91	5.49
Sum 2011-198	0.10	23.77	8.3	23.14	15.47	14.84	1.04	-17.15	-1.71
Sum 2011-199	0.10	23.70	8.3	23.14	15.40	14.84	1.04	-15.28	-1.53
Sum 2011-200	0.07	23.47	8.3	23.14	15.17	14.84	1.02	-12.96	-1.30
Sum 2011-201	0.10	23.70	8.3	23.14	15.40	14.84	1.04	-15.28	-1.53
Sum 2011-202	0.15	23.84	8.3	23.14	15.54	14.84	1.05	-12.67	-1.27
Sum 2011-203	0.15	23.74	8.3	23.14	15.44	14.84	1.04	-10.90	-1.09
Sum 2011-204	0.30	23.75	8.3	23.14	15.45	14.84	1.04	-5.54	-0.55
Sum 2011-205	0.30	23.45	8.3	23.14	15.15	14.84	1.02	-2.84	-0.28
Sum 2011-206	0.12	23.71	8.3	23.14	15.41	14.84	1.04	-12.95	-1.30
Sum 2011-207	0.14	23.75	8.3	23.14	15.45	14.84	1.04	-11.87	-1.19
Sum 2011-208	0.11	23.73	8.3	23.14	15.43	14.84	1.04	-14.62	-1.46
Sum 2011-209	0.05	23.82	8.3	23.14	15.52	14.84	1.05	-36.95	-3.70
Sum 2011-210	0.10	23.79	8.3	23.14	15.49	14.84	1.04	-17.68	-1.77
Sum 2011-211	0.10	23.78	8.3	23.14	15.48	14.84	1.04	-17.41	-1.74
Sum 2011-212	0.18	23.82	8.3	23.14	15.52	14.84	1.05	-10.27	-1.03

Sum 2011-213	0.07	24.38	8.3	23.14	16.08	14.84	1.08	-47.28	-4.73
Sum 2011-214	0.10	24.22	8.3	23.14	15.92	14.84	1.07	-28.97	-2.90
Sum 2011-215	0.10	25.44	8.3	23.14	17.14	14.84	1.15	-59.42	-5.94
Sum 2011-216	0.10	24.92	8.3	23.14	16.62	14.84	1.12	-46.72	-4.67
Sum 2011-217	0.08	25.27	8.3	23.14	16.97	14.84	1.14	-69.14	-6.91
Sum 2011-218	0.08	23.67	8.3	23.14	15.37	14.84	1.04	-18.09	-1.81
Sum 2011-219	0.05	25.85	8.3	23.14	17.55	14.84	1.18	-138.35	-13.83
Sum 2011-220	0.45	19.71	8.3	23.14	11.41	14.84	0.77	24.09	2.41
Sum 2011-221	0.10	19.15	8.3	23.14	10.85	14.84	0.73	129.15	12.92
Sum 2011-222	0.20	20.85	8.3	23.14	12.55	14.84	0.85	34.56	3.46
Feb27th-1	0.15	2.11	8.3	0.85	-6.19	-7.45	0.83	50.94	5.09
Feb27th-2	0.15	2.16	8.3	0.85	-6.14	-7.45	0.82	53.17	5.32
Feb27th-3	0.20	1.31	8.3	0.85	-6.99	-7.45	0.94	13.14	1.31
Feb27th-4	0.20	1.09	8.3	0.85	-7.21	-7.45	0.97	6.75	0.68
Feb27th-5	0.15	0.97	8.3	0.85	-7.33	-7.45	0.98	4.46	0.45
Feb27th-6	0.18	1.09	8.3	0.85	-7.21	-7.45	0.97	7.50	0.75
Feb27th-7	0.15	0.98	8.3	0.85	-7.32	-7.45	0.98	4.84	0.48
Feb27th-8	0.18	1.00	8.3	0.85	-7.30	-7.45	0.98	4.66	0.47
Feb27th-9	0.20	0.99	8.3	0.85	-7.31	-7.45	0.98	3.91	0.39
Feb27th-10	0.20	0.98	8.3	0.85	-7.32	-7.45	0.98	3.63	0.36
Feb27th-11	0.20	1.01	8.3	0.85	-7.29	-7.45	0.98	4.48	0.45
Feb27th-12	0.20	1.03	8.3	0.85	-7.27	-7.45	0.98	5.04	0.50
Feb27th-13	0.20	0.96	8.3	0.85	-7.34	-7.45	0.99	3.07	0.31
Feb27th-14	0.20	1.14	8.3	0.85	-7.16	-7.45	0.96	8.19	0.82
Feb27th-15	0.19	1.21	8.3	0.85	-7.09	-7.45	0.95	10.75	1.08
Feb27th-16	0.20	1.45	8.3	0.85	-6.85	-7.45	0.92	17.31	1.73
Feb27th-17	0.22	1.49	8.3	0.85	-6.81	-7.45	0.91	16.84	1.68
Feb27th-18	0.22	1.57	8.3	0.85	-6.73	-7.45	0.90	19.05	1.91
Feb27th-19	0.24	1.70	8.3	0.85	-6.60	-7.45	0.89	20.82	2.08
Feb27th-20	0.25	3.51	8.3	0.85	-4.79	-7.45	0.64	72.86	7.29
Feb27th-21	0.22	1.95	8.3	0.85	-6.35	-7.45	0.85	29.95	2.99
Feb27th-22	0.20	2.57	8.3	0.85	-5.73	-7.45	0.77	54.13	5.41
Feb27th-23	0.20	2.71	8.3	0.85	-5.59	-7.45	0.75	59.23	5.92
Feb27th-24	0.22	3.24	8.3	0.85	-5.06	-7.45	0.68	72.52	7.25
Feb27th-25	0.20	2.41	8.3	0.85	-5.89	-7.45	0.79	48.45	4.84
Feb27th-26	0.22	2.20	8.3	0.85	-6.10	-7.45	0.82	37.48	3.75
Feb27th-27	0.20	2.13	8.3	0.85	-6.17	-7.45	0.83	38.87	3.89
Feb27th-28	0.20	1.41	8.3	0.85	-6.89	-7.45	0.92	16.11	1.61
Feb27th-29	0.20	1.87	8.3	0.85	-6.43	-7.45	0.86	30.36	3.04

Feb27th-30	0.20	1.26	8.3	0.85	-7.04	-7.45	0.94	11.67	1.17
Feb27th-31	0.20	1.37	8.3	0.85	-6.93	-7.45	0.93	14.92	1.49
Feb27th-32	0.20	1.06	8.3	0.85	-7.24	-7.45	0.97	5.90	0.59
Feb27th-33	0.23	1.04	8.3	0.85	-7.26	-7.45	0.97	4.63	0.46
Feb27th-34	0.22	0.97	8.3	0.85	-7.33	-7.45	0.98	3.04	0.30
Feb27th-35	0.21	0.94	8.3	0.85	-7.36	-7.45	0.99	2.39	0.24
Feb27th-36	0.22	1.02	8.3	0.85	-7.28	-7.45	0.98	4.33	0.43
Feb27th-37	0.25	1.08	8.3	0.85	-7.22	-7.45	0.97	5.17	0.52
Feb27th-1a	0.20	1.72	8.3	0.85	-6.58	-7.45	0.88	25.61	2.56

**NA* = Not Applicable

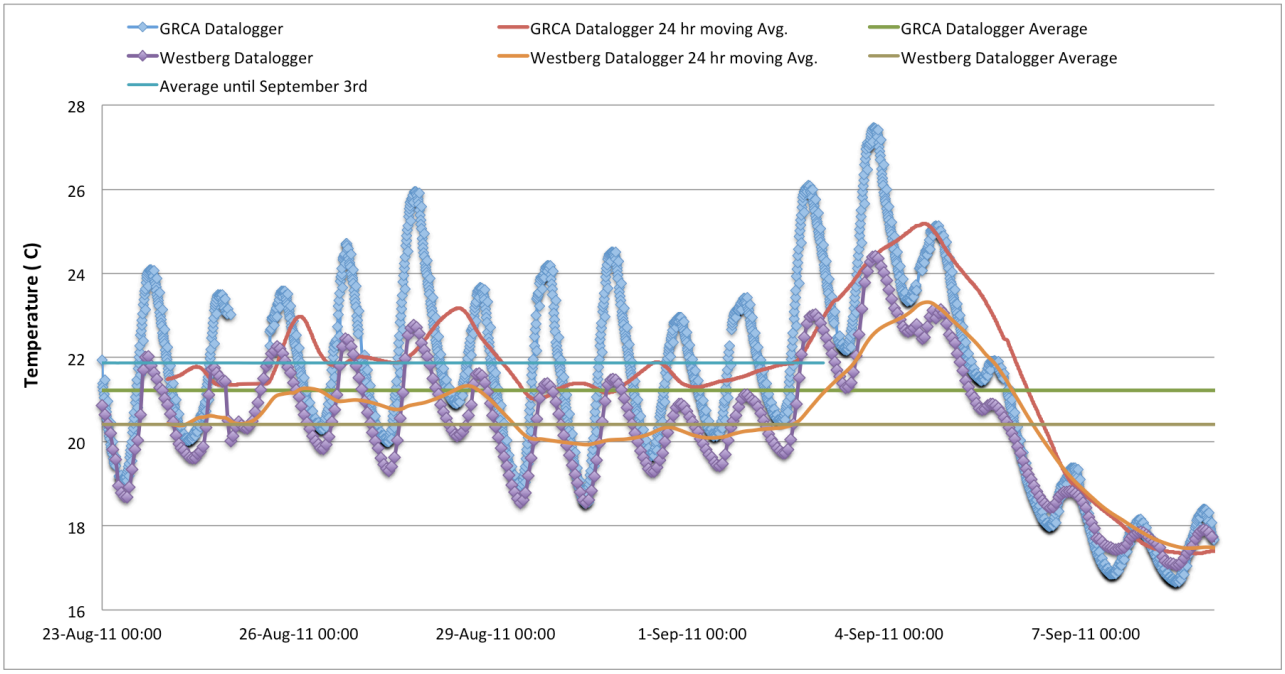

Figure AA. 1 Surface water trends for the determination of T_O for riverbed sampling locations (See Chapter five for the determination of T_O for February 27th 2011 and summer 2011 temperature profiling). Over the timespan riverbed sampling took place, there is clearly a decreasing temperature trend in the 24 hr moving average of surface water temperatures, violating the requirement that temperatures are quasi-steady state. If only temperatures until the 3rd of September are considered, however, the 24 hr moving average of the surface water temperatures does appear to be more or less consistent. This was used to estimate a T_O value for the flux estimates at riverbed sampling locations. This T_O value, however, is not valide for locations sampled after September 3rd 2011 – RB-15, RB-16, RB-17, and RB-18. Vertical fluxes calculated for RB-17 and RB-18 are to be taken as ballpark estimates only.

Appendix B – Domestic Well Samples

ID	Well Depth (m)*	Well Type*	pH	Temp (°C)	DO (mg/L)	Condc. (uS/cm)	DOC (mg/L)	Cl^- (mg/L)	NO_3^- (mg·N/L)	SO_4^{2-} (mg/L)	NH_4^+ (mg N/L)	$\delta^{34}S\text{-}SO_4^{2-}$ (‰ VCDT)	$\delta^{18}O\text{-}SO_4^{2-}$ (‰ VSMOW)	$\delta^{15}N\text{-}NO_3^-$ (‰ N_2)	$\delta^{18}O\text{-}NO_3^-$ (‰ VSMOW)
DW-1	26.21	OB	7.1	15.6	7.1	748.8	1.0	25.3	11.1	28.4	0.04	2.11, 1.99	-3.10, -2.48	-	-
DW-2	63.10	BR	7.2	13.2	8.6	592.0	0.4	15.4	8.7	18.5	0.04	2.79	-1.38	3.56	-0.56
DW-3	9.14	OB	7.1	10.8	9.5	684.4	2.0	35.5	8.8	18.1	0.04	4.56	0.41	4.09	-1.00
DW-4	NN	NN	7.1	14.2	5.1	747.0	1.1	39.9	0.2	13.9	0.02	-	-	-	-
DW-5	NN	NN	7.2	9.2	1.9	643.8	-0.1	27.9	0.2	45.3	0.04	-0.84	-3.43	-	-
DW-6	12.80	OB	7.2	14.4	8.6	656.0	0.9	10.0	0.5	14.6	0.04	2.46, 1.94	-0.35	-	-
DW-7	81.69	BR	7.3	10.7	0.1	483.0	1.1	3.9	0.2	4.4	0.22	-	-	-	-
DW-8	36.59	OB	7.4	12.8	9.4	504.0	4.0	10.7	0.2	15.8	0.15	28.21	15.35	-	-
DW-9	NN	NN	6.9	14.7	1.8	750.7	1.8	40.9	0.8	8.6	-0.01	-	-	-	-
DW-10	51.82	NN	7.4	12.6	0.1	560.7	-	11.6	0.2	37.0	0.00	-	-	-	-
DW-11	NN	NN	7.3	15.8	0.4	629.0	-	29.2	0.2	61.7	0.01	-	-	-	-
DW-12	49.70	OB	7.2	13.4	5.1	630.0	0.3	7.0	0.6	34.9	-0.01	-	-	-	-
DW-13	60.96	NN	7.2	15.1	0.1	581.0	-	4.2	0.2	29.8	0.20	-	-	-	-
DW-14	NN	OB	7.1	17.8	0.3	835.7	2.2	30.4	0.2	74.7	-0.01	-	-	-	-
DW-15	53.64	NN	7.2	13.4	0.4	622.0	0.9	16.5	0.2	50.8	0.01	-	-	-	-
DW-16	10.70	OB	7.0	11.6	0.4	790.3	0.9	30.9	1.3	60.0	0.00	9.92	4.28	-	-
DW-17	34.14	BR	7.3	14.5	1.4	573.0	0.7	19.4	0.2	43.7	1.43, 0.003	-	-	-	-
DW-18	57.90	BR	7.2	12.7	0.1	618.0	5.7	7.8	0.2	5.5	0.003, 1.43	-	-	-	-
DW-19	28.00	OB	7.1	10.8	0.1	933.0	0.4	92.7	0.3	83.2	0.01	-1.44, -1.32	-2.46	-	-
DW-20	36.58	OB	7.1	11.3	0.2	700.0	-	15.8	0.2	50.3	0.00	1.29	-2.40	-	-
DW-21	6.10	NN	6.9	12.8	0.4	641.0	-	19.0	0.2	23.8	0.08, 0.08	-	-	-	-
DW-22	6.10	NN	7.0	15.8	7.7	652.0	-	10.9	5.8	11.7	-0.01	-	-	-	-

DW-23	37.50	BR	7.1	13.5	0.2	3340.0	2.5	12.1	0.2	1197.7	-0.01	27.14	12.63, 12.95	27.33	21.56
DW-24	39.01	OB	7.2	11.0	7.2	613.7	1.2	26.4	1.8	17.9	-0.02	-	-	-	-
DW-25	18.29	OB	7.5	9.8	4.7	639.0	1.3	14.4	2.3	32.4	-0.02	5.49	-0.28	-	-
DW-26	68.59	BR	7.1	16.0	6.8	1686.7	1.3	15.1	0.2	670.3	-0.02	28.05	13.32	16.31	2.68
DW-27	68.30	BR	7.6	14.7	0.1	884.3	-0.2	32.2	0.2	118.7	-0.02	16.24, 16.07	6.55	-	-
DW-28	12.19	NN	6.8	13.0	2.8	805.0	3.6	46.9	3.8	14.9	-0.02	-	-	-	-
DW-29	12.80	OB	7.0	15.8	9.9	799.0	0.9	40.8	7.9	17.4	-0.02	6.28	-0.30	-	-
DW-30	10.7 or 43.59	NN	7.2	12.1	9.0	632.0	-	36.7	3.5	12.9	-0.01	-	-	-	-
DW-31	NN	NN	7.0	13.3	4.7	1068.0	1.7	116.7	5.0	84.1	-0.02	-	-	-	-
DW-32	24.38	OB	7.2	15.0	7.0	920.3	1.8	62.5	0.2	79.2	-0.01	1.88	-5.02	-	-
DW-33	11.58 or 63.4	BR	7.4	16.4	9.1	783.0	1.9	54.2	4.8	19.0	-0.01	4.78	1.91	-	-
DW-34	NN	NN	7.2	16.2	13.1	723.3	1.7	121.3	2.2	23.2	-0.01	-	-	-	-
DW-35	NN	NN	6.9	14.6	13.1	723.3	8.8	46.8	0.2	15.7	0.00	-	-	-	-
DW-36	39.62	BR	7.4	9.8	7.4	507.7	2.1	3.4	0.2	24.9	0.29, 0.25	33.37, 32.80	12.93	-	-
DW-37	8.53	NN	7.2	15.5	9.5	541.7	0.9	2.6	1.0	9.6	-0.01	-	-	-	-
DW-38	21.34	NN	7.3	10.9	6.4	672.0	3.9	24.4	6.1	31.5	-0.01	-	-	-	-
DW-39	NN	NN	7.3	14.6	9.7	628.3	1.5	5.1	4.5	15.4	-0.01	-	-	-	-
DW-40a	6.10	NN	6.9	15.7	1.8	1036.0	3.3	63.3	4.1	21.1	0.02, 0.02	-	-	-	-
DW-40b	6.10	NN	7.1	14.9	4.8	1025.7	3.0	76.3	3.8	20.0	-0.01	-	-	-	-
DW-41	45.72	NN	7.4	9.6	0.2	520.0	1.0	11.0	0.2	37.7	0.03	-	-	-	-

*BR = Bedrock; NN = Unknown; OB = Overburden;

Appendix C – Seep Samples

Sample ID	pH	Temp (°C)	DO (mg/L)	Condc. (uS/cm)	DOC (mg/L)	Cl^- (mg/L)	NO_3^- (mg·N/L)	SO_4^{2-} (mg/L)	NH_4^+ (mg/L)	Type*	$\delta^{34}S$-SO_4^{2-} (‰ VCDT)	$\delta^{18}O$-SO_4^{2-} (‰ VSMOW)	$\delta^{15}N$-NO_3^- (‰ N_2)	$\delta^{18}O$-NO_3^- (‰ VSMOW)
GRS-1	7.8	19.0	8.0	2973	3.2	599.3	0.5	59.2	0.2	Eff	-	-	-	-
GRS-2	7.4	8.9	4.7	644	0.5	26.1	2.8	31.2	nd	S	-1.3	-2.4	3.4	0.0
GRS-3	7.3	10.6	6.7	776	0.3	55.0	4.3	18.5	nd	S	-	-	3.0	-1.4
GRS-4	7.3	11.2	8.3	626	1.4	11.9	0.6	28.1	nd	S	-	-	-	-
GRS-5	8.4	16.3	9.5	627	1.0	15.6	2.7	24.6	nd	T	-	-	-	-
GRS-6	8.3	15.3	9.5	638	2.7	14.1	0.4	33.6	nd	T	-	-	-	-
GRS-7	8.5	16.5	9.8	535	4.6	14.0	0.2	8.3	nd	T	-	-	-	-
GRS-8	8.2	10.2	11.3	618	0.7	23.1	5.0	15.0	nd	S	-	-	-	-
GRS-9	7.6	9.9	4.7	611	0.1	22.2	0.1	20.1	nd	S	7.7	4.8	-	-
GRS-10	7.2	10.2	0.1	2480	0.2	4.3	0.1	1253.6	0.2	S	27.8	12.5	-	-
GRS-11	8.1	13.1	10.0	658	3.1	16.2	6.2	24.6	nd	T/S	-	-	-	-
GRS-12	8.3	15.4	9.4	625	2.0	17.1	0.3	5.4	nd	T	-	-	-	-
GRS-13	8.4	13.9	10.5	715	1.4	33.1	4.9	30.0	nd	T/S	-	-	-	-
GRS-14	8.3	19.4	8.6	1290	4.4	157.3	1.7	46.9	nd	T	-	-	-	-
GRS-15	8.0	15.0	9.6	1309	6.4	145.4	1.5	44.2	nd	T	-	-	-	-
GRS-16	7.5	20.1	7.6	2330	6.7	355.0	20.9	214.7	nd	T	-	-	11.4	-1.5
GRS-17	7.5	10.4	9.5	692	0.4	26.7	3.8	32.1	nd	S	-	-	-	-
GRS-18	8.0	11.3	10.8	561	2.3	20.8	3.6	19.7	nd	S	-	-	-	-
GRS-19	8.3	16.4	8.4	675	1.9	36.6	0.2	38.2	nd	T	-	-	-	-
GRS-20	7.6	12.1	7.2	709	0.2	21.5	4.3	42.4	nd	S/T	-	-	7.9	1.1
GRS-21	7.4	12.0	3.5	706	3.5	25.7	4.1	39.7	nd	S/T	-	-	3.5	-0.9

GRS-22	7.6	15.6	4.7	626	3.4	8.5	1.1	43.9	nd	T	-	-	-	-
GRS-23	7.4	10.0	9.5	662	0.0	16.2	14.1	18.8	nd	S	-	-	3.3	-0.7
GRS-24	8.4	16.3	9.6	970	4.6	116.6	0.7	23.4	nd	T	-	-	-	-
GRS-25	7.8	12.9	9.9	773	4.4	52.9	3.6	18.6	nd	T/S	6.9	2.1	12.1	4.0
GRS-26	8.1	13.2	10.6	822	5.0	54.5	4.4	45.8	nd	T/S	-	-	-	-
GRS-27	8.4	17.2	9.6	832	3.6	46.9	1.9	131.4	nd	T	21.0	10.0	8.0	1.5
GRS-28	7.6	20.3	7.3	2890	9.6	390.2	6.6	309.9	0.1	T	-	-	-	-
GRS-28a	-	-	-	-	2.5	70.4	2.6	159.6	nd		-	-	-	-
GRS-29	7.3	10.0	8.9	1016	1.6	97.3	6.2	32.1	nd	S	13.4	3.0	2.4	-1.8
GRS-30	8.2	14.9	10.2	1241	3.7	169.2	0.8	18.7	nd	Trib	-	-	-	-
GRS-31	8.5	14.9	10.9	772	11.7	40.6	3.0	116.9	nd	T	17.2	9.1	6.9	2.1
GRS-32	7.7	9.5	11.0	656	0.5	14.8	11.3	31.7	nd	S	5.2	4.3	3.7	1.1
GRS-33	8.4	14.0	10.5	800	2.0	72.3	3.1	52.4	nd	T/S	-	-	-	-
GRS-34	8.2	18.7	12.9	769	4.0	76.2	0.1	107.0	nd	T	-	-	-	-
GRS-35	7.6	9.9	11.2	866	2.9	55.4	2.5	43.6	nd	S	10.3	5.0	1.9	-2.3
GRS-36	8.2	11.9	11.1	1073	2.7	132.7	2.0	38.1	nd	S	7.7	2.9	3.6	0.7
GRS-37	8.4	16.0	9.8	896	2.1	128.1	1.0	21.1	nd	T	-	-	-	-
GRS-38	7.3	12.2	-	758	2.1	16.6	6.2	41.7	nd	S	-	-	10.2	-1.1
GRS-39	7.9	13.8	9.0	718	0.9	31.1	1.0	16.8	-	T/S	-	-	-	-
GRS-40a	8.2	13.9	9.0	900	2.5	97.2	2.0	30.3	nd	T/S	6.1	1.2	4.5	2.2
GRS-43	8.3	11.8	10.9	1150	0.9	122.3	5.4	55.3	-	S	-	-	3.8	-1.5
GRS-44	8.3	16.8	8.8	980	4.0	113.3	2.6	55.0	nd	T	-	-	-	-
GRS-45	8.2	11.9	11.1	1073	2.7	132.7	2.0	38.1	nd	S	-	-	-	-
GRS-60	7.0	9.8	2.9	752	-	-	-	-	-	S	-	-	-	-
GRS 61	7.0	9.8	2.9	752	-	-	-	-	-	S	-	-	-	-
GRS-62	6.8	12.7	4.1	2105	1.5	139.8	1.3	576.8	-	S/T	27.3	10.6	9.9	-0.3

*nd = non-detectable; S = Seep: < 12.00°C; S/T = Seep/Trib: 12.00°C to 13.00°C; T/S = Trib/Seep: 13.00°C to 14.00°C; T = Trib: > 14.00°C; E = Effluent;

Appendix D – Riverbed Samples

ID	Depth (m)	pH	Temp (°C)	DO (mg/L)	Condc. (uS/cm)	DOC (mg/L)	Cl^- (mg/L)	NO_3^- (mg·N/L)	SO_4^{2-} (mg/L)	NH_4^+ (mg/L)	$\delta^{34}S\text{-}SO_4^{2-}$ (‰ VCDT)	$\delta^{18}O\text{-}SO_4^{2-}$ (‰ VSMOW)	$\delta^{15}N\text{-}NO_3^-$ (‰ N_2)	$\delta^{18}O\text{-}NO_3^-$ (‰ VSMOW)
GRP-1A	0	8.2	23.6	10.8	757	-	98.9	2.3	36.8	0.1	13.6	6.4	-	-
GRP-1B	0.25	7.2	-	7.2	952	-	98.2	3.2	32.6	nd	6.6	1.6	-	-
GRP-1C	0.5	7.3	24.6	7.7	986	-	109.1	3.6	35.3	nd	5.1	0.0	-	-
GRP-1D	0.75	7.2	-	6.6	956	-	105.7	3.5	34.0	nd	5.8	0.2	-	-
GRP-2A	0	8.3	24.2	15.0	724	-	93.7	2.1	38.6	0.1	-	-	-	-
GRP-2B	0.25	7.0	22.2	0.6	817	-	94.3	0.3	32.2	0.1	-	-	-	-
GRP-2C	0.5	6.9	20.1	0.7	784	-	86.4	0.6	31.8	nd	-	-	-	-
GRP-2D	0.75	7.0	20.2	1.0	766	-	63.7	1.3	31.0	nd	-	-	-	-
GRP-2E	1	7.2	19.3	1.6	714	-	54.5	1.6	30.4	nd	-	-	-	-
GRP-3A	0	7.8	20.4	6.9	748	-	89.9	2.3	35.1	0.1	-	-	-	-
GRP-3B	0.25	7.3	19.8	2.5	680	-	62.0	0.3	27.1	nd	-	-	-	-
GRP-3C	0.5	7.3	19.1	3.5	694	-	61.6	0.3	26.3	nd	-	-	-	-
GRP-3D	0.75	7.4	18.7	4.3	698	-	62.8	0.4	25.8	nd	-	-	-	-
GRP-3E	1	7.4	18.0	3.0	695	-	65.8	0.2	25.5	nd	-	-	-	-
GRP-4A	0	8.5	21.9	10.9	714	-	85.4	2.5	34.6	nd	-	-	-	-
GRP-4B	0.25	7.6	24.3	8.4	663	-	-	-	0.0	nd	-	-	-	-
GRP-5A	0	8.4	21.6	9.9	724	-	91.7	2.6	37.2	nd	12.9	7.0	-	-
GRP-5B	0.25	8.0	23.6	5.4	709	-	89.2	2.6	35.2	nd	12.8	5.8	-	-
GRP-5C	0.5	7.4	21.0	4.0	697	-	27.9	5.0	45.7	nd	3.5	-1.6	-	-

GRP-5D	0.75	7.3	22.3	3.6	718	-	28.4	5.0	44.1	nd	2.5	-1.5	-	-
GRP-5E	1	7.3	23.3	5.2	644	-	27.3	4.8	43.1	nd	3.2	-1.6	5.0	-0.4
GRP-6A	0	8.2	23.3	12.4	670	-	51.5	1.9	25.2	nd	12.3	5.1	-	-
GRP-6B	0.25	7.1	17.3	6.2	590	-	25.0	2.8	15.0	nd	7.7	3.4	-	-
GRP-6C	0.5	7.2	17.1	5.7	568	-	23.5	2.9	14.5	nd	7.5	3.3	-	-
GRP-6D	0.75	7.2	19.2	6.3	598	-	21.6	2.9	14.1	nd	6.8	2.7	-	-
GRP-6E	1	7.3	20.2	7.6	573	-	21.8	2.8	13.9	nd	6.7	3.1	3.3	-2.1
GRP-7A	0	8.7	25.5	16.1	734	-	100.5	2.8	38.3	nd	-	-	-	-
GRP-7B	0.25	7.1	19.5	5.3	627	-	12.1	1.4	43.2	nd	-	-	-	-
GRP-7C	0.5	7.1	19.7	7.2	621	-	10.5	1.4	43.4	nd	-	-	-	-
GRP-7D	0.75	7.1	19.6	6.3	631	-	9.3	1.4	44.2	nd	-	-	-	-
GRP-7E	1	7.1	18.7	3.6	613	-	9.2	1.3	43.6	nd	-	-	-	-
GRP-8A	0	8.0	19.6	11.0	858	-	93.8	0.8	25.9	nd	-	-	-	-
GRP-8B	0.25	7.0	21.5	2.0	1061	-	100.9	0.1	164.3	nd	-	-	-	-
GRP-8C	0.5	7.1	21.7	1.0	1068	-	98.4	0.1	167.4	nd	-	-	-	-
GRP-8D	0.75	7.1	22.9	1.8	1038	-	91.5	0.1	165.4	nd	-	-	-	-
GRP-8E	1	7.1	24.2	1.9	1007	-	94.2	0.1	175.3	nd	-	-	-	-
GRP-9A	0	8.5	22.4	-	876	-	93.4	2.4	93.2	nd	21.6	10.4	-	-
GRP-9B	0.25	6.9	18.5	1.0	1750	-	32.4	0.8	592.1	nd	27.1	12.5	-	-
GRP-9C	0.5	7.0	20.3	0.8	1746	-	32.5	0.8	603.8	nd	25.0	12.0	-	-
GRP-9D	0.75	7.0	16.5	0.4	1759	-	32.3	0.8	610.1	nd	26.0	11.0	-	-
GRP-9E	1	7.0	19.5	0.7	1783	-	32.9	0.8	639.0	nd	26.4	12.8	16.9	9.1
GRP-10A	0	8.4	21.2	14.1	826	8.45	114.8	3.2	40.0	-	-	-	-	-

GRP-10B	0.25	7.3	15.8	7.1	593	1.19	13.6	0.7	47.9	nd	-	-	-	-
GRP-10C	0.5	7.2	17.5	6.5	596	0.11	12.8	0.8	47.9	nd	-	-	-	-
GRP-10D	0.75	7.2	17.0	6.7	598	-	12.6	0.8	48.4	nd	-	-	-	-
GRP-10E	1	7.2	18.2	5.4	596	1.40	12.5	0.7	47.8	nd	-	-	-	-
GRP-11A	0	7.9	20.9	9.0	812	4.05	93.2	2.7	72.7	nd	-	-	-	-
GRP-11B	0.25	7.5	21.0	4.4	800	6.30	91.3	1.4	71.3	0.1	-	-	-	-
GRP-11C	0.5	7.4	21.4	2.3	810	6.60	89.8	1.2	68.4	nd	-	-	-	-
GRP-12A	0	8.4	24.1	15.6	775	-	98.2	2.8	62.3	nd	-	-	-	-
GRP-12B	0.25	6.9	23.4	2.1	1168	4.84	42.1	4.6	327.8	nd	-	-	-	-
GRP-13A	0	8.4	24.2	15.6	799	-	101.3	2.6	71.2	nd	-	-	-	-
GRP-13B	0.25	7.2	26.3	1.1	1045	-	81.4	0.4	154.3	nd	-	-	-	-
GRP-13C	0.5	6.7	24.7	0.6	2069	-	33.1	0.2	828.9	3.0	-	-	-	-
GRP-13D	0.75	7.1	25.6	2.1	1012	-	-	-	-	0.4	-	-	-	-
GRP-14A	0	8.5	25.1	14.9	805	4.82	104.5	3.0	72.6	nd	19.5	7.9	-	-
GRP-14B	0.25	6.9	24.7	2.5	2140	4.07	23.8	0.5	952.2	nd	25.3	11.5	-	-
GRP-14C	0.5	7.0	25.1	3.0	2119	2.40	22.8	0.5	912.2	nd	26.5	12.6	-	-
GRP-14D	0.75	7.0	23.1	2.7	2129	1.94	23.7	0.4	939.9	nd	25.7	12.3	-	-
GRP-14E	1	7.0	24.7	2.9	2132	0.92	23.5	0.5	918.2	nd	25.5	12.1	17.2	7.7
GRP-15A	0	8.3	26.7	15.9	820	8.60	100.5	2.6	86.0	-	-	-	-	-
GRP-15B	0.25	7.3	24.6	0.7	806	-	90.6	0.1	73.0	0.6	-	-	-	-
GRP-15C	0.5	7.1	24.9	0.3	831	-	100.2	0.1	66.3	1.0	-	-	-	-
GRP-15D	0.75	7.1	24.9	0.9	826	5.70	98.2	0.1	77.4	0.6	-	-	-	-

GRP-15E	1	6.9	24.0	0.3	1236	3.60	65.8	0.1	270.9	0.2	-	-	-	-
GRP-16A	0	7.9	17.2	9.2	813	4.57	87.9	2.7	76.8	0.0	-	-	-	-
GRP-16B	0.25	6.9	16.9	1.9	803	2.12	57.4	0.8	41.7	0.2	-	-	-	-
GRP-16C	0.5	6.9	18.0	0.6	797	5.47	43.4	0.1	33.6	0.0	-	-	-	-
GRP-16D	0.75	6.9	18.3	0.8	832	2.33	51.6	0.3	41.1	0.0	-	-	-	-
GRP-16E	1	7.0	18.4	0.4	831	2.79	51.8	0.3	41.5	0.0	-	-	-	-
GRP-17A	0	8.1	18.0	11.5	816	-	90.7	2.8	71.7	0.0	-	-	-	-
GRP-17B	0.25	7.1	18.4	2.6	844	-	83.5	1.8	49.5	0.8	-	-	-	-
GRP-17C	0.5	7.6	25.3	7.9	768	-	77.8	0.5	60.1	0.0	-	-	-	-
GRP-18A	0	8.1	19.1	11.3	838	2.74	95.0	2.9	73.8	0.0	-	-	-	-
GRP-18B	0.25	7.3	21.4	0.6	855	-	99.3	0.1	43.1	0.2	-	-	-	-
GRP-18C	0.5	7.3	22.2	0.6	765	0.36	78.1	0.1	38.4	0.2	-	-	-	-
GRP-18D	0.75	7.3	23.2	0.6	630	-0.20	45.4	0.1	31.9	0.1	-	-	-	-
GRP-18E	1	-	-	-	-	4.98	-	-	0.0	0.0	-	-	-	-
GRP-19A	0	8.1	20.1	11.9	855	4.01	99.1	3.4	74.6	0.0	2.0	8.5	-	-
GRP-19B	0.25	7.3	21.7	3.0	823	-	89.3	1.1	67.6	0.0	19.7	8.7	-	-
GRP-19C	0.5	7.4	21.2	2.8	824	-	88.9	1.4	67.6	0.0	19.3	8.8	-	-
GRP-19D	0.75	7.6	25.1	8.1	774	-	79.5	0.5	60.6	0.0	19.6	8.5	-	-
GRP-19E	1	7.5	24.7	4.3	761	-	78.6	1.1	60.5	0.0	19.3	8.1	8.9	-2.2

Appendix E – Riverbed Profiles Not Discussed in the Thesis

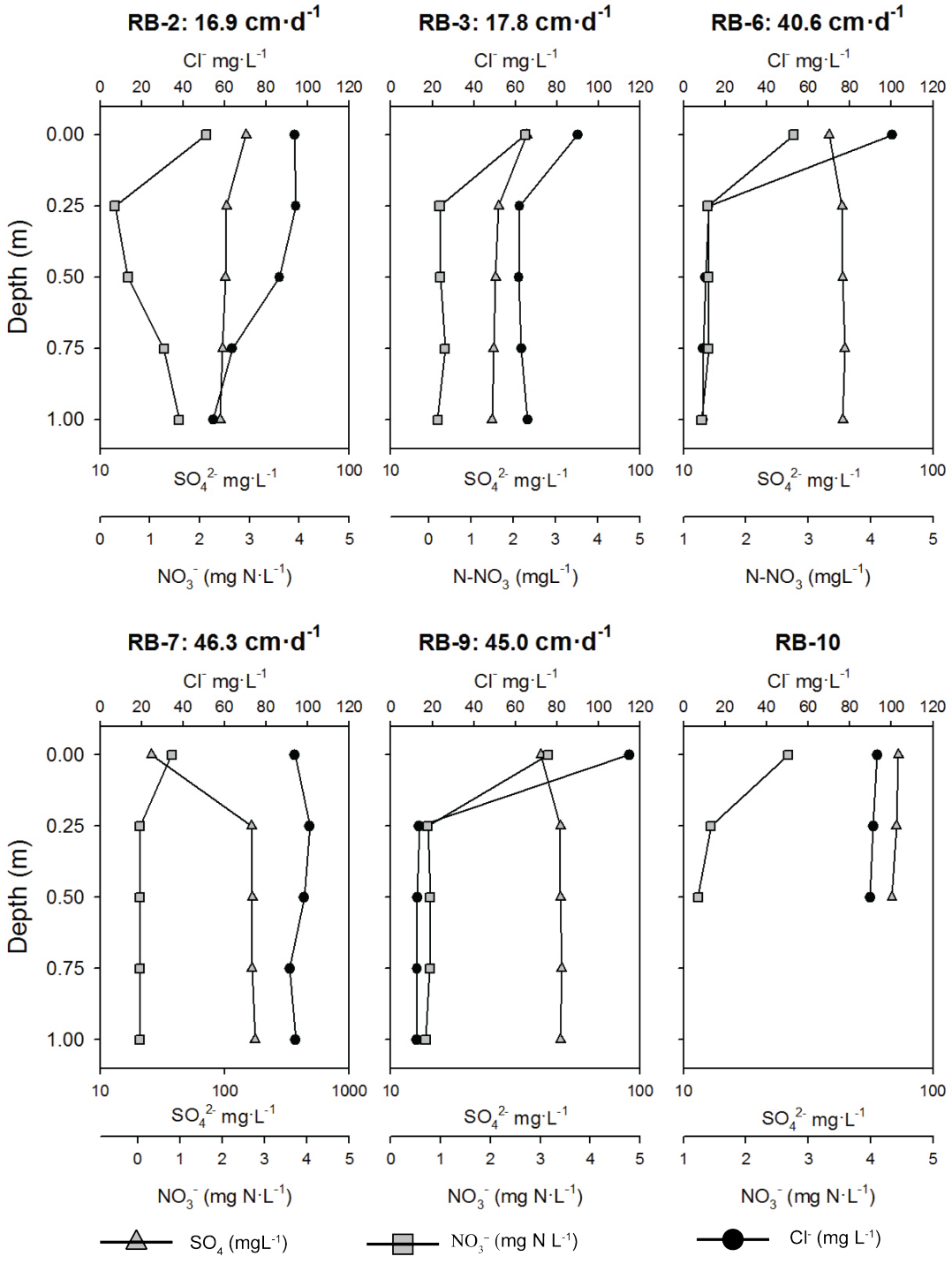

Figure AE.1 Riverbed locations where samples were not analyzed for sulfate isotopes.

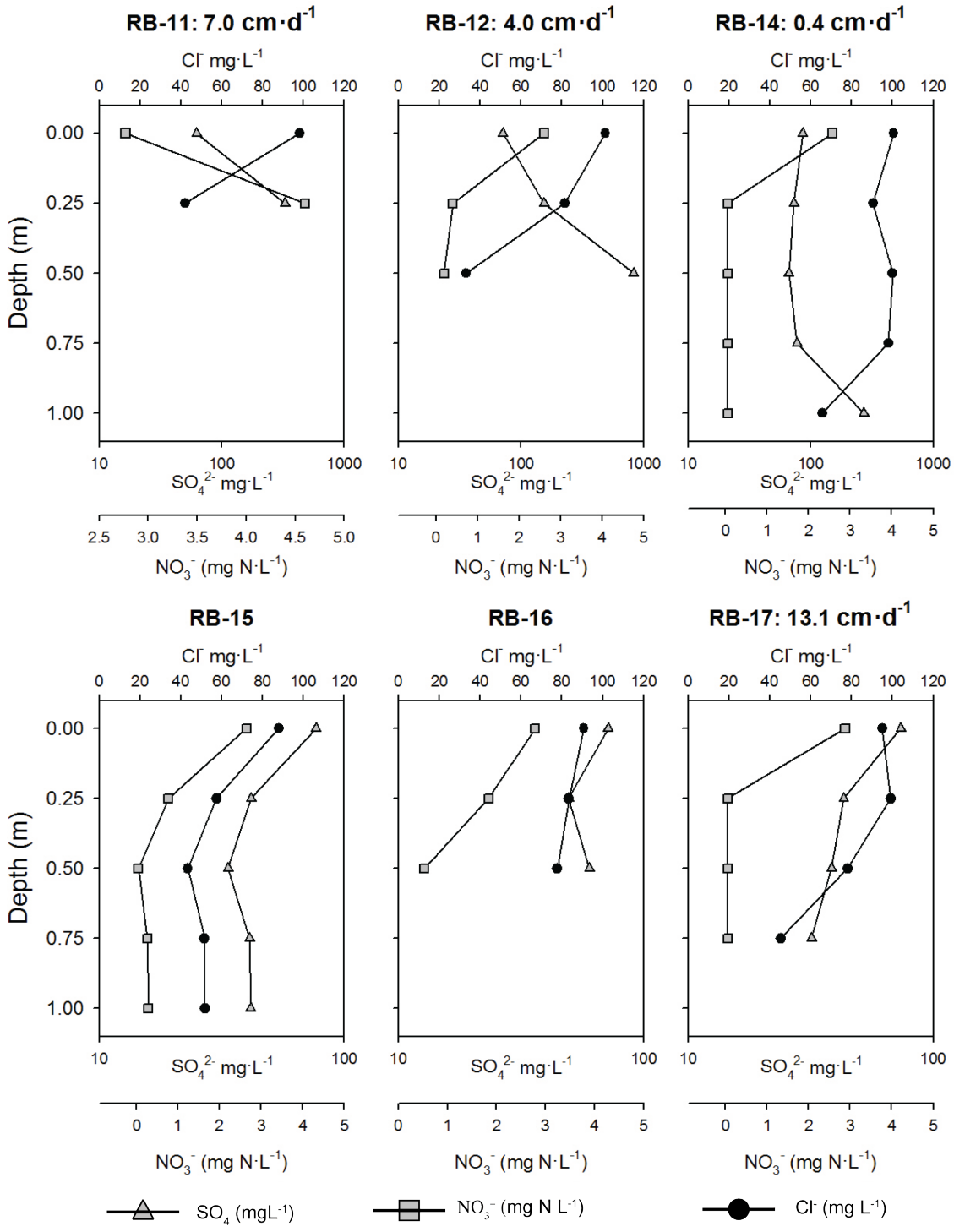

Figure AE.2 Riverbed locations where samples were not analyzed for sulfate isotopes.

Figures AF.1 and AF.2 show profiles of riverbed sampling locations not selected for sulfate isotope analysis. At some locations, only one or two samples have been collected in the riverbed, after which low flow materials were encountered or the Waterloo Profiler could not be driven deeper, making it possible to collect more samples. RB-10 and RB-11 appeared to be locations where the profiler bottomed out on bedrock, and RB-12 and RB-16 both entered silty layers that clogged the profiler ports and made sample collection impossible (Figure AF.3).

Figure AE.3 Silt clogging the profiler ports at RB-16.

Without sulfate isotopes, there is no conclusive evidence of the presence of various water-types at these locations, but chloride concentrations define hyporheic-zone water, temperature measurements permit flux estimates, and high sulfate concentrations suggest a Salina formation source. Consistent chloride concentrations within the riverbed at RB-3, RB-6, and RB-9, suggest a different water type than the river. Temperature measurements result in relatively high flux estimates of 40.6 $cm \cdot d^{-1}$, and 45.0 $cm \cdot d^{-1}$ for RB-6 and RB-9, respectively, and a lower flux estimate of 17.8 $cm \cdot d^{-1}$ for RB-3. Dissolved oxygen in the riverbed samples from all three locations was above 2.5 mgL^{-1}, and generally greater than 5 mgL^{-1}. Nitrate concentrations are below 1.0 $mgNL^{-1}$ at RB-3 and RB-9, and below 1.5 $mgNL^{-1}$ at RB-6; all lower than the river samples. All three of these locations suggest reasonably strong groundwater discharge from overburden or Guelph formation aquifers. RB-6 and RB-9 appear to have similar water types based on sulfate and chloride concentrations.

RB-7 is unique in that chloride was not helpful in distinguishing between water types. RB-7 is located in an alcove - much like RB-5 - separated from the main channel, with significant cold-water tributaries discharging nearby (Figure AF.4). The river-water chloride concentrations are approximately 40 mgL^{-1} lower here than in the main channel; i.e., the surface water type in this alcove may be different than the Grand. RB-7 has similar chloride concentrations in the riverbed as the river, but considerably, consistently higher sulfate concentrations down profile. Temperature measurements suggested a relatively high discharge flux of 42.60 cmd^{-1}. It is unclear why chloride would stay the same yet sulfate would be significantly greater in the riverbed. Low nitrate values suggest redox conditions may allow for sulfate reduction, but in that case sulfate should be lower in the riverbed, not higher.

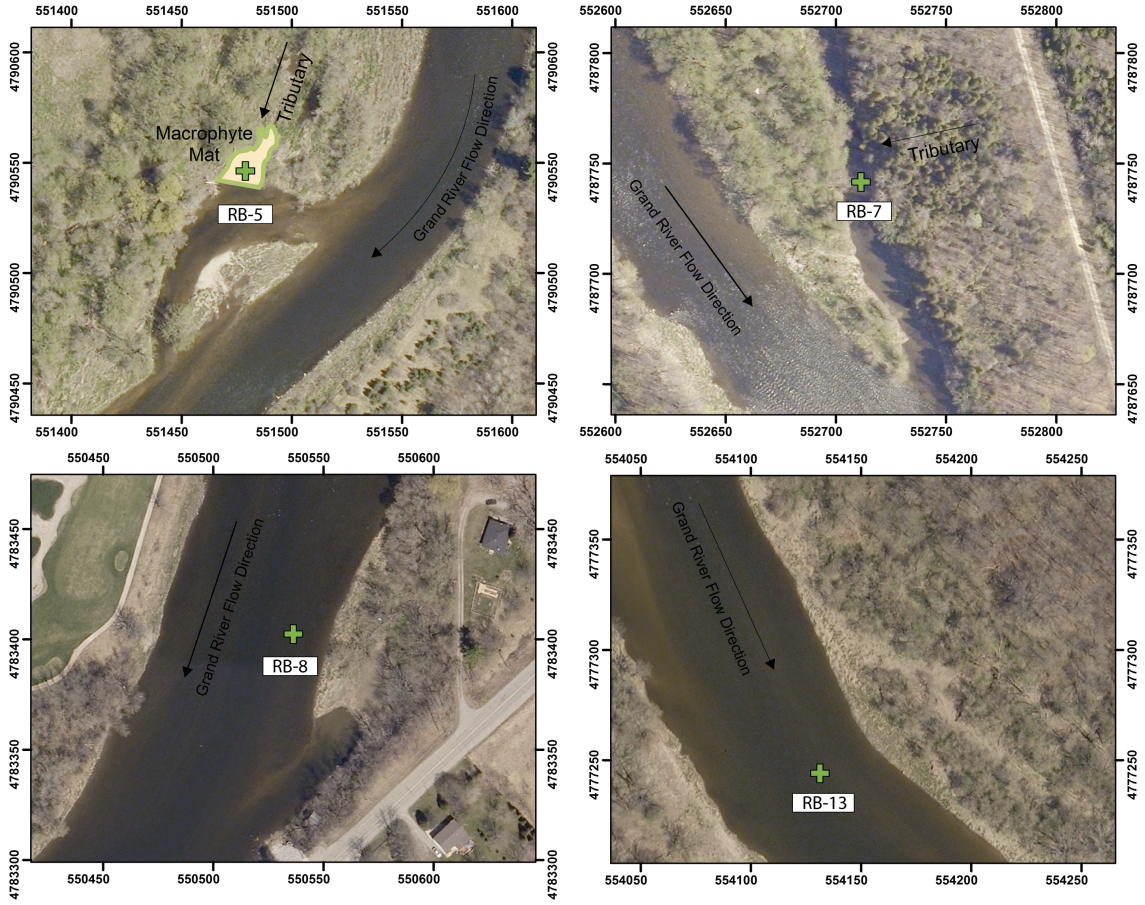

Figure AE.4 Side channel vs. main channel locations of RB-5 and RB-7 vs. RB-8 and RB-13. The side channel nature of RB-5 and RB-7, as well as several other locations, resulted in samples taken in the water column over the riverbed having different chemistry than the river in the main channel.

The profile for RB-14 may suggest a change in water type at depth. Although nitrate values are negligible in the riverbed, sulfate and chloride stay similar to river values until 1m, where sulfate more than triples and chloride drops off significantly. Low dissolved oxygen concentrations and non-detectable nitrate suggests, along with the slow decrease in sulfate concentrations from the river values to 50cm, that sulfate reduction may be occurring. Temperatures indicated a discharge flux of essentially zero. This appears consistent at least to 0.75m into the riverbed.

RB-2 and RB-17 suggest a transition between water types is taking place, with both chloride and sulfate concentrations decreasing with depth. At both RB-2 or RB-17 temperature data indicates a low to moderate vertical flux of groundwater discharge.

RB-15 may suggest a low flow barrier around 50cm into the riverbed; chloride, sulfate, and nitrate all dip at this depth from higher concentrations both deeper in the riverbed and in the river. Nitrate concentrations below detection level could indicate redox conditions sufficient to reduce sulfate.

Appendix F – Grand River Samples

ID*	Downstream** Distance (km)	pH	DO (mg/L)	Condc. (uS/cm)	DOC (mg/L)	Cl^- (mg/L)	NO_3^- (mg·N/L)	SO_4^{2-} (mg/L)	NH_4^+ (mg·N/L)	$\delta^{34}S\text{-}SO_4^{2-}$ (‰ VCDT)	$\delta^{18}O\text{-}SO_4^{2-}$ (‰ VSMOW)	$\delta^{15}N\text{-}NO_3^-$ (‰ N_2)	$\delta^{18}O\text{-}NO_3^-$ (‰ VSMOW)
GR-J1	0.11	-	9.0	749	6.6	87.7	2.9	31.5	0.20	13.5	4.4	8.6	0.5
GR-J2	1.14	8.0	8.9	742	6.5	88.5	3.2	31.5	-	-	-	-	-
GR-J3	2.15	8.1	10.1	743	5.9	86.9	3.1	30.9	0.10	-	-	-	-
GR-J4	3.15	8.2	10.7	741	5.7	88.5	3.2	31.7	-	-	-	-	-
GR-J5	4.18	8.2	11.2	754	6.3	88.8	3.2	30.8	0.10	13.2	6.4	8.0	-0.6
GR-J6	5.15	8.2	11.7	763	6.9	95.5	3.6	33.7	-	-	-	-	-
GR-J7	6.13	8.3	12.5	743	6.8	89.7	2.9	30.7	nd	-	-	-	-
GR-J8	7.17	8.3	12.9	770	10.1	98.1	3.8	34.8	-	-	-	-	-
GR-J9	8.13	8.4	13.9	758	6.6	88.3	2.7	29.7	nd	13.0	6.4	8.1	-1.0
GR-J10	9.13	8.4	13.8	760	6.1	96.3	3.7	34.0	-	-	-	-	-
GR-J11	10.17	8.5	13.9	745	8.9	91.1	3.0	31.7	nd	-	-	-	-
GR-J12	11.16	8.4	13.3	755	5.6	94.0	3.6	33.5	-	-	-	-	-
GR-J13	12.28	8.4	13.7	748	6.8	91.3	3.4	31.3	nd	13.2	6.2	8.6	-0.4
GR-J14	13.13	8.4	13.1	737	6.7	90.1	3.5	32.2	-	-	-	-	-
GR-J15	14.27	8.4	13.0	743	6.5	88.6	3.3	30.9	nd	-	-	-	-
GR-J16	15.34	8.4	12.9	740	5.9	91.4	3.5	32.3	-	-	-	-	-
GR-J17	16.20	8.4	13.0	739	7.2	88.9	3.3	31.2	nd	13.9	6.0	8.3	-1.0
GR-J18	17.35	8.4	12.9	739	8.9	91.3	3.5	32.8	-	-	-	-	-
GR-J19	18.19	8.4	13.0	738	5.8	89.3	3.4	31.7	nd	-	-	-	-
GR-J20	19.13	8.4	13.0	740	7.0	90.9	3.5	32.9	-	-	-	-	-
GR-J21	20.18	8.4	13.3	740	5.5	90.3	3.4	33.5	nd	13.7	6.2	7.7	-1.8
GR-J22	21.34	8.4	13.0	748	7.8	92.7	3.6	36.5	-	-	-	-	-
GR-J23	22.24	8.2	9.7	768	5.0	94.7	3.6	40.1	nd	-	-	-	-

GR-J24	23.24	8.2	10.2	771	5.8	81.5	3.4	63.8	-	-	-	-	-
GR-J25	24.26	8.2	10.1	775	6.3	88.2	3.4	48.7	nd	17.7	8.8	8.0	-0.8
GR-J26	25.23	8.2	10.8	773	7.0	88.2	3.3	50.5	-	-	-	-	-
GR-J27	26.26	8.2	11.1	772	5.8	86.1	3.3	52.1	nd	-	-	-	-
GR-J28	27.28	8.2	11.2	772	7.4	88.6	3.5	52.1	-	-	-	-	-
GR-J29	28.25	8.3	11.6	772	5.7	84.6	3.4	56.4	nd	16.9	9.0	8.2	-0.5
GR-J30	29.27	8.2	11.9	773	7.5	89.7	3.5	52.7	-	-	-	-	-
GR-J31	30.50	8.3	12.3	771	5.7	77.8	3.2	59.9	nd	-	-	-	-
GR-J32	31.28	8.3	12.2	772	6.2	85.7	3.4	58.7	-	-	-	-	-
GR-J33	32.31	8.3	12.2	772	7.4	85.1	3.4	57.5	nd	18.3	8.1	8.4	-0.8
GR-J34	33.33	8.2	12.1	774	6.7	83.2	3.3	61.9	-	-	-	-	-
GR-J35	34.36	8.2	12.1	763	6.0	77.4	3.2	61.1	nd	-	-	-	-
GR-J36	35.45	8.2	11.7	764	7.2	78.4	3.4	63.6	-	-	-	-	-
GR-J37	36.56	8.2	10.1	758	6.8	75.5	3.2	63.4	nd	18.4	10.2	7.7	-0.1
GR-J38	37.43	8.2	11.3	771	8.0	82.3	3.2	60.1	-	-	-	-	-
GR-J39	38.45	8.3	13.1	757	5.7	79.3	3.1	58.9	nd	-	-	-	-
GR-J40	39.43	8.4	13.6	763	5.7	81.3	3.4	62.3	-	-	-	-	-
GR-S1	0.11	6.9	8.7	766	6.0	100.0	2.9	36.4	nd	13.9	6.2	12.82	-2.26
GR-S2	1.14	8.2	9.5	768	4.7	108.9	3.4	40.3	-	-	-	-	-
GR-S3	2.15	8.5	11.9	875	3.2	115.4	3.9	43.8	nd	-	-	-	-
GR-S4	3.15	8.7	12.1	767	6.3	112.6	3.2	42.3	-	-	-	-	-
GR-S5	4.18	8.7	12.9	802	4.3	113.5	3.5	44.2	nd	14.1	6.2	-	-
GR-S6	5.15	8.8	13.6	811	7.1	114.2	3.5	42.2	-	-	-	-	-
GR-S7	6.13	8.8	13.5	759	2.9	94.4	2.8	35.4	nd	-	-	-	-
GR-S8	7.17	8.8	13.5	792	-	111.6	3.3	41.4	-	-	-	-	-
GR-S9	8.13	8.8	13.1	757	2.4	106.8	3.3	40.8	nd	14.3	6.5	14.76	0.33

GR-S10	9.13	8.8	12.1	786	5.4	110.1	3.2	40.2	-	-	-	-	-
GR-S11	10.17	8.8	12.7	781	4.2	108.8	3.1	39.7	nd	-	-	-	-
GR-S12	11.16	8.8	13.3	753	4.6	103.4	3.0	38.9	-	-	-	-	-
GR-S13	12.28	8.8	12.9	771	5.2	108.2	3.2	39.6	nd	13.9	6.1	-	-
GR-S14	13.13	8.8	12.6	778	5.1	107.7	3.2	39.7	-	-	-	-	-
GR-S15	14.27	8.8	12.5	772	4.7	106.5	3.0	39.8	nd	-	-	-	-
GR-S16	15.34	8.7	12.4	777	4.8	107.6	3.0	40.4	-	-	-	-	-
GR-S17	16.20	8.8	12.5	783	2.8	108.9	3.1	40.5	nd	14.5	6.2	11.96	-0.31
GR-S18	17.35	8.8	12.5	785	5.0	109.6	3.1	40.4	-	-	-	-	-
GR-S19	18.19	8.8	12.3	793	4.9	110.9	3.1	41.7	nd	-	-	-	-
GR-S20	19.13	8.7	12.4	801	4.0	114.7	3.5	44.8	-	-	-	-	-
GR-S21	20.18	8.7	12.2	808	2.6	112.9	3.2	44.6	nd	15.4	6.3	-	-
GR-S22	21.34	8.0	-	818	5.3	112.0	3.4	48.1	-	-	-	-	-
GR-S23	22.24	8.2	10.6	828	1.7	79.5	2.7	85.8	nd	-	-	-	-
GR-S24	23.24	8.3	11.0	831	-	95.8	3.0	77.4	-	-	-	-	-
GR-S25	24.26	8.3	11.0	831	2.2	103.7	3.1	62.3	nd	18.9	8.4	11.58	-2.14
GR-S26	25.23	8.4	11.5	833	3.8	103.0	3.1	66.1	-	-	-	-	-
GR-S27	26.26	8.5	12.0	832	6.3	102.7	3.3	67.0	nd	-	-	-	-
GR-S28	27.28	8.5	13.5	833	3.9	101.4	3.0	71.4	-	-	-	-	-
GR-S29	28.25	8.6	13.6	832	8.6	101.0	3.0	71.6	nd	19.2	8.9	-	-
GR-S30	29.27	8.6	13.6	829	-	101.7	3.2	72.7	-	-	-	-	-
GR-S31	30.50	8.7	14.6	825	5.1	95.6	3.0	77.4	nd	-	-	-	-
GR-S32	31.28	8.7	14.4	824	-	88.6	2.9	82.5	-	-	-	-	-
GR-S33	32.31	8.7	14.0	825	3.7	99.2	3.0	75.0	nd	19.5	8.9	13.975	-0.19
GR-S34	33.33	8.6	13.8	824	4.2	93.8	3.1	82.2	-	-	-	-	-
GR-S35	34.36	8.6	13.1	821	3.2	93.7	2.9	80.4	nd	-	-	-	-
GR-S36	35.45	8.5	12.3	816	3.4	94.6	3.0	79.7	-	-	-	-	-

GR-S37	36.56	8.5	10.5	813	5.5	93.2	2.9	80.1	nd	20.1	7.9	12.30	0.05
GR-S38	37.43	8.5	11.0	813	5.8	96.4	2.6	76.4	-	-	-	-	-
GR-S39	38.45	8.5	11.5	810	3.3	94.3	2.7	78.7	nd	-	-	-	-
GR-S40	39.43	8.5	11.7	810	5.3	94.1	2.6	76.1	-	-	-	-	-

* For brevity's sake, on figures 6.7 and 7.5, J and S, as in the ID labels GR-***J***1 and GR-***S***1, are omitted to reduce clutter. J indicates a sample collected in June, and S indicates a sample collected in September. As both samples are collected from approximately the same place down the Grand River, however, GR-1, on the plan map, shows the location of both.

** *Downstream Distance* refers to the distance each sample is collected from the GRCA canoe launch in Galt, Cambridge (i.e., kilometer zero).